Silicon-Hydrogen (Si-H), Aryl-Fluorine (Aryl-F) and Carbon-Carbon (C-C) Bond Activations by Iridium Porphyrin Complexes

LI, Baozhu

Thesis Submitted to the Department of Chemistry in Partial Fulfillment of the Requirement of the Degree of

Doctor of Philosophy

in

Chemistry

The Chinese University of Hong Kong

March 2010

ProQuest LLC
789 East Eisenhower Parkway
P.O. Box 1346
Ann Arbor, MI 48106-1346

Thesis/Assessment Committee

Professor LEE, Hung Kay (Chair)

Professor CHAN, Kin Shing (Thesis Supervisor)

Professor MIAO, Qian (Committee Member)

Professor KWONG, Hoi-Lun (External Examiner)

Table of Contents

Acknowledgement

I would like to express my most sincere gratitude to my supervisor, Professor Kin Shing Chan, for his guidance, valuable advice and continuous encouragement in my postgraduate studies and the preparation of this thesis.

Through his teaching, I have laid solid foundation on chemical knowledge and cultivated the attitude to integrate chemical knowledge into daily research. In addition, I have grown up to be better in logical thinking and much more eager to ask why in scientific studies.

I would also like to give thanks to all members of the Department of Chemistry for their selfless help and technical support in all circumstances. Especially, thanks Ms. Hoi Shan Chan for X-ray crystallographic determination, and Mr. Chi Chung Lee as well as Ms. Hau Yan Ng for mass spectrometric analysis.

Then many thanks to all my dear former and current group members in Chan's group, especially Ms. Lirong Zhang, Mr. Peng Fai Chiu, Mr. Tsz Ho Lai, Mr. Yun Wai Chan, Mr. Chi Wai Cheung, Ms. Xu Song, Mr. Kwong Shing Choi, Mr. Man Ho Lee, Mr. Hong Sang Fung, Mr. Chung Yin Chan, Ms. Ching Chi Au and Ms. Ying Ying Qian for their encouragement and helpful discussion.

In the end, I would like to express my thanks to my family for their unfailing support and love. Without their love and understanding, I would not be able to finish the course of my study.

December, 2009.

Baozhu Li

Department of Chemistry

The Chinese University of Hong Kong

Abbreviations

δ	: chemical shift
Anal	: analytical
Ar	: aryl
Bn	: benzyl
BDE	: bond dissociation energy
^{t}Bu	: *tert*-butyl
Calcd.	: calculated
CCA	: carbon-carbon bond activation
CFA	: carbon-fluorine bond activation
CHA	: carbon-hydrogen bond activation
d	: day(s)
d	: doublet (NMR)
dd	: doublet of doublets (NMR)
ddd	: doublet of doublet of doublets (NMR)
dddd	: doublet of doublet of doublet of doublets (NMR)
ddt	: doublet of doublet of triplets (NMR)
EN	: electronegativity
ESI	: electrospray ionization
FABMS	: fast atom bombardment mass spectrometry
g	: gram(s)
GC-MS	: gas chromatography mass spectrometry
h	: hour(s)
HRMS	: high resolution mass spectrometry
Hz	: hertz
J	: coupling constant
K	: equilibrium constant
L	: ligand
m	: multiplet (NMR)
M	: molarity
M^+	: molecular cation
M^-	: molecular anion
Me	: methyl
mg	: milligram (s)
MHz	: megahertz

min	: minute (s)
mL	: milliliter (s)
mmol	: millimole (s)
MS	: mass spectrometry
NMR	: nuclear magnetic resonance
OEt	: ethoxyl
ppm	: part per million
Ph	: phenyl
Por	: porphyrin dianion
Pr	: propyl
q	: quartet (NMR)
R	: alkyl group
r.t.	: room temperature
s	: singlet (NMR)
SiHA	: silicon-hydrogen bond activation
t	: triplet (NMR)
TEMPO	: 2,2,6,6-Tetramethyl-piperidin-1-oxyl
THF	: tetrahydrofuran
TLC	: thin-layer chromatography
TMS	: tetramethylsilane
tt	: triplet of triplets (NMR)
X	: halide
μL	: microliter(s)

Abstract

The objectives of the research focus on the bond activation chemistry by iridium porphyrin complexes with three organic substrates, (1) hydrosilanes ($HSiR_3$), (2) fluorobenzenes ($C_6H_nF_{6-n}$, n = 0-6), and (3) aromatic or aliphatic ketones (RCOR, R = alkyl or aryl).

Part I describes the silicon-hydrogen bond activation (SiHA) of silanes with both electron-deficient iridium porphyrin carbonyl chloride (Ir(ttp)Cl(CO)) and electron-rich iridium porphyrin methyl (Ir(ttp)Me) to give iridium(III) porphyrin silyls ($Ir(ttp)SiR_3$). Firstly, $Ir(ttp)SiR_3$ were synthesized in moderate to good yields conveniently from the reactions of Ir(ttp)Cl(CO) and Ir(ttp)Me with silanes, via SiHA in solvent-free conditions and non-polar solvents at 200 °C. Base facilitated the SiHA reaction even at lower temperature of 140 °C. Specifically, K_3PO_4 accelerated the SiHA with Ir(ttp)Cl(CO), while KOAc promoted the SiHA by Ir(ttp)Me. Mechanistic experiments suggest that Ir(ttp)Cl(CO) initially forms iridium porphyin cation ($Ir(ttp)^+$), which then reacts with silanes likely via heterolysis to give iridium porphyrin hydride (Ir(ttp)H). Ir(ttp)H further reacts with silanes to yield $Ir(ttp)SiR_3$. On the other hand, Ir(ttp)Me and $Ir(ttp)SiR_3$ undergo either oxidative addition (OA) or sigma-bond metathesis (SBM) to form the products. In the presence of base, a penta-coordinated silicon hydride species likely forms and reacts with Ir(ttp)Me to form iridium porphyin anion ($Ir(ttp)^-$) that can further react with silane to yield Ir(ttp)H after protonation. Ir(ttp)H finally reacts with excess silane to give $Ir(ttp)SiR_3$.

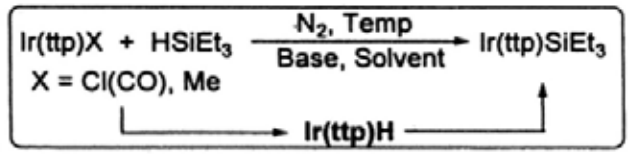

Part II describes successful base promoted aromatic carbon-fluorine (C-F) and carbon-hydrogen (C-H) bond activation of fluorobenzenes in neat conditions to give the corresponding iridium(III) porphyrin aryls (Ir(ttp)Ar) at 200 °C in up to 95% yield. Mechanistic studies suggested that $Ir(ttp)SiEt_3$ is firstly converted to $Ir(ttp)^-$ in the presence of KOH. $Ir(ttp)^-$ cleaves the aromatic C-F bond via an S_NAr process. As the reaction proceeds, a hydroxide anion can coordinate to the iridium center of Ir(ttp)Ar to form an iridium porphyrin trans aryl hydroxyl anion (*trans*-$[ArIr(ttp)OH]^-$). In the presence of water, *trans*-$[ArIr(ttp)OH]^-$ can give Ir(ttp)OH and ArH. Ir(ttp)OH then undergoes aromatic C-H bond activation reaction to give Ir(ttp)Ar'. Furthermore, the aromatic C-F bond activation products were found as the kinetic products, and aromatic C-H bond activation products were the thermodynamic ones.

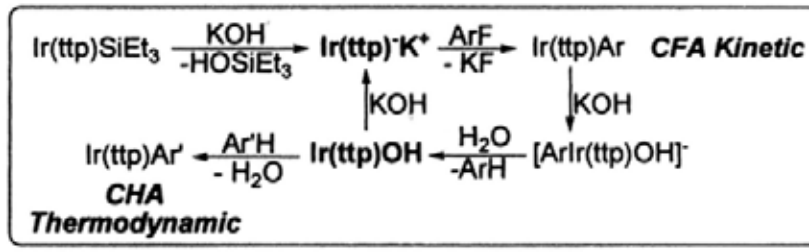

Part III describes the successful C(C=O)-C(α) bond activation of acetophenones by high-valent iridium porphyrin complexes (Ir(ttp)X, X = Cl(CO), $(BF_4)(CO)$, Me) in solvent-free conditions at 200 °C to give the corresponding iridium porphyrin benzoyls (Ir(ttp)COAr) in up to 92% yield. Mechanistic studies suggest that Ir(ttp)X reacts with acetophenones to give α-CHA product as the primary product, which can re-convert back to the active intermediate Ir(ttp)OH or Ir(ttp)H in the presence of

water formed from the concurrent iridium-catalyzed aldol condensation of acetophenones. Then Ir(ttp)OH cleaves the aromatic C-H bonds to produce the aromatic CHA products, which are more thermally stable than the α-CHA product. Both Ir(ttp)H and Ir(ttp)OH were the possible intermediates to cleave the C(C=O)-C(α) bond to give thermodynamic products of Ir(ttp)COAr. On the other hand, only Ir(ttp)(BF_4)(CO) can react with the aliphatic ketones, likely due to the stronger Lewis acidity and the HBF_4 generated in catalyzing the aldol condensation of aliphatic ketones to facilitate the formation of Ir(ttp)OH and Ir(ttp)H.

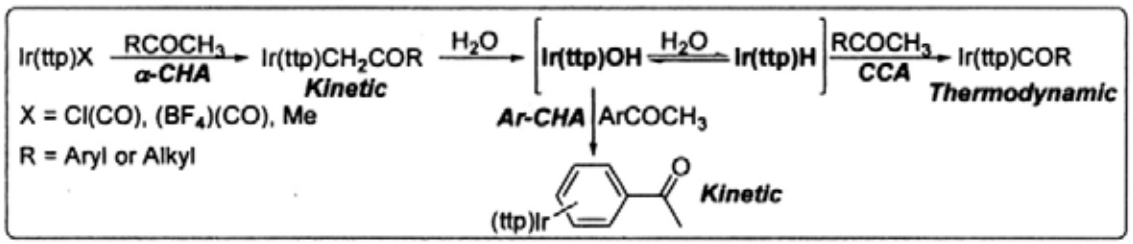

摘要

本論文主要研究了銥卟啉絡合物在鍵的活化中的應用，包括三類有機分子，有機矽烷（$HSiR_3$），氟代苯衍生物（$C_6H_nF_{6-n}$，n = 0-6）以及芳香酮和脂肪酮（RCOR，R = 芳基或烷基）。

第一部分主要介紹了缺電子的銥卟啉羰基氯絡合物（Ir(ttp)Cl(CO)）以及多電子的銥卟啉甲基絡合物（Ir(ttp)Me）與有機矽烷的反應，通過矽-氫鍵活化得到相應的銥卟啉矽烷基絡合物（$Ir(ttp)SiR_3$）。首先，在 200 °C，非溶劑或非極性溶劑的條件下，Ir(ttp)Cl(CO)或 Ir(ttp)Me 與有機矽烷反應，通過矽-氫鍵活化可以方便的得到中等產率或高產率的銥卟啉矽烷基絡合物。在低溫條件下，比如 140 °C，添加鹼可以促進矽-氫鍵的活化。具體來說，磷酸鉀（K_3PO_4）可以加速 Ir(ttp)Cl(CO)與有機矽烷反應時的矽-氫鍵活化，而醋酸鉀（KOAc）則有效的提高 Ir(ttp)Me 與有機矽烷反應時的矽-氫鍵活化的速度。對其機理的研究表明，首先，Ir(ttp)Cl(CO)形成銥卟啉絡合正離子（$Ir(ttp)^+$），然後 $Ir(ttp)^+$與有機矽烷反應，通過異裂產生銥卟啉絡合氫化物（Ir(ttp)H）。Ir(ttp)H 繼續和有機矽烷反應產生相應的銥卟啉矽烷基絡合物作爲最終產物。另外，Ir(ttp)Me 或 $Ir(ttp)SiR_3$ 與有機矽烷反應，可以通過氧化加成（OA）或者 σ-鍵交換（SBM）得到相應的銥卟啉矽烷基絡合物。在添加鹼的條件下，有機矽烷首先與鹼反應，形成五配位的矽氫絡合物，然後再與 Ir(ttp)Me 反應，得到銥卟啉絡合負離子（$Ir(ttp)^-$），$Ir(ttp)^-$繼續與有機矽烷反應，經過質子化作用產生 Ir(ttp)H。最終 Ir(ttp)H 與過量的有機矽烷反應得到 $Ir(ttp)SiR_3$。

第二部分主要描述了在 200 °C，非溶劑的條件下，鹼性添加劑成功的促進了氟代苯衍生物的芳香族碳-氟（C-F）鍵跟碳-氫（C-H）鍵的活化，得到了相應的

銥卟啉芳基絡合物（Ir(ttp)Ar），產率最高可達 95%。對其機理的研究表明，銥卟啉三乙基矽烷絡合物（Ir(ttp)$SiEt_3$）在添加氫氧化鉀（KOH）的條件下，首先形成 Ir(ttp)$^-$。Ir(ttp)$^-$直接與氟代苯衍生物反應，通過親核性芳香取代（S_NAr）斷裂芳香族 C-F 鍵。隨著反應的進行，氫氧根離子（^-OH）與銥卟啉芳基絡合物的銥金屬中心配位，形成反式銥卟啉芳基羥基絡合負離子（*trans*-[ArIr(ttp)OH]$^-$）。在有水的條件下，*trans*-[ArIr(ttp)OH]$^-$可以與水反應，得到銥卟啉羥基絡合物（Ir(ttp)OH）以及相應的芳香烴化合物。然後 Ir(ttp)OH 與過量的氟代苯衍生物繼續反應，通過芳香族 C-H 鍵的活化產生銥卟啉含氟芳基絡合物（Ir(ttp)Ar'）。此外，我們發現，芳香族 C-F 鍵活化的產物是動力學的產物，而芳香族 C-H 鍵活化的產物則是熱力學的產物。

第三部分闡述了高價銥卟啉絡合物（Ir(ttp)X，X = Cl(CO), (BF_4)(CO)或 Ir(ttp)Me）與苯乙酮衍生物的反應。在 200 °C，非溶劑的條件下，成功的斷裂羰基碳及 α-碳（C(C=O)-C(α)）鍵，得到相應的銥卟啉苯醯基絡合物，產率最高可達 92%。對其機理的研究表明，Ir(ttp)X 與苯乙酮衍生物進行反應，產生相應的 α-碳氫鍵活化的產物作爲一級產物。同時，銥卟啉絡合物可以催化苯乙酮衍生物的醇醛縮合反應，產生水。在有水的條件下，α-碳氫鍵活化的產物可以重新形成活性中間體 Ir(ttp)OH 或者 Ir(ttp)H。然後，Ir(ttp)OH 繼續與苯乙酮反應，斷裂苯環上的芳香族 C-H 鍵，產生芳香族 C-H 鍵活化的產物，這些芳香族碳氫鍵活化的產物比 α-碳氫鍵活化的產物在熱力學上更穩定。Ir(ttp)H 和 Ir(ttp)OH 都有可能是斷裂 C(C=O)-C(α)鍵的活性中間體，從而產生熱力學穩定的銥卟啉苯醯基絡合物（Ir(ttp)COAr）。另外，只有 Ir(ttp)(BF_4)(CO)能夠與脂肪酮進行反應，這可能是因爲 Ir(ttp)(BF_4)(CO)具有很強的 Lewis 酸性，並通過 α-碳氫鍵的活化形成強酸

性的 HBF_4，催化脂肪酮的醇醛縮合反應形成水，從而促進 Ir(ttp)OH 和 Ir(ttp)H 的形成。

Chapter 1 General Introduction

1.1 Macrocycle Ligands (Schiff Base, Phthalocyanine and Porphyrin)

Bulky ligands can protect the periphery of the metal complexes from external attack and also can impose the coordination numbers or geometrical constraints to stabilize the metal complexes.[1] Macrocycles provide a unique platform for organometallic chemistry.

1.1.1 Schiff Base

A Schiff base (or azomethine) is a functional group that contains a carbon-nitrogen double bond with the nitrogen atom connected to an aryl or alkyl group. The general formula of a Schiff base is $R_1R_2C=N-R_3$, where R_3 is an aryl or alkyl group that makes the Schiff base a stable imine. Schiff bases can be generated from an amine and a carbonyl compound by condensation. Figure 1.1 shows some examples of Schiff bases. Schiff bases metal complexes are a class of compounds that have been studied extensively because of their attractive chemical and physical properties, and their wide-ranging applications in numerous scientific areas.[2] In addition, as a kind of imines, Schiff base played a high reactivity towards organic reactions.[3] However, the synthesis of Schiff base suffers from drawbacks including low yield, long reaction time and difficult work-up.[4] The labile imine functionality imposes acid and base lability.

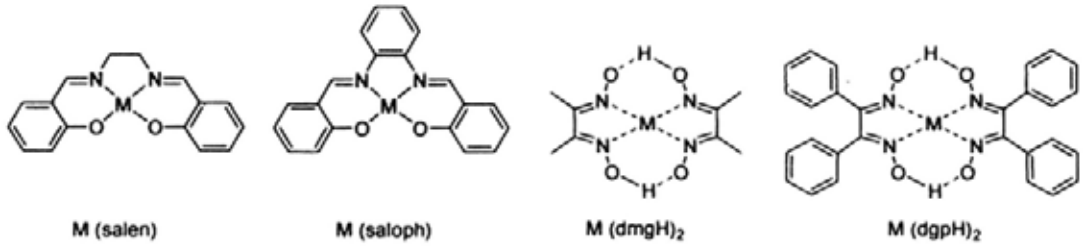

Figure 1.1 Structures of metal Schiff base

1.1.2 Phthalocyanine

A phthalocyanine (pc) is a symmetrical macrocyclic compound with an alternating nitrogen-carbon ring structure (Figure 1.2), and exhibits aromatic behavior owing to its planar conjugated array of 18 π-electrons.[5] Pc can coordinate hydrogen and various metal cations in its center by coordinate bonds with the four isoindole nitrogen atoms. Besides well known as dyes, pcs have also been utilized for photoconductor, nonlinear optical applications and supramolecular chemistry,[6] but the poor solubility of metallophthalocyanines and the difficulties of functionalization limit their applications.[7]

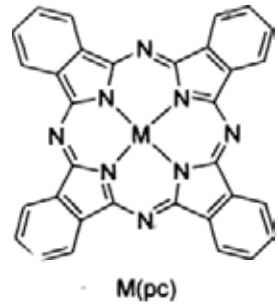

Figure 1.2 Structure of metallophthalocyanine

1.1.3 Porphyrin

Porphyrins (por) are heterocyclic macrocycles characterized by the presence of four modified pyrrole subunits interconnected at α carbon atoms via methine bridges (=CH-) (Figure 1.3). Porphyrins are aromatic with 18 π-electrons that are delocalized

in the inner 16-membered ring. Therefore, porphyrins are highly-conjugated system and consequently are deeply colored.[8-11]

Porphyrins can form very stable tetradentate chelated metal complexes by replacement of two inner pyrrole protons with metal ions, usually with a charge of +2 or +3. Metallopophyrins are important as model compounds for understanding the chemical reactivities and relationships of several biologically important macromolecules.[12] Porphyrins can also be applied in a variety of reactions in organic chemistry,[13] and porphyrin-based compounds are of interest in molecular electronics and supramolecular building blocks.[6c,14] Comparing with other macrocycles, porphyrins present an extra stability, and are more easily accessible and tamable, therefore, the properties of metalloporphyrins are easily modified.[15]

M(por)

Figure 1.3 Structure of metalloporphyrin

1.2 Metalloporphyrins (Co, Rh, Ir)

The Chan's group has a continuing interests in the chemistry of metalloporphyrins,[16] so the porphyrin ligands are the focus in this work. Table 1.1 summarizes a SciFinder Scholar search of the group 9 metal macrocycles publications from 1965 to 2009 September. We can see that among group 9 metal porphyrin complexes, iridium porphyrins are less studied comparing with the cobalt and

rhodium porphyrins.

Table 1.1 Summary of Publications of Metallomacrocycles (SciFinder Search Data, Accessd in September, 2009)

M	salen	saloph	Pc	Porphyrin
Co	308	74	2356	1071
Rh	5	5	39	197
Ir	5	0	5	26
Total	318	79	2400	1294

1.2.1 Properities of Iridium Porphyrin Complexes

Comparing with Co and Rh porphyrin complexes, Ir porphyrins are more stable and less reactive due to the stronger Ir-H and Ir-C and Ir-Ir bonds than that of Co and Rh.[17] (Table 1.2 and Table 1.3)

Table 1.2 Bond Dissociation Enthalpies of M(oep)X (kcal mol^{-1})[17]

M-X	Co	Rh	Ir
M-H	52 ± 2	61 ± 1	70 ± 2
M-Me	41 ± 2	58 ± 1	62 ± 2

Table 1.3 Metal-Metal Bond Dissociation Energies[17]

M^{II}(por) (d^7)	$\Delta H_f^{\neq}$ (kcal mol $^{-1}$)	$\Delta H^{\cdot}$ (kcal mol $^{-1}$)
Co(por)	momomers (s = 1/2)	
$[Rh(oep)]_2$	18.5	15.5
$[Ir(oep)]_2$	26	23
$[Rh(txp)]_2$	15	12
$[Ir(txp)]_2$	23	20
Rh(tmp)	monomers (s = 1/2)	
$[Ir(tmp)]_2$	<10	
Ir(ttipp)	monomers (s = 1/2)	

1.2.2 Bond Activation by Iridium Porphyrin Complexes

Although the bond activations by iridium porphyrins are rare, some successful examples related have been reported in Chan's group.[18, 19]

Benzylic Carbon-Hydrogen Bond Activation of Toluenes[18]

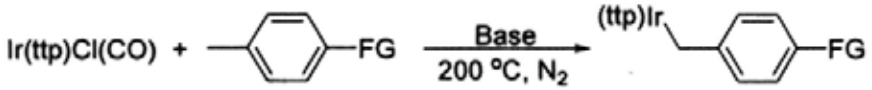

FG = Me, H, F, NO_2
Base = K_2CO_3, NaOPh

up to 80%

Aldehydic Carbon-Hydrogen Bond Activation of Aldehydes[19]

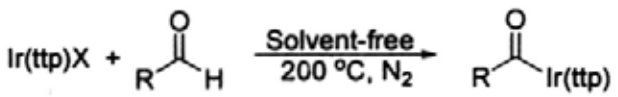

X = Cl(CO), Me
R = Ar, Alkyl

up to 92%

1.3 Scope of Thesis

The objectives of the research focus on the studies of the reactivity of iridium(III) porphyrin complexes towards bond activation chemistry involving

(1) silicon-hydrogen bond activation of silanes

(2) base-promoted competitive aromatic carbon-fluorine and carbon-hydrogen bond activation of fluorobenzenes

(3) carbon (C=O)-carbon (α) bond activation of ketones

References

(1) DeWit, D. G. *Coord. Chem. Rev.* **1996**, *147*, 209-246.

(2) (a) Leung, A. C. W.; MacLachlan, M. J. *J. Inorg. Organomet. Polym. Mater.* **2007**, *17*, 57-89. (b) Alexander, V. *Chem. Rev.* **1995**, *95*, 273-342.

(3) Layer, R. W. *Chem. Rev.* **1963**, *63*, 489-510.

(4) Keypour, H.; Rezaeivala, M.; Fall, Y.; Dehghani-Firouzabadi, A. A. *Solvent-Free Synthesis of Some N_4O_2, N_4S_2 and N_6 Schiff Base Lligands Assisted by Microwave Irradiation.* ARKIVOC, **2009**, *X*, 292-301.

(5) Claessens, C. G.; Blau, W. J.; Cook, M.; Hanack, M.; Nolte, R. J. M.; Torres, T.; Wöhrle, D. *Monatsh. Chem.* **2001**, *132*, 3-11.

(6) (a) Inabe, T.; Tajima, H. *Chem. Rev.* **2004**, *104*, 5503-5533. (b) de la Torre, G.; Vázquez, P.; Agulló-López, F.; Torres, T. *Chem. Rev.* **2004**, *104*, 3723-3750. (c) Beletskaya, I.; Tyurin, V. S.; Tsivadze, A. Y.; Guilard, R.; Stern, C. *Chem. Rev.* **2009**, *109*, 1659-1713.

(7) (a) Wang, B.; Zuo, X.; Wu, Y.; Chen, Z.; Li, Z. *Mater. Lett.* **2005**, *59*, 3073-3077. (b) Ingrosso, C.; Curri, M. L.; Fini, P.; Giancane, G.; Agostiano, A.; Valli, L. *Langmuir* **2009**, *25*, 10305-10313. (c) Chen, X.; Thomas, J.; Gangopadhyay, P.; Norwood, R. A.; Peyghambarian, N.; McGrath, D. V. *J. Am. Chem. Soc.* **2009**, *131*, 13840-13843.

(8) Fleischer, E. B. *Acc. Chem. Res.* **1970**, *3*, 105-112.

(9) Ogoshi, H.; Mizutani, T. *Acc. Chem. Res.* **1998**, *31*, 81-89.

(10) Kadish, K. M.; Smith, K. M.; Guilard, R. *The Porphyrin Handbook Volumn 3*, Eds.; Academic Press: Boston, 2000.

(11) Smith, K. M. *Porphyrins and Metalloporphyrins*, Ed.; Elservier Scientific Pub. Co.: New York, 1975.

(12) (a) Schrauzer, G. N. *Angew. Chem. Int. Ed. Engl.* **1976**, *15*, 417-426. (b) Schrauzer, G. N. *Acc. Chem. Res.* **1968**, *1*, 97-103.

(13) (a) Nam, W. *Acc. Chem. Res.* **2007**, *40*, 522-531. (b) Xia, Q.-H.; Ge, H.-Q.; Ye, C.-P.; Liu, Z.-M.; Su, K.-X. *Chem. Rev.* **2005**, *105*, 1603-1662. (c) Li, S.; Sarkar, S.; Wayland, B. B. *Inorg. Chem.* **2009**, *48*, 8550-8558. (d) Zhang, J.; Li, S.; Fu, X.; Wayland, B. B. *Dalton Trans.* **2009**, 3661-3663. (e) Fu, X.; Li, S.; Wayland, B. B. *J. Am. Chem. Soc.* **2006**, *128*, 8947-8954.

(14) Oliveri, C. G.; Ulmann, P. A.; Wiester, M. J.; Mirkin, C. A. *Acc. Chem. Res.* **2008**, *41*, 1618-1629.

(15) (a) Shinokubo, H.; Osuka, A. *Chem. Commun.* **2009**, 1011-1021. (b) Kadish, K. M.; Smith, K. M.; Guilard, R. *The Porphyrin Handbook Volumn 1*, Eds.;

Academic Press: Boston, 2000.

(16) (a) Chan, Y. W.; Chan, K. S. *Organometallics* **2008**, *27*, 4625-4635. (b) Chan, K. S.; Li, X. Z.; Dzik, W. I.; de Bruin, B. *J. Am. Chem. Soc.* **2008**, *130*, 2051-2061. (c) Chan, K. S.; Mak, K. W.; Tse, M. K.; Yeung, S. K.; Li, B. Z.; Chan, Y. W. *J. Organomet. Chem.* **2008**, *693*, 399-407. (d) Song, X.; Chan, K. S. *J. Chin. Chem. Soc.* **2009**, *56*, 667-670.

(17) Wayland, B. B. Temple University, Philadelphia, PA. Personal communication, 2007.

(18) Cheung, C. W.; Chan, K. S. *Organometallics* **2008**, *27*, 3043-3055.

(19) Song, X.; Chan, K. S. *Organometallics* **2007**, *26*,965-970.

Chapter 2 Base-Promoted Silicon-Hydrogen Bond Activation (SiHA) by Iridium Porphyrin (por) Complexes

2.1 Introduction

2.1.1 Properties of Silanes

Silane is the silicon analogue of methane with chemical formula SiH_4. As silicon atom (1.9) is less electronegative than both carbon (2.5) and hydrogen (2.1),[1] the polarity of the Si-H bond is opposite to that of C-H bond.[2] Comparing with carbon atom (5.3 cm^3 mol^{-1}), silicon atom has a larger size (12.1 cm^3 mol^{-1}),[3] therefore the Si-H bond is longer than C-H bond, which more easily undergoes nucleophilic attack.[4] A Si-H bond is considered mostly covalent, since charge separation in Si-H bond is not as great as other ionic hydrides. However, the Si-H bond is stronger than corresponding C-H bond for selected silanes and hydrocarbons. Table 2.1 shows the selected bond dissociation energy (BDE) of silanes.[5]

Table 2.1 Selected BDE of Si-H and C-H in Silanes and Hydrocarbons

Silane	BDE_{Si-H} / kcal mol^{-1}	Hydrocarbon	BDE_{C-H} / kcal mol^{-1}
$H-SiEt_3$	94.6	$H-CEt_3$	---
$H-SiPh_2Me$	86.3	$H-CPh_2Me$	82.8
H-SiHPhMe	91.3	H-CHPhMe	85.4
$H-SiHPh_2$	90.6	$H-CHPh_2$	84.5
$H-SiH_2Ph$	91.3	$H-CH_2Ph$	88.5

The reaction of hydrosilanes with transition-metal can proceed to give a "classical" (two-center, two-electron) or a "nonclassical" (three-center, two-electron) interaction (Scheme 2.1).[6] The orbital interactions between the Si-H unit and the metal center are illustrated in Figure 2.1. A σ-interaction can exist between a metal *d*-orbital and the Si-H σ-bonding orbital (Figure 2.1a). A π-component may arise when a metal dπ-orbital interacts with the Si-H σ*-antibonding orbital (Figure 2.1b).[7] The greater basicity of the Si-H bond relative to the H-H or C-H bond makes the Si-H unit a better σ-donor.[8]

Scheme 2.1

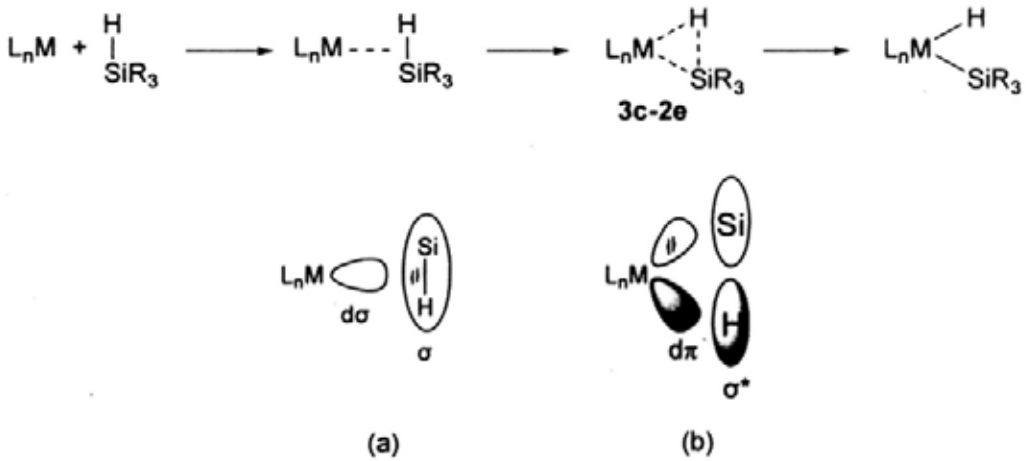

Figure 2.1 (a) M-(η^2-HSi) σ-bonding interaction; (b) M-(η^2-HSi) π-back-bonding interaction

2.1.2 Properties of Transition Metal Silyls

In 1956, the first transition-metal silyl derivative $Cp(CO)_2FeSiMe_3$ (Cp = η^5-C_5H_5) was prepared by Wilkinson and co-workers.[9] Stimulated by the discovery of the transition-metal catalyzed hydrosilation of olefins, further interest in transition-metal-silicon bonded compounds grew.[10]

Metal-silicon bond distances are commonly shorter than expected for single covalent bonds (Table 2.2).[11] These observations have often been attributed to d_π-d_π π-bonding involving donation of d-electron density from the transition metal to empty silicon d orbitals of appropriate symmetry.[12] The greatest difference between the expected and observed M-Si bond distance occurs with late transition metals which display unique structural and bonding properties.[13] Alternatively, it is possible that a $-SiR_3$ group is simply a very strong σ-donor to account for the shorter bonds.

Table 2.2 Selected M-Si Distances in Late Transition-Metal Silyl Complexes

Compound	M-Si Obsvd. / Å	M-Si Calcd. / Å
$(CO)_5MnSiMe_3$	2.497(5)[14]	2.63
π-$Cp(CO)FeH(SiCl_3)_2$	2.252(3)[15]	2.51
$(CO)_4CoSiH_3$	2.381(4)[16]	2.51
$RhHCl(SiCl_3)(PPh_3)_2$	2.203(4)[17]	2.48

2.1.3 Importance of SiHA by Transition Metal Complexes

Silicon-hydrogen bond activation (SiHA) is an important process for catalytic application in organic synthesis.[18-20] Among these reactions, transition metal silyls[18,19] or silylenes[21,22] have been proposed as the active intermediates for the catalytic functionalization of hydrocarbons with transition metal complexes (Scheme 2.2). The preparation of transition metal silyls from the reactions of metal halides with silanes have been extensively utilized,[7a] and Table 2.3 summarized some examples of organic or polymer synthesis involving SiHA reaction.

Scheme 2.2 Metal Silyl or Silylene as Intermediate in Catalytic Reaction

Metal-Silyl[18,19]

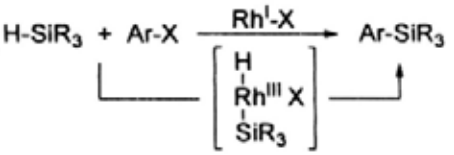

Metal-Silylene[21,22]

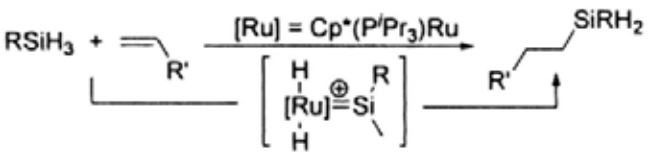

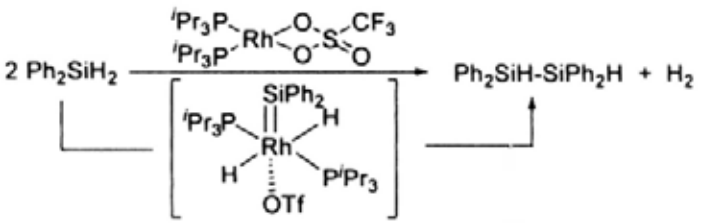

Table 2.3 Application of SiHA in Organic and Polymer Synthesis

Reaction	Example
Arylation[19,20b,23]	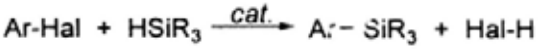
Dehydrogenative Coupling[18]	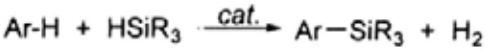
Dehalogenation[20a,24]	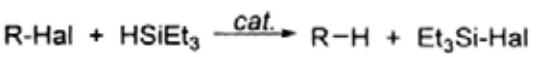
Addition[25]	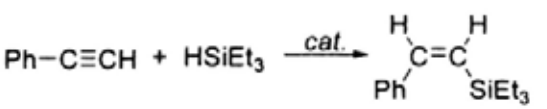
Hydrosilylation[26]	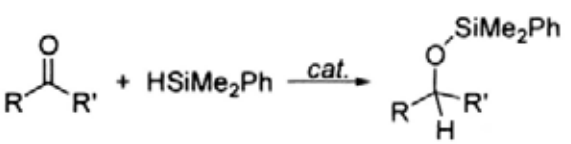
Alkylation of Amine[27]	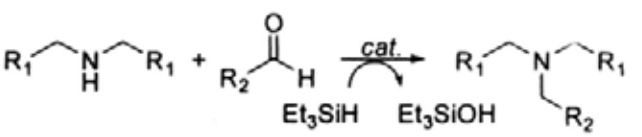

Silane Alcoholysis[28]	$ROH + R'_3SiH \xrightarrow{cat.} RCH_2\text{-}OSiR'_3$
Polymer Synthesis[29]	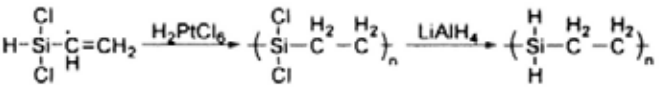

The silicon-hydrogen bond activation with late high valent transition metals such as rhodium (III) or iridium (III) complexes is interesting.[7a,30] So far, the mechanistic possibilities of silicon-hydrogen bonds activation by these late transition metal complexes have been proposed via heterolysis,[31] oxidative addition[30b,32] or sigma-bond metathesis[33](Scheme 2.3). One key supporting evidence for the oxidative addition is the isolation of iridium(V) silyl intermediate that has been characterized by X-ray diffraction (Figure 2.2).[30b,32b]

Scheme 2.3 Possible Pathways for SiHA Reaction

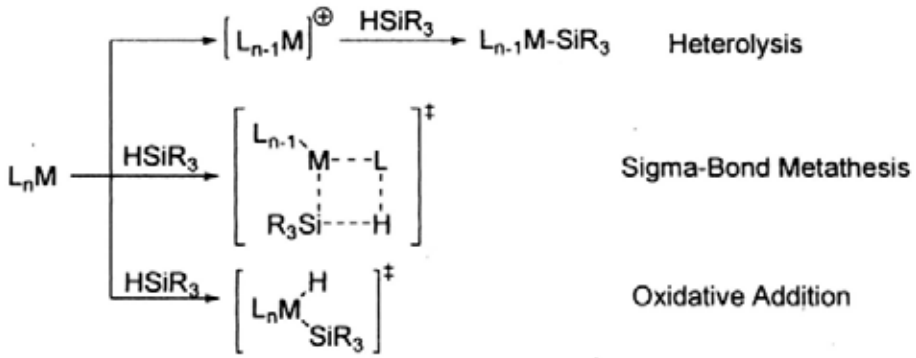

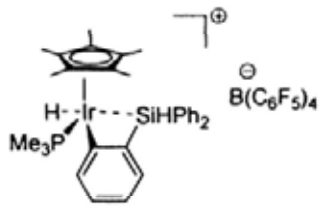

(a)

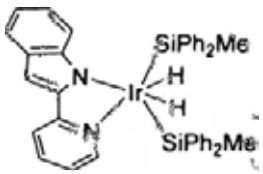

(b)

Figure 2.2 ORTEP diagram of molecular structures for Ir(V) silyl species.

2.1.4 Si-H Bond Activation by Rhodium Porphyrin Complexes

The Chan's group has reported that silicon-hydrogen bonds activation by rhodium(III) porphyrins (por) can provide a facile synthetic route of rhodium silyl complexes.[31a] Rhodium(III) porphyrin halides and methyls react with silanes to give high yields of rhodium porphyrin silyls via silicon-hydrogen bond activation in solvent-free conditions. Rh(por)Cl was proposed to undergo ionization into $Rh(por)^{+}Cl^{-}$, which then undergoes silylation to yield rhodium porphyrin silyls. On the other hand, Rh(por)Me also reacts with silanes via either oxidative addition or sigma-bond metathesis (Scheme 2.4). These reactions are mechanistically puzzling since *cis*-interaction on the same face of a porphyrin by the methyl group and silane could be sterically very demanding.

Scheme 2.4 Mechanisms of SiHA of Silanes with Rh(por)Cl or Rh(por)Me

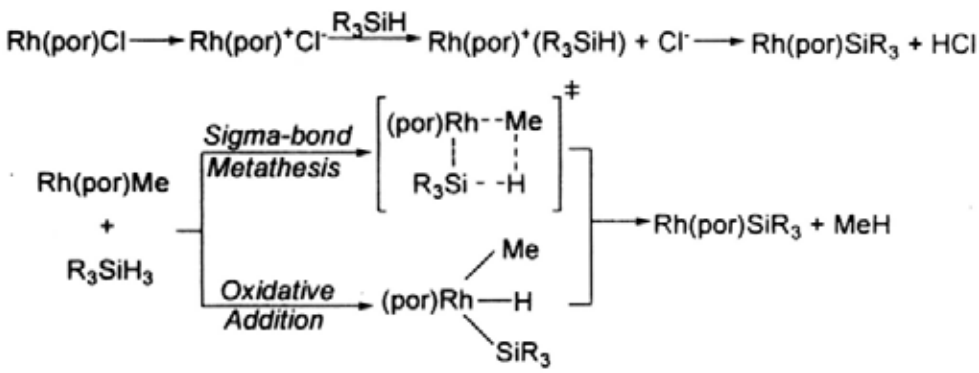

2.1.5 Objective of This Work

The objectives of this work are to broaden the synthetic scope and to gain further mechanistic understanding of these metalloporphyrin-based SiHA.

2.2 Preparation of Iridium Porphyrin Complexes

Tetrakis-4-tolylporphyrin (H_2ttp) **1a** was synthesized by co-tetramerization of pyrrole and 4-tolualdehyde according to the literature method in 20 % yield (eq 2.1).[34]

Iridium tetrakis-4-tolylporphyrin carbonyl chloride (Ir(ttp)Cl(CO)) **1b** was synthesized according to the literature report.[35] Iridium(I) cyclooctadiene chloride dimer $[Ir(COD)Cl]_2$ **1c** was prepared by the reaction of $IrCl_3 \cdot xH_2O$ with 1,5-cyclooctadiene (COD) in 62 % yield (eq 2.2).[36] Metalation of porphyrin ligand **1a** with $[Ir(COD)Cl]_2$ **1c** in refluxing *p*-xylene gave purple solids of $Ir^{III}(ttp)Cl(CO)$ **1b** in 64% yield (eq 2.3).[35]

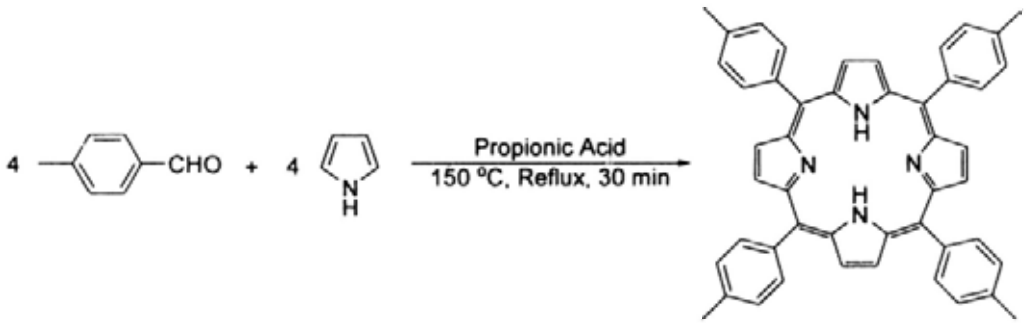

(2.1)

Tetrakis-4-tolylporphyrin H_2ttp **1a** 20 %

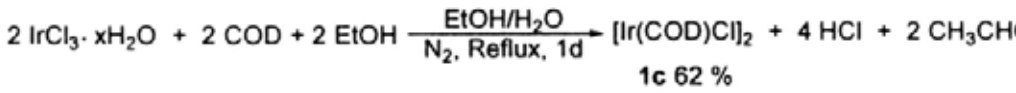

(2.2)

1c 62 %

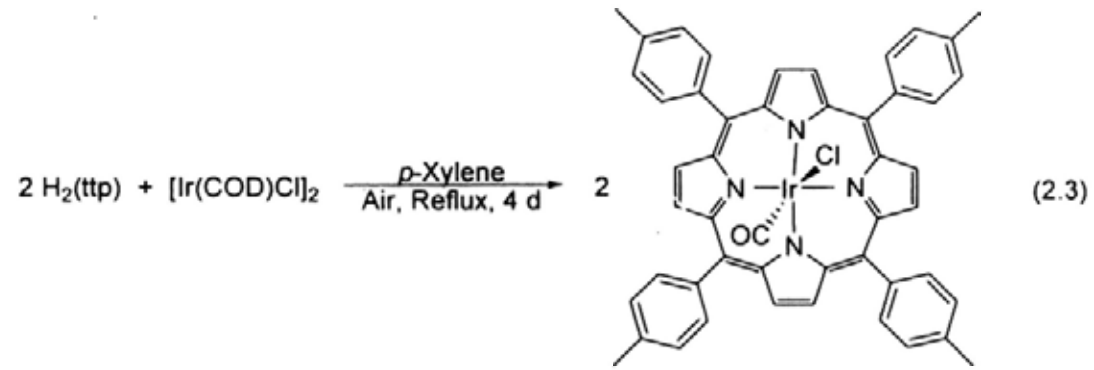

(2.3)

Ir(ttp)Cl(CO) **1b** 64 %

Ir(ttp)H **1d**, $Ir(ttp)(BF_4)(CO)$ **1e** and Ir(ttp)Me **1f** were synthesized according to literature method.[35,37] Ir(ttp)Cl(CO) **1b** was reduced by $NaBH_4$ and then protonated by HCl to give Ir(ttp)H **1d** in 95% yield (eq 2.4).[35b] Ir(ttp)Cl(CO) reacted with $AgBF_4$ in

CH_2Cl_2 at room temperature after 1 day to give a mixture of Ir(ttp)(BF_4) and Ir(ttp)(BF_4)(CO) in 80% yield (Ir(ttp)(BF_4) : Ir(ttp)(BF_4)(CO) = 1:1 to 1:4) (eq 2.5).[37] Ir(ttp)Cl(CO) **1b** was reduced by $NaBH_4$ and then alkylation by MeI to give Ir(ttp)Me **1e** in 75% yield (eq 2.6).[35]

$$\underset{\textbf{1b}}{\text{Ir(ttp)Cl(CO)}} \xrightarrow[\text{2. THF, 70 °C, 2h}\\ \text{3. HCl, 0 °C, 15min}]{\text{1. NaBH}_4\text{ / 1M NaOH}} \underset{\textbf{1d 95\%}}{\text{Ir(ttp)H}} \qquad (2.4)$$

$$\underset{\textbf{1b}}{\text{Ir(ttp)Cl(CO)}} + \text{AgBF}_4 \xrightarrow[1\text{ d}]{\text{rt, CH}_2\text{Cl}_2} \underset{\textbf{1e 80\%}}{\text{Ir(ttp)(BF}_4\text{) / Ir(ttp)(BF}_4\text{)(CO)}} + \text{AgCl} \qquad (2.5)$$

$$\underset{\textbf{1b}}{\text{Ir(ttp)Cl(CO)}} \xrightarrow[\text{2. THF, 70 °C, 2 h}\\ \text{3. MeI, 70 °C, 2 h}]{\text{1. NaBH}_4\text{ / 1 M NaOH}} \underset{\textbf{1f 75\%}}{\text{Ir(ttp)Me}} \qquad (2.6)$$

2.3 Si-H Bond Activation by Iridium Porphyrin Carbonyl Chloride

2.3.1 Optimization of Solvent-Free Conditions

Initially, Ir(ttp)Cl(CO) **1b** reacted with $HSiEt_3$ **2a** in solvent-free conditions at 120 °C (Table 2.4, entry 1). However, only a trace amount of Ir(ttp)$SiEt_3$ **3a** (<5%) was obtained even after 9 days, while Ir(ttp)H **1d** was observed as the major product according to ^{1}H NMR analysis of the crude reaction mixture. At 140 °C, 10% yield of Ir(ttp)$SiEt_3$ **3a** was isolated after 6 days (Table 2.4, entry 2). When the reaction temperature was further increased to 200 °C, after 4.5 hours, Ir(ttp)H was generated as the major product together with Ir(ttp)$SiEt_3$ **3a** isolated in a low yield of 6% (Table 2.4, entry 3). After 4 days, Ir(ttp)$SiEt_3$ **3a** was isolated in 84% yield (Table 2.4, entry 4). Therefore, the temperature of 200 °C was employed for subsequent studies.

Table 2.4 Optimization of the Synthesis of Ir(ttp)$SiEt_3$

Eentry	Temp / °C	Time	**3a** / %
1	120	9 d	<5
2	140	6 d	10
3	200	4.5 h	6
4	200	4 d	84

2.3.2 Synthetic Application

When the optimized solvent-free conditions at 200 °C were applied to the reactions of Ir(ttp)Cl(CO) **1b** with various silanes, moderate to good yields of iridium porphyrin silyl complexes were obtained (Table 2.5, eq 2.7). Ir(ttp)Cl(CO) **1b** dissolved in alkyl substituted silanes only upon heating, but dissolved in aromatic silanes even at room temperature.

The yields of the products depended on the steric hindrance of silanes.[31a] Cone angles obtained from phosphines have been used as a measure of steric hindrance and cone angles of silanes are identical to the corresponding phosphines[38] [H_3SiPh (101 °), $HSi(OEt)_3$ (109 °), H_2SiPh_2 (128 °), $HSiEt_3$ (132 °), $HSiPr_3$ (132 °), $HSiPh_2Me$ (136 °)].[38,39] In general, more bulky silanes with larger cone angles reacted with slower rates and gave lower yields. No SiHA product was found when Ir(ttp)Cl(CO) **1b** reacted with the more hindered $HSiPr_3$ or HSi^tBuMe_2. However, the rate of SiHA was also dependent on the solubility of Ir(ttp)Cl(CO) **1b** in silane. A better solvent, such as $H_2SiPhMe$, or $HSiPhMe_2$, gave a faster rate (Table 2.5, entries 5 and 7), while a poor solvent such as $HSiEt_3$ gave a slower rate (Table 2.5, entry 1).

Table 2.5 Solvent-Free SiHA of Silanes by Ir(ttp)Cl(CO)

$$\underset{\textbf{1b}}{Ir(ttp)Cl(CO)} + \underset{\textbf{2a-g}}{HSiR_1R_2R_3} \xrightarrow[Time]{N_2,\ Temp} \underset{\textbf{3a-g}}{Ir(ttp)SiR_1R_2R_3} \quad (2.7)$$

Entry	$HSiR_1R_2R_3$	Temp / °C	Time	Product (yield / %)
1	$HSiEt_3$ **2a**	200	4 d	$Ir(ttp)SiEt_3$ **3a** (84)
2	$HSi(OEt)_3$ **2b**	200	6 h	$Ir(ttp)Si(OEt)_3$ **3b** (54)
3	$HSiBnMe_2$ **2c**	200	1 d	$Ir(ttp)SiBnMe_2$ **3c** (78)
4	H_3SiPh **2d**	140	5 h	$Ir(ttp)SiPhH_2$ **3d** (90)
5	$H_2SiPhMe$ **2e**	200	0.5 h	Ir(ttp)SiPhMeH **3e** (34)
6	H_2SiPh_2 **2f**	140	2 d	$Ir(ttp)SiPh_2H$ **3f** (68)
7[a]	$HSiPh_2Me$ **2g**	200	6 h	$Ir(ttp)SiPh_2Me$ **3g** (42)

[a] 30% yield of Ir(ttp)SiPhMeH **3e** was also generated according to ^1H NMR analysis of the crude reaction mixture.

Iridium porphyrin silyls are thermally stable when the silyl group is tri-substituted. However, the mono-substituted $Ir(ttp)SiPhH_2$ **3d** decomposed at 200 °C even in a nitrogen atmosphere. Therefore, the reaction of Ir(ttp)Cl(CO) **1b** and H_3SiPh **2d** was carried out at a lower temperature of 140 °C (Table 2.5, entry 4). $Ir(ttp)SiPhH_2$ **3d** and Ir(ttp)SiPhMeH **3e** could not be purified by column chromatography on alumina or recrystallization from CH_2Cl_2/MeOH. However, these two complexes could be purified simply by washing off the impurities with methanol under N_2.

For $HSiPh_2Me$ **2g** only, besides the SiHA reaction, silicon-carbon bond activation (SiCA) was also observed. When **2g** reacted with Ir(ttp)Cl(CO) **1b** at 200

°C, according to ^{1}H NMR analysis Ir(ttp)H initially formed. Then both the SiHA product **3g** and SiCA product **3e** were generated slowly and simultaneously in the ratio of 1.00 to 1.15 with the slow disappearance of Ir(ttp)H (Figure 2.3). In addition, Ir(ttp)H also reacted with $HSiPh_2Me$ to generate both **3g** and **3e** at 200 °C in about 1.00 to 0.71 ratio (Figure 2.4), which suggested that Ir(ttp)H was the intermediate for the parallel formation of both **3g** and **3e** in the reaction of **1a** and **2g** at 200 °C.

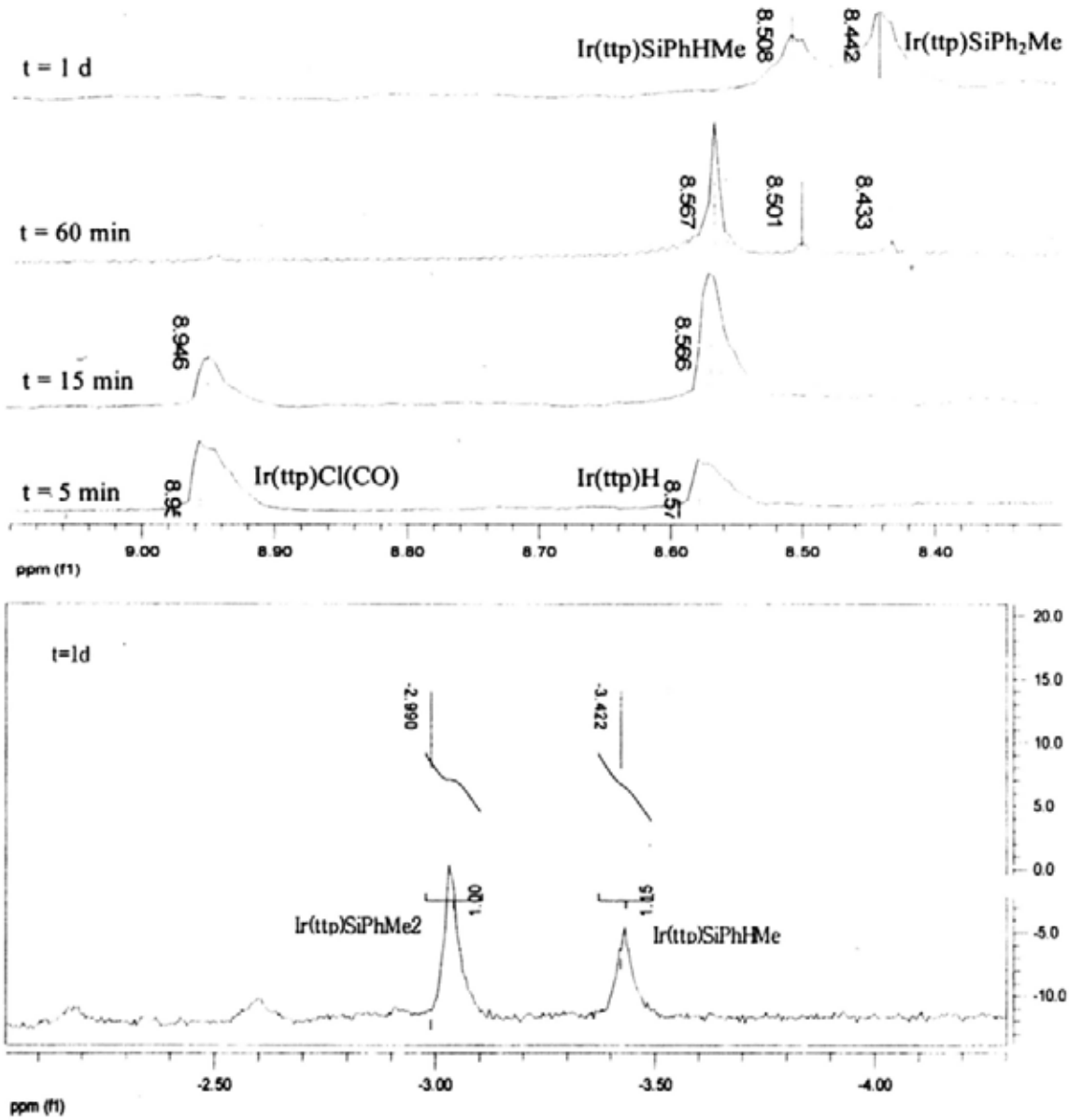

Figure 2.3 Partial ^{1}H NMR spectra for reaction sequence between Ir(ttp)Cl(CO) **1b** and $HSiPh_2Me$ **2g**

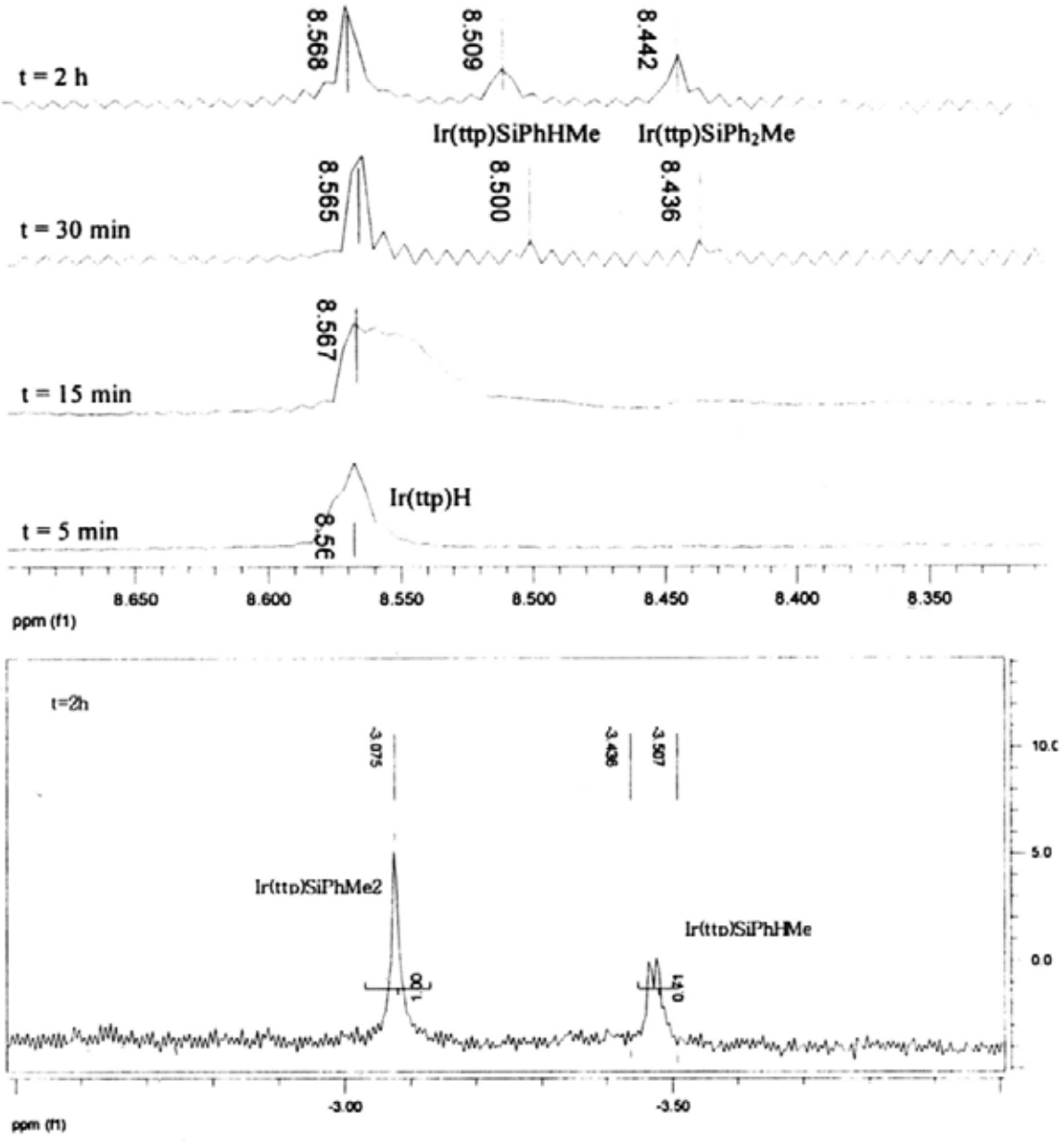

Figure 2.4 Partial ^{1}H NMR spectra for reaction sequence between Ir(ttp)H **1d** and $HSiPh_2Me$ **2g**

2.3.3 Base-Promoted Si-H Bond Activation

Yamanoi and his coworker reported that a base, especially K_3PO_4 can promote catalysis of a SiHA reaction.[19] Chan's group also found that 2,6-dimethylpyridine can increase the rate of SiHA of Rh(ttp)X (X = Cl and OTf) and $HSiEt_3$.[31a] Therefore the possibility of base-promoted SiHA was examined.

Table 2.6 Base-Promoted SiHA of $HSiEt_3$ in Solvent-Free Conditions

$$\underset{\textbf{1b}}{Ir(ttp)Cl(CO)} + \underset{\textbf{2a}}{HSiEt_3} \xrightarrow[\text{Temp, Time}]{\text{n equiv Base, } N_2} \underset{\textbf{3a}}{Ir(ttp)SiEt_3} \quad (2.8)$$

Entry	Base	n	Temp / °C	Time / d	**3a** / %
1	none	0	200	4	84
2	none	0	140	6	10
3	K_3PO_4	5	140	1	46
4	K_3PO_4	10	140	1	88
5	K_3PO_4	20	140	1	80
6	K_2CO_3	10	140	1	16
7	KOH	10	140	1	37
8	KF	10	140	5	50
9	CsCl	10	140	6	<5
10	KI	10	140	5	14
11	KOAc	10	140	5	12

Table 2.6 and eq 2.8 show the successful results of base-promoted SiHA reaction of Ir(ttp)Cl(CO) **1b** and $HSiEt_3$ **2a** in solvent-free conditions. Addition of 5 equivalents of K_3PO_4 enhanced the reaction rate and yield slightly (Table 2.6, entries 3 and 2), while addition of 10 equivalents of K_3PO_4 enhanced the reaction rate and yield remarkably even at a lower temperature of 140 °C (Table 2.6, entry 4). However, the addition of 20 equivalents of K_3PO_4 decreased the reaction yield slightly (Table 2.6, entry 5), and this may be due to the decomposition of intermediates or the

occurrence of side-reaction caused by excess base. The optimal amount of K_3PO_4 was therefore found to be 10 equivalents.

We further screened other salts with anions of different basicity and nucleophilicity of anion in the reaction of Ir(ttp)Cl(CO) and $HSiEt_3$. The p*K*a values for conjugated acids have been used to compare the basicities of anions [H_2O (15.7) > HPO_4^{2-} (12.32) > HCO_3^- (10.3) > HOAc (4.76) > HF (3.17) > HCl (-8.0) > HI (<-9.0)].[40] In general, a stronger base can promote SiHA of silane effectively (Table 2.6, entries 4 and 7). However, the very strong base such as KOH gave lower product yield, which was likely due to base-promoted decomposition of either the intermediate or the product.[41]

2.3.4 Si-H Bond Activation in Solvent Conditions

Chan's group have reported that the SiHA of silanes with rhodium porphyrin complexes should be carried out in solvent-free conditions due to the competitive activation of solvent, such as benzene and dichloromethane.[31a] However, iridium porphyrin complexes appeared to be less reactive towards solvents. So the SiHA reaction was carried out in a non-polar solvent, such as benzene or cyclohexane.

Table 2.7 and eq 2.9 show the results of SiHA of silanes by Ir(ttp)Cl(CO) **1b** in benzene and cyclohexane. For $HSiEt_3$ **2a**, the reaction rate was slower than that in neat solvent-free conditions as expected by the lower concentration of **2a** used (Table 2.7, entries 1 and 2 vs Table 2.5, entry 1). The lower yielding reaction of **3a** is likely due to the poor reactivity of **2a**. However, a higher yield was obtained for $HSi(OEt)_3$ **2b** even in a solvent (Table 2.7, entries 3 and 4 vs Table 2.5, entry 2). The faster rate

and higher yield may be due to the better solubility of Ir(ttp)Cl(CO) in solvent and the higher reactivity of $HSi(OEt)_3$. Therefore, benzene and cyclohexane were both suitable solvents for this reaction. Ir(ttp)Cl(CO) **1b** also underwent rate-enhanced SiHA in benzene in the presence of K_3PO_4 (eq 2.10).

Table 2.7 SiHA of Silanes by Ir(ttp)Cl(CO)

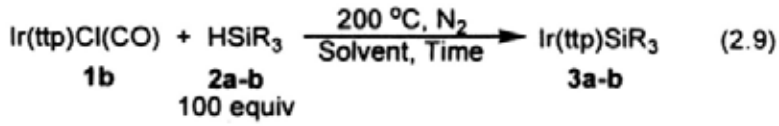

Entry	$HSiR_3$	Solvent	Time	Product (yield / %)
1	$HSiEt_3$ **2a**	Benzene	9 d	$Ir(ttp)SiEt_3$ **3a** (58)
2	$HSiEt_3$ **2a**	Cyclohexane	9 d	$Ir(ttp)SiEt_3$ **3a** (60)
3	$HSi(OEt)_3$ **2b**	Benzene	6 h	$Ir(ttp)Si(OEt)_3$ **3b** (85)
4	$HSi(OEt)_3$ **2b**	Cyclohexane	12 h	$Ir(ttp)Si(OEt)_3$ **3b** (88)

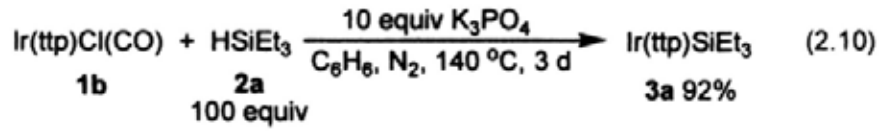

2.3.5 Mechanistic Study of Si-H Bond Activation by Ir(ttp)Cl(CO)

Scheme 2.5 illustrates the proposed mechanism for the SiHA. Initially, Ir(ttp)Cl(CO) ionizes into $Ir(ttp)^+Cl^-$ upon heating. This step is supported by the rate-enhanced reaction with $Ir(ttp)(BF_4)(CO)$[37] **1e** bearing a more labile anion. At 200 °C, Ir(ttp)Cl(CO) required 4 days to give $Ir(ttp)SiEt_3$ in 84% yield (Table 2.5, entry 1). $Ir(ttp)(BF_4)(CO)$ only took 1 day to complete the reaction to produce 61% yield of **3a** (eq 2.11). The slightly lower yield may be caused by the lower stability of **1e** at high

temperature.[37] Then Ir(ttp)$^+$ forms a silane complex **A** which reacts to give the observed intermediate Ir(ttp)H **1d** together with Et_3SiCl presumably. Further reaction of Ir(ttp)H with excess silane produces the iridium porphyrin silyl product. In the presence of a strong base (K_3PO_4, KOH, KF), Ir(ttp)H is formed more rapidly by the facile attack on silicon atom in the iridium-silane complex by a base. The intermediate Ir(ttp)H then reacts with excess silane to yield $Ir(ttp)SiEt_3$. Indeed, when the reaction mixture of Ir(ttp)Cl(CO) **1b** and 100 equiv of $HSiEt_3$ **2a** with the addition of K_3PO_4 (10 equiv) in benzene-d_6 was heated for 1.5 hours at 140 °C in a sealed-NMR tube, Ir(ttp)H was observed first without any $Ir(ttp)SiEt_3$ (Figure 2.5). Therefore, the base-promoted SiHA is due to the accelerated formation of Ir(ttp)H intermediate. Furthermore, in an independent experiment, Ir(ttp)H reacted with $HSiEt_3$ to give 92% yield of $Ir(ttp)SiEt_3$ at 140 °C after 2 days (eq 2.12).

$$\underset{\textbf{1e}}{Ir(ttp)(BF_4)(CO)} + \underset{\textbf{2a}}{HSiEt_3} \xrightarrow[1\ d]{N_2,\ 200\ ^\circ C} \underset{\textbf{2b}\ 61\%}{Ir(ttp)SiEt_3} \qquad (2.11)$$

$$\underset{\textbf{1d}}{Ir(ttp)H} + \underset{\textbf{2a}}{HSiEt_3} \xrightarrow[2d]{N_2,\ 140\ ^\circ C} \underset{\textbf{3a}\ 92\%}{Ir(ttp)SiEt_3} \qquad (2.12)$$

Scheme 2.5 Mechanism of Base-Promoted SiHA of Ir(ttp)Cl(CO) with $HSiEt_3$

$$Ir(ttp)Cl(CO) \xrightarrow[heat]{-CO,\ -Cl^-} Ir(ttp)^+ \xrightarrow{HSiEt_3} \underset{\textbf{A}}{\left[Ir(ttp)^+\text{—}H\text{—}SiEt_3\right]} \xrightarrow{base} Ir(ttp)H \xrightarrow{HSiEt_3} Ir(ttp)SiEt_3$$

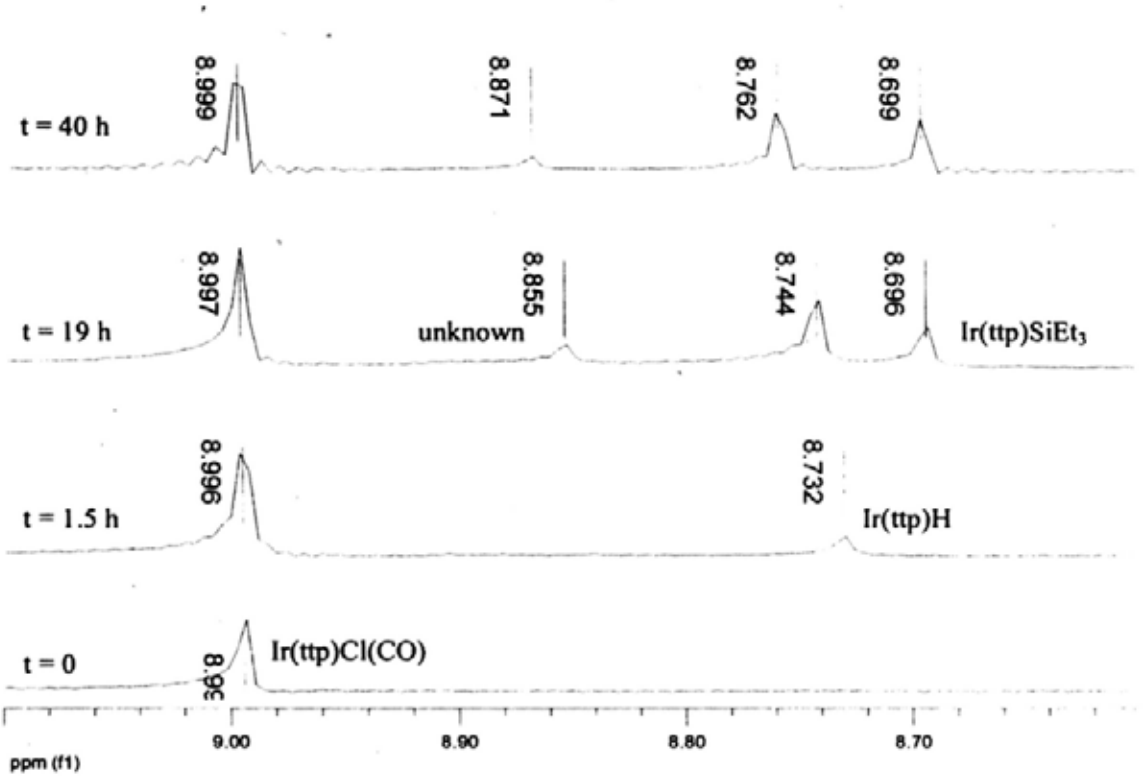

Figure 2.5 Partial ^{1}H NMR spectra for reaction sequence between Ir(ttp)Cl(CO) **1b** and $HSiEt_3$ **2a**

Scheme 2.6 illustrates the proposed mechanism for the reaction of Ir(ttp)Cl(CO) with $HSiPh_2Me$ with SiHA, SiCA and silyl exchange reactions. Ir(ttp)Cl(CO) reacts with $HSiPh_2Me$ to give Ir(ttp)H initially, which then reacts with excess $HSiPh_2Me$ to yield both SiHA product **3g** and SiCA product **3e** concurrently. In addition, iridium porphyrin silyls could undergo silyl exchange reaction to give **3e** or **3g** in solvent-free conditions in a higher concentration of silanes. Indeed, the silyl exchange reactions were demonstrated by the separate reactions of **3g** or **3e** with $HSiPh_2Me$ to give a mixture of **3g** and **3e** (eqs 2.13 and 2.14).

Scheme 2.6 Mechanism of SiHA and SiCA of Ir(ttp)Cl(CO) with $HSiPh_2Me$

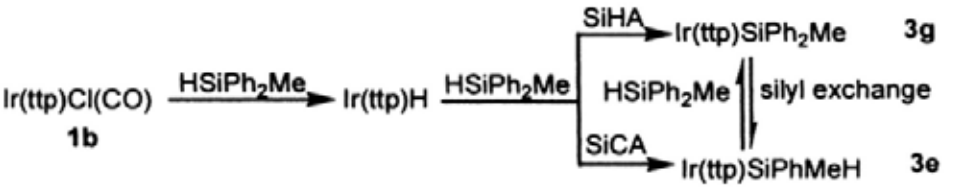

$$Ir(ttp)SiPh_2Me\ (\mathbf{3g}) + HSiPh_2Me\ (\mathbf{2g}) \xrightarrow[2d]{N_2,\ 200^oC} Ir(ttp)SiPh_2Me\ (\mathbf{3g}\ 33\%) + Ir(ttp)SiPhMeH\ (\mathbf{3e}\ 31\%) \quad (2.13)$$

$$Ir(ttp)SiPhMeH\ (\mathbf{3e}) + HSiPh_2Me\ (\mathbf{2g}) \xrightarrow[2d]{N_2,\ 200^oC} Ir(ttp)SiPh_2Me\ (\mathbf{3g}\ 40\%) + Ir(ttp)SiPhMeH\ (\mathbf{3e}\ 46\%) \quad (2.14)$$

2.4 X-Ray Structures of $Ir(ttp)SiEt_3$, $Ir(ttp)Si(OEt)_3$, $Ir(ttp)SiBnMe_2$ and $Ir(ttp)SiPh_2Me$

The structures of $Ir(ttp)SiEt_3$ **3a**, $Ir(ttp)Si(OEt)_3$ **3b**, $Ir(ttp)SiBnMe_2$ **3c** and $Ir(ttp)SiPh_2Me$ **3g** were confirmed by single-crystal X-ray diffraction studies and are shown in Figures 2.6, 2.7, 2.8 and 2.9 (30% thermal ellipsoids). Crystals were grown from dichloromethane/methanol solution. Tables 2.8, 2.9, 2.10 and 2.11 list the selected bond lengths and angles for **3a, 3b**, **3c** and **3g,** respectively.

From Figure 2.6 and Table 2.8, the Ir-Si bond length is 2.3527 Å, which is longer than that of $Rh(oep)SiEt_3$ (Rh-Si = 2.305 Å).[42a] The Ir atom is displaced 0.161 Å from the mean plane of porphyrin ring. The dihedral angles between toyl plane and the mean porphyrin plane are 69.85°, 67.86°, 67.10°, and 87.09°, respectively. The dihedral angles between NC_4 pyrroles and mean plane are 2.77°, 2.43°, 4.55°, and 1.98°, respectively.

For $Ir(ttp)Si(OEt)_3$ **3b**, the coordination sphere of the iridium atom forms a triclinic geometry with the four porphyrinato nitrogen atoms occupying the basal sites while the silicon atom resides at the axial site. The Ir-Si length is 2.277 Å, which is

slightly shorter than that of reported Rh-Si (2.329 Å for Rh(tmp)$SiPh_2Me$, 2.305 Å for Rh(tpp)$SiMe_3$).[31a,42b] It is also shorter than that of Ir-Si in iridium complexes.[43] The Ir atom is displaced 0.193 Å from the mean plane of porphyrin ring, which is slightly larger than that of Ir(ttp)$SiEt_3$. The dihedral angles between toyl plane and the mean porphyrin plane are 82.97°, 87.12°, 82.48°, and 69.53°, respectively. The dihedral angles between NC_4 pyrroles and mean plane are 8.28°, 0.87°, 5.51°, and 2.22°, respectively.

The Ir-Si bond length of Ir(ttp)$SiBnMe_2$ **3c** is 2.328 Å, which is longer than that of Ir(ttp)$Si(OEt)_3$ **3b**, while shorter tnan that of Ir(ttp)$SiEt_3$ **3a**. The Ir atom is displaced 0.113 Å from the mean plane of porphyrin ring. The dihedral angles between toyl plane and the mean porphyrin plane are 82.98°, 62.80°, 77.26°, and 55°, respectively. The dihedral angles between NC_4 pyrroles and mean plane are 1.25°, 3.46°, 1.86°, and 4.04°, respectively.

The Ir-Si bond length of Ir(ttp)$SiPh_2Me$ **3g** is 2.329 Å, which is similar than that of Rh(tmp)$SiPh_2Me$ (Rh-Si = 2.329 Å)[31a], while shorter than that of Ir(ttp)$SiEt_3$. The Ir atom is displaced 0.139 Å from the mean plane of porphyrin ring. The dihedral angles between toyl plane and the mean porphyrin plane are 56.74°, 75.82°, 76.93°, and 63.24°, respectively. The dihedral angles between NC_4 pyrroles and mean plane are 6.58°, 3.44°, 4.17°, and 4.61°, respectively.

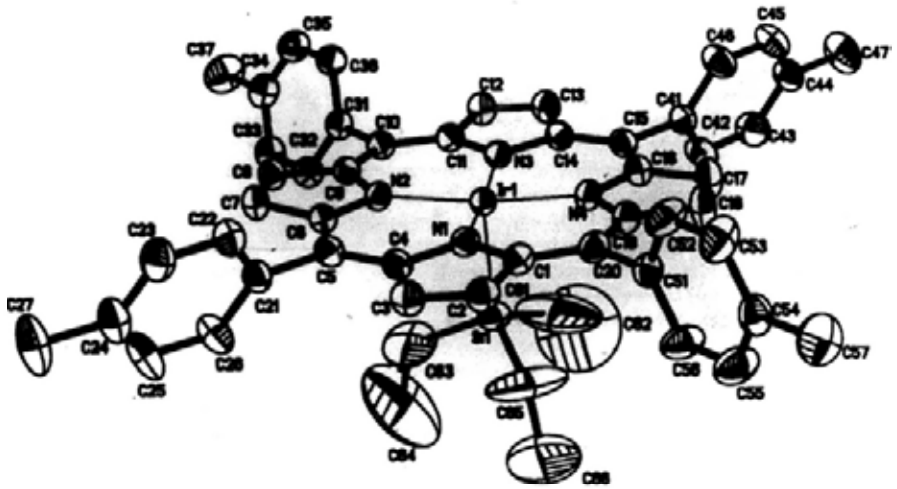

Figure 2.6 Molecular structure of $Ir(ttp)SiEt_3$ (30% thermal ellipsoids).

Table 2.8 Selected Bond Lengths and Angles of $Ir(ttp)SiEt_3$

Bond Lengths / Å			
Ir(1)-N(1)	2.035 (3)	Ir(1)-N(2)	2.017 (3)
Ir(1)-N(3)	2.028 (3)	Ir(1)-N(4)	2.026 (4)
Ir(1)-Si(1)	2.3527 (14)	Si(1)-C(61)	1.916 (13)
Si(1)-C(63)	1.865 (10)	Si(1)-C(65)	1.851 (9)
Bond Angles / deg			
N(1)-Ir(1)-Si(1)	92.51 (11)	N(2)-Ir(1)-Si(1)	94.05 (11)
N(3)-Ir(1)-Si(1)	93.94 (11)	N(4)-Ir(1)-Si(1)	92.81 (11)
C(61)-Si(1)-Ir(1)	110.3 (3)	C(63)-Si(1)-Ir(1)	109.9 (3)
C(65)-Si(1)-Ir(1)	110.9 (3)	C(63)-Si(1)-C(61)	110.5 (6)
C(65)-Si(1)-C(61)	106.3 (7)	C(65)-Si(1)-C(63)	108.8 (6)

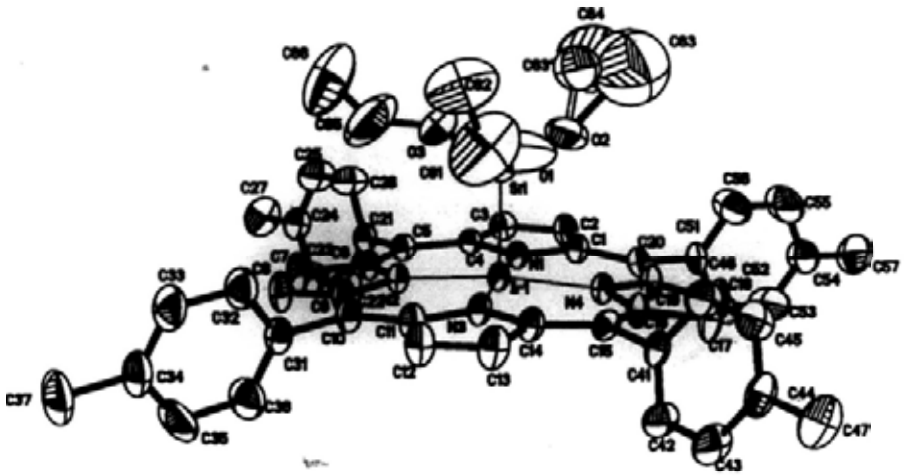

Figure 2.7 Molecular structure of Ir(ttp)Si(OEt)$_3$ (30% thermal ellipsoids).

Table 2.9 Selected Bond Lengths and Angles of Ir(ttp)Si(OEt)$_3$

Bond Lengths / Å			
Ir(1)-N(1)	2.040 (6)	Ir(1)-N(2)	2.022 (6)
Ir(1)-N(3)	2.029 (6)	Ir(1)-N(4)	2.029 (6)
Ir(1)-Si(1)	2.277 (3)	Si(1)-O(1)	1.552 (11)
Si(1)-O(2)	1.616 (9)	Si(1)-O(3)	1.604 (10)
Bond Angles / deg			
N(1)-Ir(1)-Si(1)	90.88 (19)	N(2)-Ir(1)-Si(1)	95.1 (2)
N(3)-Ir(1)-Si(1)	94.3 (2)	N(4)-Ir(1)-Si(1)	92.9 (2)
O(1)-Si(1)-Ir(1)	112.7 (5)	O(2)-Si(1)-Ir(1)	109.6 (3)
O(3)-Si(1)-Ir(1)	113.3 (4)	O(1)-Si(1)-O(2)	103.9 (8)
O(1)-Si(1)-O(3)	113.6 (8)	O(3)-Si(1)-O(2)	102.7 (6)

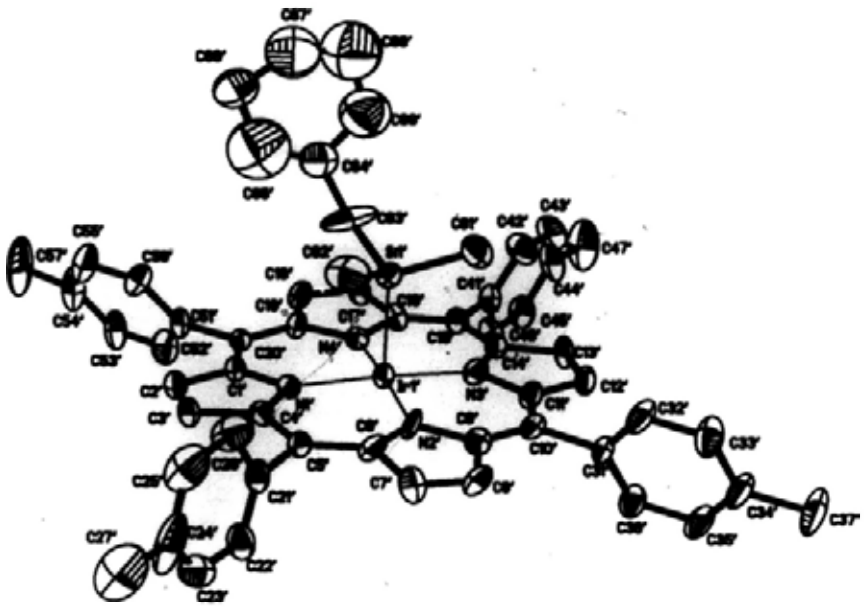

Figure 2.8 Molecular structure of Ir(ttp)SiBnMe$_2$ (30% thermal ellipsoids).

Table 2.10 Selected Bond Lengths and Angles of Ir(ttp)SiBnMe$_2$

Bond Lengths / Å			
Ir(1)-N(1)	2.036 (12)	Ir(1)-N(2)	2.026 (14)
Ir(1)-N(3)	2.025 (13)	Ir(1)-N(4)	2.030 (13)
Ir(1)-Si(1)	2.328 (5)	Si(1)-C(61)	1.865 (2)
Si(1)-C(62)	1.852 (6)	Si(1)-C(63)	1.85 (3)
Bond Angles / deg			
N(1)-Ir(1)-Si(1)	93.5 (4)	N(2)-Ir(1)-Si(1)	92.3 (5)
N(3)-Ir(1)-Si(1)	92.7 (4)	N(4)-Ir(1)-Si(1)	91.6 (4)
C(61)-Si(1)-Ir(1)	110.4 (8)	C(62)-Si(1)-Ir(1)	110.8 (9)
C(63)-Si(1)-Ir(1)	110.2 (8)	C(61)-Si(1)-C(62)	106.6 (14)
C(61)-Si(1)-C(63)	109.4 (15)	C(63)-Si(1)-C(62)	109.8 (14)

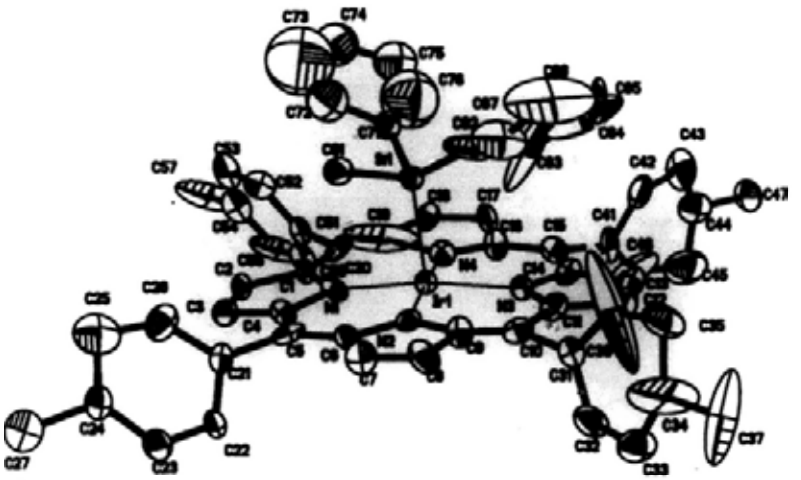

Figure 2.9 Molecular structure of Ir(ttp)$SiPh_2Me$ (30% thermal ellipsoids).

Table 2.11 Selected Bond Lengths and Angles of Ir(ttp)$SiPh_2Me$

Bond Lengths / Å			
Ir(1)-N(1)	2.00 (2)	Ir(1)-N(2)	2.047 (19)
Ir(1)-N(3)	2.028 (17)	Ir(1)-N(4)	2.03 (2)
Ir(1)-Si(1)	2.329 (6)	Si(1)-C(61)	1.91 (3)
Si(1)-C(62)	1.725 (15)	Si(1)-C(71)	1.80 (2)
Bond Angles / deg			
N(1)-Ir(1)-Si(1)	92.2 (6)	N(2)-Ir(1)-Si(1)	88.5 (5)
N(3)-Ir(1)-Si(1)	96.4 (5)	N(4)-Ir(1)-Si(1)	95.6 (6)
C(61)-Si(1)-Ir(1)	112.3 (8)	C(62)-Si(1)-Ir(1)	117.0 (6)
C(71)-Si(1)-Ir(1)	111.2 (7)	C(61)-Si(1)-C(62)	97.6 (9)
C(61)-Si(1)-C(71)	102.3 (11)	C(71)-Si(1)-C(62)	114.6 (10)

2.5 Si-H Bond Activation by Iridium Porphyrin Methyl and Silyls

2.5.1 Si-H Bond Activation by Ir(ttp)Me

SiHA by a more electron-rich Ir(ttp)Me **1f** bearing a non-dissociating methyl group was also successful (Table 2.12, eq 2.15). In solvent-free conditions, Ir(ttp)Me **1f** reacted with $HSiEt_3$ **2a** to give a poor yield (12%) of Ir(ttp)$SiEt_3$ **3a** at 150 °C (Table 2.12, entry 1). When increased the temperature to 200 °C after 5 days, **1f** reacted with $HSiEt_3$ **2a** to give 83% yield of Ir(ttp)$SiEt_3$ **3a** (Table 2.12, entry 2). However, **1f** reacted with $HSi(OEt)_3$ **2b** to produce only 16% yield of Ir(ttp)$Si(OEt)_3$ **3b** (Table 2.12, entry 3). The lower yield was attributed to the poor reactivity and selectivity, since most Ir(ttp)Me remained unreactive and Ir(ttp)Et generated via carbon-oxygen bond activation was observed. When the reaction was carried out in benzene solvent, a higher reaction temperature of 200 °C was required but still poor product yields were observed (Table 2.12, entries 4 and 5).

Table 2.12 Silicon-Hydrogen Bond Activation by Ir(ttp)Me

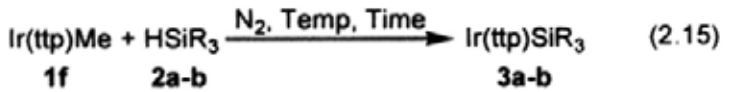

1f **2a-b** **3a-b** (2.15)

Entry	$HSiR_3$	Temp / °C	Time / d	Product (yield / %)
1	$HSiEt_3$ **2a**	150	8	Ir(ttp)$SiEt_3$ **3a** (12)
2	$HSiEt_3$ **2a**	200	5	Ir(ttp)$SiEt_3$ **3a** (83)
3	$HSi(OEt)_3$ **2b**	200	7	Ir(ttp)$Si(OEt)_3$ **3b** (16)
4[a]	$HSiEt_3$ **2a**	200	7	Ir(ttp)$SiEt_3$ **3a** (10)
5[a]	$HSi(OEt)_3$ **2b**	200	4	Ir(ttp)$Si(OEt)_3$ **3b** (8)

[a] In benzene solvent, Ir(ttp)Me : Silane = 1 : 100.

2.5.2 Base-Promoted Si-H Bond Activation by Ir(ttp)Me

To further enhance the SiHA by Ir(ttp)Me, base effect on SiHA was then examined. Table 2.13 and eq 2.16 list the results of base-promoted of SiHA by Ir(ttp)Me. We were delighted to find that the addition of K_3PO_4, KF or KOAc gave higher product yields (Table 2.13, entries 2, 5 and 8), although KOH and CsCl were proved to be detrimental (Table 2.13, entries 4 and 6).

Table 2.13 Base Promoted SiHA of $HSiEt_3$ by Ir(ttp)Me in Solvent-Free Conditions

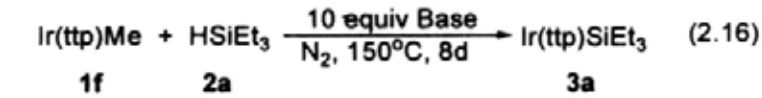

1f **2a** **3a**

Entry	Base	**3a** / %	Entry	Base	**3a** / %
1	none	12	5	KF	15
2	K_3PO_4	44	6	CsCl	6
3	K_2CO_3	14	7	KI	9
4	KOH	<5	8	KOAc	60

2.5.3 Silyl Exchange

The SiHA reaction was also observed with the electron rich $Ir(ttp)SiEt_3$ and $Ir(ttp)SiBnMe_2$ complexes. $Ir(ttp)SiBnMe_2$ **3c** reacted with $HSiEt_3$ **2a** at 200 °C in 4 days to give 20% of $Ir(ttp)SiEt_3$ **3a** and 71% of **3c** was recovered, while $Ir(ttp)SiEt_3$ **3a** reacted with $HSiBnMe_2$ to give 82% of $Ir(ttp)SiBnMe_2$ **3c** after 2 days, and **3a** was completely consumed (eqs 2.17 and 2.18). The higher conversion of $Ir(ttp)SiEt_3$ into

3c (eq 2.18) is likely due to the preferred formation of a less hindered Ir(ttp)SiBnMe$_2$ complex.

$$\underset{\text{Recorvey 71\%}}{\underset{\textbf{3c}}{Ir(ttp)SiBnMe_2}} + \underset{\textbf{2a}}{HSiEt_3} \xrightarrow[4\ d]{N_2,\ 200^\circ C} \underset{\textbf{3a 20\%}}{Ir(ttp)SiEt_3} + \underset{\textbf{2c}}{HSiBnMe_2} \quad (2.17)$$

$$\underset{\textbf{3a}}{Ir(ttp)SiEt_3} + \underset{\textbf{2c}}{HSiBnMe_2} \xrightarrow[2\ d]{N_2,\ 200^\circ C} \underset{\textbf{3c 82\%}}{Ir(ttp)SiBnMe_2} + \underset{\textbf{2a}}{HSiEt_3} \quad (2.18)$$

2.5.4 Mechanistic Study of Si-H Bond Activation by Ir(ttp)R (R=Me and Silyl)

Scheme 2.7 shows the proposed reaction pathways for the reaction of Ir(ttp)Me and Ir(ttp)SiR$_3$ with silanes without the addition of base. Oxidative addition can occur via the formation of an Ir(V) intermediate since an Ir(V) intermediate in SiHA has been reported by Bergman and coworkers.[32b] Alternatively, sigma-bond metathesis or sigma-complex-assisted metathesis[33d] via a 4-centered transition state is also possible. The distinction of oxidative addition and sigma-bond metathesis has been attempted by theoretical methods since it is experimentally difficult.[44] Dissociative mechanism via homolysis of Ir(ttp)Me is unlikely since the Ir-Me bond is stronger than Rh-Me bond which is about 58 kcal/mol[45] and will require a very long reaction time. An alternative dissociative mechanism via heterolytic cleavage of Ir-Me is not probable since Ir^-/Me^+ or Ir^+/Me^- ion pairs are unstable and the energetic requirement would be expected to be even much higher than that of homolysis.[37]

Scheme 2.7 Mechanism of SiHA of Ir(ttp)Me and Ir(ttp)SiR$_3$ with Silanes

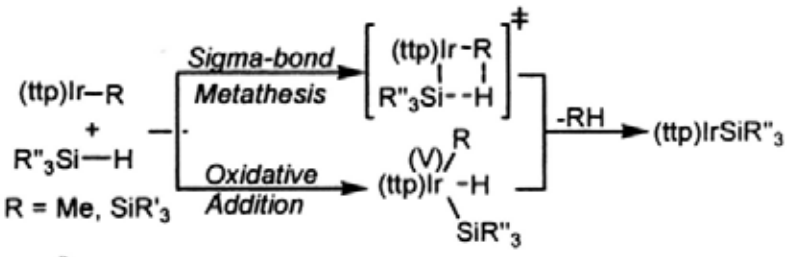

While we do not understand very well the mechanism of the base-promoted SiHA by Ir(ttp)Me, we speculate in Scheme 2.8 that a base (B = $K_2PO_4^-$ and OAc^-) can attack Et_3SiH to form a penta-valent BEt_3SiH^-[46] which is more reactive to convert Ir(ttp)Me into Ir(ttp)$^\cdot$. Then rapid proton abstraction of Ir(ttp)$^\cdot$ with Et_3SiH or other proton source forms Ir(ttp)H which subsequently undergoes facile SiHA with Et_3SiH to produce $Ir(ttp)SiEt_3$. Indeed, Ir(ttp)H was observed by ^1H NMR spectroscopy when the reactions were run only in the presence of base, such as K_3PO_4 or KOAc, while no Ir(ttp)H was found without the addition of base. This proposed mechanism further accounts the effect of base strength. In the presence of weak base, such as CsCl or KI, the formation of BEt_3SiH^- is disfavored. On the other hand, in the presence of very strong base, such as KOH, Ir(ttp)$^\cdot$ is formed rapidly, but undergoes facile competitive decomposition and only trace amount of $Ir(ttp)SiEt_3$ is observed.

Scheme 2.8 Mechanism of SiHA of Ir(ttp)Me and Silane with Base

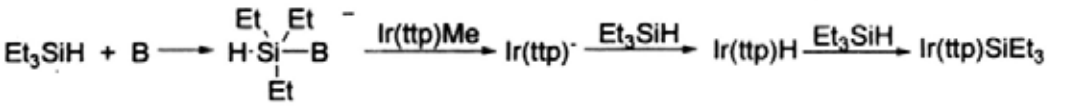

2.6 Conclusion

We have discovered that iridium porphyrin silyl complexes were synthesized from the reactions of iridium(III) porphyrin carbonyl chloride and methyl with silanes via silicon-hydrogen bond activation in both solvent and solvent-free conditions. SiHA reactions were promoted by basic additives. K_3PO_4 facilitated the SiHA of silane by Ir(ttp)Cl(CO) most efficiently, while KOAc acceleratd the SiHA with Ir(ttp)Me best. Preliminary mechanistic experiments suggested that iridium porphyrin carbonyl chloride initially formed iridium porphyrin cation, which then reacted with

silanes to generate iridium porphyrin hydride. Ir(ttp)H further reacted with excess silane via silicon-hydrogen bond activation reaction to yield iridium porphyrin silyls. On the other hand, the silicon-hydrogen bond activation reaction of silanes by iridium(III) porphyrin methyl and silyls likely underwent oxidative addition or sigma-bond metathesis. In the presence of base, an anionic penta-coordinated silicon hydride species likely formed, which would further react with iridium porphyrin methyl to generate iridium porphyrin anion. Ir(ttp)H was produced after protonation and finally reacted with excess silane to give iridium porphyrin silyl complexes.

2.7 Experimental Section

Unless otherwise noted, all chemicals were obtained from commercial suppliers and used without further purification. Hexane for chromatography was distilled from anhydrous calcium chloride. Thin-layer chromatography was performed on precoated alumina plates for thin-layer analysis of reaction mixture. All preparation reactions were carried out in a teflon screw-head stoppered tube in N_2 in the absence of light. The purification of iridium silyl complexes was carried out by flash column chromatography in air using alumina (90 active neutral, 70-230 mesh). Samples for microanalysis were recrystallized from CH_2Cl_2/MeOH and were then dried at 40-60 °C in vacuum (0.005 mmHg) for 3 days.

^{1}H NMR spectra were recorded on a Bruker DPX-300 (300 MHz). Chemical shifts were reported with reference to the residual solvent protons in $CDCl_3$ (δ 7.26 ppm) as the internal standard. Chemical shifts (δ) were reported in parts per million (ppm) in δ scale downfield from TMS. Coupling constants (J) are reported in hertz

(Hz). ^{13}C NMR spectra were recorded on a Bruker DPX 300 (75 MHz) spectrometer and referenced to $CDCl_3$ (δ 77.1 ppm) spectra. High-resolution mass spectra (HRMS) were performed on a Thermofinnign MAT 95 XL in FAB (using 3-nitrobenzyl alcohol (NBA) matrix and CH_2Cl_2 as the solvent) and ESI model (MeOH:CH_2Cl_2 = 1:1 as the solvent).

Preparation of 5,10,15,20-Tetratolylporphyrin [H_2ttp] (1a).[34]

Pyrrole (24 mL, 340 mmol) was added dropwise to a refluxing solution of benzaldehyde (35 mL, 340 mmol) in propionic acid (1.25 L). The resulting mixture was refluxed in air for 30 min. The resulting black solution was cooled to room temperature, and MeOH (1.5 L) was added to crystallize the purple porphyrin. The mixture was filtered and washed with MeOH. Purple crystals (11.7 g, 17 mmol, 20%) were obtained. R_f = 0.39 (hexane/CH_2Cl_2 = 1:1). ^1H NMR ($CDCl_3$, 300 MHz): δ -2.78 (s, 2 H), 2.70 (s, 12 H), 7.54 (d, 8 H, J = 7.8 Hz), 8.08 (d, 8 H, J = 8.0 Hz), 8.85 (s, 8 H).

Preparation of 5,10,15,20-(Tetratolylporphyrinato)(carbonyl)iridium(III) Chloride [Ir(ttp)Cl(CO)] (1b).[35,36]

A solution mixture of $IrCl_3 \cdot xH_2O$ (2.00 g, 5.67 mmol), 1,5-cyclooctadiene (6.0 mL, 49 mmol), EtOH (34 mL) and water (17 mL) was placed in a three-necked round bottom flask. One neck of the flask was equipped with an inlet for N_2, another neck was equipped with a water condenser. A slow stream of N_2 was passed through the system and the solution was refluxed for 1 day to give a brick red precipitates. EtOH was removed by rotary evaporate and extra water was added. The mi · · was cooled

in an ice both and orange solid of $[Ir(COD)Cl]_2$ **1c** (1.18 g, 1.76 mmol, 62%) was collected by filtration, washed with ice-cold methanol and then dried in vacuum at room temperature for 1 day.

H_2ttp **1a** (350 mg, 0.52 mmol) and $[Ir(COD)Cl]_2$ **1c** (524 mg, 0.78 mmol) were added into *p*-xylene (200 mL) and the solution was refluxed for 3 days. The color of the solution changed from purple to red. The crude mixture was dried under high vacuum and purified by silica gel (70-230 mesh) column chromatography eluting with a solvent mixture of hexane/CH_2Cl_2 (2:1). The fast moving purple fraction was discarded and the following red fraction was collected. Reddish purple solids Ir(ttp)Cl(CO) (307 mg, 0.33 mmol, 64 %) were obtained by recrystallization from CH_2Cl_2/CH_3OH. R_f = 0.32 (hexane/CH_2Cl_2 = 1:2). ^{1}H NMR ($CDCl_3$, 300 MHz) δ 2.71 (s, 12 H), 7.56 (d, 8 H, J = 7.8 Hz), 8.08 (d, 4 H, J = 8.1 Hz), 8.14 (d, 4 H, J = 8.4 Hz), 8.94 (s, 8 H).

Preparation of 5, 10, 15, 20-(Tetratolylporphyrinato)iridium(III) Hydride [Ir(ttp)H] (1d).[35]

A suspension of Ir(ttp)Cl(CO) **1b** (100 mg, 0.11 mmol) in THF (50 mL) and a solution of $NaBH_4$ (83 mg, 2.20 mmol) in aq. NaOH (0.1 M, 4 mL) were purged with N_2 for 15 minutes separately. The solution of $NaBH_4$ was added slowly to the suspension of Ir(ttp)Cl(CO) via a cannula. The mixture was heated at 70°C under N_2 for 2 hours to give a brown solution. The solution was then cooled to 0 °C under N_2 and degassed 0.1 M HCl (200 mL) was added via a cannula. A brick red suspension was formed. After stirred at room temperature for another 15 minutes under N_2, the

brick red precipitate was collected after filtration and washing with water (2 x 10 mL) under N_2. The brick red residues (89 mg, 0.10 mmol, 95 %) were obtained after vacuum dried. ^{1}H NMR (C_6D_6, 300 MHz): δ -56.61 (s, 1 H), 2.39 (s, 12 H), 7.20 (d, 4 H, J = 6.0 Hz), 7.33 (d, 4 H, J = 9.0 Hz), 7.91 (d, 4 H, J = 9.0 Hz), 8.18 (d, 4 H, J = 9.0 Hz), 8.81 (s, 8 H).

Preparation of 5,10,15,20-(Tetratolylporphyrinato)(carbonyl)iridium(III) Tetrafluoroborate [Ir(ttp)(BF_4)(CO)] (1e).[37]

Ir(ttp)Cl(CO) **1b** (100 mg, 0.11 mmol) and $AgBF_4$ (203 mg, 1.10 mmol) were added into anhydrous CH_2Cl_2 (50 mL), and stirred for 1 day at room temperature. The mixture was changed from red to reddish brown in color. The product was purified by recrystallization from CH_2Cl_2 /hexane after filtration. The mixed product Ir(ttp)(BF_4)/ Ir(ttp)(BF_4)(CO) (1:1 to 1:4) (86 mg, 0.09 mmol, 80%) was obtained.

Preparation of 5, 10, 15, 20-(Tetratolylporphyrinato)iridium(III) Methyl [Ir(ttp)Me] (1f).[35]

A suspension of Ir(ttp)Cl(CO) **1b** (100 mg, 0.11 mmol) and THF (50 mL) was placed in a Telfon screw capped tube and a solution of $NaBH_4$ (83 mg, 2.20 mmol) in aq. NaOH (1 M, 4 mL) were purged with N_2 for 15 minutes separately. The solution of $NaBH_4$ was added slowly to the suspension of Ir(ttp)Cl(CO) via a cannula. The mixture was heated at 70 °C under N_2 for 2 hours to give a brown suspension. The mixture was then cooled to room temperature under N_2 and iodomethane (0.2 mL, 3.2 mmol) was added. The reaction mixture was further heated at 70 °C under N_2 for 2 hours. A reddish brown suspension was formed. The reaction mixture was worked up

by extraction with CH_2Cl_2/H_2O. The combined organic extract was dried ($MgSO_4$), filtered and rotary evaporated. The reddish orange residue was purified by column chromatography on alumina eluting with a solvent mixture of hexane/CH_2Cl_2 (2:1). The major red fraction was collected and gave reddish purple solid of Ir(ttp)Me (72 mg, 0.08 mmol, 75 %) as the product after rotary evaporation. The product was further purified by recrystallization from CH_2Cl_2/CH_3OH. R_f = 0.24 (hexane/CH_2Cl_2 = 2:1). ^{1}H NMR ($CDCl_3$, 300 MHz): δ -6.28 (s, 3 H), 2.68 (s, 12 H), 7.50 (d, 8 H, J = 8.1 Hz), 8.97 (t, 8 H, J = 7.5 Hz), 8.52 (s, 8 H).

Reactions between Ir(ttp)Cl(CO) 1b and Silanes. General Procedure. The reaction between Ir(ttp)Cl(CO) **1b** and triethylsilane (**2a**) is described as a typical example. Triethylsilane (1.1 mL, 500 equiv) was added to Ir(ttp)Cl(CO) (12.5 mg, 0.014 mmol), and the mixture was degassed by the freeze-pump-thaw method (3 cycles). Then the mixture was heated at 200 °C for 4 days. The crude product was purified by column chromatography on alumina eluting with hexane. A purple solid of Ir(ttp)$SiEt_3$ **3a** (11.5 mg, 0.0118 mmol, 84%) was isolated. R_f = 0.52 (hexane/CH_2Cl_2 = 5:1). ^{1}H NMR ($CDCl_3$, 300 MHz): δ -3.22 (q, 6 H, J = 7.8 Hz), -1.25 (t, 9 H, J = 7.8 Hz), 2.68 (s, 12 H), 7.50 (d, 8 H, J = 8.4 Hz), 7.96 (t, 8 H, J = 6.0 Hz), 8.51 (s, 8 H). ^{13}C NMR ($CDCl_3$, 75 MHz): δ 0.1, 5.3, 21.7, 29.9, 124.82, 127.6, 127.7, 131.3, 133.4, 133.8, 137.3, 138.8, 143.8. HRMS (FAB): calcd for $(C_{54}H_{51}N_4SiIr)^+$ *m/z* 976.3507; found *m/z* 976.3526. Anal. Calcd for $C_{54}H_{51}N_4SiIr$: C, 66.43; H, 5.26; N, 5.74. Found: C, 66.43; H, 5.24; N, 5.64.

Reaction between Ir(ttp)Cl(CO) 1b and Triethylsilane (2a). Triethylsilane (1.0 mL, 500 equiv) and Ir(ttp)Cl(CO) (11.2 mg, 0.012 mmol) were heated at 120 °C for 9 days. Only trace amount of Ir(ttp)$SiEt_3$ **3a** (<5%) was observed according to ^1H NMR spectroscopy.

Reaction between Ir(ttp)Cl(CO) 1b and Triethylsilane (2a). Triethylsilane (1.0 mL, 500 equiv) and Ir(ttp)Cl(CO) (11.2 mg, 0.012 mmol) were heated at 200 °C for 4.5 hours. A purple solid of Ir(ttp)$SiEt_3$ **3a** (0.7 mg, 0.0007 mmol, 6%) was isolated after column chromatography.

Reaction between Ir(ttp)Cl(CO) 1b and Triethylsilane (2a). Triethylsilane (1.2 mL, 500 equiv) and Ir(ttp)Cl(CO) (14.1 mg, 0.015 mmol) were heated at 140 °C for 6 days. A purple solid of Ir(ttp)$SiEt_3$ **3a** (1.2 mg, 0.0012 mmol, 10%) was isolated after column chromatography.

Reaction between Ir(ttp)Cl(CO) 1b and Triethoxysilane (2b). Triethoxysilane (1.3 mL, 500 equiv) and Ir(ttp)Cl(CO) (13.3 mg, 0.014 mmol) were heated at 200 °C for 6 hours. A purple solid of Ir(ttp)$Si(OEt)_3$ **3b** (7.7 mg, 0.0075 mmol, 54%) was isolated after column chromatography. R_f = 0.28 (hexane/CH_2Cl_2 = 5:1). ^1H NMR ($CDCl_3$, 300 MHz): δ -0.22 (t, 9 H, J = 6.9 Hz), 0.91 (q, 6 H, J = 6.9 Hz), 2.68 (s, 12 H), 7.50 (d, 8 H, J = 8.1 Hz), 7.99 (d, 8 H, J = 8.1 Hz), 8.58 (s, 8 H). ^{13}C NMR ($CDCl_3$, 75 MHz): δ 17.3, 21.8, 55.1, 124.3, 127.7, 127.8, 131.2, 133.9, 137.4, 139.2, 143.6. HRMS (FAB): calcd for $(C_{54}H_{51}N_4SiIr)^+$ *m/z* 1024.3354; found *m/z* 1024.2260. Anal. Calcd for $C_{54}H_{51}N_4O_3SiIr$: C, 63.32; H, 5.02; N, 5.47. Found: C, 63.15; H, 4.98; N, 5.38.

Reaction between Ir(ttp)Cl(CO) 1b and Benzyldimethylsilane (2c). Benzyldimethylsilane (1.2 mL, 500 equiv) and Ir(ttp)Cl(CO) (13.6 mg, 0.015 mmol) were heated at 200 °C for 1 day. A purple solid of Ir(ttp)SiBnMe$_2$ **3c** (11.8 mg, 0.0117 mmol, 78%) was isolated after column chromatography. R_f = 0.55 (hexane/CH_2Cl_2 = 5:1). ^{1}H NMR ($CDCl_3$, 300 MHz): δ –3.83 (s, 6 H), -2.21 (s, 2 H), 2.69 (s, 12 H), 5.32 (t, 2 H, J = 3.6 Hz), 6.47 (t, 3 H, J = 3.6 Hz), 7.50 (t, 8 H, J = 7.2 Hz), 7.96 (d, 4 H, J = 7.5 Hz), 8.04 (d, 4 H, J = 7.5 Hz), 8.58 (s, 8 H). ^{13}C NMR ($CDCl_3$, 75 MHz): δ -7.3, 21.7, 21.1, 123.2, 125.2, 127.5, 128.1, 128.2, 131.8, 133.9, 134.3, 137.9, 139.2, 144.0. HRMS (FAB): calcd for $(C_{57}H_{49}N_4SiIr)^+$ *m/z* 1010.3350; found *m/z* 1010.3340. Anal. Calcd for $C_{54}H_{51}N_4O_3SiIr$: C, 67.76; H, 4.89; N, 5.54. Found: C, 67.65; H, 4.948; N, 5.41.

Reaction between Ir(ttp)Cl(CO) 1b and Phenylsilane (2d). Phenylsilane (1.0 mL, 500 equiv) and Ir(ttp)Cl(CO) (15.6 mg, 0.017 mmol) were heated at 140 °C for 5 hours. A dark brown solid of Ir(ttp)SiPhH$_2$ **3d** (14.8 mg, 0.0153 mmol, 90%) was isolated when the reaction mixture was washed by MeOH. ^{1}H NMR ($CDCl_3$, 300 MHz): δ –2.16 (s, 2 H, $^1J_{Si-H}$ = 202.8 Hz), 2.69 (s, 12 H), 4.33 (d, 2 H, J = 6.3 Hz), 6.37 (t, 2 H, J = 6.3 Hz), 6.76 (t, 1 H, J = 6.3 Hz), 7.51 (d, 8 H, J = 7.5 Hz), 7.88 (d, 4 H, J = 7.2 Hz), 8.00 (d, 4 H, J = 7.2 Hz), 8.53 (s, 8 H). ^{13}C NMR ($CDCl_3$, 75 MHz): δ 21.7, 124.2, 126.1, 127.5, 127.6, 131.3, 131.4, 133.6, 133.9, 137.3, 138.7, 143.0. HRMS (FAB): calcd for $(C_{54}H_{43}N_4SiIr)^+$ *m/z* 968.2881; found *m/z* 968.2872.

Reaction between Ir(ttp)Cl(CO) 1b and Phenylmethylsilane (2e). Phenylmethylsilane (0.8 mL, 500 equiv) and Ir(ttp)Cl(CO) (11.2 mg, 0.012 mmol)

were heated at 200 °C for 0.5 hour. A purple solid of Ir(ttp)SiPhMeH **3e** (4.0 mg, 0.0041 mmol, 34%) was isolated when the reaction mixture was washed by MeOH. R_f = 0.46 (hexane/CH_2Cl_2 = 5:1). ^{1}H NMR ($CDCl_3$, 300 MHz): δ –3.45 (d, 3 H, J = 3.3 Hz), -2.24 (q, 1 H, J = 3.3 Hz, $^1J_{Si-H}$ = 200.1 Hz), 2.68 (s, 12 H), 4.34 (d, 2 H, J = 6.9 Hz), 6.40 (t, 2 H, J = 7.5 Hz), 6.78 (t, 1 H, J = 7.4 Hz), 7.53 (t, 8 H, J = 5.7 Hz), 7.86 (d, 4 H, J = 8.4 Hz), 7.98 (d, 4 H, J = 8.4 Hz), 8.49 (s, 8 H). ^{13}C NMR ($CDCl_3$, 75 MHz): δ -9.8, 21.8, 124.5, 126.2, 127.5, 127.7, 127.8, 130.6, 131.4, 133.8, 134.0, 137.4, 138.9, 143.3. HRMS (FAB): calcd for $(C_{55}H_{45}N_4SiIr)^+$ *m/z* 982.3037; found *m/z* 982.3032.

Reaction between Ir(ttp)Cl(CO) 1b and Diphenylsilane (2f). Diphenylsilane (1.6 mL, 500 equiv) and Ir(ttp)Cl(CO) (16.0 mg, 0.017 mmol) were heated at 140 °C for 2 days. A purple solid of Ir(ttp)$SiPh_2H$ **3f** (12.1 mg, 0.0116 mmol, 68%) was isolated after column chromatography. R_f = 0.56 (hexane/CH_2Cl_2 = 5:1). ^{1}H NMR ($CDCl_3$, 300 MHz): δ -1.76 (s, 1 H, $^1J_{Si-H}$ = 204.6 Hz), 2.68 (s, 12 H), 4.50 (d, 4 H, J = 7.5 Hz), 6.39 (t, 4 H, J = 7.5 Hz), 6.75 (t, 2 H, J = 7.5 Hz), 7.48 (t, 8 H, J = 7.5 Hz), 7.72 (d, 4 H, J = 7.5 Hz), 7.95 (d, 4 H, J = 7.5 Hz), 8.45 (s, 8 H). ^{13}C NMR ($CDCl_3$, 75 MHz): δ 21.8, 124.5, 126.2, 127.5, 127.7, 131.4, 132.0, 133.8, 134.0, 137.4, 138.9, 143.2. HRMS (FAB): calcd for $(C_{60}H_{47}N_4SiIr)^+$ *m/z* 1044.3194; found *m/z* 1044.3209. Anal. Calcd for $C_{60}H_{47}N_4SiIr$: C, 69.00; H, 4.54; N, 5.36. Found: C, 69.11; H, 4.54; N, 5.38.

Reaction between Ir(ttp)Cl(CO) 1b and Diphenylmethylsilane (2g). Diphenylmethylsilane (1.5 mL, 500 equiv) and Ir(ttp)Cl(CO) (14.0 mg, 0.015 mmol) were heated at 200 °C for 6 hours. A purple solid of Ir(ttp)$SiPh_2Me$ **3g** (6.7 mg,

0.0063 mmol, 42%) was isolated after column chromatography. R_f = 0.51 (hexane/CH_2Cl_2 = 5:1). ^1H NMR ($CDCl_3$, 300 MHz): δ –3.07 (s, 3 H), 2.68 (s, 12 H), 4.61 (d, 4 H, J = 7.2 Hz), 6.46 (t, 4 H, J = 7.5 Hz), 6.77 (t, 2 H, J = 7.2 Hz), 7.46 (q, 8 H, J = 7.5 Hz), 7.78 (d, 4 H, J = 7.8 Hz), 7.89 (d, 4 H, J = 7.8 z), 8.42(s, 8 H). ^{13}C NMR ($CDCl_3$, 75 MHz): δ -8.2, 21.8, 124.7, 126.1, 127.0, 127. 7, 127.7, 131.4, 131.6, 133.6, 133.7, 133.9, 137.4, 138.9, 143.4. HRMS (FAB): calcd for $(C_{61}H_{49}N_4SiIr)^+$ *m/z* 1058.3350; found *m/z* 1058.3367. Anal. Calcd for $C_{54}H_{51}N_4O_3SiIr$: C, 69.22; H, 4.67; N, 5.29. Found: C, 69.21; H, 4.65; N, 5.03. Ir(ttp)SiPhMeH **3e** (4.4 mg, 0.0045 mmol, 30%) was also generated according to the ^1H NMR spectrum of the crude reaction mixture.

Reaction between Ir(ttp)Cl(CO) 1b and Diphenylmethylsilane (2g). Diphenylmethylsilane (1.4 mL, 500 equiv) was added to Ir(ttp)Cl(CO) (13.4 mg, 0.014 mmol), and the mixture was degassed by the freeze-pump-thaw method (3 cycles). Then the mixture was heated at 200 °C. The reaction mixture was monitored by ^1H NMR spectroscopy by taking aliquot of the reaction mixture. After 1 day, the ratio of Ir(ttp)$SiPh_2Me$ **3g** and Ir(ttp)SiPhMeH **3e** was about 1.00:1.15.

Reaction between Ir(ttp)Cl(CO) 1b and Silanes with Base Added. General Procedure. The reaction between Ir(ttp)Cl(CO) **1b** and triethylsilane (**2a**) with the addition of K_3PO_4 is described as a typical example. Triethylsilane (1.1 mL, 500 equiv) was added to a mixture of Ir(ttp)Cl(CO) (12.6 mg, 0.014 mmol) and K_3PO_4 (29.7 mg, 0.140 mmol, 10 equiv), and the mixture was degassed by the freeze-pump-thaw method (3 cycles). Then the mixture was heated at 140 °C for 1

day. The crude product was purified by chromatography on alumina eluting with hexane. A purple solid of Ir(ttp)$SiEt_3$ **2b** (12.0 mg, 0.0123 mmol, 88%) was isolated.

Reaction between Ir(ttp)Cl(CO) 1b and Triethylsilane (2a) with K_3PO_4 (5 equiv). Triethylsilane (1.3 mL, 500 equiv) was added to a mixture of Ir(ttp)Cl(CO) (14.8 mg, 0.016 mmol) and K_3PO_4 (17.0 mg, 0.080 mmol, 5 equiv), then the mixture was heated at 140 °C for 1 day. A purple solid of Ir(ttp)$SiEt_3$ **3a** (7.2 mg, 0.0074 mmol, 46%) was isolated after column chromatography.

Reaction between Ir(ttp)Cl(CO) 1b and Triethylsilane (2a) with K_3PO_4 (20 equiv). Triethylsilane (1.4 mL, 500 equiv) was added to a mixture of Ir(ttp)Cl(CO) (15.8 mg, 0.017 mmol) and K_3PO_4 (72.2 mg, 0.340 mmol, 20 equiv), then the mixture was heated at 140 °C for 1 day. A purple solid of Ir(ttp)$SiEt_3$ **3a** (13.3 mg, 0.0136 mmol, 80%) was isolated after column chromatography.

Reaction between Ir(ttp)Cl(CO) 1b and Triethylsilane (2a) with K_2CO_3. Triethylsilane (1.0 mL, 500 equiv) was added to a mixture of Ir(ttp)Cl(CO) (12.2 mg, 0.013 mmol) and K_2CO_3 (18.0 mg, 0.130 mmol, 10 equiv), then the mixture was heated at 140 °C for 1 day. A purple solid of Ir(ttp)$SiEt_3$ **3a** (2.0 mg, 0.0020 mmol, 16%) was isolated after column chromatography.

Reaction between Ir(ttp)Cl(CO) 1b and Triethylsilane (2a) with KOH. Triethylsilane (1.0 mL, 500 equiv) was added to a mixture of Ir(ttp)Cl(CO) (12.2 mg, 0.013 mmol) and KOH (7.3 mg, 0.130 mmol, 10 equiv), then the mixture was heated at 140 °C for 1 day. A purple solid of Ir(ttp)$SiEt_3$ **3a** (4.7 mg, 0.0048 mmol, 37%) was isolated after column chromatography.

Reaction between Ir(ttp)Cl(CO) 1a and Triethylsilane (2a) with KF. Triethylsilane (1.3 mL, 500 equiv) was added to a mixture of Ir(ttp)Cl(CO) (15.3 mg, 0.017 mmol) and KF (9.9 mg, 0.170 mmol, 10 equiv), then the mixture was heated at 140 °C for 5 days. A purple solid of Ir(ttp)$SiEt_3$ **3a** (8.3 mg, 0.0085 mmol, 50%) was isolated after column chromatography.

Reaction between Ir(ttp)Cl(CO) 1a and Triethylsilane (2a) with CsCl. Triethylsilane (1.2 mL, 500 equiv) was added to a mixture of Ir(ttp)Cl(CO) (14.0 mg, 0.015 mmol) and CsCl (25.3 mg, 0.150 mmol, 10 equiv), then the mixture was heated at 140 °C for 6 days. A purple solid of Ir(ttp)$SiEt_3$ **3a** (<5%) was isolated after column chromatography.

Reaction between Ir(ttp)Cl(CO) 1a and Triethylsilane (2a) with KI. Triethylsilane (1.1 mL, 500 equiv) was added to a mixture of Ir(ttp)Cl(CO) (13.2 mg, 0.014 mmol) and KI (23.2 mg, 0.140 mmol, 10 equiv), then the mixture was heated at 140 °C for 5 days. A purple solid of Ir(ttp)$SiEt_3$ **3a** (1.9 mg, 0.0019 mmol, 14%) was isolated after column chromatography.

Reaction between Ir(ttp)Cl(CO) 1a and Triethylsilane (2a) with KOAc. Triethylsilane (1.2 mL, 500 equiv) was added to a mixture of Ir(ttp)Cl(CO) (14.4 mg, 0.016 mmol) and KOAc (15.7 mg, 0.160 mmol, 10 equiv), then the mixture was heated at 140 °C for 5 days. A purple solid of Ir(ttp)$SiEt_3$ **3a** (1.9 mg, 0.0019 mmol, 12%) was isolated after column chromatography.

Reactions between Ir(ttp)Cl(CO) 1a and Silanes in Solvent. General Procedure. The reaction of Ir(ttp)Cl(CO) **1a** with triethylsilane **(2a)** in benzene is described as a

typical example. Triethylsilane (0.22 mL, 100 equiv) was added to Ir(ttp)Cl(CO) (12.9 mg, 0.014 mmol) in benzene (1.0 mL), and the mixture was degassed by the freeze-pump-thaw method (3 cycles). Then the mixture was heated at 200 °C for 9 days. The crude product was purified by chromatography on alumina eluting with hexane. A purple solid of Ir(ttp)$SiEt_3$ **3a** (7.9 mg, 0.0081 mmol, 58%) was isolated.

Reaction between Ir(ttp)Cl(CO) 1a and Triethylsilane (2a) in Cyclohexane. Triethylsilane (0.22 mL, 100 equiv) was added to Ir(ttp)Cl(CO) (12.6 mg, 0.014 mmol) in cyclohexane (1.0 mL). Then the mixture was heated at 200 °C for 9 days. A purple solid of Ir(ttp)$SiEt_3$ **3a** (8.2 mg, 0.0084 mmol, 60%) was isolated after column chromatography.

Reaction between Ir(ttp)Cl(CO) 1a and Triethoxylsilane (2b) in Benzene. Triethoxylsilane (0.24 mL, 100 equiv) was added to Ir(ttp)Cl(CO) (12.2 mg, 0.013 mmol) in benzene (1.0 mL). Then the mixture was heated at 200 °C for 6 hours. A purple solid of Ir(ttp)$Si(OEt)_3$ **3b** (11.3 mg, 0.0110 mmol, 85%) was isolated after column chromatography.

Reaction between Ir(ttp)Cl(CO) 1a and Triethoxylsilane (2b) in Cyclohexane. Triethoxylsilane (0.26 mL, 100 equiv) was added to Ir(ttp)Cl(CO) (12.9 mg, 0.014 mmol) in cyclohexane (1.0 mL). Then the mixture was heated at 200 °C for 12 hours. A purple solid of Ir(ttp)$Si(OEt)_3$ **3b** (12.6 mg, 0.0123 mmol, 88%) was isolated after column chromatography.

Reaction between Ir(ttp)Cl(CO) 1a and Triethylsilane (2a) in Benzene with K_3PO_4 Added. Triethylsilane (0.26 mL, 100 equiv) was added to a mixture of

Ir(ttp)Cl(CO) (14.4 mg, 0.016 mmol) and K_3PO_4 (34.0 mg, 0.160 mmol, 10 equiv) in benzene (1.0 mL), and the mixture was degassed by the freeze-pump-thaw method (3 cycles). Then the mixture was heated at 140 °C for 3 days. The crude product was purified by chromatography on alumina eluting with hexane. A purple solid of $Ir(ttp)SiEt_3$ **3a** (14.4 mg, 0.0147 mmol, 92%) was isolated.

Reaction between Ir(ttp)Cl(CO) 1a and Triethylsilane (2a) in Benzene-d_6 with K_3PO_4 Added in Sealed-NMR Tube. Triethylsilane (90 μL, 100 equiv) was added to a mixture of Ir(ttp)Cl(CO) (5.4 mg, 0.0058 mmol) and K_3PO_4 (12.3 mg, 0.058 mmol, 10 equiv) in benzene-d_6 (0.5 mL) in a NMR tube with a rotaflo stopper, and the mixture was degassed by the freeze-pump-thaw method (3 cycles). The NMR tube was flame-sealed under vacuum. Then the mixture was heated at 140 °C. Monitor the reaction by ^1H NMR spectroscopy. After 1.5 hours, Ir(ttp)H was observed first without any $Ir(ttp)SiEt_3$.

Reaction between Ir(ttp)(BF_4)(CO) 1c and Triethylsilane (2a). Triethylsilane (1.0 mL, 500 equiv) was added to Ir(ttp)(BF_4)(CO) (12.8 mg, 0.013 mmol) and the mixture was degassed by the freeze-pump-thaw method (3 cycles). Then the mixture was heated at 200 °C for 1 day. The crude product was purified by chromatography on alumina eluting with hexane. A purple solid of $Ir(ttp)SiEt_3$ **3a** (7.7 mg, 0.0079 mmol, 61%) was isolated.

Reaction between Ir(ttp)H 1d and Triethylsilane (2a). Triethylsilane (1.3 mL, 500 equiv) was added to Ir(ttp)H (14.0 mg, 0.016 mmol), and the mixture was degassed by the freeze-pump-thaw method (3 cycles). Then the mixture was heated at 140 °C for 2

days. The crude product was purified by chromatography on alumina eluting with hexane. A purple solid of Ir(ttp)$SiEt_3$ **3a** (14.4 mg, 0.0147 mmol, 92%) was isolated.

Reaction between Ir(ttp)H 1d and Diphenylmethylsilane (2g). Diphenylmethylsilane (1.0 mL, 500 equiv) was added to Ir(ttp)H (9.0 mg, 0.010 mmol), and the mixture was degassed by the freeze-pump-thaw method (3 cycles). Then the mixture was heated at 200 °C. The reaction mixture was monitored by ^1H NMR spectroscopy by taking aliquot of the reaction mixture. After 2 hours, the ratio of Ir(ttp)$SiPh_2Me$ **3g** and Ir(ttp)SiPhMeH **3e** was about 1.00:0.71.

Reactions between Ir(ttp)Me 1b and Silanes. General Procedure. The reaction of Ir(ttp)Me **1b** with triethylsilane **(2a)** is described as a typical example. Triethylsilane (1.0 mL, 500 equiv) was added to Ir(ttp)Me (11.1 mg, 0.013 mmol), and the mixture was degassed by the freeze-pump-thaw method (3 cycles). Then the mixture was heated at 200 °C for 5 days. The crude product was purified by chromatography on alumina eluting with hexane. A purple solid of Ir(ttp)$SiEt_3$ **3a** (10.5 mg, 0.0108 mmol, 83%) was isolated.

Reaction between Ir(ttp)Me 1b and Triethylsilane (2a). Triethylsilane (1.2 mL, 500 equiv) and Ir(ttp)Me (13.4 mg, 0.015 mmol) were heated at 150 °C for 8 days. A purple solid of Ir(ttp)$SiEt_3$ **3a** (1.8 mg, 0.0018 mmol, 12%) was isolated after column chromatography.

Reaction between Ir(ttp)Me 1b and Triethoxysilane (2b). Triethoxysilane (1.1 mL, 500 equiv) and Ir(ttp)Me (10.9 mg, 0.012 mmol) were heated at 200 °C for 7 days. A

purple solid of Ir(ttp)Si(OEt)$_3$ **3b** (2.0 mg, 0.0019 mmol, 16%) was isolated after column chromatography.

Reactions between Ir(ttp)Me 1b and Silanes in Benzene. General Procedure. The reaction between Ir(ttp)Me **1b** and triethylsilane (**2a**) in benzene is described as a typical example. Triethylsilane (0.24 mL, 100 equiv) was added to Ir(ttp)Me (12.9 mg, 0.015 mmol) in benzene (1.0 mL), and the mixture was degassed by the freeze-pump-thaw method (3 cycles). Then the mixture was heated at 200 °C for 7 days. The crude product was purified by chromatography on alumina eluting with hexane. A purple solid of Ir(ttp)SiEt$_3$ **3a** (1.5 mg, 0.0015 mmol, 10%) was isolated.

Reaction between Ir(ttp)Me 1b and Triethoxylsilane (2b) in Benzene. Triethoxylsilane (0.26 mL, 100 equiv) was added to Ir(ttp)Me (11.9 mg, 0.014 mmol) in benzene (1.0 mL). Then the mixture was heated at 200 °C for 4 days. A purple solid of Ir(ttp)Si(OEt)$_3$ **3b** (1.1 mg, 0.0011 mmol, 8%) was isolated after column chromatography.

Reaction between Ir(ttp)Me 1b and Triethylsilane (2a) with Base Added. General Procedure. The reaction between Ir(ttp)Me **1b** and triethylsilane (**2a**) with the addition of K_3PO_4 is described as a typical example. Triethylsilane (1.2 mL, 500 equiv) was added to a mixture of Ir(ttp)Me (13.1 mg, 0.015 mmol) and K_3PO_4 (31.8 mg, 0.150 mmol, 10 equiv), and the mixture was degassed by the freeze-pump-thaw method (3 cycles). Then the mixture was heated at 150 °C for 8 days. The crude product was purified by chromatography on alumina eluting with hexane. A purple solid of Ir(ttp)SiEt$_3$ **3a** (6.4 mg, 0.0066 mmol, 44%) was isolated.

Reaction between Ir(ttp)Me 1b and Triethylsilane (2a) with KOH. Triethylsilane (1.1 mL, 500 equiv) was added to a mixture of Ir(ttp)Me (12.3 mg, 0.014 mmol) and KOH (7.8 mg, 0.140 mmol, 10 equiv). Then the mixture was heated at 150 °C for 8 days. Only trace amount of Ir(ttp)$SiEt_3$ **3a** (<5%) was observed according to ^1H NMR spectroscopy of the crude reaction mixture.

Reaction between Ir(ttp)Me 1b and Triethylsilane (2a) with K_2CO_3. Triethylsilane (1.0 mL, 500 equiv) was added to a mixture of Ir(ttp)Me (11.8 mg, 0.013 mmol) and K_2CO_3 (18.0 mg, 0.130 mmol, 10 equiv). Then the mixture was heated at 150 °C for 8 days. A purple solid of Ir(ttp)$SiEt_3$ **3a** (1.8 mg, 0.0018 mmol, 14%) was isolated after column chromatography.

Reaction between Ir(ttp)Me 1b and Triethylsilane (2a) with KF. Triethylsilane (1.2 mL, 500 equiv) was added to a mixture of Ir(ttp)Me (12.8 mg, 0.015 mmol) and KF (8.7 mg, 0.150 mmol, 10 equiv). Then the mixture was heated at 150 °C for 8 days. A purple solid of Ir(ttp)$SiEt_3$ **3a** (2.2 mg, 0.0023 mmol, 15%) was isolated after column chromatography.

Reaction between Ir(ttp)Me 1b and Triethylsilane (2a) with CsCl. Triethylsilane (1.3 mL, 500 equiv) was added to a mixture of Ir(ttp)Me (14.1 mg, 0.016 mmol) and CsCl (26.9 mg, 0.160 mmol, 10 equiv). Then the mixture was heated at 150 °C for 8 days. A purple solid of Ir(ttp)$SiEt_3$ **3a** (0.9 mg, 0.0009 mmol, 6%) was isolated after column chromatography.

Reaction between Ir(ttp)Me 1b and Triethylsilane (2a) with KI. Triethylsilane (1.1 mL, 500 equiv) was added to a mixture of Ir(ttp)Me (12.1 mg, 0.014 mmol) and KI

(23.2 mg, 0.140 mmol, 10 equiv). Then the mixture was heated at 150 °C for 8 days. A purple solid of Ir(ttp)$SiEt_3$ **3a** (1.2 mg, 0.0012 mmol, 9%) was isolated after column chromatography.

Reaction between Ir(ttp)Me 1b and Triethylsilane (2a) with KOAc. Triethylsilane (1.2 mL, 500 equiv) was added to a mixture of Ir(ttp)Me (13.3 mg, 0.015 mmol) and KOAc (14.7 mg, 0.150 mmol, 10 equiv). Then the mixture was heated at 150 °C for 8 days. A purple solid of Ir(ttp)$SiEt_3$ **3a** (8.8 mg, 0.0090 mmol, 60%) was isolated.

Reaction between Ir(ttp)$SiPh_2$Me 3g and Diphenylmethylsilane (2g). Diphenylmethylsilane (1.2 mL, 500 equiv) was added to Ir(ttp)$SiPh_2$Me (12.2 mg, 0.012 mmol) and the mixture was degassed by the freeze-pump-thaw method (3 cycles). Then the mixture was heated at 200 °C for 2 days. The crude product was purified by chromatography on alumina eluting with hexane. A purple solid of Ir(ttp)$SiPh_2$Me **3g** (4.2 mg, 0.0040 mmol, 33%) was recovered, and 31% yield of Ir(ttp)SiPhMeH **3e** was produced according to ^{1}H NMR spectrum of the crude reaction mixture.

Reaction between Ir(ttp)SiPhMeH 3e and Diphenylmethylsilane (2g). Diphenylmethylsilane (1.5 mL, 500 equiv) was added to Ir(ttp)SiPhMeH (14.6 mg, 0.015 mmol) and the mixture was degassed by the freeze-pump-thaw method (3 cycles). Then the mixture was heated at 200 °C for 2 days. The crude product was purified by chromatography on alumina eluting with hexane. A purple solid of Ir(ttp)$SiPh_2$Me **3g** (6.4 mg, 0.0060 mmol, 40%) was isolated, and 46% yield of

Ir(ttp)SiPhMeH **3e** remained according to ^{1}H NMR spectrum of the crude reaction mixture.

Reaction between Ir(ttp)SiEt$_3$ 3a and Benzyldimethylsilane (2c). Benzyldimethylsilane (1.0 mL, 500 equiv) was added to Ir(ttp)SiEt$_3$ (12.2 mg, 0.012 mmol) and the mixture was degassed by the freeze-pump-thaw method (3 cycles). Then the mixture was heated at 200 °C for 2 days. The crude product was purified by chromatography on alumina eluting with hexane. A purple solid of Ir(ttp)SiBnMe$_2$ **3c** (9.9 mg, 0.0098 mmol, 82%) was isolated.

Reaction between Ir(ttp)SiBnMe$_2$ 3c and Triethylsilane (2a). Triethylsilane (1.2 mL, 500 equiv) was added to Ir(ttp)SiBnMe$_2$ (15.2 mg, 0.015 mmol) and the mixture was degassed by the freeze-pump-thaw method (3 cycles). Then the mixture was heated at 200 °C for 4 days, and **3c** was not consumed completely. The crude product was purified by chromatography on alumina eluting with hexane. A purple solid of Ir(ttp)SiEt$_3$ **3a** (2.9 mg, 0.0030 mmol, 20%) was isolated, and Ir(ttp)SiBnMe$_2$ **3c** (10.8 mg, 0.0106 mmol, 71%) was recovered.

References

(1) *http://www.twtor_homework.com/Chemistry_Help/electronegativity_table/electro-negativity. html.* Accessed on December 6, 2009.

(2) Mazumder, B. *Silicon and its Compounds,* Science Publishers, Inc.: Enfield, NH, USA, 2000.

(3) *http://web.mit.edu/course/3/3.091/www3/pt/pert2.html.* Accessed on December 6, 2009.

(4) Bassindale, A. R.; Glynn, S. J ; Taylor, P. G. In *The Chemistry of Organic Silicon Compounds*, Vol. 2 Rappoport, Z., Apeloig, Y., Eds.; Wiley: Chichester, U.K, 1998, Part 1, pp 495-511.

(5) Luo, Y.-R. *Handbook of Bond Dissociation Energies in Organic Compounds*, CRC Press: Boca Raton, FL, 2003.

(6) (a) Schubert, U. *Advances in Organosilicon Chemistry*, Marcinicec, B.; Chojnowski, J.; Eds.; Gordon and Breach: Yverdon-lesBains, Switzerland, 1994. (b) Schubert, U. *Adv. Organomet. Chem.* **1990**, *30*, 151-187.

(7) (a) Corey, J. Y.; Braddock-Wilking, J. *Chem. Rev.* **1999**, *99*, 175-292. (b) Kubas, G. J. *Metal Dihydrogen and Sigma-Bond Complexes: Structure, Theory, and Reactivity*, Kluwer Academic/Plenum Publishers: New York, 2001.

(8) Crabtree, R. H. *Angew. Chem. Int. Ed. Engl.* **1993**, *32*, 789-805.

(9) Piper, T. S.; Lemal, D.; Wilkinson, G. *Naturwissenschaften* **1956**, *43*, 129.

(10) Speier, J. L.; Webster, J. A.; Barnes, G. H. *J. Am. Chem. Soc.* **1957**, *79*, 974-979.

(11) (a) Tilley, T. D. *The Chemistry of Organic Silicon Compounds Part I*, Patai, S.; Rappoport, Z. Eds.; John Wiley & Sons Ltd.: New York, 1989, Vol. 2, Chapter 24. (b) Tilley, T. D. *The Silicon-Heteroatom Bond*, Patai, S.; Rappoport, Z. Eds.; John Wiley & Sons Ltd.: New York, 1991, Chapter 10.

(12) (a) Albright, T. A.; Burdett, J. K.; whangbo, M. H. *Orbital Interactions in Chemistry*, John Wiley & Sons Ltd.: New York, 1985. (b) Berry, A. D.; Corey, E. R.; Hagen, A. P.; MacDiarmid, A. G.; Saalfeld, F. E.; Wayland, B. B. *J. Am. Chem. Soc.* **1970**, *92*, 1940-1945.

(13) Lin, Z. *Chem. Soc. Rev.* **2002**, *31*, 239-245.

(14) Hamilton, R. S.; Corey, E. R. *Abstracts, 156th National Meeting of the American Chemical Society*, Atlantic City, K, J., Sept 1968.

(15) Manojlović-Muir, L.; Muir, K. W.; Ibers, J. A. *Inorg. Chem.* **1970**, *9*, 447-452.

(16) Robiette, A. G.; Sheldrick, G. M.; Simpson, R. N. F.; Aylett, B. J.; Campbell, J. A. *J. Organomet. Chem.* **1968**, *14*, 279-283.

(17) Muir, K. W.; Ibers, J. A. *Inorg. Chem.* **1970**, *9*, 440-447.

(18) Tsukada, N.; Hartwig, J. F. *J. Am. Chem. Soc.* **2005**, *127*, 5022-5023

(19) Yamanoi, Y.; Nishihara, H. *Tetrahedron Lett.* **2006**, *47*, 7157-7161.

(20) (a) Yang, J.; Brookhart, M. *J. Am. Chem. Soc.* **2007**, *129*, 12656-12657. (b) Yamanoi, Y.; Taira, T.; Sato, J.-i.; Nakamula, I.; Nishihara, H. *Org. Lett.* **2007**, *22*, 4543-4546.

(21) Rankin, M. A.; MacLean, D. F.; Schatte, G.; McDonald, R.; Stradiotto, M. *J. Am. Chem. Soc.* **2007**, *129*, 15855-15864.

(22) Goikhman, R.; Milstein, D. *Chem. Eur. J.* **2005**, *11*, 2983-2988.

(23) Yamanoi, Y.; Nishihara, H. *J. Org. Chem.* **2008**, *73*, 6671-6678.

(24) Esteruelas, M. A.; Herrero, J.; Oliván, M. *Organometallics* **2004**, *23*, 3891-3897.

(25) Esteruelas, M. A.; Herrero, J.; Oro, L. A. *Organometallics* **1993**, *12*, 2377-2379.

(26) Reis, P. M.; Romão, C. C.; Royo, B. *Dalton Trans.* **2006**, 1842-1846.

(27) Mizuta, T.; Sakaguchi, S.; Ishii, Y. *J. Org. Chem.* **2005**, *70*, 2195-2199.

(28) Mirza-Aghayan, M.; Boukherroub, R.; Bolourtchian, M. *J. Organomet. Chem.* **2005**, *690*, 2372-2375.

(29) Boury, B.; Corriu, R. J. P.; Leclercq, D.; Mutin, P. H.; Planeix, J.-M.; Vioux, A. *Organometallics* **1991**, *10*, 1457-1461.

(30) (a) Taw, F. L.; Bergman, R. G.; Brookhart, M. *Organometallics* **2004**, *23*, 886-890. (b) Karshtedt, D.; Bell, A. T.; Tilley, T. D. *Organometallics* **2006**, *25*, 4471-4482.

(31) (a) Zhang, L.; Chan, K. S. *Organometallics* **2006**, *25*, 4822-4829. (b) Klei, S. R.; Tilley, T. D.; Bergman, R. G. *Organometallics* **2002**, *21*, 3376-3387.

(32) (a) Fernandez, M. J.; Maitlis, P. M. *J. Chem. Soc., Dalton Trans.* **1984**, 2063-2066. (b) Klei, S. R.; Tilley, T. D.; Bergman, R. G. *J. Am. Chem. Soc.* **2000**, *122*, 1816-1817.

(33) (a) Radu, N. S.; Tilley, T. D. *J. Am. Chem. Soc.* **1995**, *117*, 5863-5864. (b) Ziegler, T.; Folga, E. *J. Organomet. Chem.* **1994**, *478*, 57-65. (c) Woo, H.-G.; Walzer, J. F.; Tilley, T. D. *J. Am. Chem. Soc.* **1992**, *114*, 7047-7055. (d) Perutz, R. N.; Sabo-Etienne, S. *Angew. Chem., Int. Ed.* **2007**, *46*, 2578-2592.

(34) Wagner, R. W.; Lawrence, D. S.; Lindsey, J. S. *Tetrahedron Lett.* **1987**, *28*, 3069-3070.

(35) (a) Yeung, S. K.; Chan, K. S. *Organometallics* **2005**, *24*, 6426-6430. (b) Yeung, S. K. *Ph. D. Thesis,* The Chinese University of Hong Kong, 2005.

(36) van der Ent, A.; Onderdelinden, A. L. *Inorg. Synth.* **1973**, *14*, 92-95.

(37) Song, X.; Chan, K. S. *Organometallics* **2007**, *26*, 965-970.

(38) Tolman, C. A. *Chem. Rev.* **1977**, *77*, 313-348.

(39) (a) Hester, D. M.; Sun, J.; Harper, A. W.; Yang, G. K. *J. Am. Chem. Soc.* **1992**, *114*, 5234-5240. (b) Goikhman, R.; Milstein, D. *Chem. Eur. J.* **2005**, *11*, 2983-2988. (c) Bunten, K. A.; Chen, L.; Fernandez, A. L.; Poë, A. J. *Coord. Chem. Rev.* **2002**, *233-234*, 41-51.

(40) *http://evans.harvard.edu/pdf/evans_pKa_table.pdf.* Accessed on December 6, 2009.

(41) Ogoshi, H.; Setsune, J.-I.; Yoshida, Z.-I. *J. Organomet. Chem.* **1978**, *159*, 317-328.

(42) (a) Mizutani, T.; Uesaka, T.; Ogoshi, H. *Organometallics* **1995**, *14*, 341-346. (b) Tse, A. K.-S.; Wu, B.-M.; Mak, T. C. W.; Chan, K. S. *J. Organomet. Chem.* **1998**, *568*, 257-261.

(43) (a) Goikhman, R.; Aizenberg, M.; Kraatz, H.-B.; Milstein, D. *J. Am. Chem. Soc.* **1995**, *117*, 5865-5866. (b) Simons, R. S.; Gallucci, J. C.; Tessier, C. A.; Youngs, W. J. *J. Organomet. Chem.* **2002**, *654*, 224-228. (c) Klei, S. R.; Tilley, T. D.; Bergman, R. G. *Organometallics* **2001**, *20*, 3220-3222. (d) Diversi, P.; Marchetti, F.; Ermini, V.; Matteoni, S. *J. Organomet. Chem.* **2000**, *593-594*, 154-160.

(44) (a) Vastine, B. A.; Hall, M. B. *J. Am. Chem. Soc.* **2007**, *129*, 12068-12069. (b) Webster, C. E.; Hall, M. B. *Coord. Chem. Rev.* **2003**, *238-239*, 315-331.

(45) Wayland, B. B.; Ba, S.; Sherry, A. E. *J. Am. Chem. Soc.* **1991**, *113*, 5305-5311.

(46) (a) Corriu, R. J. P.; Guerin, C.; Henner, B. J. L.; Wang, Q. *Orgnaometallics* **1991**, *10*, 3200-3205. (b) Wan, Y.; Verkade, J. G. *J. Am. Chem. Soc.* **1995**, *117*, 141-156. (c) Damrauer, R.; Crowell, A. J.; Craig, C. F. *J. Am. Chem. Soc.* **2003**, *125*, 10759-10766. (d) Kinrade, S. D.; Del Nin, J. W.; Schach, A. S.; Sloan, T. A.; Wilson, K. L.; Knight, C. T. G. *Science* **1999**, *285*, 1542-1545. (e) Damrauer, R.; O'Connell, B.; Danahey, S. E.; Simon, R. *Organometallics* **1989**, *8*, 1167-1171.

Chapter 3 Base-Promoted Competitive Aromatic Carbon-Fluorine (C-F) and Carbon-Hydrogen (C-H) Bond Activation of Fluorobenzenes by Iridium Porphyrin Triethylsilyl

3.1 Introduction

3.1.1 Properties of Fluorobenzenes

The electronegativity (EN) of fluorine atom (4.0) is the largest among all the elements.[1] The aryl carbon-fluorine (C-F) bond length (1.34 Å) is the shortest next to an aryl carbon-hydrogen (C-H) bond (1.08 Å).[2] However, the bond dissociation energy (BDE) of an aryl C-F bond (126 kcal mol^{-1}) is much larger than that of an aryl C-H bond (110 kcal mol^{-1}) and other aryl carbon-halogen (C-X) bonds (X = Cl, 95 kcal mol^{-1}; X = Br, 79 kcal mol^{-1}).[3] Table 3.1 shows some selected properties of aryl hydrogen and halogen bonds.

Table 3.1 Selected Properties of Aryl Hydrogen and Halogen Bonds

Element	Electronegativity[1] (Pauling)	Ph-X / Å	BDE[3] Ph-X / kcal mol^{-1}
H	2.1	1.08[2]	110
F	4.0	1.34[4]	126
Cl	3.0	1.70[4]	95
Br	2.8	1.90[5]	79

Due to the large electronegativity of fluorine atom, an inductive ($-I_\sigma$) effect is induced to reduce the electron density at the carbon of a C-F bond. On the other hand, unshared electron pairs of fluorine bonded to a sp^2-carbon interact with π-electrons

repulsively to push the π-electrons to a *β*-carbon ($+I_\pi$ effect). Same as other halogen atoms, the lone pair electrons of fluorine can also resonate with the π-electron system (+R effect). Therefore, the electron density at the *ortho-* or *para*-carbon of aromatic compounds increases (Figure 3.1a). Fluorobenzene can give *ortho-* and *para*-substituted products via electrophilic aromatic substitution (S_EAr) by a predominant +R effect on the stabilization of intermediates (Figure 3.1b). Similarly, fluorobenzene can also undergo nucleophilic aromatic substitution (S_NAr) to give mainly *meta*-substitution product via +I stabilization effect on the intermediates (Figure 3.1c).

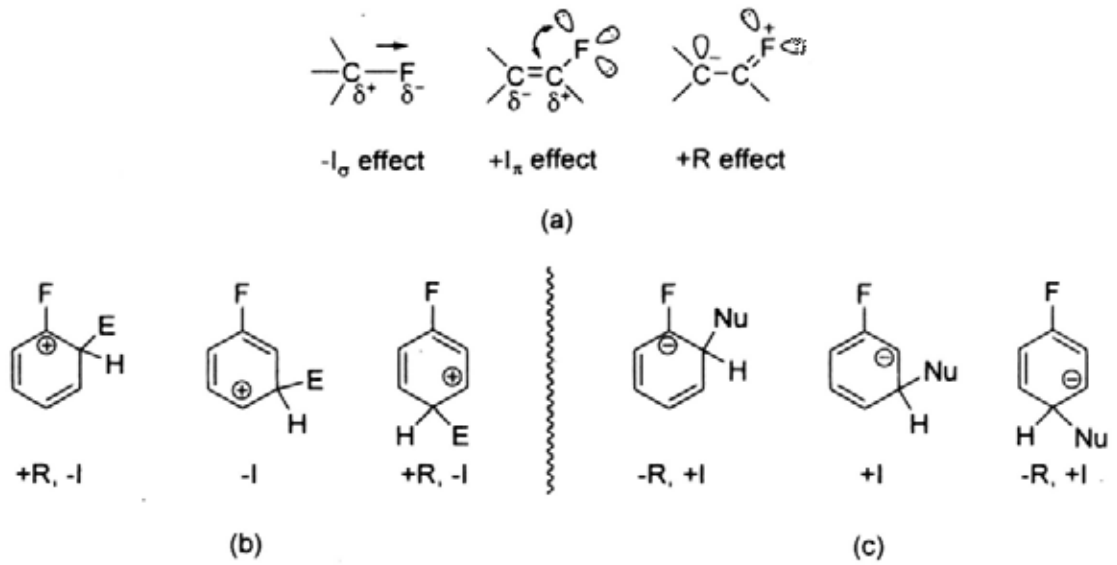

Figure 3.1 (a) Fluorine electronic effect; (b) Regioselectivity of electrophilic aromatic substitution; (c) Regioselectivity of nucleophilic aromatic substitution.

3.1.2 History of C-F Bond Activations

Carbon-fluorine bond activation of fluorocarbons with transition metal complexes has been extensively investigated due to the interests in the fundamental understanding, and the search for new routes to defluorinate or synthesize fluoroorganic and fluoroorganometallic compounds.[6] Table 3.2 summarizes some

reviews relevant to the C-F bond activation with transition metal complexes.[6-16] The C-F bond activation has been widely applied in defluorination,[8] coordination,[9] and organic synthesis.[10]

Table 3.2 Reviews Relevant to C-F Bond Activation in Chronological Order

Year	Topic
1988[7]	Transition-metal dihalocarbene complexes
1994[6]	Activation of carbon-fluorine bonds by metal complexes
1997[11]	Recent advances in C-F bond activation
1997[9]	The coordination chemistry of the CF unit in fluorocarbons
2000[12]	Organometallic transformations demonstrate that fluorocarbons are reactive moleculaes
2002[13]	Routes to fluorinated organic derivatives by nickel mediated C-F activation of heteroaromatics
2002[8]	Metal-mediated reductive hydrodehalogenation of organic halides
2003[14]	Carbon-fluorine bond activation-looking at and learning from unsolvated systems
2003[15]	Activation of C-F bonds using $Cp^*_2ZrH_2$: a diversity of mechanisms
2005[16]	Carbon-fluorine bond activation by platinum group metal complexes
2009[10]	C-F bond activation in organic synthesis

3.1.3 Mechanistic Possibilities in Aromatic C-F Bond Activation

Transition-metal-mediated intermolecular aromatic C-F bond activation processes usually occur via the following possible pathways: (i) Oxidative addition (OA); (ii) Sigma bond metathesis (SBM); (iii) Nucleophilic aromatic substitution (S_NAr); (iv) Electron transfer (ET) (Table 3.3).[17]

Table 3.3 Possible Pathways for Aromatic C-F Bond Activation[17]

Process	Chemical Transformation
(i) Oxidative Addition	[M] + Ar-F ⟶ Ar-[M]-F
(ii) Sigma Bond Metathesis	
a. M-C Bond Formation, HF Elimination	H-[M] + Ar-F ⟶ Ar-[M] + H-F
b. M-C Bond Formation, SiF Elimination	R_3Si-[M] + Ar-F ⟶ Ar-[M] + R_3Si-F
c. Hydrodefluorination, M-F Bond Formation	H-[M] + Ar-F ⟶ F-[M] + Ar-H
(iii) Nucleophilic Aromatic Substitution	$[M]^-$ + Ar-F ⟶ Ar-[M] + F^-
(iv) Electron Transfer	$[M]^-$ + Ar-F ⟶ [M]· + $Ar\text{-}F^-$·
	$Ar\text{-}F^-$· ⟶ Ar· + X^-
	[M]· + Ar· ⟶ [M]-Ar

3.1.4 Competitive Aromatic C-F and C-H Bond Activation

Besides the aromatic C-F bonds, aromatic carbon-hydrogen (C-H) bonds in fluorobenzenes can compete for the bond activation. Generally, aromatic C-H bonds are weaker than C-F bonds by 16~25 kcal mol^{-1} (Table 3.4), therefore, the cleavage of aromatic C-H bonds is more kinetically favorable. Furthermore, the resultant fluoroaryl metal complexes are more stable (Table 3.5).[18a] It is also found that the bond strength of the rhodium aryl complexes is correlated with the p*K*a values of the

proton in fluorobenzenes.

Table 3.4 Bond Dissociation Energy (BDE) of C-F Bond and C-H Bond and p*Ka* values of Fluorobenzenes

Entry	ArF	BDE of C-F / kcal mol^{-1}	BDE[18a] of C-H / kcal mol^{-1}	p*Ka*[18b] (DMSO)
1	C_6H_6	---	117.1	44.7
2	C_6H_5F	125.6[2]	*o*-119.6	*o*-36.8
			m-117.3	*m*-42.3
			p-118.1	*p*-43.7
3	1,2-F_2-C_6H_4	---	*o*-119.6	*o*-33.9
			m-118.2	*m*-41.7
4	1,3-F_2-C_6H_4	---	*o*,o-122.4	*o*,*o*-28.7
			o-120.6	*o*-35.8
			m-117.6	*m*-39.9
5	1,4-F_2-C_6H_4	---	*o*-119.8	*o*-40.1
6	1,3,5-F_3-C_6H_3	138[19]	*o*,*o*-123.2	*o*,*o*-31.5
7	C_6HF_5	150[20]	*o*,*o*-123.0	*o*,*o*-29.0
8	C_6F_6	154[20]	---	---

Table 3.5 Calculated BDE and Relative BDE (kcal mol^{-1}) for Rh(η^5-C_5H_5)(H)(Ar^F)(PH_3)[18a]

Ar^F-H	Ar^F	D(Rh-Ar^F)	ΔD(Rh-Ar^F)$_{rel}$
C_6H_5-H	C_6H_5	61.3	0
C_6H_4F-H	2-F-C_6H_4	67.1	5.7
	3-F-C_6H_4	62.1	0.8
	4-F-C_6H_4	62.1	0.8
1,2-F_2-C_6H_3-H	2,3-F_2-C_6H_3	67.9	6.5
	3,4-F_2-C_6H_3	62.8	1.5
1,3-F_2-C_6H_3-H	2,4-F_2-C_6H_3	67.9	6.5
	2,6-F_2-C_6H_3	73.6	12.3
	3,5-F_2-C_6H_3	62.9	1.6
1,4-F_2-C_6H_3-H	2,5-F_2-C_6H_3	68.0	6.7
1,3,5-F_3-C_6H_2-H	2,4,6-F_3-C_6H_2	74.3	13.0
C_6F_5-H	C_6F_5	76.4	15.1

Tomás *et al.* reported the reaction of a hexahydride-osmium complex with aromatic ketones to generate *ortho*-selective C-H or C-F bond activation products, and the selectivity was substrate-dependent.[21] The reaction of hexahydride-osmium with aromatic ketones, such as acetophenone and benzophenone, the *ortho*-selective aromatic CHA products were isolated with the release of hydrogen molecule (eq 3.1). When 2,6-difluoroacetophenone and pentafluoroacetophenone were used, *ortho*-CFA

reaction occurred selectively with the concomitant loss of HF (eq 3.2). These results suggest that both aromatic C-F and C-H bonds can be broken under the reaction conditions. Then unsymmetrical non-perfluoroketones were used to examine the preference for the CFA and CHA in an aromatic ketone as shown in eq 3.3. For monofluorophenyl methyl ketone (a), the *ortho*-CHA is preferred over the *ortho*-CFA, whereas the *ortho*-CFA was preferred over the *ortho*-CHA for pentafluorophenyl phenyl ketone (b). In addition, the DFT calculations suggested that both C-H bond and C-F bond ruptures are thermodynamically favorable. The disfavored C-F bond activation process is likely due to the higher energy required to cleave a stronger C-F bond, although the C-F bond activation turns out to be much more exothermic than the C-H bond activation.

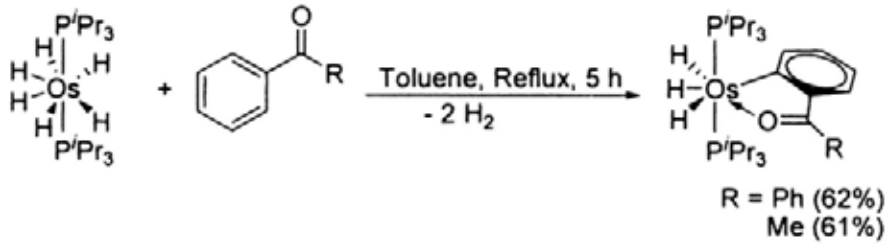

(3.1)

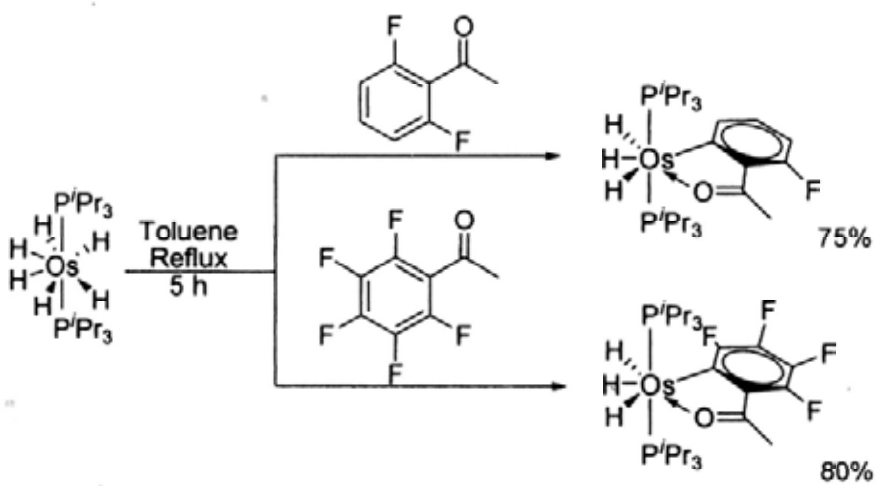

(3.2)

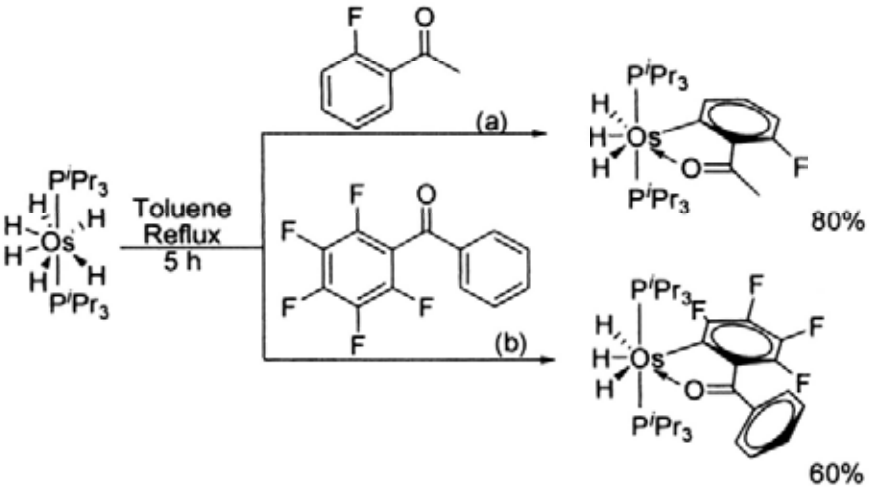

(3.3)

The absence of fluorine chelation-assistance effect has been demonstrated by Milstein and co-workers in 2003.[22] The electron-rich cationic Ir(I) system underwent facile aromatic C-H bond activation of haloarenes to give unsaturated, stable Ir(III) hydridophenyl complexes (Scheme 3.1). In this reaction system, the halogen (Cl or Br) was found to act as a directing group, leading to the high regioselective *ortho*-C-H bond activation kinetically and thermodynamically. However, the statistical C-H bond activation was observed in fluorobenzene, and also accounted by the poor ligating ability of fluorine atom.

Scheme 3.1 Aromatic C-H Bond Activation of Haloarenes by Ir(PNP) Complex

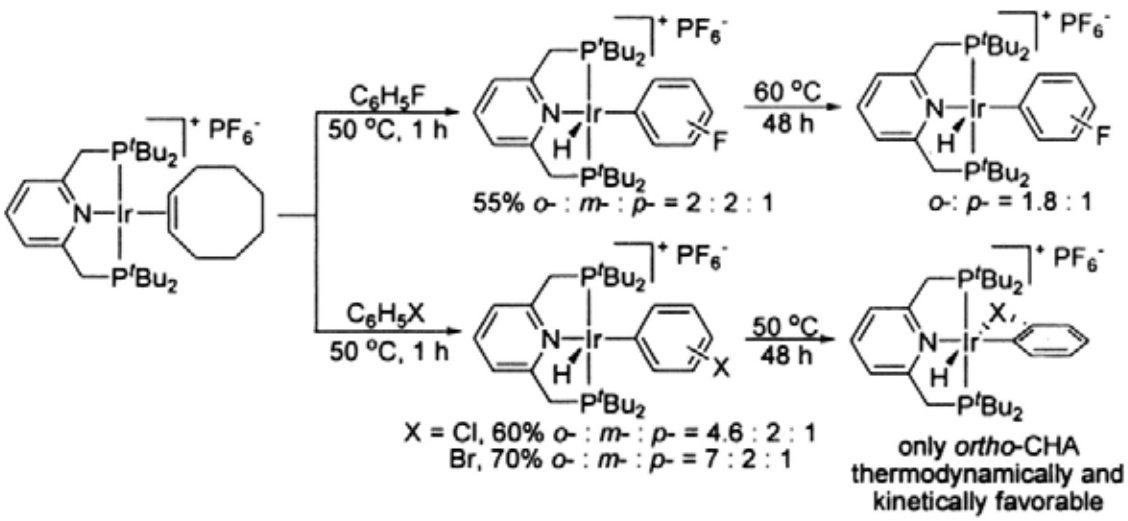

Later, Ozerov and co-workers explored a neutral PNP-iridium pincer complex reacted with chlorobenzene.[23] The reaction of C-H oxidative addition at room temperature firstly occurred to form a mixture of CHA products kinetically. Thermolysis of the mixture at 70 °C gave the *ortho*-selective C-H bond activation isomer. At a higher temperature of 120 °C, the C-Cl bond activation thermodynamic product was produced (Scheme 3.2a). X-ray structure of the *ortho*-CHA product indicated that the *ortho*-Cl was oriented appropriately for additional Cl→Ir donation which stabilized the product. It was also proposed that the *ortho*-ClC_6H_4 product simply formed the strongest σ-Ir-C bond among these isomeric ClC_6H_4 ligands. In addition, a mixture of four CHA products was produced at room temperature when neat fluorobenzene was used. Upon thermolysis (100 °C, 20 h), this mixture evolved into a mixture of only two isomers of CHA products without any C-F bond activation product observed (Scheme 3.2b). The *ortho* chelation stabilizing effect of fluorine is absent in comparison with that of chlorine.

Scheme 3.2 Competitive C-H and C-Cl Bond Activation by Ir(PNP) Complex

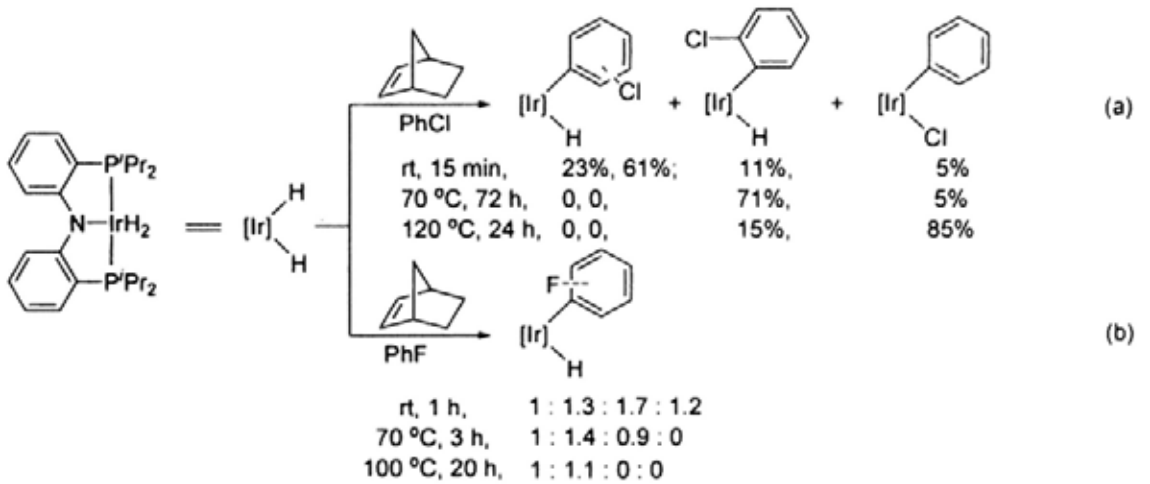

Recently, Jones and co-workers have reported that Tp'Rh(CNneophentyl)(Ar^F)H reacted with fluorobenzenes via photolysis to form C-H bond activation products.[24] They found that the stability of the Rh-C_{Ar} products was highly related to the number of *ortho* fluorines and mildly dependent on the total number of fluorine substituents. So the thermodynamic selectivity displayed a strong preference for C-H bond activation *ortho* to the maximum number of fluorine atoms, while the kinetic selectivity was directed by the steric hindrance of η^2-arene species (Scheme 3.3).

The above examples show that the origins of the competitive aromatic CHA and CFA as well as the regioselectivity in CHA of aryl fluorides, are not well understood.

Scheme 3.3 CHA of 1,3-F_2-C_6H_4 with [Tp'Rh(CNneophentyl)] Complex

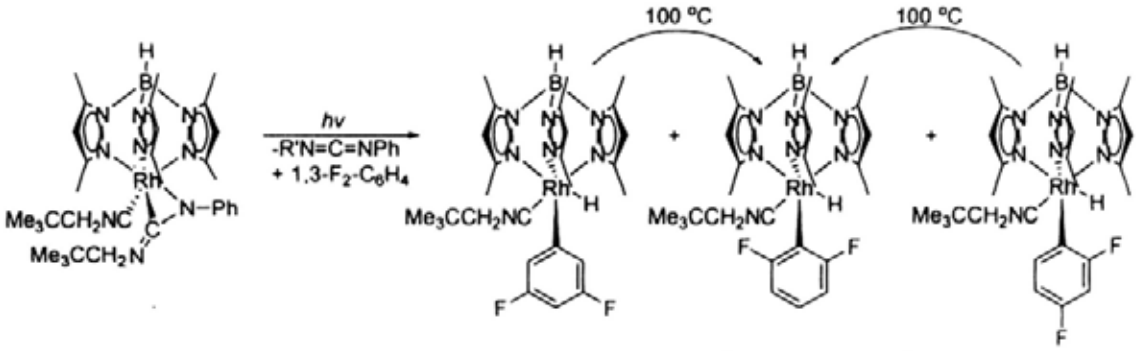

In Chan's group, Rh(ttp)Cl has been found to react with various fluorobenzenes in basic media to undergo competitive aromatic C-F bond and *ortho*-selective C-H bond activation reactions (eq 3.4).[25] Preliminary mechanistic studies suggested that Rh(ttp)$^-$ was the active intermediate towards the aromatic CFA reaction via an S_NAr pathway (Scheme 3.4), while the mechanism of the *ortho*-selective aromatic CHA reaction remains unclear.

$$\underset{100\ \text{equiv}}{\text{Rh(ttp)Cl + Ar-F}} \xrightarrow[1\ \text{d, 120 °C, N}_2]{\text{C}_6\text{H}_6\text{, KOH (10 equiv)}} \underset{\text{ArCFA}}{\text{Rh(ttp)Ar}} + \underset{\textit{ortho}\text{-CHA}}{\text{Rh(ttp)(}o\text{-F-Ar')}} \qquad (3.4)$$

Scheme 3.4 Proposed Mechanism for Aromatic C-F Bond Activation of Fluororbenzenes by Rh(ttp)Cl

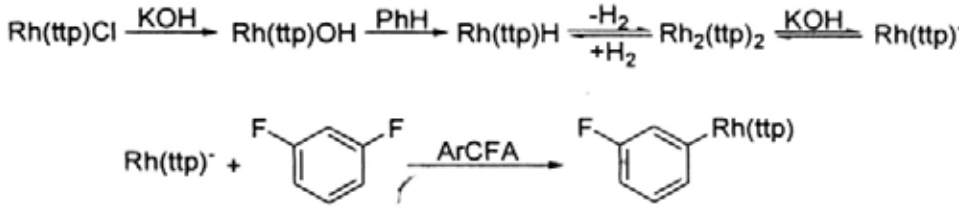

3.1.5 Objectives of This Work

The objectives of this work are (1) to extend the chemistry from rhodium to iridium porphyrin complexes to investigate the bond activation chemistry of fluorobenzenes, (2) to identify the active intermediates for aromatic carbon-fluorine and carbon-hydrogen bond activation, (3) to gain mechanistic understandings for the competitive reactions and (4) to find out the origins of the kinetic and thermodynamic stability of the aromatic CFA and CHA products.

3.2 Competitive Aromatic C-F and C-H Bond Activation of Fluorobenzenes by Iridium Porphyrin Triethylsilyl

3.2.1 Optimization of the Reaction Conditions

3.2.1.1 Temperature Effect

Initially, the reaction between Ir(ttp)$SiEt_3$[26] **1a** and 1,4-difluorobenzene **2d** was carried out in benzene at 120 °C with the addition of 10 equivalents of KOH. Only 29% yield of the aromatic CFA product Ir(ttp)(4-F-C_6H_4) **3e** was isolated together with the *ortho*-CHA product Ir(ttp)(2,5-F_2-C_6H_3) **3f** in trace amount (<5%), and the recovery of Ir(ttp)$SiEt_3$ **1a** in 56% yield (Table 3.6, entry 1). Upon increasing the reaction temperature to 150 °C, after 5 days, Ir(ttp)$SiEt_3$ **1a** almost completely reacted

and the ArCFA product **3e** was isolated in 85% yield together with a trace amount of the *ortho*-CHA product **3f** (Table 3.6, entry 2).

Table 3.6 Temperature Effect on Activation of 1,4-Difluorobenzene in Benzene by Ir(ttp)SiEt$_3$

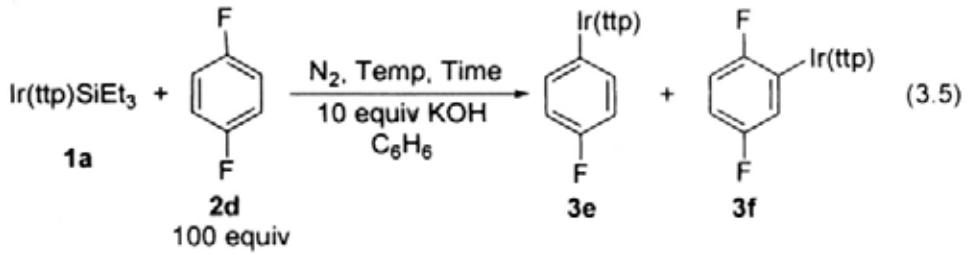

(3.5)

Entry	Temp / °C	Time / d	Yield / %			
			1a	**3e**	**3f**	Total
1	120	6	56	29	<5	85
2	150	5	6	85	<5	91[a]
3	200	3	<5	52	8	89[b]
4[c]	200	3	97	---	---	97

[a] Ir(ttp)C$_6$H$_5$ **3a** was isolated in trace amount (<5%). [b] Ir(ttp)C$_6$H$_5$ **3a** was isolated in 29% yield. [c] No KOH.

At 200 °C, besides the formation of the ArCFA product **3e** in 52% yield and the *ortho*-CHA product **3f** in 8% yield, Ir(ttp)C$_6$H$_5$ **3a** was also isolated in 29% yield (Table 3.6, entry 3). Ir(ttp)C$_6$H$_5$ **3a** was most likely generated from the competitive aromatic CHA reaction of benzene solvent. Upon more carefully monitoring the reaction by thin-layer chromatography (TLC) analysis, the ArCFA product **3e** was observed in 1 day before the formation of the *ortho*-CHA product **3f** after 2 days. Since Ir(ttp)SiEt$_3$ was stable at 200 °C for 3 days without the addition of KOH (Table

3.6, entry 4), KOH must play a key role for the conversion from **1a** to the active intermediates for the further reactions.

In order to examine the origin of $Ir(ttp)C_6H_5$ **3a** (Table 3.6, entry 3), benzene-d_6 was used instead of benzene as the solvent (eq 3.6). No $Ir(ttp)C_6H_5$ **3a**, but only $Ir(ttp)C_6D_5$ **3a'** was isolated in 6% yield. The result supports that $Ir(ttp)C_6H_5$ **3a** was formed from the ArCHA of benzene at higher temperature. The lower yield of **3a'** than **3a** is likely caused by the kinetic isotopic effect with the C-H bond cleavage involving in the rate determining step and the competitive decomposition of the intermediates.[27]

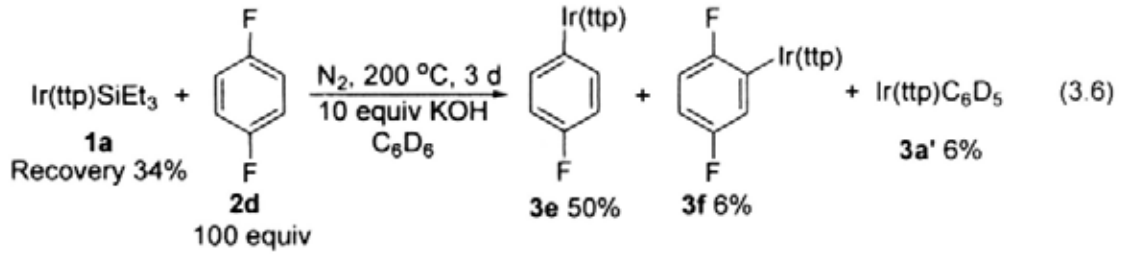

3.2.1.2 Base Effect

At 200 °C, the side-reaction of ArCHA of benzene occurred, therefore, the reaction conditions were further optimized at a lower temperature of 150 °C. Since the bond dissociation energy of silicon-fluorine bond (160 kcal mol^{-1})[3] is much larger than that of silicon-oxygen bond (132 kcal mol^{-1})[3], KF was also used to replace KOH as the basic additive. However, no reaction occurred even after 8 days and 94% yield of $Ir(ttp)SiEt_3$ **1a** was recovered (Table 3.7, entry 2). The stability of $Ir(ttp)SiEt_3$ towards KF is more likely due to the much poorer solubility and nucleophilicity of KF in benzene comparing with KOH.[28]

Table 3.7 Base Effect on Activation of 1,4-Difluorobenzene by Ir(ttp)SiEt$_3$

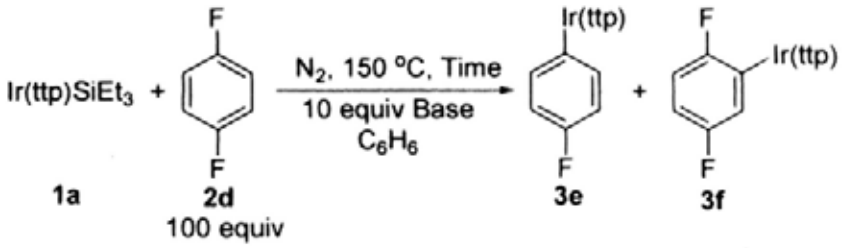

1a 2d 100 equiv 3e 3f

Entry	Base	Time / d	Yield / %			
			1a	**3e**	**3f**	Total
1	KOH	5	6	85	<5	91[a]
2	KF	8	94	---	---	94

[a] Ir(ttp)C$_6$H$_5$ **3a** was isolated in trace amount (<5%).

3.2.1.3 Base Loading Effect

Table 3.8 shows the KOH loading effect for the reaction between Ir(ttp)SiEt$_3$ **1a** and 1,4-difluorobenzene **2d** at 150 °C in benzene. When the KOH was decreased from 10 to 5 equivalents, the reaction rate and the ArCFA product yield were decreased although the yield of the *ortho*-CHA product was increased slightly (Table 3.8, entry 1). However, when KOH was increased to 20 equivalents, the reaction rate was enhanced and the total yield of iridium porphyrin species was slightly lower (Table 3.8, entry 3), which could be caused by the base-promoted decomposition of intermediates or products.

Table 3.8 Base Loading Effect on Activation of 1,4-difluorobenzene by Ir(ttp)SiEt$_3$

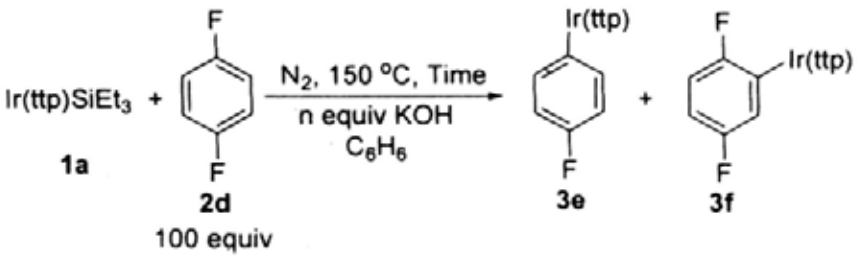

(3.8)

Entry	n	Time / d	Yield[a] / %			
			1a	**3e**	**3f**	Total
1	5	5	17	61	11	89
2	10	5	6	85	<5	91
3	20	4	<5	74	<5	74

[a] Ir(ttp)C$_6$H$_5$ **3a** was isolated in trace amount (<5%).

3.2.1.4 Aromatic CFA and CHA of 1,4-Difluorobenzene by Ir(ttp)SiEt$_3$ in Solvent-Free Conditions

From the above findings, at 150 °C, the ArCFA and *ortho*-CHA products yields were not good while at 200 °C, the side reaction of ArCHA of benzene was competitive. The reaction was further carried out in solvent-free conditions at 200 °C with the addition of 10 equivalents of KOH to minimize the reaction with benzene solvent. To our delight, after 3 days, the ArCFA product **3e** and the *ortho*-CHA product **3f** were isolated in 47% and 41% yield, respectively, with only a small amount of Ir(ttp)SiEt$_3$ **1a** (10%) left (eq 3.9). According to TLC analysis in the course of the reaction, the ArCFA product **3e** was observed within two hours, while the *ortho*-CHA product **3f** was formed after three hours. It suggests that the aromatic CFA

reaction is more kinetically favorable than the *ortho*-CHA reaction. Therefore, the optimal reaction conditions require KOH (10 equiv) at 200 °C.

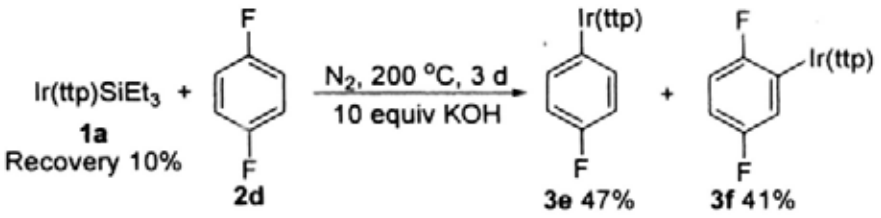

(3.9)

3.2.2 Bond Activations of Various Fluorobenzenes

To explore the scope of the activation reactions, various fluorobenzenes **2a-g** were applied to the optimal reaction conditions. The results are summarized in Table 3.9 and eq 3.10. Generally, the less fluorine-substituted fluorobenzenes reacted faster, likely due to the better solubility of $Ir(ttp)SiEt_3$ and the products (Table 3.9, entries 1-4 vs entries 5-7).

In particular, $Ir(ttp)SiEt_3$ **1a** reacted with fluorobenzene **2a** for 2 days gave the ArCFA product $Ir(ttp)C_6H_5$ **3a** in 64% yield, as well as three isomers of the aromatic CHA products **3b** and **3d-e** (Table 3.9, entry 1). Among these three isomers, the *meta*-CHA product **3d** was the major one and isolated in 18% yield. On the other hand, for 1,2-difluorobenzene **2b** and pentafluorobenzene **2f**, the *ortho*-selective aromatic CHA was observed. The ArCHA products **3c** and **3i** were also isolated as the major products in 89% and 56% yield, respectively (Table 3.9, entries 2 and 6). For 1,3-difluorobenzene **2c** and 1,3,5-trifluorobenzene **2e**, only the aromatic CFA products were isolated in 80% and 24% yield, respectively, while no aromatic CHA products were observed (Table 3.9, entries 3 and 5).

Table 3.9 Base-Promoted Competitive Aromatic CFA and CHA of fluorobenzenes by Ir(ttp)SiEt$_3$ in Solvent-Free Conditions

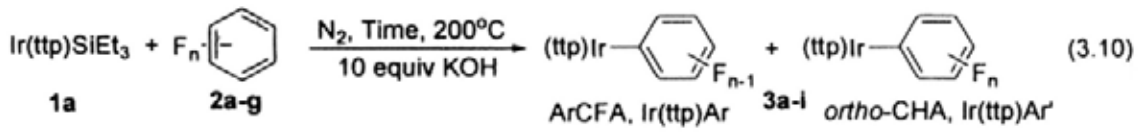

(3.10)

Entry	Sub	Time / d	Yield / %		
			Ar	Ar'	Total
1		2	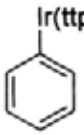	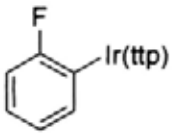	87[a]
	2a		**3a** 64	**3b** <5	
2	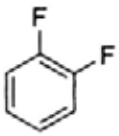	2	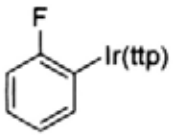	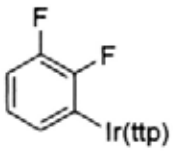	95
	2b		**3b** 6	**3c** 89	
3	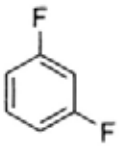	4	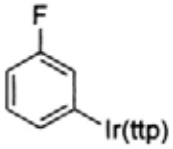	---	80
	2c		**3d** 80		
4		3	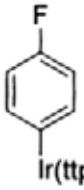	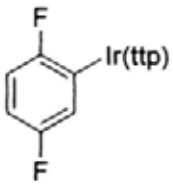	98[b]
	2d		**3e** 47	**3f** 41	
5	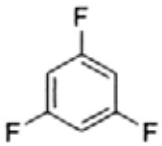	8	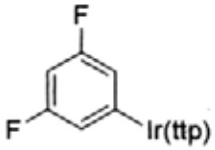	---	98[c]
	2e		**3g** 24		

6	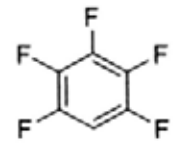 **2f**	6	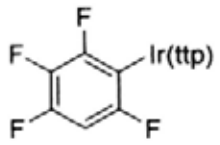 **3h** <5	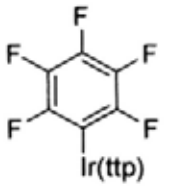 **3i** 56	94[d]
7	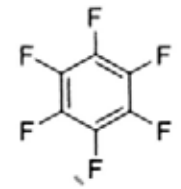 **2g**	8	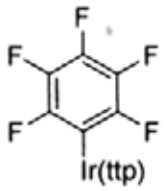 **3i** 50	---	74[e]

[a] Both *meta*- and *para*-CHA products **3d** and **3e** were isolated in 18% and 5% yield, respectively. [b] **1a** was recovered in 10% yield. [c] **1a** was recovered in 74% yield. [d] **1a** was recovered in 38% yield. [e] **1a** was recovered in 24% yield.

Perutz *et al.* has reported that fluorine-substituents, especially the *ortho*-fluorine substituent stabilize the Rh-C(α) bond of some rhodium aryl complexes.[18a] They also found that the total charge on the aryl ring (Figure 3.2a) but not the charge on C_{ipso} (Figure 3.2b) increased with the increasing Rh-C bond energy indicating that the more ionic Rh-C bond is stronger. However, it does not correlate with the bond strength of the iridium porphyrin aryls. In most cases, *meta*-fluorine substituent aryl iridium porphyrin complexes, such as **3c-d**, **3f**, **3g** and **3i**, are the major products.

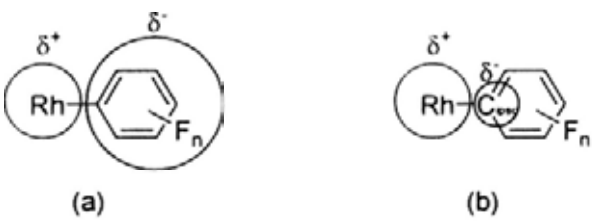

Figure 3.2 Ionization of covalent Rh-C bond driven by the fluorine substituents

The Hammett constants correlate better with the thermodynamic stability of the iridium porphyrin aryls. The *meta*-fluorine substituent (σ_m = 0.34)[28] exerts stronger inductive effect in strengthening the covalent Ir-C bond by polarization comparing with the *para*-fluorine substituent (σ_p = 0.06).[28] For the *ortho*-fluorine substituent, some steric destabilizing effect probably exists, since there is no chelation interaction observed between the Ir center and the *ortho*-fluorine atom (Table 3.11). More probably electron withdrawing effect of fluorine exists. On the other hand, in *ortho*- and *para*-fluorine substituted aromatic CHA products, a resonance structure with positive charge on fluorine atom, releases electrons and destabilizes the Ir-C bonds in the products. This destabilizing effect does not exist for *meta*-fluorine substituent (Figure 3.3). The ground state effect argues for the observed *meta*-CHA product **3d** being the major product from the reaction of **1a** and **2a** (Table 3.9, entry 1).

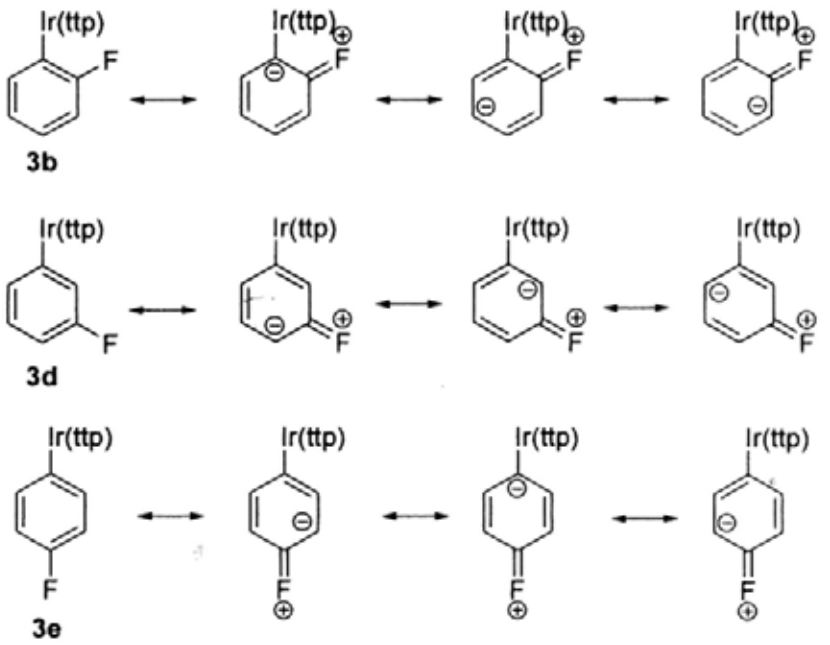

Figure 3.3 Resonance structures for the isomers of aromatic CHA of fluorobenzene

3.2.3 Kinetic and Thermodynamic Consideration for the Competitive Aromatic CFA and CHA

During the course of the reaction of Ir(ttp)$SiEt_3$ **1a** and 1,4-difluorobenzene **2d**, the aromatic CFA product **3e** was observed before the formation of the *ortho*-CHA product **3f**. Therefore, the aromatic CFA reaction is more likely a kinetic process. Indeed, when the reaction of **1a** and **2d** was stopped in a shorter reaction time of 2 hours, the ArCFA product **3e** was isolated as the major product in 29 % yield, as well as trace amount of *ortho*-CHA product **3f** (eq 3.11).[29]

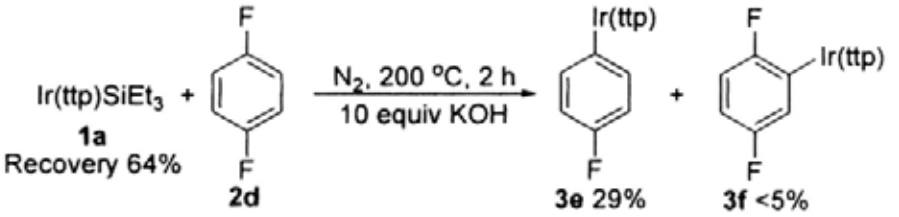

(3.11)

In addition, in an independent reaction between Ir(ttp)(4-F-C_6H_4) **3e** and 1,4-difluorobenzene **2d**, the *ortho*-CHA product Ir(ttp)(2,5-F_2-C_6H_4) **3f** was isolated in 30% yield with the recovery of **3e** in 57% yield after 3 days (eq 3.12). Therefore, most likely, Ir(ttp)$SiEt_3$ converts to the active intermediate in the presence of KOH, which further reacts with fluorobenzenes to cleave the C-F bond kinetically. Then the ArCFA products react with fluorobenzenes to form the CHA products as the thermodynamic products.

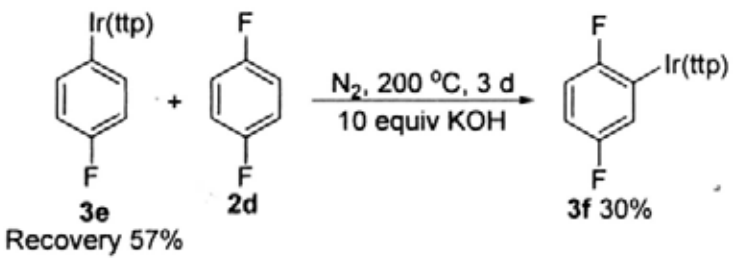

(3.12)

On the other hand, the *ortho*-CHA product **3f** reacted with **2d** in the presence of KOH at 200 °C to give the aromatic CFA product **3e** in a slower reaction rate (eq 3.13). These results suggest that the aromatic CFA and CHA products are interconvertible and equilibrating in the reaction system after prolonged heating for 6 days. The *ortho*-CHA product **3f** is more thermally stable comparing with the ArCFA product **3e**.

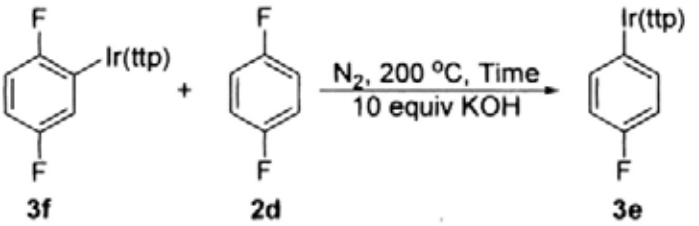

3f **2d** **3e** (3.13)

t = 3 d, **3e** 9%, **3f** Recovery 79%

t = 6 d, **3e** 58%, **3f** Recovery 25%

3.2.4 Mechanistic Investigation of the Competitive Aromatic CFA and CHA by Ir(ttp)SiEt$_3$

3.2.4.1 Active Intermediate for Aromatic CFA

In order to gain further insight into the reaction intermediates, the progress of the reaction of Ir(ttp)SiEt$_3$ **1a** with KOH (10 equiv) in benzene-d_6 at 200 °C was monitored by ^{1}H NMR spectroscopy. After 5 days, Ir(ttp)$^{\cdot}$ **1b** was observed in 11% yield[30] together with KOSiEt$_3$ (20%) and $(Et_3Si)_2O$ (6%). After 25 days, KOSiEt$_3$ completely converted to $(Et_3Si)_2O$, and Ir(ttp)H **1c** formed in a low yield of 2%, likely due to the protonation of Ir(ttp)$^{\cdot}$ with residual water present[31] (eq 3.14, Scheme 3.5, Figure 3.4). These results support that a hydroxide anion attacks the silicon center by a nucleophilic substitution to generate Ir(ttp)$^{\cdot}$ or Ir(ttp)H upon protonation.

$$\underset{\textbf{1a}}{Ir(ttp)SiEt_3} + \underset{10\ equiv}{KOH} \xrightarrow[Benzene\text{-}d_6]{200\ ^oC} \underset{\textbf{1b}}{Ir(ttp)^-K^+} + \underset{\textbf{1c}}{Ir(ttp)H} + KOSiEt_3 + (Et_3Si)_2O \qquad (3.14)$$

11%		t = 5 d,	11%		20%	6%
6%		t = 25 d,	14%	2%		17%

Scheme 3.5 ^{1}H NMR Spectra of $Ir(ttp)SiEt_3$ in Benzene-d_6 with the Addition of KOH

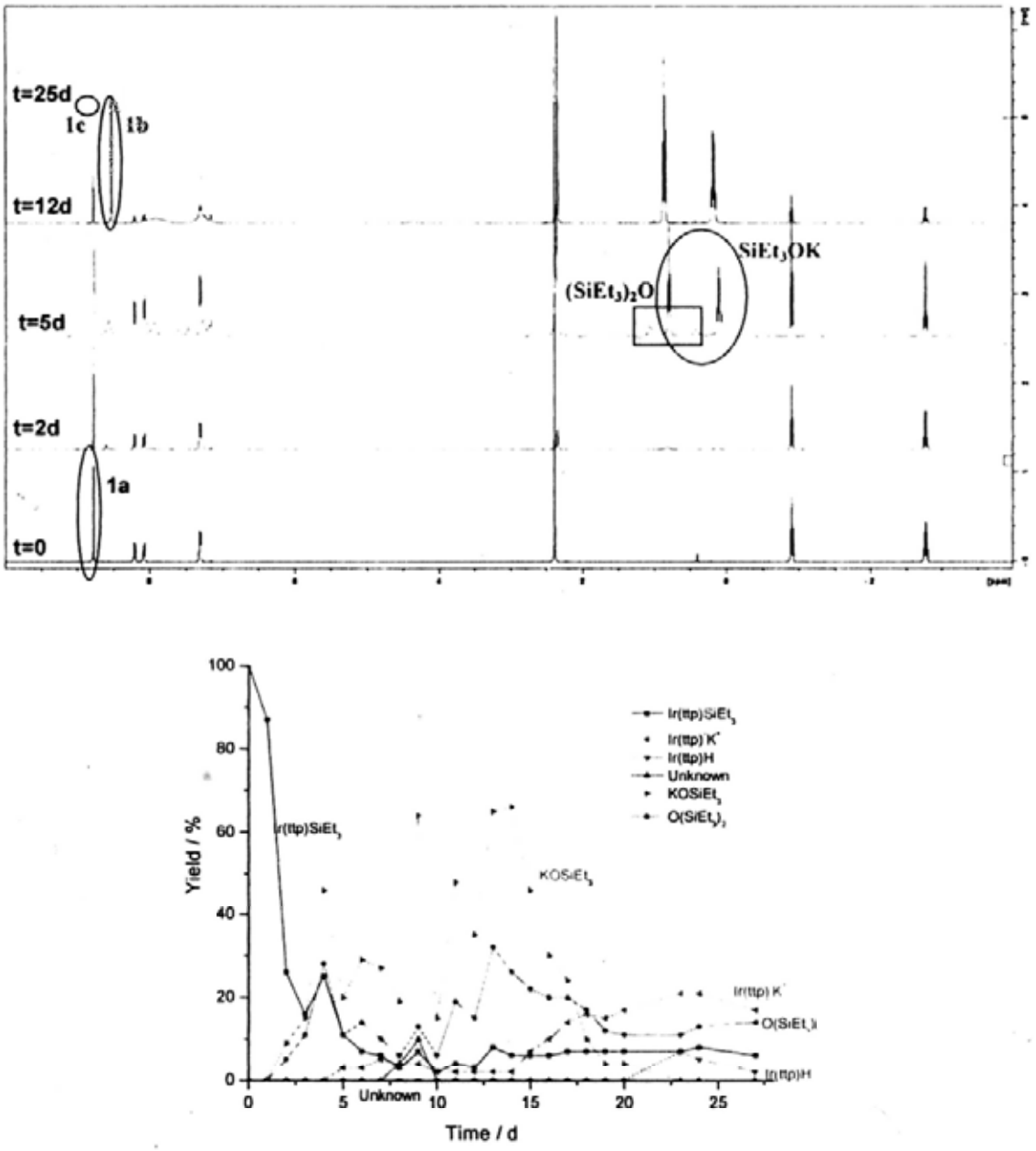

Figure 3.4 Time profile for the reaction of $Ir(ttp)SiEt_3$ in the presence of KOH

To further confirm the intermediacy of $Ir(ttp)^-$ **1b** in the ArCFA of fluorobenzenes, $Ir(ttp)^-Na^+$, independently synthesized from the reduction of

Ir(ttp)Cl(CO) by Na/Hg in THF,[32] was reacted with neat fluorobenzene **2a** at 120 °C (eq 3.15). After 2 days, Ir(ttp)C_6H_5 **3a** was isolated as the sole product in 40% yield. Ir(ttp)$^{\cdot}$ **1b** was confirmed to be the active intermediate for the ArCFA reaction, which likely operates via a nucleophilic aromatic substitution (S_NAr) (Scheme 3.6).[33]

$$\text{Ir(ttp)Cl(CO)} \xrightarrow[\text{THF, Na/Hg}]{\text{N}_2,\ 60\ ^\circ\text{C},\ 10\ \text{min}} \underset{\text{quantitative}}{\text{Ir(ttp)}^{\cdot}\text{Na}^{+}} \xrightarrow[\text{C}_6\text{H}_5\text{F }\mathbf{2a}]{\text{N}_2,\ 120\ ^\circ\text{C},\ 2\ \text{d}} \underset{\mathbf{3a}\ 40\%}{\text{Ir(ttp)C}_6\text{H}_5} \qquad (3.15)$$

Scheme 3.6 Nucleophilic Substitution (Addition-Elimination) of Fluorobenzene by Ir(ttp)$^{\cdot}$

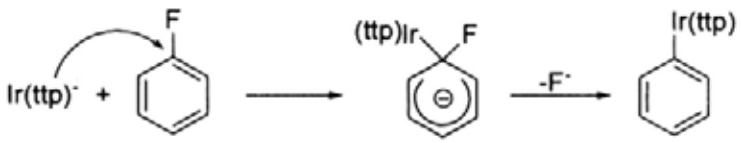

In addition, Ir(ttp)H[31,34a] **1c** and $[Ir(ttp)]_2$[34b] **1d** were found to convert into or exist in equilibrium with Ir(ttp)$^{\cdot}$ **1b** in the presence of base,[35] therefore, their possible intermediacy for aromatic CFA and CHA was also examined (Table 3.10, eq 3.16).

Without KOH, both Ir(ttp)H **1c** and $[Ir(ttp)]_2$ **1d** reacted with fluorobenzene **2a** at 200 °C to give a complex mixture without any aromatic CFA and CHA products (Table 3.10, entries 2 and 5). Only with the addition of KOH (10 equiv), the aromatic CFA and CHA products were isolated (Table 3.10, entries 1 and 4). These results suggested that both Ir(ttp)H **1c** and $[Ir(ttp)]_2$ **1d** were not the direct active intermediates for the aromatic CFA and CHA reactions, but the precursors of intermediates. In addition, Ir(ttp)H **1c** reacted with **2a** at a lower temperature of 120 °C in the presence of KOH, to give only the ArCFA product **3a** without any aromatic CHA products. Therefore, the aromatic CHA requires a higher reaction temperature than the aromatic CFA.

Table 3.10 Aromatic CFA and CHA of Fluorobenzene by Ir(ttp)X (X = H, Ir(ttp))

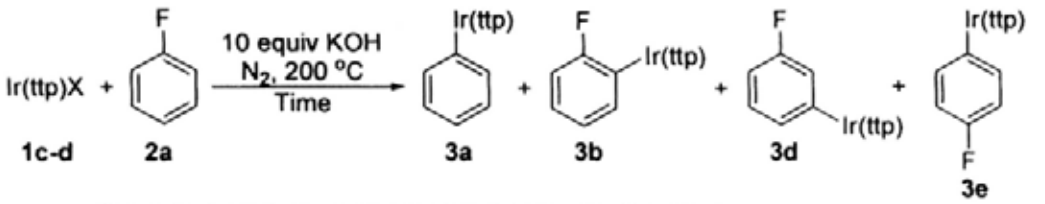

(3.16)

Entry	X	Time / d	Yield / %				
			3a	**3b**	**3d**	**3e**	Total
1	H **1c**	1	50	7	22	6	85
2[a]	H **1c**	4	A mixture of unknowns				28
3[b]	H **1c**	2	91	---	---	---	91
4	Ir(ttp) **1d**	1	52	9	13	5	79
5[a]	Ir(ttp) **1d**	2	A mixture of unknowns				65

[a] No KOH, no aromatic CFA and CHA products were observed. [b] The reaction was carried out at 120 °C.

3.2.4.2 Active Intermediate for Aromatic CHA

In order to examine the reaction mechanism of the aromatic CHA without the competitive aromatic CFA, the reaction of Ir(ttp)$SiEt_3$ **1a** with benzene **2h** in the presence of KOH (10 equiv) was carried out at 200 °C. After 4 days, Ir(ttp)C_6H_5 **3a** was isolated in a low yield of 7% (eq 3.17), which was much lower than the reaction with 1,4-difluorobenzene (Table 3.6, entry 3). Therefore, Ir(ttp)$^{\cdot}$ does not appear to be the major intermediate for the aromatic CHA.

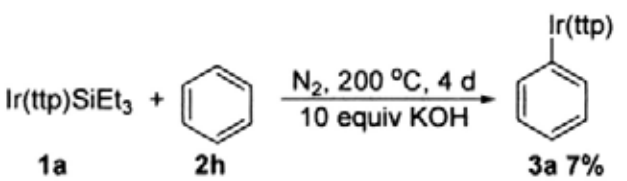

(3.17)

Furthermore, Rossi and co-workers have reported nucleophilic aromatic substitution of fluorobenzene by highly basic (p*K*a = 44.9 for Me_3SiH in DMSO)[36a] and nucleophilic trimethylsiliconide anion (Me_3Si^-) to give the aromatic CFA product, as well as the *ortho*- and *para*-CHA products simultaneously without the observation of *meta*-CHA product (eq 3.18).[33d] Scheme 3.7 shows the reported proposed mechanism for the S_NAr of fluorobenzene.

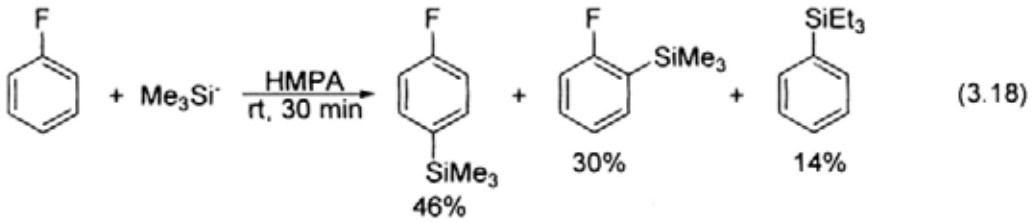

(3.18)

Scheme 3.7 Proposed Mechanism for the S_NAr of Fluorobenzene by Me_3Si^-

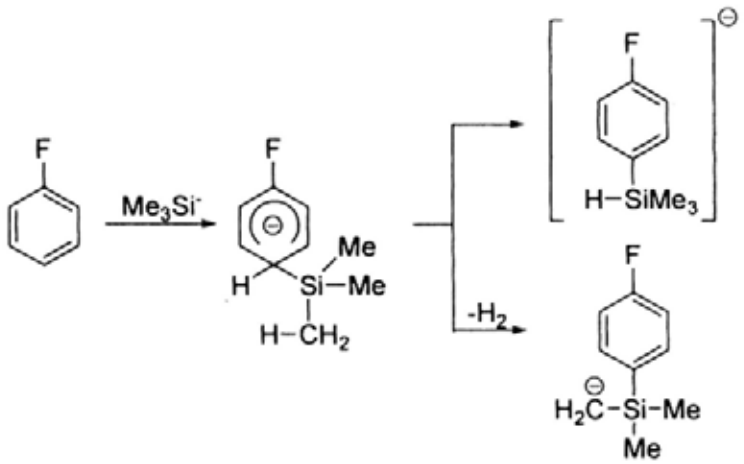

Later, trimethylstannide (Me_3Sn^-) (p*K*a = 23.5 for Me_3SnH in DME)[36b] was reported to react with fluorobenzene to give trace amount of aromatic CFA product together with *para*-CHA product in ca 15% yield (eq 3.19).[33e] An analogous mechanism with that of Me_3Si^- ion was proposed and is shown in Scheme 3.8. The lower yield was attested to the lower reactivity of Me_3Sn^- than Me_3Si^-.

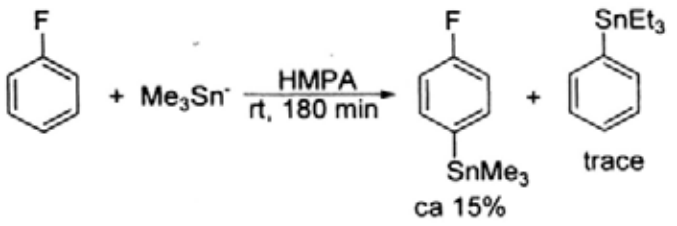

(3.19)

Scheme 3.8 Proposed Mechanism for the S_NAr of Fluorobenzene by Me_3Sn^-

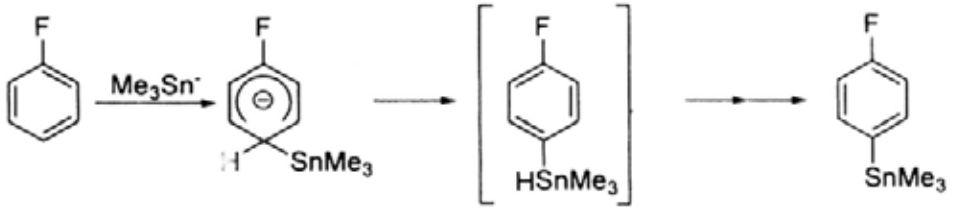

Based on these two reported examples, the aromatic CHA process of fluorobenzenes is unlikely via S_NAr of an iridium porphyrin anion. Firstly, S_NAr reaction usually gives high regioselectivity due to the electronic effect, while a mixture of three isomers (*o* : *m* : *p* = 1 : 4 : 1 in molar ratio) was generated in the reaction of Ir(ttp)$SiEt_3$ **1a** with fluorobenzene **2a**. Secondly, these three isomers were observed simultaneously as a result of competitive S_NAr reactions with fluorobenzene by Me_3Si^- (eq 3.18). However, the aromatic CFA product was observed before the formation of the aromatic CHA products, which unlikely operates as a competitive S_NAr with $Ir(ttp)^-$. Thirdly, $Ir(ttp)^-$ (p*K*a = ca 15 for Ir(oep)H estimated with higher p*K*a value than Rh(oep)H,[31c] p*K*a = 11 in DMSO for Rh(tpp)H[31a]) is much less basic and nucleophilic than Me_3Si^- and Me_3Sn^-, so an S_NAr attack on the carbon atom in fluorobenzene with a leaving hydride anion (H^-) is not thermodynamically favorable. Therefore, S_NAr of fluorobenzene with iridium porphyrin anion to form aromatic CHA products is mechanistically difficult, and other mechanistic possibilities were considered.

We found that Ir(ttp)(4-F-C_6H_4) **3e** reacted with 1,4-difluorobenzene **2d** in the presence of KOH to give the *ortho*-CHA product **3f** in 30% yield (eq 3.12), therefore, we assumed that **3e** can yield an intermediate that cleave the aromatic C-H bonds to give the aromatic CHA product. However, **3e** was found thermally stable in fluorobenzene **2a** at 200 °C for 4 days in the absence of KOH, and 95% yield of **3e** was recovered. For the reaction of **3e** and **2a** in the presence of 10 equivalents of KOH, the *meta*-CHA product **3d** was isolated as the major product in 42% yield (eq 3.20). These two reactions show that the KOH must be necessary for the transformation of iridium porphyrin aryls (Ir(ttp)Ar) to aromatic CHA products.

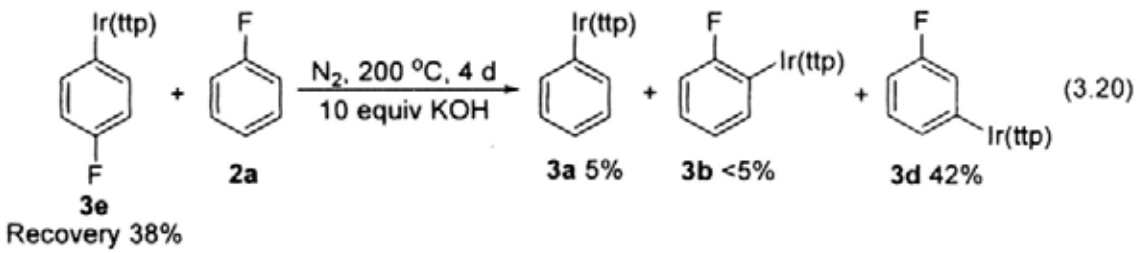

(3.20)

We were fortunate to discover that a new iridium porphyrin species was observed, when Ir(ttp)(4-F-C_6H_4) **3e** was heated in benzene-d_6 in the presence of KOH (10 equiv) for 7 days. Upon cooling down the reaction mixture in a sealed-NMR tube and taking ^{1}H NMR spectrum quickly (within 10 minutes), the signal of this species at δ -10.94 ppm was assigned to the hydroxyl proton of the proposed structure of [(4-F-C_6H_4)Ir(ttp)OH]$^-$ **4a** (eq 3.21, Figure 3.5). Likewise, [(2,5-F_2-C_6H_3)Ir(ttp)OH]$^-$ **4b** was observed in the reaction with Ir(ttp)(2,5-F_2-C_6H_3) **3f** (eq 3.22, Figure 3.6).

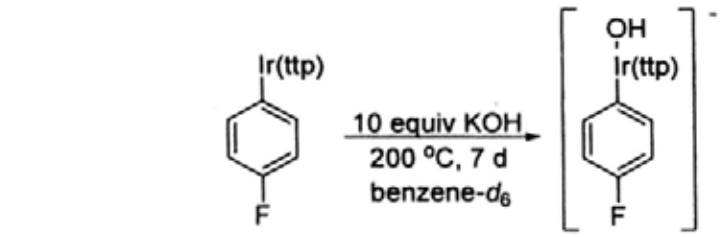

4a 47%

(3.21)

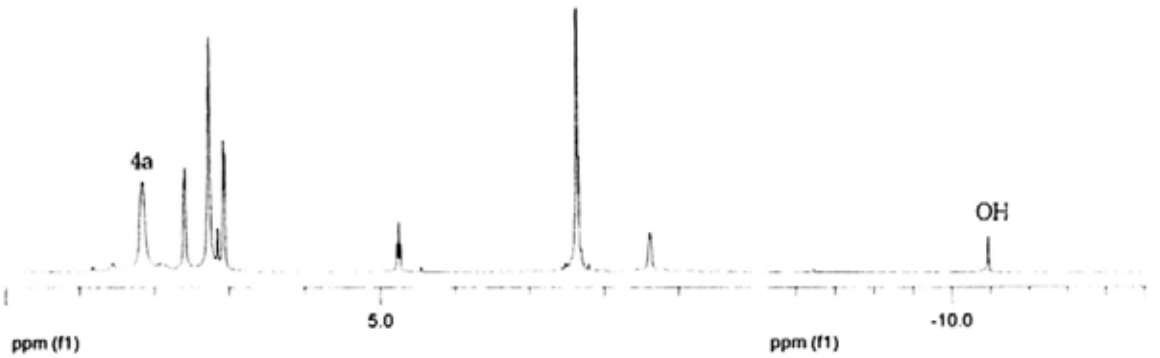

Figure 3.5 Partial ^{1}H NMR spectrum of [(4-F-C_6H_4)Ir(ttp)OH]$^-$ **4a**

Same as **3e**, when Ir(ttp)(2,5-F_2-C_6H_3) **3f** was heated in benzene-d_6 added with the KOH (10 equiv), [(2,5-F_2-C_6H_3)Ir(ttp)OH]$^-$ **4b** was observed after 3 days, togther with Ir(ttp)$^-$ and 1,4-difluorobenzene **2d** (eq 3.22, Figure 3.6). After the neutralization of the reaction mixture by dilute aqueous H_2SO_4, no 2,5-difluorophenol was observed by both ^{1}H NMR spectroscopy and GC-MS analyses. Therefore, Ir(ttp)$^-$ was not formed from the direct nucleophilic attack carbon of Ir-aryl(C) bond, but from the further reaction of *trans*-[ArIr(ttp)OH]$^-$ as shown in Scheme 3.9. [ArIr(ttp)OH]$^-$ reacted with water to form Ir(ttp)OH[37] **1e** and 1,4-difluorobenzene **2d**. Then Ir(ttp)OH can undergo reduction at high temperature to yield Ir^{II}(ttp),[38] Ir^{II}(ttp) further rapidly disproportionates into Ir^{III}(ttp)$(OH_2)_n^+$ and Ir^{I}(ttp)$^-$.[39]

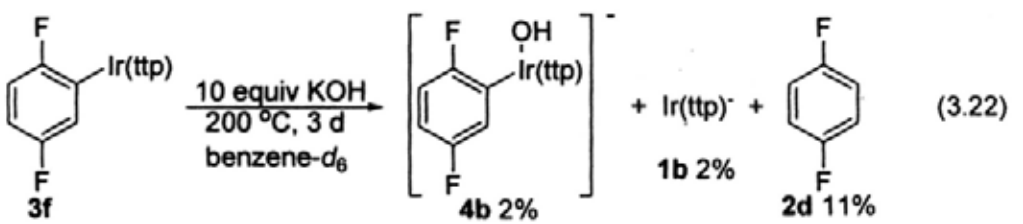

3f

4b 2%

1b 2%

2d 11%

(3.22)

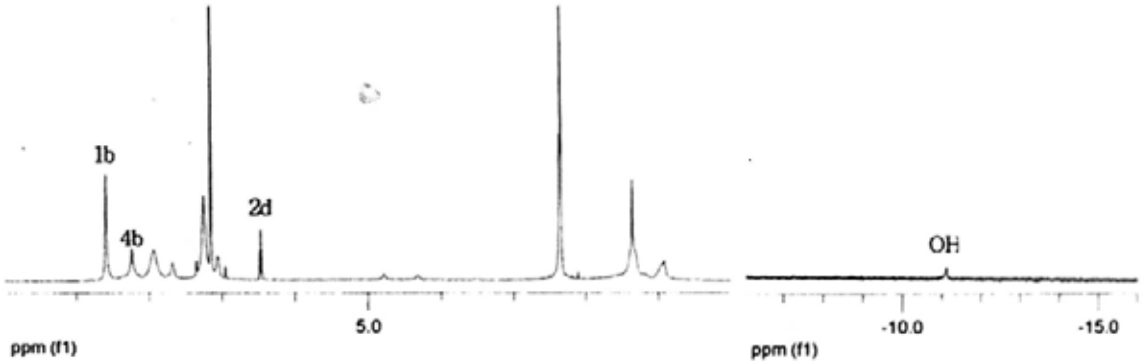

Figure 3.6 Partial ^{1}H NMR spectrum of [(2,5-F_2-C_6H_3)Ir(ttp)OH]$^-$ **4b**

Scheme 3.9 Transformation From Ir(ttp)OH to Ir(ttp)$^-$

$$[(2,5\text{-}F_2\text{-}C_6H_3)Ir(ttp)OH]^- + H_2O \longrightarrow Ir(ttp)OH + 1,4\text{-}F_2\text{-}C_6H_4 + {}^-OH \quad (i)$$

$$2\ Ir(ttp)OH \longrightarrow 2\ Ir^{II}(ttp) + H_2O_2 \quad (ii)$$

$$2\ Ir^{II}(ttp) \longrightarrow [Ir(ttp)]_2 \quad (iii)$$

$$[Ir(ttp)]_2 + H_2O \longrightarrow Ir^{III}(ttp)(OH_2)_n^+ + Ir(ttp)^- \quad (iv)$$
$$n = 1 \text{ or } 2$$

Since [ArIr(ttp)OH]$^-$ **4a-b** were observed in the above two independent reactions, we proposed that Ir(ttp)OH **1e** is the possible active intermediates towards the aromatic CHA reactions. Actually, when Ir(ttp)(4-F-C_6H_4) **3e** reacted with benzene **2h** for 4 days at 200 °C in the presence of KOH (10 equiv), Ir(ttp)C_6H_5 **3a** was isolated in a higher yield of 58% (eq 3.23). When benzene-d_6 was used instead of benzene, at 200 °C with the addition of KOH for 4 days, Ir(ttp)C_6H_5 **3a** and Ir(ttp)C_6D_5 **3a'** were isolated in 7% and 12% yield, respectively, together with fluorobenzene **2a** in 16% yield (eq 3.24). Therefore, Ir(ttp)OH **1e** is indeed a reasonable intermediate to cleave the aromatic C-H bonds to give the aromatic CHA products. The formation of stable water co-product (eq 3.25) further provides the driving force of the reaction.

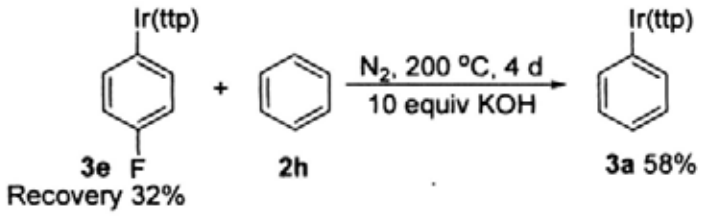

(3.23)

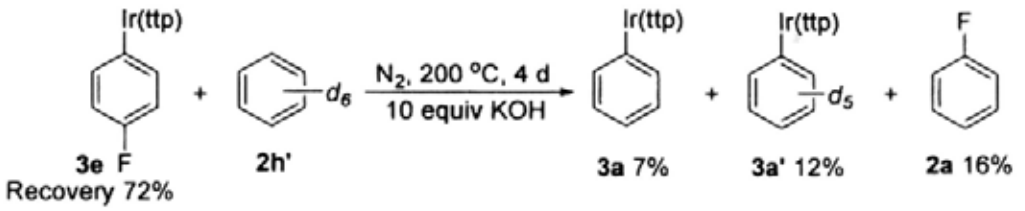

(3.24)

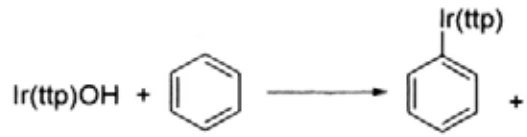

(3.25)

This proposed Ir(ttp)OH intermediate for aromatic CHA is supported by a literature precedent.[40] Periana and co-workers have reported that an iridium-hydroxyl complex can cleave the aromatic C-H bonds of benzene to generate corresponding phenyl complex.[40a] In addition, experimental and theoretical studies suggest that the reaction proceeds via rate-determining formation of an arene complex followed by faster C-H bond cleavage by a sigma bond metathesis reaction. Scheme 3.10 shows the proposed mechanism for this reaction with the calculated ΔG values.

Scheme 3.10 Proposed Mechanism for the Reaction of Iridium-Hydroxyl Complex with Benzene

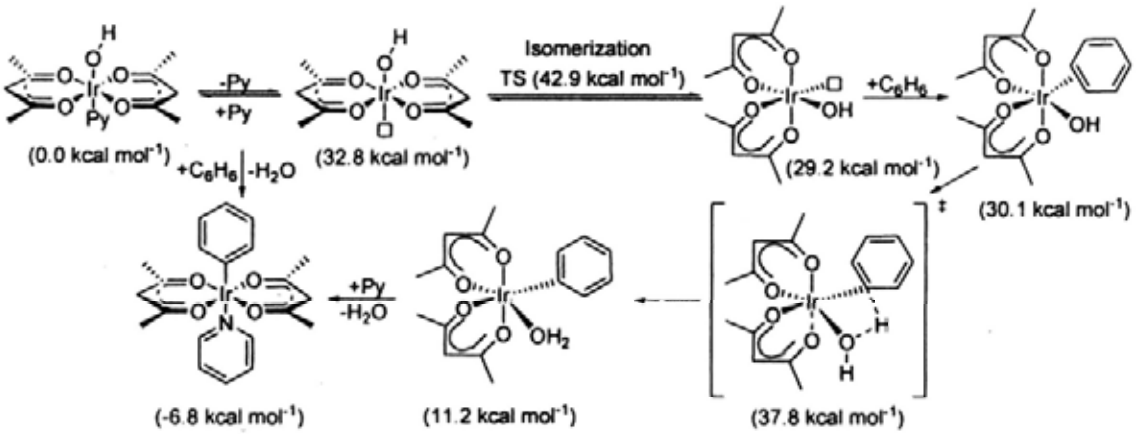

3.2.4.3 Proposed Mechanism for the Base-Promoted Competitive Aromatic CFA and CHA of Fluorobenzenes

Based on the above findings, the proposed mechanism for the base-promoted competitive aromatic CFA and CHA of fluorobenzenes with iridium porphyrin triethylsilyl is shown in Scheme 3.11. Firstly, in the presence of KOH, Ir(ttp)$SiEt_3$ **1a** is converted to Ir(ttp)$^-$ **1b** and $HOSiEt_3$ formed (pathway i). Then Ir(ttp)$^-$ cleaves the aromatic C-F bond directly via S_NAr to give Ir(ttp)Ar as the kinetic product (pathway ii). $HOSiEt_3$ can react with KOH to form $KOSiEt_3$ and $(Et_3Si)_2O$ (pathway iii). As the reaction proceeds, a hydroxide anion can coordinate to the iridium center of Ir(ttp)Ar to form an iridium porphyrin *trans* aryl hydroxyl anion *trans*-[ArIr(ttp)OH]$^-$. In the presence of water, *trans*-[ArIr(ttp)OH]$^-$ can give Ir(ttp)OH and ArH (pathway iv). Finally, Ir(ttp)OH reacts with fluorobenzenes to cleave the aromatic C-H bonds to form the ArCHA products and water as the thermodynamic products (pathway v).

Scheme 3.11 Proposed Mechanism for the Base-Promoted Competitive Aromatic CFA and CHA of Fluorobenzenes with Ir(ttp)$SiEt_3$

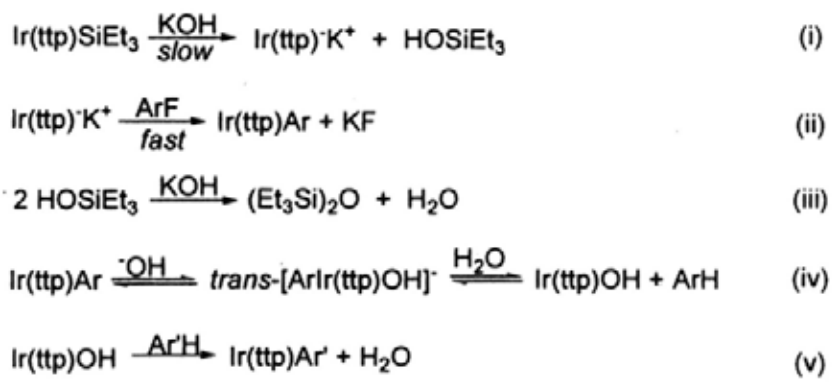

3.2.4.4 Rationalization of Kinetic CFA and Thermodynamic CHA

This proposed mechanism is also consistent with that the aromatic CFA reaction is a kinetic process, while the aromatic CHA process is the thermodynamic one.

Firstly, Ir(ttp)$^-$ was formed from Ir(ttp)$SiEt_3$ in the presence of KOH, which kinetically reacts with fluorobenzene via S_NAr to give the aromatic CFA product. In addition, the S_NAr process at an aromatic carbon of the C-H bonds is mechanistically difficult as the formation of hydride leaving group is energetically very demanding.

Secondly, the water co-product from the aromatic CHA increases the entropy and provided the additional driving force for this reaction.

Thirdly, the BDE of KF and H_2O are similar (118 vs 119 kcal mol^{-1} K^{-1}),[3,41] while the Ir-C bond is strengthened by the fluorine substituent in the phenyl ligand,[18a] therefore, the aromatic CHA product is more thermally stable than the aromatic CFA product.

3.2.5 X-Ray Structures of Iridium Porphyrin Aryls

Table 3.11 lists the selected bond lengths and angles for **3a-e**, **3g** and **3i**. *Meta*-fluorine substituted iridium porphyrin aryls, such as **3d** and **3g**, display larger bond lengths between iridium center and α-carbon.

The fluorine atom does not appear to coordinate to the iridium center, but electron repulsion exists between the *ortho*-fluorine atom and iridium center as judged the larger Ir-C_α-C(*ortho*-F) angle (129°) than the Ir-C_α-C_β' angle (119°) in Ir(ttp)(2-F-C_6H_4) **2b**. However, it is interesting that in Ir(ttp)(3-F-C_6H_4) **3d**, the Ir-C_α-C_β(*meta*-F) angle (114°) is smaller than Ir-C_α-C_β' angle (123°), which can also

account for the smaller difference between Ir-C_α-C_β (*ortho*- and *meta*-F) angle (125.8°) and Ir-C_α-C_β' angle (120.7°) in Ir(ttp)(2,3-F_2-C_6H_3) **3c**, but the larger difference (128.6° and 116.3°) in Ir(ttp)(2,5-F_2-C_6H_3) **3f**. Furthermore, for symmetric iridium porphyrin aryls, such as **3e** and **3i**, the two Ir-C_α-C_β angles are the same, while two Ir-C_α-C_β angles in **3g** are different. The origin remains unclear at this stage.

In addition, the iridium-fluorine(*ortho*) distance (3.321 Å for **3b**, 3.331 Å for **3c**, 3.373 Å for **3f** and 3.278 Å for **3i**) is larger than the sum of the van der Waal radius of the two atoms (3.25 Å)[42]. It suggests that the chelation assistance effect between Ir center and *ortho*-fluorine atom does not exist.

In order to give more structural understanding of the *trans*- iridium porphyrin aryl hydroxide complexes, the structure analogure, Ir(ttp)Ar(PPh_3) were further studied. Table 3.12 lists the selected bond lengths and angles for **3b'-d'**, **3g'** and **3i'**. The iridium-carbon(α) bond of *meta*-fluorine substituent (2.074 Å for **3d'** and 2.069 Å for **3g'**) is significantly shorten than that of *ortho*-fluorine substituent (2.108 Å for **3b'** and 2.112 Å for **3c'**), which suggests that the coordination of PPh_3 to the iridium center strengthens the Ir-C(α) bond. In addition, the electron repulsion still exists between the *ortho*-fluorine atom and iridium center as judged the larger Ir-C_α-C(*ortho*-F) angle (124.7°) than the Ir-C_α-C_β' angle (116.6°) in Ir(ttp)(2-F-C_6H_4)(PPh_3) **2b'**. While different from **3d**, in Ir(ttp)(3-F-C_6H_4)(PPh_3) **3d'**, the Ir-C_α-C_β(*meta*-F) angle (122.3°) is slightly larger than Ir-C_α-C_β' angle (120.9°).

On the other hand, the coordination of PPh_3 to the iridium center lengthens the Ir-C(α) bond in *ortho*-fluorine substituent iridium porphyrin aryl complex (2.04 Å for

3b vs 2.108 Å for 3**b'**), while the the Ir-C(α) bond length of *meta*-fluorine substituent iridium porphyrin aryl complexes (2.08 Å for **3d** vs 2.074 Å for **3d'**) remain the same. However, for Ir(ttp)(3,5-F_2-C_6H_3), the coordination of PPh_3 shortens the Ir-C(α) bond obviously (2.141 Å for **3g** vs 2.069 Å for **3g'**), which can also account the *meta*-fluorine substituent iridium porphyrin aryl complexes are the most stable one.

Due to the poor quality of the X-ray crystal of **3b**, **3d**, **3f** and **3g**, we can only make a prediction but can not come up with a precise conclusion.

3.3 Conclusion

Base-promoted competitive aromatic C-F and C-H bond activation reactions of fluorobenzenes were successfully achieved by iridium(III) porphyrin triethylsilyl to give the corresponding iridium(III) porphyrin aryl complexes. Mechanistic studies suggest that Ir(ttp)$^{\cdot}$ acts as the active intermediate to cleave the aromatic C-F bond via an S_NAr process, while Ir(ttp)OH was the intermediate towards aromatic C-H bond activation reaction. Furthermore, the aromatic C-F bond activation products were found as the kinetic products, and aromatic C-H bond activation products were the thermodynamic ones.

Table 3.11 Selected Bond Lengths (Å) and Angles (deg) for Ir(ttp)Ar

Ir(ttp)Ar (Final R indices [I>2sigma(I)])	Ir(ttp)(C_6H_5)[35] **3a** (R1 = 0.0553)	Ir(ttp)(2-F-C_6H_4) **3b** (R1 = 0.0978)	Ir(ttp)(3-F-C_6H_4) **3d** (R1 = 0.0941)	Ir(ttp)(4-F-C_6H_4) **3e** (R1 = 0.0214)	Ir(ttp)(2,3-F_2-C_6H_3) (MeOH) **3c** (R1=0.0546)	Ir(ttp)(2,5-F_2-C_6H_3)(DMSO)**3f** (R1 = 0.0728)	Ir(ttp)(3,5-F_2-C_6H_3) **3g** (R1 = 0.0765)	Ir(ttp)(C_6F_5)(MeOH) **3i** (R1 = 0.0398)
Ir-C_α-C_β angle / deg	120.1(10)	129(2) (*o*-F)	114(3) (*m*-F)	121.1(2)	125.8(6) (*o*-F)	128.6(8) (*o*-F)	121.1(4)	123.9(4)
Ir-C_α-C_β' angle / deg	119.1(10)	119(2)	123(2)	121.4(2)	120.7(7)	116.3(6)	115.5(13)	124.4(4)
F(*o*)-C_β-C_α angle / deg	---	118(3)	---	---	120.1(7)	124.7(12)	---	120.7(5); 121.2(5)
F(*o*)-C_β-C_γ angle / deg	---	114(3)	---	---	116.2(7)	106.7(14)	---	114.4(5); 114.0(4)
Ir-C(α) Distance / Å	2.168(11)	2.04(3)	2.08(3)	2.016(3)	2.062(8)	2.144(7)	2.141(15)	2.049(5)
C-F Distance / Å	---	*o*-1.35(4)			*o*-1.355(9)	*o*-1.392(14)		*o*-1.348(6) / 1.356(6)
			m-1.29(4)		*m*-1.333(10)	*m*-1.367(13)	*m*-1.31(4) / 1.37(4)	*m*-1.341(6) / 1.358(6)
				p-1.364(4)				*p*-1.331(7)
Ir-F(*o*) Distance / Å	---	3.321	---	---	3.331	3.373	---	3.283 / 3.278
Ir-H(*o*) Distance / Å	3.022 / 3.115	---	2.509(*m*-F) / 2.969	3.032 / 3.020	3.076	3.058	3.008 / 3.101	---

Table 3.11 Selected Bond Lengths (Å) and Angles (deg) for Ir(ttp)Ar (Continued)

Ir(ttp)Ar (Final R indices [I>2sigma(I)])	Ir(ttp)(C_6H_5)[35] **3a** (R1 = 0.0553)	Ir(ttp)(2-F-C_6H_4) **3b** (R1 = 0.0978)	Ir(ttp)(3-F-C_6H_4) **3d** (R1 = 0.0941)	Ir(ttp)(4-F-C_6H_4) **3e** (R1 = 0.0214)	Ir(ttp)(2,3-F_2-C_6H_3) (MeOH) **3c** (R1=0.0546)	Ir(ttp)(2,5-F_2-C_6H_3)(DMSO)**3f** (R1 = 0.0728)	Ir(ttp)(3,5-F_2-C_6H_3) **3g** (R1 = 0.0765)	Ir(ttp)(C_6F_5)(MeOH) **3i** (R1 = 0.0398)
C-H Distance / Å	*o*-0.929 / 0.931	---	*o*-0.944 / 0.948	*o*-0.929 / 0.930	*o*-0.931	*o*-0.931	*o*-0.950 / 0.952	---
	m-0.925 / 0.929		*m*-0.953	*m*-0.930 / 0.930	*m*-0.931	*m*-0.930	*p*-0.951	
	p-0.928		*p*-0.952		*p*-0.930	*p*-0.930		
Ir-Main Plane Distance / Å	0	0.071	0.139	0.004	0.053	0.038	0	0.213
C-C Distance / Å	α-β-1.365(9)/	**α-β-1.381(10)**/	α-β-1.03(11)/	α-β-1.386(4)/	**α-β-1.408(11)**/	**α-β-1.201(18)**/	α-β-1.364(10)/	**α-β-1.388(7)**/
	1.357(9)	1.381(10)	1.24(5)	1.383(4)	1.414(11)	1.442(13)	1.351(10)	**1.394(7)**
	β-γ-1.375(10)/	**β-γ-1.375(10)**/	**β-γ-1.64(9)**/	β-γ-1.388(4)/	**β-γ-1.360(12)**/	**β-γ-1.452(19)**/	**β-γ-1.375(10)**/	**β-γ-1.374(7)**/
	1.362(10)	1.383(10)	1.33(4)	1.379(4)	1.410(14)	**1.355(16)**	**1.378(10)**	**1.358(8)**
	β-δ-1.385(10)/	β-δ-1.380(10)/	**β-δ-1.38(4)**/	**β-δ-1.359(5)**/	**β-δ-1.343(14)**/	β-δ-1.408(18)/	**β-δ-1.379(10)**/	**β-δ-1.363(8)**/
	1.381(10)	1.382(10)	1.44(4)	**1.367(5)**	1.360(13)	**1.403(18)**	**1.382(10)**	**1.370(8)**

Table 3.12 Selected Bond Lengths (Å) and Angles (deg) for Ir(ttp)Ar(PPh_3)

Ir(ttp)Ar (Final R	Ir(ttp)(2-F-C_6H_4)(PPh_3)	Ir(ttp)(3-F-C_6H_4)(PPh_3)	Ir(ttp)(2,3-F_2-C_6H_3)(PPh_3)	Ir(ttp)(3,5-F_2-C_6H_3)(PPh_3)	Ir(ttp)(C_6F_5)(PPh_3)
indices [I>2sigma(I)])	**3b'** (R1 = 0.0368)	**3d'** (R1 = 0.0358)	**3c'** (R1 = 0.0446)	**3g'** (R1 = 0.0235)	**3i'** (R1 = 0.0236)
Ir-C_α-C_β angle / deg	124.7(5) (*o*-F)	122.3(4) (*m*-F)	125.5(5) (*o*-F)	122.1(2)	123.2(2)
Ir-C_α-C_β' angle / deg	116.6(4)	120.9(4)	117.7(5)	120.4(3)	125.1(2)
F(*o*)-C_β-C_α angle / deg	124.7(8)	---	124.4(7)	---	122.0(3); 121.4(3)
F(*o*)-C_β-C_γ angle / deg	108.2(8)	---	113.3(8)	---	113.6(3); 113.3(3)
Ir-C(α) Distance / Å	2.108(5)	2.074(5)	2.112(6)	2.069(3)	2.140(3)
C-F Distance / Å	*o*-1.224(10)		*o*-1.292(9)		*o*-1.341(4) / 1.349(4)
		m-1.394(9)	*m*-1.337(11)	*m*-1.372(5) / 1.374(5)	*m*-1.353(5) / 1.352(5)
					p-1.345(4)
Ir-F(*o*) Distance / Å	3.330	---	3.388	---	3.344 / 3.369
Ir-H(*o*) Distance / Å	3.182	3.108 (*m*-F) / 3.087	3.098	3.106 / 3.074	---

Table 3.12 Selected Bond Lengths (Å) and Angles (deg) for Ir(ttp)Ar(PPh_3) (Continued)

Ir(ttp)Ar (Final R	Ir(ttp)(2-F-C_6H_4)(PPh_3)	Ir(ttp)(3-F-C_6H_4)(PPh_3)	Ir(ttp)(2,3-F_2-C_6H_3)(PPh_3)	Ir(ttp)(3,5-F_2-C_6H_3)(PPh_3)	Ir(ttp)(C_6F_5)(PPh_3)
indices [I>2sigma(I)])	**3b'** (R1 = 0.0368)	**3d'** (R1 = 0.0358)	**3c'** (R1 = 0.0446)	**3g'** (R1 = 0.0235)	**3i'** (R1 = 0.0236)
C-H Distance / Å	*o*-0.930	*o*-0.929 / 0.928 (*m*-F)	*o*-0.930	*o*-0.930 / 0.930	---
	m-0.930 / 0.930	*m*-0.930	*m*-0.930	*p*-0.930	
	p-0.931	*p*-0.930	*p*-0.930		
Ir-Main Plane Distance / Å	0.030	0.060	0.030	0.063	0.017
Ir-P Distance / Å	2.5007(13)	2.5243(13)	2.5004(14)	2.5144 (8)	2.4585 (7)
C-C Distance / Å	α-β-**1.352(9)** / 1.490(8)	α-β-1.385(8) / 1.409(8)	α-β-**1.369(10)** / 1.437(10)	α-β-1.390(5) / 1.397(5)	α-β-**1.398(5) / 1.382(5)**
	β-γ-**1.369(11)** / 1.420(8)	β-γ-**1.391(9)** / 1.392(9)	β-γ-**1.388(11)** / 1.423(11)	β-γ-**1.383(6) / 1.376(6)**	β-γ-**1.386(5) / 1.384(5)**
	β-δ-1.330(17) / 1.355(19)	β-δ-**1.352(11)** / 1.373(11)	β-δ-**1.362(16)** / 1.326(16)	β-δ-**1.361(6) / 1.358(7)**	β-δ-**1.363(6) / 1.355(6)**

3.4 Experimental Section

Unless otherwise noted, all chemicals were obtained from commercial suppliers and used without further purification. Hexane for chromatography was distilled from anhydrous calcium chloride. Benzene used as solvent was distilled from sodium. Thin-layer chromatography was performed on precoated silica gel 60 F_{254} plates for thin-layer analyses for the reaction mixture. All preparation reactions were carried out in a teflon screw-head stoppered tube in N_2. For purification of iridium aryl complexes, fresh column chromatography was used and carried out in air using alumina (90 active neutral, 70-230 mesh). Samples for microanalyses were recrystallized from CH_2Cl_2/MeOH and were then dried at 40-60 °C in vacuum (0.005 mmHg) for 3 days.

^{1}H NMR spectra were recorded on a Bruker 400. Chemical shifts were reported with reference to the residual solvent protons in C_6D_6 (δ 7.15 ppm) or in $CDCl_3$ (δ 7.26 ppm) as the internal standard. Coupling constants (J) are reported in hertz (Hz). ^{13}C NMR spectra were recorded on a Bruker 400 (100 MHz) spectrometer and referenced to $CDCl_3$ (δ 77.1 ppm) or CD_2Cl_2 (δ 53.8 ppm) or THF (δ 67.4 ppm). ^{19}F NMR spectra were recorded on a Varian XL-400 spectrometer at 376 MHz. Chemical shifts were referenced with the external standard fluorine in $C_6H_5CF_3$ using a sealed melting point tube and put into the NMR tube (δ = 0.00 ppm). Chemical shifts (δ) were reported as part per million (ppm) in δ scale downfield from $C_7H_5F_3$.[43] Coupling constants (J) were reported in Hertz (Hz). High-resolution mass spectra (HRMS) were performed on a Thermofinnign MAT 95 XL in FAB (using 3-nitrobenzyl alcohol (NBA) matrix and CH_2Cl_2 as the solvent) and ESI model (MeOH:CH_2Cl_2 = 1:1 as the solvent).

Preparation of 5, 10, 15, 20-Tetratolylporphyrinatoiridium(I) Anion [Ir(ttp)$^-$Na$^+$] (1b).[32]

A solution of Ir(ttp)Cl(CO) (20.0 mg, 0.022 mmol) in freshly distilled THF (4.0 ml) was added to Na:Hg (4%, 500 mg) under N_2. The red solution was stirred at 60 °C under N_2 for 10 minutes to form a greenish-brown solution. The residue and the solvent were removed to give brown solid of Ir(ttp)$^-$Na$^+$ **1b** in quantitative yield and was used without further purification. ^{1}H NMR (THF-d_8, 400 MHz): δ 2.57 (s, 12 H), 7.39 (d, 8 H, J = 7.2 Hz), 7.79 (d, 8 H, J = 7.6 Hz), 8.04 (s, 8 H).

Preparation of 5, 10, 15, 20-Tetratolylporphyrinatoiridium(II) Dimer [Ir(ttp)]$_2$ (1d).[34b]

Ir(ttp)H (18.2 mg, 0.021mmol) and TEMPO (8.2 mg, 0.053 mmol, 2.5 equiv) were dissolved in benzene (10 mL) under N_2, and the reaction mixture was degassed by the freeze-pump-thaw method (3 cycles). The deep red solution was stirred for 5 minutes under N_2. The solvent as well as the excess TEMPO and TEMPOH were removed by high vacuum, and a dark red solid of [Ir(ttp)]$_2$ **1d** was obtained in quantitative yield and was used without further purification. ^{1}H NMR (C_6D_6, 400 MHz): δ 2.47 (s, 12 H), 7.06 (d, 8 H, J = 7.5 Hz), 7.66 (d, 4 H, J = 7.6 Hz), 8.33 (s, 8 H), 9.48 (d, 4 H, J = 7.2 Hz).

Reaction between Ir(ttp)SiEt$_3$ 1a and 1,4-Difluorobenzenes (2d) in Benzene with the Addition of Base. General Procedure. The reaction of Ir(ttp)SiEt$_3$ **1a** with 1,4-difluorobenzene (**2b**) in benzene at 120 °C with the addition of 10 equivalents of KOH is described as a typical example. Benzene (0.9 mL) and 1,4-difluorobenzene (0.2 mL, 100 equiv) were added to a mixture of Ir(ttp)SiEt$_3$ (19.6 mg, 0.020 mmol) and KOH (11.2 mg, 0.200 mmol, 10 equiv), and the mixture was degassed by the freeze-pump-thaw method (3 cycles). Then the mixture was heated at 120 °C for 6

days. The crude product was purified by column chromatography on alumina eluting with a mixture of hexane/CH_2Cl_2 (3:1), and a purple solid of Ir(ttp)$SiEt_3$ **1a** (11.0 mg, 0.0113 mmol, 56%) was recovered. Then changed the solvent to hexane/CH_2Cl_2 (2:1), and a purple solid of Ir(ttp)(4-F-C_6H_4) **3e** (5.6 mg, 0.0059 mmol, 29%) was isolated. R_f = 0.35 (hexane/CH_2Cl_2 = 1:1). ^{1}H NMR (C_6D_6, 400 MHz): δ 0.92 (dd, 2 H, $^4J_{H\text{-}F}$ = 6.0 Hz, J = 8.8 Hz), 2.39 (s, 12 H), 4.65 (dd, 2 H, $^3J_{H\text{-}F}$ = 9.2 Hz, J = 9.2 Hz), 7.21 (d, 4 H, J = 7.4 Hz), 7.33 (d, 4 H, J = 7.6 Hz), 7.91 (dd, 4 H, J = 1.6, 7.8 Hz), 8.15 (dd, 4 H, J = 1.6, 7.6 Hz), 8.82 (s, 8 H). ^{13}C NMR ($CDCl_3$, 100 MHz): δ 21.5, 109.7 (d, $^2J_{C\text{-}F}$ = 19.5 Hz), 123.8, 127.4, 127.5, 129.0 (d, $^3J_{C\text{-}F}$ = 6.0 Hz), 131.4, 133.5, 134.1, 137.3, 138.6, 142.8, 156.9 (d, $^1J_{C\text{-}F}$ = 236.2 Hz). ^{19}F NMR ($CDCl_3$, 376 MHz): δ -62.36 (s, 1 F, 4-F). HRMS (FABMS): Calcd. for $(C_{54}H_{40}FN_4Ir)^+$: *m/z* 956.2861; found *m/z* 956.285545. A single crystal for X-ray analysis was grown from CH_2Cl_2/Hexane. Changing the solvent to hexane/CH_2Cl_2 (1:1), and a purple solid of Ir(ttp)(2,5-F_2-C_6H_3) **3f** was isolated in trace amount (less than 5% yield). R_f = 0.20 (hexane/CH_2Cl_2 = 1:1). ^{1}H NMR (C_6D_6, 400 MHz): δ 0.71 (ddd, 1 H, $^3J_{H\text{-}F}$ = 11.6 Hz, $^4J_{H\text{-}F}$ = 4.8 Hz, J = 3.2 Hz), 2.37 (s, 12 H), 4.23 (ddd, 1 H, $^3J_{H\text{-}F}$ = 14.0 Hz, $^4J_{H\text{-}F}$ = 5.2 Hz, J = 7.0 Hz), 4.78 (ddd, 1 H, $^3J_{H\text{-}F}$ = 11.4 Hz, $^4J_{H\text{-}F}$ = 3.2 Hz, J = 7.2 Hz), 7.19 (d, 4 H, J = 7.6 Hz), 7.28 (d, 4 H, J = 7.6 Hz), 8.01 (dd, 4 H, J = 1.6, 7.6 Hz), 8.11 (dd, 4 H, J = 2.0, 7.6 Hz), 8.87 (s, 8 H). ^{13}C NMR (CD_2Cl_2, 100 MHz): δ 21.5, 86.8 (d, $^2J_{C\text{-}F}$ = 31.9 Hz), 107.0 (dd, $^2J_{C\text{-}F}$ = 24.2 Hz, $^3J_{C\text{-}F}$ = 9.3 Hz), 110.3 (dd, $^2J_{C\text{-}F}$ = 31.0 Hz, $^3J_{C\text{-}F}$ = 8.9 Hz), 119.6 (dd, $^2J_{C\text{-}F}$ = 21.8 Hz, $^3J_{C\text{-}F}$ = 12.9 Hz), 123.5, 127.7, 127.8, 131.6, 133.8, 134.5, 137.8, 139.0, 143.3, 152.4 (d, $^1J_{C\text{-}F}$ = 236.8 Hz), 160.8 (d, $^1J_{C\text{-}F}$ = 234.2). ^{19}F NMR (CD_2Cl_2, 376 MHz): δ -61.40 ~ -61.29 (m, 1 F, 5-F), -52.63 ~ -52.55 (m, 1 F, 2-F). HRMS (FABMS): Calcd. for $(C_{54}H_{39}F_2N_4Ir)^+$: *m/z* 974.2767; found *m/z* 974.276253.

Reaction between Ir(ttp)SiEt$_3$ 1a and 1,4-Difluorobenzenes (2d) in Benzene with the addition of 10 equivalents of KOH at 150 °C. Benzene (0.9 mL) and 1,4-difluorobenzene (0.2 mL, 100 equiv) were added to a mixture of Ir(ttp)SiEt$_3$ (18.7 mg, 0.019 mmol) and KOH (10.8 mg, 0.190 mmol, 10 equiv). Then the mixture was heated at 150 °C for 5 days. The crude product was purified by column chromatography eluting with a mixture of hexane/CH_2Cl_2 (3:1), and a purple solid of Ir(ttp)SiEt$_3$ **1a** (1.2 mg, 0.0012 mmol, 6%) was recovered. Then changed the solvent to hexane/CH_2Cl_2 (2:1), and a purple solid mixture of Ir(ttp)(4-F-C_6H_4) **3e** (15.4 mg, 0.0161 mmol, 85%) and Ir(ttp)C_6H_5 **3a** (<5%) was isolated. Ir(ttp)C_6H_5 **3a**, R_f = 0.35 (hexane/CH_2Cl_2 = 1:1). ^{1}H NMR (C_6D_6, 400 MHz): δ 1.10 (d, 2 H, J = 8.0 Hz), 2.39 (s, 12 H), 4.89 (t, 2 H, J = 7.2 Hz), 5.23 (t, 1 H, J = 7.2 Hz), 7.19 (d, 4 H, J = 7.6 Hz), 7.32 (d, 4 H, J = 7.6 Hz), 7.87 (dd, 4 H, J = 1.6, 7.6 Hz), 8.14 (dd, 4 H, J = 1.6, 7.6 Hz), 8.80 (s, 8 H). ^{13}C NMR ($CDCl_3$, 75 MHz): δ 21.7, 95.3, 120.2, 123.2, 124.2, 127.6, 129.1, 131.6, 133.7, 134.2, 137.4. HRMS (FABMS): Calcd. for $(C_{54}H_{41}N_4Ir)^+$: *m/z* 938.2955; found *m/z* 938.294798. When changed the solvent to hexane/CH_2Cl_2 (1:1), a purple solid of Ir(ttp)(2,5-F_2-C_6H_3) **3f** (<5%) was isolated.

Reaction between Ir(ttp)SiEt$_3$ 1a and 1,4-Difluorobenzenes (2d) in Benzene with the Addition of 10 equivalents of KOH at 200 °C. Benzene (0.9 mL) and 1,4-difluorobenzene (0.2 mL, 100 equiv) were added to a mixture of Ir(ttp)SiEt$_3$ (18.4 mg, 0.019 mmol) and KOH (10.6 mg, 0.190 mmol, 10 equiv). Then the mixture was heated at 200 °C for 3 days. The crude product was purified by column chromatography eluting with a mixture of hexane/CH_2Cl_2 (3:1), and a purple solid of Ir(ttp)SiEt$_3$ **1a** (<5%) was recovered. Then changed the solvent to hexane/CH_2Cl_2 (2:1), and a purple solid mixture of Ir(ttp)(4-F-C_6H_4) **3e** (9.4 mg, 0.0098 mmol, 52%) and Ir(ttp)C_6H_5 **3a** (5.2 mg, 0.0055 mmol, 29%) was isolated. When changed the

solvent to hexane/CH_2Cl_2 (1:1), a purple solid of Ir(ttp)(2,5-F_2-C_6H_3) **3f** (1.5 mg, 0.0015 mmol, 8%) was isolated.

Reaction between Ir(ttp)$SiEt_3$ 1a and 1,4-Difluorobenzenes (2d) in Benzene without the Addition of KOH at 200 °C. Benzene (0.8 mL) and 1,4-difluorobenzene (0.2 mL, 100 equiv) were added to Ir(ttp)$SiEt_3$ (18.2 mg, 0.019 mmol). Then the mixture was heated at 200 °C for 3 days. The crude product was purified by column chromatography eluting with a mixture of hexane/CH_2Cl_2 (3:1), and a purple solid of Ir(ttp)$SiEt_3$ **1a** (17.6 mg, 0.0180 mmol, 96%) was recovered.

Reaction between Ir(ttp)$SiEt_3$ 1a and 1,4-Difluorobenzenes (2d) in Benzene-d_6 with the Addition of KOH at 200 °C. Benzene-d_6 (0.9 mL) and 1,4-difluorobenzene (0.2 mL, 100 equiv) were added to a mixture of Ir(ttp)$SiEt_3$ (18.5 mg, 0.019 mmol) and KOH (10.6 mg, 0.190 mmol, 10 equiv). Then the mixture was heated at 200 °C for 3 days. The crude product was purified by column chromatography eluting with a mixture of hexane/CH_2Cl_2 (3:1), and a purple solid of Ir(ttp)$SiEt_3$ **1a** (6.4 mg, 0.0066 mmol, 34%) was recovered. Then changed the solvent to hexane/CH_2Cl_2 (2:1), and a purple solid mixture of Ir(ttp)(4-F-C_6H_4) **3e** (9.0 mg, 0.0094 mmol, 50%) and Ir(ttp)C_6D_5 **3a'** (1.2 mg, 0.0013 mmol, 6%) was isolated. When changed the solvent to hexane/CH_2Cl_2 (1:1), a purple solid of Ir(ttp)(2,5-F_2-C_6H_3) **3f** (1.2 mg, 0.0012 mmol, 6%) was isolated.

Reaction between Ir(ttp)$SiEt_3$ 1a and 1,4-Difluorobenzenes (2d) in Benzene with the Addition of KF at 150 °C. Benzene (0.9 mL) and 1,4-difluorobenzene (0.2 mL, 100 equiv) were added to a mixture of Ir(ttp)$SiEt_3$ (18.2 mg, 0.019 mmol) and KF (10.8 mg, 0.190 mmol, 10 equiv). Then the mixture was heated at 200 °C for 8 days. The crude product was purified by column chromatography eluting with a mixture of

hexane/CH_2Cl_2 (3:1), and a purple solid of Ir(ttp)$SiEt_3$ **1a** (17.4 mg, 0.0178 mmol, 94%) was recovered.

Reaction between Ir(ttp)$SiEt_3$ 1a and 1,4-Difluorobenzenes (2d) in Benzene with the Addition of 5 equivalents of KOH at 150 °C. Benzene (0.8 mL) and 1,4-difluorobenzene (0.2 mL, 100 equiv) were added to a mixture of Ir(ttp)$SiEt_3$ (17.8 mg, 0.018 mmol) and KOH (5.1 mg, 0.090 mmol, 5 equiv). Then the mixture was heated at 150 °C for 5 days. The crude product was purified by column chromatography eluting with a mixture of hexane/CH_2Cl_2 (3:1), and a purple solid of Ir(ttp)$SiEt_3$ **1a** (3.1 mg, 0.0032 mmol, 17%) was recovered. Then changed the solvent to hexane/CH_2Cl_2 (2:1), and a purple solid of Ir(ttp)(4-F-C_6H_4) **3e** (10.6 mg, 0.0111 mmol, 61%) and Ir(ttp)C_6H_5 **3a** (<5%) was isolated. When changed the solvent to hexane/CH_2Cl_2 (1:1), a purple solid of Ir(ttp)(2,5-F_2-C_6H_3) **3f** (1.9 mg, 0.0020 mmol, 11%) was isolated.

Reaction between Ir(ttp)$SiEt_3$ 1a and 1,4-Difluorobenzenes (2d) in Benzene with the Addition of 20 equivalents of KOH at 150 °C. Benzene (0.9 mL) and 1,4-difluorobenzene (0.2 mL, 100 equiv) were added to a mixture of Ir(ttp)$SiEt_3$ (18.6 mg, 0.019 mmol) and KOH (21.4 mg, 0.380 mmol, 20 equiv). Then the mixture was heated at 150 °C for 4 days. The crude product was purified by column chromatography eluting with a mixture of hexane/CH_2Cl_2 (3:1), and a purple solid of Ir(ttp)$SiEt_3$ **1a** was recovered in trace amount (<5%). Then changed the solvent to hexane/CH_2Cl_2 (2:1), and a purple solid of Ir(ttp)(4-F-C_6H_4) **3e** (13.5 mg, 0.0141 mmol, 74%) and Ir(ttp)C_6H_5 **3a** (<5%) was isolated. When changed the solvent to hexane/CH_2Cl_2 (1:1), a purple solid of Ir(ttp)(2,5-F_2-C_6H_3) **3f** (<5%) was isolated.

Reaction between Ir(ttp)$SiEt_3$ 1a and Fluorobenzenes (2a-g) with the Addition of 10 equivalents of KOH at 200 °C in Solvent-Free Conditions. General Procedure.

The reaction of Ir(ttp)$SiEt_3$ **1a** with fluorobenzene (**2a**) at 200 °C with the addition of 10 equivalents of KOH is described as a typical example. Fluorobenzene (0.9 mL, 500 equiv) was added to a mixture of Ir(ttp)$SiEt_3$ (18.4 mg, 0.019 mmol) and KOH (10.6 mg, 0.190 mmol, 10 equiv), and the mixture was degassed by the freeze-pump-thaw method (3 cycles). Then the mixture was heated at 200 °C for 2 days. The crude product was purified by column chromatography on alumina eluting with a mixture of hexane/CH_2Cl_2 (2:1), and a purple solid mixture of Ir(ttp)C_6H_5 **3a** (11.4 mg, 0.0122 mmol, 64%), Ir(ttp)(2-F-C_6H_4) **3b** (<5%), Ir(ttp)(3-F-C_6H_3) **2d** (3.2 mg, 0.0033 mmol, 18%) and Ir(ttp)(4-F-C_6H_4) **3e** (0.9 mg, 0.0009 mmol, 5%) was isolated. Ir(ttp)(2-F-C_6H_4) **3b**, R_f = 0.35 (hexane/CH_2Cl_2 = 1:1). ^{1}H NMR (C_6D_6, 400 MHz): δ 0.79 (ddd, 1 H, $^4J_{H\text{-}F}$ = 8.4 Hz, J = 1.6, 6.8 Hz), 2.38 (s, 12 H), 4.44 (ddd, 1 H, $^3J_{H\text{-}F}$ = 11.5 Hz, J = 1.2, 7.8 Hz), 4.80 (ddd, 1 H, $^5J_{H\text{-}F}$ = 7.0 Hz, J = 1.2, 7.0 Hz), 5.09 (dddd, 1 H, $^4J_{H\text{-}F}$ = 9.6 Hz, J = 1.6, 4.9, 5.4 Hz), 7.20 (d, 4 H, J = 7.6 Hz), 7.31 (d, 4 H, J = 7.6 Hz), 7.95 (dd, 4 H, J = 1.6, 7.6 Hz), 8.13 (dd, 4 H, J = 1.6, 7.6 Hz), 8.85 (s, 8 H). ^{13}C NMR (CD_2Cl_2, 100 MHz): δ 21.6, 110.8 (d, $^2J_{C\text{-}F}$ = 27.9 Hz), 119.2 (d, $^4J_{C\text{-}F}$ = 2.4 Hz), 121.7 (d, $^3J_{C\text{-}F}$ = 8.2 Hz), 123.7, 127.7, 127.8, 131.6, 133.9, 134.0 (d, $^3J_{C\text{-}F}$ = 11.6 Hz), 134.4, 137.7, 139.0, 143.4, 163.9 (d, $^1J_{C\text{-}F}$ = 240.1 Hz). ^{19}F NMR (CD_2Cl_2, 376 MHz): δ -45.55 ~ -45.49 (m, 1 F, 2-F). HRMS (FABMS): Calcd. for $(C_{54}H_{40}FN_4Ir)^+$: *m/z* 956.2861; found *m/z* 956.284725. A single crystal for X-ray analysis was grown fron CH_2Cl_2/methanol. Ir(ttp)(3-F-C_6H_4) **3d**, R_f = 0.35 (hexane/ CH_2Cl_2 = 1:1). ^{1}H NMR (C_6D_6, 400 MHz): δ 0.85 (d, 1 H, J = 8.4 Hz), 0.88 (ddd, 1 H, $^3J_{H\text{-}F}$ = 12.0 Hz, J = 1.6, 2.0 Hz), 2.39 (s, 12 H), 4.64 (dd, 1 H, $^3J_{H\text{-}F}$ = 15.2 Hz, J = 8.0 Hz), 4.94 (dt, 1 H, $^4J_{H\text{-}F}$ = 2.4 Hz, J = 8.4 Hz), 7.18 (d, 4 H, J = 7.6 Hz), 7.32 (d, 4 H, J = 7.6 Hz), 7.90 (dd, 4 H, J = 2.0, 7.6 Hz), 8.14 (dd, 4 H, J = 2.0, 7.8 Hz), 8.82 (s, 8 H). ^{13}C NMR ($CDCl_3$, 100 MHz): δ 21.7, 106.6 (d, $^2J_{C\text{-}F}$ = 20.8 Hz), 115.4 (d, $^2J_{C\text{-}F}$ = 19.6 Hz),

123.2 (d, $^{3}J_{C\text{-}F}$ = 8.0 Hz), 123.9, 124.9, 127.6, 127.7, 131.6, 133.6, 134.3, 137.4, 138.7, 142.9, 155.5 (d, $^{1}J_{C\text{-}F}$ = 243.1 Hz). ^{19}F NMR ($CDCl_3$, 376 MHz): δ -54.19 ~ -54.12 (m, 1 F, 3-F). HRMS (FABMS): Calcd. for $(C_{54}H_{40}FN_4Ir)^+$: *m/z* 956.2861; found *m/z* 956.286859. A single crystal for X-ray analysis was grown from CH_2Cl_2/methanol.

Reaction between Ir(ttp)SiEt$_3$ 1a and 1,2-Difluorobenzenes (2b) with the Addition of 10 equivalents of KOH at 200 °C in Solvent-Free Conditions. 1,2-Difluorobenzene (1.0 mL, 500 equiv) was added to a mixture of Ir(ttp)SiEt$_3$ (19.4 mg, 0.020 mmol) and KOH (11.2 mg, 0.200 mmol, 10 equiv). Then the mixture was heated at 200 °C for 2 days. The crude product was purified by column chromatography eluting with a mixture of hexane/CH_2Cl_2 (2:1), and a purple solid of Ir(ttp)(2-F-C_6H_4) **3b** (1.1 mg, 0.0012 mmol, 6%) was isolated. Then changed the solvent to hexane/CH_2Cl_2 (1:1), and a purple solid of Ir(ttp)(2,3-F_2-C_6H_3) **3c** (17.2 mg, 0.0177 mmol, 89%) was isolated. R_f = 0.25 (hexane/CH_2Cl_2 = 1:1). ^{1}H NMR (C_6D_6, 400 MHz): δ 0.52 (dddd, 1 H, $^{5}J_{H\text{-}F}$ = 1.4 Hz, $^{4}J_{H\text{-}F}$ = 6.8 Hz, *J* = 1.2, 6.8 Hz), 2.38 (s, 12 H), 4.54 (ddt, 1 H, $^{5}J_{H\text{-}F}$ = 1.2 Hz, $^{4}J_{H\text{-}F}$ = 8.0 Hz, *J* = 7.0 Hz), 4.93 (dddd, 1 H, $^{4}J_{H\text{-}F}$ = 12.4 Hz, $^{3}J_{H\text{-}F}$ = 12.7 Hz, *J* = 1.2, 8.2 Hz), 7.19 (d, 4 H, *J* = 7.2 Hz), 7.30 (d, 4 H, *J* = 7.6 Hz), 7.96 (dd, 4 H, *J* = 1.6, 7.6 Hz), 8.11 (dd, 4 H, *J* = 1.6, 8.6 Hz), 8.86 (s, 8 H). ^{13}C NMR (CD_2Cl_2, 100 MHz): δ 21.6, 108.3 (d, $^{2}J_{C\text{-}F}$ = 17.3 Hz), 118.1 (dd, $^{3}J_{C\text{-}F}$ = 6.6 Hz, $^{4}J_{C\text{-}F}$ = 3.1 Hz), 123.5, 127.6, 127.8, 129.2 (dd, $^{3}J_{C\text{-}F}$ = 11.0 Hz, $^{4}J_{C\text{-}F}$ = 3.2 Hz), 131.5, 134.0, 134.4, 137.7, 139.1, 143.3, 144.6 (dd, $^{1}J_{C\text{-}F}$ = 242.9 Hz, $^{2}J_{C\text{-}F}$ = 18.1 Hz), 152.3 (dd, $^{1}J_{C\text{-}F}$ = 239.4 Hz, $^{2}J_{C\text{-}F}$ = 10.2 Hz). ^{19}F NMR (CD_2Cl_2, 376 MHz): δ -79.80 ~ -79.70 (m, 1 F, 3-F), -73.02 ~ -72.95 (m, 1 F, 2-F). HRMS (FABMS): Calcd. for $(C_{54}H_{39}F_2N_4Ir)^+$: *m/z* 974.2767; found *m/z* 974.278921. A single crystal for X-ray analysis was grown from CH_2Cl_2/DMSO.

Reaction between Ir(ttp)$SiEt_3$ 1a and 1,3-Difluorobenzenes (2c) with the Addition of 10 equivalents of KOH at 200 °C in Solvent-Free Conditions. 1,3-Difluorobenzene (1.0 mL, 500 equiv) was added to a mixture of Ir(ttp)$SiEt_3$ (18.8 mg, 0.019 mmol) and KOH (10.8 mg, 0.190 mmol, 10 equiv). Then the mixture was heated at 200 °C for 4 days. The crude product was purified by column chromatography eluting with a mixture of hexane/CH_2Cl_2 (2:1), and a purple solid of Ir(ttp)(3-F-C_6H_4) **3b** (14.6 mg, 0.0153 mmol, 80%) was isolated.

Reaction between Ir(ttp)$SiEt_3$ 1a and 1,4-Difluorobenzenes (2d) with the Addition of 10 equivalents of KOH at 200 °C in Solvent-Free Conditions for Three Days. 1,4-Difluorobenzene (1.0 mL, 500 equiv) was added to a mixture of Ir(ttp)$SiEt_3$ (18.0 mg, 0.018 mmol) and KOH (10.3 mg, 0.180 mmol, 10 equiv). Then the mixture was heated at 200 °C for 3 days. The crude product was purified by column chromatography eluting with a mixture of hexane/CH_2Cl_2 (3:1), and a purple solid of Ir(ttp)$SiEt_3$ **1a** (1.7 mg, 0.0017 mmol, 10%) was recovered. Then changed the solvent to hexane/CH_2Cl_2 (2:1), and a purple solid of Ir(ttp)(4-F-C_6H_4) **3e** (8.2 mg, 0.0086 mmol, 47%) was isolated. When changed the solvent to hexane/CH_2Cl_2 (1:1), a purple solid of Ir(ttp)(2,5-$C_6H_3F_2$) **3f** (7.2 mg, 0.0074 mmol, 41%) was isolated.

Reaction between Ir(ttp)$SiEt_3$ 1a and 1,3,5-Trifluorobenzenes (2e) with the Addition of 10 equivalents of KOH at 200 °C in Solvent-Free Conditions. 1,3,5-Trifluorobenzene (1.1 mL, 500 equiv) was added to a mixture of Ir(ttp)$SiEt_3$ (20.2 mg, 0.021 mmol) and KOH (11.6 mg, 0.210 mmol, 10 equiv). Then the mixture was heated at 200 °C for 8 days. The crude product was purified by column chromatography eluting with a mixture of hexane/CH_2Cl_2 (3:1), and a purple solid of Ir(ttp)$SiEt_3$ **1a** (15.2 mg, 0.0155 mmol, 74%) was recovered. Then changed the solvent to hexane/CH_2Cl_2 (1:1), and a purple solid of Ir(ttp)(3,5-F_2-C_6H_3) **3g** (4.9 mg,

0.0050 mmol, 24%) was isolated. R_f= 0.30 (hexane/CH_2Cl_2 = 1:1). ^{1}H NMR (C_6D_6, 400 MHz): δ 0.62 (dd, 2 H, $^3J_{H\text{-}F}$ = 9.6 Hz, J = 2.0 Hz), 2.39 (s, 12 H), 4.69 (tt, 1 H, $^3J_{H\text{-}F}$ = 9.2 Hz, J = 2.4 Hz), 7.17 (d, 4 H, J = 8.0 Hz), 7.33 (d, 4 H, J = 7.2 Hz), 7.92 (dd, 4 H, J = 1.6, 7.8 Hz), 8.13 (dd, 4 H, J = 1.6, 7.6 Hz), 8.82 (s, 8 H). The ^{13}C NMR and ^{19}F NMR spectra of **3g** can not be obtained since its solubility is not good enough in $CDCl_3$, CD_2Cl_2, acetone-d_6 and THF-d_8. HRMS (FABMS): Calcd. for $(C_{54}H_{39}F_2N_4Ir)^+$: *m/z* 974.2767; found *m/z* 974.273442. A single crystal for X-ray analysis was grown from CH_2Cl_2/methanol.

Reaction between Ir(ttp)SiEt$_3$ 1a and Pentafluorobenzenes (2f) with the Addition of 10 equivalents of KOH at 200 °C in Solvent-Free Conditions. Pentafluorobenzene (1.0 mL, 500 equiv) was added to a mixture of Ir(ttp)$SiEt_3$ (18.1 mg, 0.019 mmol) and KOH (10.4 mg, 0.190 mmol, 10 equiv). Then the mixture was heated at 200 °C for 6 days. The crude product was purified by column chromatography eluting with a mixture of hexane/CH_2Cl_2 (3:1), and a purple solid of Ir(ttp)$SiEt_3$ **1a** (7.0 mg, 0.0072 mmol, 38%) was recovered. Then changed the solvent to hexane/CH_2Cl_2 (1:1), and a purple solid of Ir(ttp)(C_6F_5) **3i** (10.9 mg, 0.0106 mmol, 56%) was isolated. R_f = 0.08 (hexane/CH_2Cl_2 = 1:1). ^{1}H NMR (C_6D_6, 400 MHz): δ 2.36 (s, 12 H), 7.19 (d, 4 H, J = 7.6 Hz), 7.27 (d, 4 H, J = 7.6 Hz), 8.06 (d, 4 H, J = 7.2 Hz), 8.16 (d, 4 H, J = 7.2 Hz), 8.93 (s, 8 H). ^{13}C NMR (THF-d_8, 100 MHz): δ 21.5, 123.7, 128.0 (d, $^2J_{C\text{-}F}$ = 24.5 Hz), 131.8, 134.4, 134.9, 138.1, 139.9, 144.0, 148 ~ 153 (for the C of C-F bond). ^{19}F NMR (THF-d_8, 376 MHz): δ -105.6 (t, 1 F, J = 19.9 Hz, 4-F), -103.16 (t, 2 F, J = 19.9 Hz, 3-F), -69.40 (d, 2 F, J = 20.2 Hz, 2-F). HRMS (FABMS): Calcd. for $(C_{54}H_{36}F_5N_4Ir)^+$: *m/z* 1028.2484; found *m/z* 1028.251763. A single crystal for X-ray analysis was grown from CH_2Cl_2/methanol. And ArCFA product Ir(ttp)(2,3,4,6-F_4-C_6H) **3h** (<5%) was involved in the mixture of product. R_f =

0.08 (hexane/CH_2Cl_2 = 1:1). ^{1}H NMR (C_6D_6, 400 MHz): δ 2.36 (s, 12 H), 4.69 (ddd, 1 H, $^3J_{H\text{-}F}$ = 16.4 Hz, $^4J_{H\text{-}F}$ = 9.4 Hz, $^5J_{H\text{-}F}$ = 7.2 Hz), 7.19 (dd, 8 H, J = 1.7, 8.0 Hz), 8.84 ~ 8.14 (m, 8 H (overlap with Ir(ttp)C_6F_5)), 8.91 (s, 8 H). ^{19}F NMR ($CDCl_3$, 376 MHz): δ -83.95 ~ -83.78 (m, 1 F, 4-F), -80.81 ~ -80.70 (m, 1 F, 3-F), -71.43 ~ -71.35 (m, 1 F, 2-F), -69.16 ~ -69.12 (m, 1 F, 6-F). HRMS (FABMS): Calcd. for $(C_{54}H_{37}F_4N_4Ir)^+$: *m/z* 1010.2578; found *m/z* 1010.280933.

Reaction between Ir(ttp)$SiEt_3$ 1a and Hexafluorobenzenes (2g) with the Addition of 10 equivalents of KOH at 200 °C in Solvent-Free Conditions. Hexafluorobenzene (1.2 mL, 500 equiv) was added to a mixture of Ir(ttp)$SiEt_3$ (20.7 mg, 0.021 mmol) and KOH (11.9 mg, 0.210 mmol, 10 equiv). Then the mixture was heated at 200 °C for 8 days. The crude product was purified by column chromatography eluting with a mixture of hexane/CH_2Cl_2 (3:1), and a purple solid of Ir(ttp)$SiEt_3$ **1a** (4.9 mg, 0.0050 mmol, 24%) was recovered. Then changed the solvent to hexane/CH_2Cl_2 (1:1), and a purple solid of Ir(ttp)(C_6F_5) **3i** (10.8 mg, 0.0105 mmol, 50%) was isolated.

Reaction between Ir(ttp)$SiEt_3$ 1a and 1,4-Difluorobenzenes (2d) with the Addition of 10 equivalents of KOH at 200 °C in Solvent-Free Conditions for Two Hours. 1,4-Difluorobenzene (0.9 mL, 500 equiv) was added to a mixture of Ir(ttp)$SiEt_3$ (17.0 mg, 0.017 mmol) and KOH (9.5 mg, 0.170 mmol, 10 equiv). Then the mixture was heated at 200 °C for 2 hours. The crude product was purified by column chromatography eluting with a mixture of hexane/CH_2Cl_2 (3:1), and a purple solid of Ir(ttp)$SiEt_3$ **1a** (10.6 mg, 0.0109 mmol, 64%) was recovered. Then changed the solvent to hexane/CH_2Cl_2 (2:1), and a purple solid of Ir(ttp)(4-F-C_6H_4) **3e** (4.7 mg, 0.0049 mmol, 29%) was isolated. When changed the solvent to hexane/CH_2Cl_2 (1:1), a purple solid of Ir(ttp)(2,5-F_2-C_6H_3) **3f** (<5%) was isolated.

Reaction of Ir(ttp)(4-F-C_6H_4) 3e and 1,4-Difluorobenzene (2d) with the Addition of KOH. 1,4-Difluorobenzene (1.0 mL, 500 equiv) was added to a mixture of Ir(ttp)(4-F-C_6H_4) (18.9 mg, 0.020 mmol) and KOH (11.1 mg, 0.200 mmol, 10 equiv), and the mixture was degassed by the freeze-pump-thaw method (3 cycles). Then the mixture was heated at 200 °C for 3 days. The crude product was purified by column chromatography on alumina eluting with a mixture of hexane/CH_2Cl_2 (2:1), and a purple solid of Ir(ttp)(4-F-C_6H_4) **3e** (10.9 mg, 0.0114 mmol, 57%) was recovered. Then changed the solvent to hexane/CH_2Cl_2 (1:1), and a purple solid of Ir(ttp)(2,5-F_2-C_6H_3) **3f** (5.8 mg, 0.0060 mmol, 30%) was isolated.

Reaction of Ir(ttp)(2,5-F_2-C_6H_3) 3f and 1,4-Difluorobenzene (2d) with the Addition of KOH at 200 °C for Three days. 1,4-Difluorobenzene (0.9 mL, 500 equiv) was added to a mixture of Ir(ttp)(2,5-F_2-C_6H_3) (17.5 mg, 0.018 mmol) and KOH (10.0 mg, 0.180 mmol, 10 equiv), and the mixture was degassed by the freeze-pump-thaw method (3 cycles). Then the mixture was heated at 200 °C for 3 days. The crude product was purified by column chromatography on alumina eluting with a mixture of hexane/CH_2Cl_2 (2:1), and a purple solid of Ir(ttp)(4-F-C_6H_4) **3e** (1.5 mg, 0.0016 mmol, 9%) was isolated. Then changed the solvent to hexane/CH_2Cl_2 (1:1), and a purple solid of Ir(ttp)(2,5-F_2-C_6H_3) **3f** (13.8 mg, 0.0142 mmol, 79%) was recovered.

Reaction of Ir(ttp)(2,5-F_2-C_6H_3) 3f and 1,4-Difluorobenzene (2d) with the Addition of KOH at 200 °C for Six days. 1,4-Difluorobenzene (1.1 mL, 500 equiv) was added to a mixture of Ir(ttp)(2,5-F_2-C_6H_3) (21.0 mg, 0.022 mmol) and KOH (12.1 mg, 0.220 mmol, 10 equiv), and the mixture was degassed by the freeze-pump-thaw method (3 cycles). Then the mixture was heated at 200 °C for 6 days. The crude product was purified by column chromatography on alumina eluting with a mixture of

hexane/CH_2Cl_2 (2:1), and a purple solid of Ir(ttp)(4-F-C_6H_4) **3e** (12.2 mg, 0.0128 mmol, 58%) was isolated. Then changed the solvent to hexane/CH_2Cl_2 (1:1), a purple solid of Ir(ttp)(2,5-F_2-C_6H_3) **3f** (5.4 mg, 0.0055 mmol, 25%) was recovered.

Reaction of Ir(ttp)$SiEt_3$ 1a with KOH in Benzene-d_6 in a Sealed-NMR Tube. Benzene-d_6 (0.5 mL) was added to mixture of Ir(ttp)$SiEt_3$ (9.3 mg, 0.0095 mmol) and KOH (5.3 mg, 0.0950 mmol, 10 equiv) in an NMR tube with a rotaflo stopper and degassed by the freeze-pump-thaw method (3 cycles). The mixture was frozen under liquid nitrogen and then flame-sealed under vacuum. The sealed-NMR tube was heated at 200 °C, and monitored by ^1H NMR spectroscopy and the yield of product was calibrated with the internal standard residual benzene in benzene-d_6.

Reaction of Ir(ttp)$^-Na^+$ 1b and Fluorobenzene (2a) without the Addition of KOH. Fluorobenzene (1.0 mL, 500 equiv) was added to Ir(ttp)$^-Na^+$ (18.6 mg, 0.022 mmol) under N_2, and the mixture was degassed by the freeze-pump-thaw method (3 cycles). Then the mixture was heated at 120 °C for 2 days. The crude product was purified by column chromatography on alumina eluting with a mixture of hexane/CH_2Cl_2 (2:1), and a purple solid of Ir(ttp)C_6H_5 **3a** (8.2 mg, 0.0087 mmol, 40%) was isolated.

Reaction of Ir(ttp)H 1d and Fluorobenzene (2a) without the Addition of KOH. Fluorobenzene (0.8 mL, 500 equiv) was added to Ir(ttp)H (15.4 mg, 0.018 mmol), and the mixture was degassed by the freeze-pump-thaw method (3 cycles). Then the mixture was heated at 200 °C for 4 days. The crude product was purified by column chromatography on alumina eluting with a mixture of hexane/CH_2Cl_2 (1:1), and a purple solid mixture of unknowns (4.3 mg, ca 28 %) was isolated. And no aromatic CFA or CHA product was observed.

Reaction of Ir(ttp)H 1d and Fluorobenzene (2a) with the Addition of KOH. Fluorobenzene (0.9 mL, 500 equiv) was added to a mixture of Ir(ttp)H (17.2 mg,

0.020 mmol) and KOH (11.2 mg, 0.200 mmol, 10 equiv), and the mixture was degassed by the freeze-pump-thaw method (3 cycles). Then the mixture was heated at 200 °C for 1 day. The crude product was purified by column chromatography on alumina eluting with a mixture of hexane/CH_2Cl_2 (2:1), and a purple solid mixture of Ir(ttp)C_6H_5 **3a** (9.4 mg, 0.0100 mmol, 50%), Ir(ttp)(2-F-C_6H_4) **3b** (1.3 mg, 0.0014 mmol, 7%), Ir(ttp)(3-F-C_6H_4) **3d** (4.2 mg, 0.0044 mmol, 22%) and Ir(ttp)(4-F-C_6H_4) **3e** (1.1 mg, 0.0012 mmol, 6%) was isolated.

Reaction of Ir(ttp)H 1d and Fluorobenzene (2a) with the Addition of KOH at 120 °C. Fluorobenzene (0.8 mL, 500 equiv) was added to a mixture of Ir(ttp)H (14.9 mg, 0.017 mmol) and KOH (9.7 mg, 0.170 mmol, 10 equiv), and the mixture was degassed by the freeze-pump-thaw method (3 cycles). Then the mixture was heated at 120 °C for 2 days. The crude product was purified by column chromatography on alumina eluting with a mixture of hexane/CH_2Cl_2 (2:1), and a purple solid of Ir(ttp)C_6H_5 **3a** (14.5 mg, 0.0155 mmol, 91%) was isolated. And no aromatic CHA product was observed.

Reaction of $[Ir(ttp)]_2$ 1c and Fluorobenzene (2a) without the Addition of KOH. Fluorobenzene (1.0 mL, 1000 equiv) was added to $[Ir(ttp)]_2$ (18.2 mg, 0.010 mmol), and the mixture was degassed by the freeze-pump-thaw method (3 cycles). Then the mixture was heated at 200 °C for 2 days. The crude product was purified by column chromatography on alumina eluting with a mixture of hexane/CH_2Cl_2 (1:1), and a purple solid mixture of unknowns (11.8 mg, ca 65 %) was isolated. And no aromatic CFA or CHA product was observed.

Reaction of $[Ir(ttp)]_2$ 1c and Fluorobenzene (2a) with the Addition of KOH. Fluorobenzene (1.1 mL, 1000 equiv) was added to a mixture of $[Ir(ttp)]_2$ (19.4 mg, 0.011 mmol) and KOH (12.7 mg, 0.220 mmol, 20 equiv), and the mixture was

degassed by the freeze-pump-thaw method (3 cycles). Then the mixture was heated at 200 °C for 1 day. The crude product was purified by column chromatography on alumina eluting with a mixture of hexane/CH_2Cl_2 (2:1), and a purple solid mixture of Ir(ttp)C_6H_5 **3a** (10.7 mg, 0.0114 mmol, 52%), Ir(ttp)(2-F-C_6H_4) **3b** (1.9 mg, 0.0020 mmol, 9%), Ir(ttp)(3-F-C_6H_4) **3d** (2.8 mg, 0.0029 mmol, 13%) and Ir(ttp)(4-F-C_6H_4) **3e** (1.1 mg, 0.0011 mmol, 5%) was isolated.

Reaction of Ir(ttp)$SiEt_3$ 1a and Benzene (2h) with the Addition of KOH. Benzene (0.8 mL, 500 equiv) was added to a mixture of Ir(ttp)$SiEt_3$ (17.0 mg, 0.017 mmol) and KOH (9.8 mg, 0.170 mmol, 10 equiv), and the mixture was degassed by the freeze-pump-thaw method (3 cycles). Then the mixture was heated at 200 °C for 4 days. The crude product was purified by column chromatography on alumina eluting with a mixture of hexane/CH_2Cl_2 (2:1), and a purple solid of Ir(ttp)C_6H_5 **3a** (1.1 mg, 0.0012 mmol, 7%) was isolated.

Reaction of Ir(ttp)(4-F-C_6H_4) 3e and Fluorobenzene (2a) with the Addition of KOH. Fluorobenzene (0.9 mL, 500 equiv) was added to a mixture of Ir(ttp)(4-F-C_6H_4) (17.9 mg, 0.019 mmol) and KOH (10.5 mg, 0.190 mmol, 10 equiv), and the mixture was degassed by the freeze-pump-thaw method (3 cycles). Then the mixture was heated at 200 °C for 4 days. The crude product was purified by column chromatography on alumina eluting with a mixture of hexane/CH_2Cl_2 (2:1), and a purple solid mixture of Ir(ttp)C_6H_5 **3a** (0.9 mg, 0.0010 mmol, 5%), Ir(ttp)(2-F-C_6H_4) **3b** (<5%), Ir(ttp)(3-F-C_6H_4) **3d** (7.6 mg, 0.0079 mmol, 42%) and Ir(ttp)(4-F-C_6H_4) **3e** (6.9 mg, 0.0072 mmol, 38%) was isolated.

Reaction of Ir(ttp)(4-F-C_6H_4) 3e and Fluorobenzene (2a) without the Addition of KOH. Fluorobenzene (1.0 mL, 500 equiv) was added to Ir(ttp)(4-F-C_6H_4) (19.4 mg, 0.020 mmol), and the mixture was degassed by the freeze-pump-thaw method (3

cycles). Then the mixture was heated at 200 °C for 4 days. The crude product was purified by column chromatography on alumina eluting with a mixture of hexane/CH_2Cl_2 (2:1), and a purple solid mixture of Ir(ttp)(4-F-C_6H_4) **3e** (18.2 mg, 0.0194 mmol, 97%) was recovered.

Reaction of Ir(ttp)(4-F-C_6H_4) 3e with KOH in Benzene-d_6 in a Sealed-NMR Tube. Benzene-d_6 (0.5 mL) was added to a mixture of Ir(ttp)(4-F-C_6H_4) (10.5 mg, 0.0110 mmol) and KOH (6.2 mg, 0.1100 mmol, 10 equiv) in an NMR tube with a rotaflo stopper and degassed by the freeze-pump-thaw method (3 cycles). The mixture was frozen under liquid nitrogen and then flame-sealed under vacuum. The sealed-NMR tube was heated at 200 °C, and monitored by ^{1}H NMR spectroscopy and the yield of product was calibrated with the internal standard residual benzene in benzene-d_6. After 7 days, a new species of [(4-F-C_6H_4)Ir(ttp)OH]$^-$ **4a** was proposed to be formed. ^{1}H NMR (C_6D_6, 400 MHz): δ -10.94 (s, 1 H), 1.37 (d, 2 H, J = 4.8 Hz), 2.36 (s, 12 H), 4.73 (dd, 2 H, $^3J_{H\text{-}F}$ = 8.8 Hz, J = 8.8 Hz), 7.06 (d, 4 H, J = 7.6 Hz), 7.27 (s, 8 H), 7.59 (d, 4 H, J = 6.8 Hz), 8.16 (s, 8 H). HRMS (FABMS): Calcd. for $(C_{54}H_{41}FN_4IrO)^+$: *m/z* 973.2888; found *m/z* 973.292639.

Reaction of Ir(ttp)(4-F-C_6H_4) 3e and Benzene (2h) with the Addition of KOH. Benzene (1.0 mL, 500 equiv) was added to a mixture of Ir(ttp)(4-F-C_6H_4) (21.8 mg, 0.023 mmol) and KOH (12.9 mg, 0.230 mmol, 10 equiv), and the mixture was degassed by the freeze-pump-thaw method (3 cycles). Then the mixture was heated at 200 °C for 4 days. The crude product was purified by column chromatography on alumina eluting with a mixture of hexane/CH_2Cl_2 (2:1), and a purple solid mixture of Ir(ttp)C_6H_5 **3a** (12.5 mg, 0.0133 mmol, 58%) and Ir(ttp)(4-F-C_6H_4) **3e** (7.0 mg, 0.0073 mmol, 32%) was isolated.

Reaction between Ir(ttp)(4-F-C_6H_4) 3e and Benzene-d_6 (2h') with the Addition of 10 equivalents of KOH at 200 °C in Solvent-Free Conditions. Benzene-d_6 (0.8 mL, 500 equiv) was added to a mixture of Ir(ttp)(4-F-C_6H_4) (17.6 mg, 0.018 mmol) and KOH (10.3 mg, 0.180 mmol, 10 equiv), and the mixture was degassed by the freeze-pump-thaw method (3 cycles). Then the mixture was heated at 200 °C for 4 days. The crude product was purified by column chromatography on alumina eluting with a mixture of hexane/CH_2Cl_2 (2:1), and a purple solid mixture of Ir(ttp)(C_6H_5) **3a** (1.2 mg, 0.0013 mmol, 7%) and Ir(ttp)(C_6D_5) **3a'** (2.0 mg, 0.0021 mmol, 12%) was isolated, while Ir(ttp)(4-F-C_6H_4) **3e** (12.4 mg, 0.0130 mmol, 72%) was recovered. According to ^{1}H NMR of the crude reaction mixture, C_6H_5F **2a** was observed in 16% yield calibrated with the iridium porphyrin species.

Reaction of Ir(ttp)(2,5-F_2-C_6H_3) 3e with KOH in Benzene-d_6 in a Sealed-NMR Tube. Benzene-d_6 (0.5 mL) was added to a mixture of Ir(ttp)(2,5-F_2-C_6H_3) (8.8 mg, 0.0090 mmol) and KOH (5.1 mg, 0.090 mmol, 10 equiv) in an NMR tube with a rotaflo stopper and degassed by the freeze-pump-thaw method (3 cycles). The mixture was frozen under liquid nitrogen and then flame-sealed under vacuum. The sealed-NMR tube was heated at 200 °C, and monitored by ^{1}H NMR spectroscopy and the yield of the product was calibrated with the internal standard residual benzene in benzene-d_6. After 3 days, a new species of [(2,5-F_2-C_6H_3)Ir(ttp)OH]$^-$ **4b** was proposed to be formed. ^{1}H NMR (C_6D_6, 400 MHz): δ -11.14 (s, 1 H), 0.91 (m, 1 H), 2.34 (s, 12 H), 4.31 (m, 1 H), 4.57 (m, 1 H), 7.06 (s, 4 H), 7.25 (s, 8 H), 7.67 (s, 4 H), 8.23 (s, 8 H).

Preparation of 5, 10, 15, 20-(Tetratolylporphyrinato)(triphenylphosphine) iridium(III) Aryls [Ir(ttp)($C_6H_nF_{6-n}$)(PPh_3)] 3a'-g' and 3i'. Generatal Procedure. Preparation of 5, 10, 15, 20-(Tetratolylporphyrinato)(triphenylphosphine) iridium(III)

Phenyl [Ir(ttp)(C_6H_5)(PPh_3)] **3a'** is described as a typical example. Ir(ttp)(C_6H_5) (5.5 mg, 0.0059 mmol) and PPh_3 (1.5 mg, 1 equiv) were dissolved in dichloromethane (0.5 mL) in air at room temperature, and Ir(ttp)(C_6H_5)(PPh_3) **3a'** was obtained in quantitative yield. R_f = 0.50 (hexane/CH_2Cl_2 = 1:1). ^{1}H NMR (CD_2Cl_2, 400 MHz): δ 0.37 (dd, 2 H, $^4J_{H\text{-}P}$ = 5.6 Hz, J = 6.8 Hz), 2.62 (s, 12 H), 4.10 (dd, 6 H, $^3J_{H\text{-}P}$ = 8.0 Hz, J = 8.0 Hz), 4.72 (dt, 2 H, $^5J_{H\text{-}P}$ = 2.0 Hz, J = 7.4 Hz), 5.14 (t, 1 H, J = 7.2 Hz), 6.55 (dt, 6 H, $^4J_{H\text{-}P}$ = 1.8 Hz, J = 7.7 Hz), 6.87 (dt, 3 H, $^5J_{H\text{-}P}$ = 1.0 Hz, J = 7.4 Hz), 7.44 (d, 4 H, J = 7.8 Hz), 7.48 (d, 4 H, J = 7.8 Hz), 7.63 (dd, 4 H, J = 1.7, 7.6 Hz), 7.77 (dd, 4 H, J = 1.7, 7.6 Hz), 8.45 (s, 8 H).

Preparation of 5, 10, 15, 20-(Tetratolylporphyrinato)(triphenylphosphine) iridium(III) (2-Fluorophenyl) [Ir(ttp)(2-F-C_6H_4)(PPh_3)] 3b'. Ir(ttp)(2-F-C_6H_4) (6.0 mg, 0.0063 mmol) and PPh_3 (1.6 mg, 1 equiv) were dissolved in dichloromethane (0.5 mL) in air at room temperature, and Ir(ttp)(2-F-C_6H_4)(PPh_3) **3b'** was obtained in quantitative yield. R_f = 0.48 (hexane/CH_2Cl_2 = 1:1). ^{1}H NMR (CD_2Cl_2, 400 MHz): δ 0.09 (ddd, 1 H, $^4J_{H\text{-}P}$ = 7.2 Hz, $^4J_{H\text{-}F}$ = 7.2 Hz, J = 1.2, 6.2 Hz), 2.63 (s, 12 H), 4.12 (dd, 6 H, $^3J_{H\text{-}P}$ = 8.2 Hz, J = 8.0 Hz), 4.33 (dddd, 1 H, $^5J_{H\text{-}P}$ = 3.5 Hz, $^3J_{H\text{-}F}$ = 11.0 Hz, J = 1.2, 7.8 Hz), 4.62 (t, 1 H, J = 7.4 Hz), 5.18 (dddd, 1 H, $^4J_{H\text{-}F}$ = 7.3 Hz, J = 1.2, 5.4, 7.2 Hz), 6.51 (dt, 6 H, $^4J_{H\text{-}P}$ = 1.3 Hz, J = 7.7 Hz), 6.68 (dt, $^5J_{H\text{-}P}$ = 1.0 Hz, J = 7.4 Hz), 7.42 (t, 8 H, J = 6.7 Hz), 7.47 (d, 4 H, J = 7.3 Hz), 7.71 (d, 4 H, J = 7.2 Hz), 8.45 (s, 8 H). A single crystal for X-ray analysis was grown from CH_2Cl_2/methanol.

Preparation of 5, 10, 15, 20-(Tetratolylporphyrinato)(triphenylphosphine) iridium(III) (2,3-Difluorophenyl) [Ir(ttp)(2,3-F_2-C_6H_3)(PPh_3)] 3c'. Ir(ttp)(2,3-F_2-C_6H_3) (6.2 mg, 0.0064 mmol) and PPh_3 (1.7 mg, 1 equiv) were dissolved in dichloromethane (0.5 mL) in air at room temperature, and Ir(ttp)(2,3-F_2-C_6H_3)(PPh_3) **3c'** was obtained in quantitative yield. R_f = 0.55 (hexane/CH_2Cl_2 = 1:1). ^{1}H NMR

(CD_2Cl_2, 400 MHz): δ -0.18 (ddddd, 1 H, $^4J_{H\text{-}P}$ = 6.3 Hz, $^5J_{H\text{-}F}$ = 1.2 Hz, $^4J_{H\text{-}F}$ = 6.2 Hz, J = 1.0, 6.4 Hz), 2.63 (s, 12 H), 4.11 (dd, 6 H, $^3J_{H\text{-}P}$ = 8.0 Hz, J = 8.2 Hz), 4.54 (ddt, 1 H, $^5J_{H\text{-}F}$ = 1.4 Hz, $^4J_{H\text{-}F}$ = 13.8 Hz, J = 6.4 Hz), 5.00 (dddd, 1 H, $^4J_{H\text{-}F}$ = 9.2 Hz, $^3J_{H\text{-}P}$ = 9.2 Hz, J = 1.3, 7.8 Hz), 6.51 (dt, 6 H, $^4J_{H\text{-}P}$ = 1.8 Hz, J = 7.8 Hz), 6.87 (dt, 3 H, $^5J_{H\text{-}P}$ = 1.3 Hz, J = 7.4 Hz), 7.42 (m, 8 H, overlap), 7.47 (m, 4 H, overlap), 7.72 (d, 4 H, J = 7.2 Hz), 8.47 (s, 8 H). A single crystal for X-ray analysis was grown from CH_2Cl_2/methanol.

Preparation of 5, 10, 15, 20-(Tetratolylporphyrinato)(triphenylphosphine) iridium(III) (3-Fluorophenyl) [Ir(ttp)(3-F-C_6H_4)(PPh_3)] 3d'. Ir(ttp)(3-F-C_6H_4) (7.5 mg, 0.0078 mmol) and PPh_3 (2.1 mg, 1 equiv) were dissolved in dichloromethane (0.5 mL) in air at room temperature, and Ir(ttp)(3-F-C_6H_4)(PPh_3) **3d'** was obtained in quantitative yield. R_f = 0.55 (hexane/CH_2Cl_2 = 1:1). ^{1}H NMR (CD_2Cl_6, 400 MHz): δ 0.06 (dddd, 1 H, $^4J_{H\text{-}P}$ = 2.8 Hz, $^5J_{H\text{-}F}$ = 6.5 Hz, J = 1.2, 6.0 Hz), 0.15 (ddd, 1 H, $^4J_{H\text{-}P}$ = 0.8 Hz, $^3J_{H\text{-}F}$ = 7.8 Hz, J = 5.4 Hz), 2.65 (s, 12 H), 4.09 (dd, 6 H, $^3J_{H\text{-}P}$ = 8.0 Hz, J = 8.1 Hz), 4.68 (ddd, 1 H, $^3J_{H\text{-}F}$ = 14.7 Hz, J = 2.9, 7.9 Hz), 4.84 (dt, 1 H, $^4J_{H\text{-}F}$ = 2.6 Hz, J = 8.2 Hz), 6.55 (dt, 6 H, $^4J_{H\text{-}P}$ = 1.5 Hz, J = 7.8 Hz), 6.88 (dt, 3 H, $^5J_{H\text{-}P}$ = 1.1 Hz, J = 7.4 Hz), 7.45 (d, 4 H, J = 7.8 Hz), 7.49 (d, 4 H, J = 7.7 Hz), 7.64 (dd, 4 H, J = 1.7, 7.6 Hz), 7.77 (dd, 4 H, J = 1.7, 7.6 Hz), 8.48 (s, 8 H). A single crystal for X-ray analysis was grown from CH_2Cl_2/methanol.

Preparation of 5, 10, 15, 20-(Tetratolylporphyrinato)(triphenylphosphine) iridium(III) (4-Fluorophenyl) [Ir(ttp)(4-F-C_6H_4)(PPh_3)] 3e'. Ir(ttp)(4-F-C_6H_4) (6.1 mg, 0.0064 mmol) and PPh_3 (1.7 mg, 1 equiv) were dissolved in dichloromethane (0.5 mL) in air at room temperature, and Ir(ttp)(4-F-C_6H_4)(PPh_3) **3e'** was obtained in quantitative yield. R_f = 0.58 (hexane/CH_2Cl_2 = 1:1). ^{1}H NMR (CD_2Cl_2, 400 MHz): δ 0.27 (ddd, 2 H, $^4J_{H\text{-}P}$ = 2.4 Hz, $^4J_{H\text{-}F}$ = 12.2 Hz, J = 6.6 Hz), 2.65 (s, 12 H), 4.10 (dd, 6

H, $^3J_{H\text{-}P}$ = 8.3 Hz, J = 8.1 Hz), 4.49 (ddd, 2 H, $^4J_{H\text{-}P}$ = 1.3 Hz, $^3J_{H\text{-}F}$ = 9.3 Hz, J = 9.3 Hz), 6.54 (dt, 6 H, $^4J_{H\text{-}P}$ = 1.5 Hz, J = 7.7 Hz), 6.87 (dt, 3 H, $^5J_{H\text{-}P}$ = 0.8 Hz, J = 7.4 Hz), 7.44 (d, 4 H, J = 7.7 Hz), 7.48 (d, 4 H, J = 7.8 Hz), 7.62 (dd, 4 H, J = 1.6, 7.6 Hz), 7.75 (dd, 4 H, J = 1.6, 7.6 Hz), 8.46 (s, 8 H).

Preparation of 5, 10, 15, 20-(Tetratolylporphyrinato)(triphenylphosphine) iridium(III) (2,5-Difluorophenyl) [Ir(ttp)(2,5-F_2-C_6H_3)(PPh_3)] 3f'. Ir(ttp)(2,5-F_2-C_6H_3) (6.5 mg, 0.0067 mmol) and PPh_3 (1.8 mg, 1 equiv) were dissolved in dichloromethane (0.5 mL) in air at room temperature, and Ir(ttp)(2,5-F_2-C_6H_3)(PPh_3) **3f'** was obtained in quantitative yield. R_f = 0.52 (hexane/CH_2Cl_2 = 1:1). ^{1}H NMR (CD_2Cl_2, 400 MHz): δ -0.22 (dddd, 1 H, $^4J_{H\text{-}P}$ = 7.0 Hz, $^4J_{H\text{-}F}$ = 7.5 Hz, $^3J_{H\text{-}F}$ = 7.5 Hz, J = 3.6 Hz), 2.64 (s, 12 H), 4.10 (dd, 6 H, $^3J_{H\text{-}P}$ = 8.4 Hz), 4.26 (ddd, 1 H, $^4J_{H\text{-}F}$ = 8.8 Hz, $^3J_{H\text{-}F}$ = 13.4 Hz, J = 4.4 Hz), 4.84 (ddd, 1 H, $^4J_{H\text{-}F}$ = 8.3 Hz, $^3J_{H\text{-}F}$ = 11.4 Hz, J = 3.3 Hz), 6.52 (dt, 6 H, $^4J_{H\text{-}P}$ = 1.4 Hz, J = 7.6 Hz), 6.87 (t, 3 H, J = 7.4 Hz), 7.43 (t, 8 H, J = 6.6 Hz), 7.50 (d, 4 H, J = 7.6 Hz), 7.72 (d, 4 H, J = 7.4 Hz), 8.48 (s, 8 H).

Preparation of 5, 10, 15, 20-(Tetratolylporphyrinato)(triphenylphosphine) iridium(III) (3,5-Difluorophenyl) [Ir(ttp)(3,5-F_2-C_6H_3)(PPh_3)] 3g'. Ir(ttp)(3,5-F_2-C_6H_3) (6.4 mg, 0.0066 mmol) and PPh_3 (1.8 mg, 1 equiv) were dissolved in dichloromethane (0.5 mL) in air at room temperature, and Ir(ttp)(3,5-F_2-C_6H_3)(PPh_3) **3g'** was obtained in quantitative yield. R_f = 0.58 (hexane/CH_2Cl_2 = 1:1). ^{1}H NMR (CD_2Cl_2, 400 MHz): δ -0.31 (ddd, 2 H, $^5J_{H\text{-}F}$ = 6.6 Hz, $^3J_{H\text{-}F}$ = 9.6 Hz, J = 2.0 Hz), 2.65 (s, 12 H), 4.07 (dd, 6 H, $^3J_{H\text{-}P}$ = 8.3 Hz, J = 8.4 Hz), 4.60 (tt, 1 H, $^3J_{H\text{-}F}$ = 9.2 Hz, J = 2.3 Hz), 6.55 (dt, 6 H, $^4J_{H\text{-}P}$ = 1.6 Hz, J = 7.6 Hz), 6.88 (t, 3 H, J = 7.4 Hz), 7.45 (d, 4 H, J = 7.8 Hz), 7.49 (d, 4 H, J = 7.8 Hz), 7.65 (dd, 4 H, J = 1.0, 7.6 Hz), 7.67 (dd, 4 H, J = 1.0, 7.6 Hz), 8.49 (s, 8 H). A single crystal for X-ray analysis was grown from CH_2Cl_2/methanol.

Preparation of 5, 10, 15, 20-(Tetratolylporphyrinato)(triphenylphosphine) iridium(III) Pentafluorophenyl [Ir(ttp)(C_6F_5)(PPh_3)] 3i'. Ir(ttp)(C_6F_5) (6.3 mg, 0.0061 mmol) and PPh_3 (1.6 mg, 1 equiv) were dissolved in dichloromethane (0.5 mL) in air at room temperature, and Ir(ttp)(C_6F_5)(PPh_3) **3i'** was obtained in quantitative yield. R_f = 0.65 (hexane/CH_2Cl_2 = 1:1). ^{1}H NMR (CD_2Cl_2, 400 MHz): δ 2.62 (s, 12 H), 4.08 (dd, 6 H, $^3J_{H\text{-}P}$ = 8.4 Hz, J = 8.4 Hz), 6.48 (dt, 6 H, $^4J_{H\text{-}P}$ = 1.7 Hz, J = 7.7), 6.87 (t, 3 H, J = 7.4 Hz), 7.26 (d, 4 H, J = 6.8 Hz), 7.40 (t, 8 H, J = 6.2 Hz), 7.72 (d, 4 H, J = 6.3 Hz), 8.49 (s, 8 H). A single crystal for X-ray analysis was grown from CH_2Cl_2/ methanol.

References

(1) Hiyama, T.; Kanie, K.; Kusumoto, T.; Morizawa, Y.; Shimizu, M. *Organofluorine Compounds Chemistry and Applications,* Eds.; Springer: New York, 2000.

(2) Maksić, Z. B.; Randić, M. *J. Am. Chem. Soc.* **1970**, *92*, 424-425.

(3) Luo, Y.-R. *Handbook of Bond Dissociation Energies in Organic Compounds;* CRC Press: Boca Raton, FL, 2003.

(4) Oosaka, H. *Bull. Chem. Soc. Jpn.* **1940**, *15*, 31-36.

(5) Liu, Y.-J.; Persson, P.; Karlsson, H. O.; Lunell, S.; Kadi, M.; Karlsson, D.; Davidsson, J. *J. Chem. Phys.* **2004**, *120*, 6502-6509.

(6) Kiplinger, J. L.; Richmond, T. G.; Osterberg, C. E. *Chem. Rev.* **1994**, *94*. 373-431.

(7) Brothers, P. J.; Roper, W. R. *Chem. Rev.* **1988**, *88*, 1293-1326.

(8) Alonso, F.; Beletskaya, I. P.; Yus, M. *Chem. Rev.* **2002**, *102*, 4009-4091.

(9) Plenio, H. *Chem. Rev.* **1997**, *97*, 3363-3384.

(10) Amii, H.; Uneyama, K. *Chem. Rev.* **2009**, *109*, 2119-2183.

(11) Burdeniuc, J.; Jedlicka, B.; Crabtree, R. H. *Chem. Ber./Recueil* **1997**, *130*,

145-154.

(12) Richmond, T. G. *Angew. Chem., Int. Ed.* **2000**, *39*, 3241-3244.

(13) Braun, T.; Perutz, R. N. *Chem. Commun.* **2002**, 2749-2757.

(14) Mazurek, U.; Schwarz, H. *Chem. Commun.* **2003**, 1321-1326.

(15) Jones, W. D. *Dalton Trans.* **2003**, 3991-3995.

(16) Torrens, H. *Coord. Chem. Rev.* **2005**, *249*, 1957-1985.

(17) Braun, T.; Perutz, R. N. *Comprehensive Organometallic Chemistry III*; Crabtree, R. H., Mingos, D. M. P., Eds.: Elsevier: Oxford, 2007; Vol. 1, pp 725-758.

(18) (a) Clot, E.; Mégret, C.; Eisenstein, O.; Perutz, R. N. *J. Am. Chem. Soc.* **2009**, *131*, 7817-7827. (b) Shen, K.; Fu, Y.; Li, J.-N.; Liu, L.; Guo, Q.-X. *Tetrahedron* **2007**, *63*, 1568-1576.

(19) Smart, B. E. *Mol. Struct. Energ.* **1986**, *3*, 141-191.

(20) Maron, L.; Werkema, E. L.; Perrin, L.; Eisenstein, O.; Andersen, R. A. *J. Am. Chem. Soc.* **2005**, *127*, 279-292.

(21) Barrio, P.; Castarlenas, R.; Esteruelas, M. A.; Lledós, A.; Maseras, F.; Oñate, E.; Tomàs, J. *Organometallics* **2001**, *20*, 442-452.

(22) Ben-Ari, E.; Gandelman, M.; Rozenberg, H.; Shimon, L. J. W.; Milstein, D. *J. Am. Chem. Soc.* **2003**, *125*, 4714-4715. (b) Ben-Ari, E.; Cohen, R.; Gandelman, M.; Shimon, L. J. W.; Martin, J. M. L.; Milstein, D. *Organometallics* **2006**, *25*, 3190-3210.

(23) Fan, L.; Parkin, S.; Ozerov, O. V. *J. Am. Chem. Soc.* **2005**, *127*, 16772-16773.

(24) Evans, M. E.; Burke, C. L.; Yaibuathes, S.; Colt, E.; Eisenstein, O.; Jones, W. D. *J. Am. Chem. Soc.* **2009**, *131*, 13464-13473.

(25) Lee, M. H. *M. Phil. Thesis*, The Chinese University of Hong Kong, 2008.

(26) Li, B.; Chan, K. S. *Organometallics* **2008**, *27*, 4034-4042.

(27) Kwart, H. *Acc. Chem. Res.* **1982**, *15*, 401-408.

(28) Isaacs, N. S. *Physical Organic Chemistry*; Longman Scientific and Technical: New York, 1986.

(29) Qian, Y. Y. Unpublished results, **2009**.

(30) The solubility of Ir(ttp)˙ **1b** in benzene-d_6 was poor, and the some precipitate was observed during the course of the reaction, so the lower yield of Ir(ttp)˙ was more likely due to the poor solubility of Ir(ttp)˙ in benzene-d_6.

(31) (a) Nelson, A. P.; DiMagno, S. G. *J. Am. Chem. Soc.* **2000**, *122*, 8569-8570. (b) Sanford, M. S.; Groves, J. T. *Angew. Chem., Int. Ed.* **2004**, *43*, 588-590. (c) Ogoshi, H.; Setsune, J.-I.; Yoshida, Z.-I. *J. Organomet. Chem.* **1978**, *159*, 317-328.

(32) Tse, A. K.-S.; Wu, B.-M.; Mak, T. C. W.; Chan, K. S. *J. Organomet. Chem.* **1998**, *568*, 257-261.

(33) (a) Edelbach, B. L.; Jones, W. D. *J. Am. Chem. Soc.* **1997**, *119*, 7734-7742. (b) Chan, P. K.; Leong, W. K. *Organometallics* **2008**, *27*, 1247-1253. (c) Reade, S. P.; Mahon, M. F.; Whittlesey, M. K. *J. Am. Chem. Soc.* **2009**, *131*, 1847-1861. (d) Postigo, A.; Rossi, R. A. *Org. Lett.* **2001**, *3*, 1197-1200. (e) Postigo, A.; Vaillard, S. E.; Rossi, R. A. *J. Phys. Org. Chem.* **2002**, *15*, 889-893.

(34) (a) Yeung, S. K. *Ph. D. Thesis,* The Chinese University of Hong Kong, 2005. (b) Chan, K. S.; Leung, Y.-B. *Inorg. Chem.* **1994**, *33*, 3187.

(35) Cheung, C. W. Unpublished results, **2009**.

(36) (a) Fu, Y.; Liu, L.; Li, R.-Q.; Liu, R.; Guo, Q.-X. *J. Am. Chem. Soc.* **2004**, *126*, 814-822. (b) Zavgorodnii, V. S.; Novoselov, A. V.; Mikhailov, L. E.; Skvortsov, N. K.; Fauvarque, J.-F. *Russ. J. Org. Chem.* **2003**, *39*, 242-247.

(37) For Rh(oep)OH, see: (a) Del Rossi, K. J.; Wayland, B. B. *J. Am. Chem. Soc.* **1985**, *107*, 7941-7944. For Rh(tspp)OH, see: (b) Fu, X.; Wayland, B. B. *J. Am. Chem. Soc.* **2004**, *126*, 2623-2631. (c) Fu, X.; Li, S.; Wayland, B. B. *J. Am. Chem. Soc.* **2006**, *128*, 8947-8954.

(38) Hydroxide ion is an effective one-electron reducing agent, see: Sawyer, D. T.; Roberts, J. L., Jr. *Acc. Chem. Res.* **1988**, *21*, 469-476.

(39) Analogous disproportionation reaction of Rh^{II}(por), see: (a) In excess MeOH, see: Li, S.; Cui, W.; Wayland, B. B. *Chem. Commun.* **2007**, 4024-4025. (b) By strong ligand, see: Wayland, B. B.; Balkus, K. J., Jr.; Farnos, M. D. *Organometallics* **1989**, *8*, 950-955. (c) Wayland, B. B.; Sherry, A. E.; Bunn, A. G. *J. Am. Chem.* Soc. **1993**, *115*, 7675-7684.

(40) (a) Tenn, W. J., III; Young, K. J. H.; Oxgaard, J.; Nielsen, R. J.; Goddard, W. A., III; Periana, R. A. *Organometallics* **2006**, *25*, 5173-5175. (b) Kloek, S. M.; Heinekey, D. M.; Goldberg, K. I. *Angew. Chem., Int. Ed.* **2007**, *46*, 4736-4738. (c) Hanson, S. K.; Heinekey, D. M.; Goldberg, K. I. *Organometallics* **2008**, *27*, 1454-1463. (d) Bercaw, J. E.; Hazari, N.; Labinger, J. A. *Organometallics* **2009**, *28*, 5489-5492.

(41) Lide, D. R., Ed. *CRC Handbook of Chemistry and Physics*, 84th Ed.; CRC Press: Boca Raton, FL, 2003.

(42) (a) Kulawiec, R. J.; Holt, E. M.; Lavin, M.; Crabtree, R. H. *Inorg. Chem.* **1987**, *26*, 2559-2561. (b) Pauling, L. *The Nature of the Chemical Bond*, 3rd Ed.; Cornell University Press: Ithaca, NY, 1960.

(43) Mooney, E. F. *An Introduction to ^{19}F N.M.R. Spectroscopy*, Heyden and Son Ltd.; London, 1970.

Chapter 4 Carbonyl Carbon and α-Carbon (C(C=O)-C(α)) Bond Activation of Ketones by Iridium Porphyrin Complexes

4.1 Introduction

4.1.1 Properties of Ketone

In organic chemistry, ketone is a type of compound that features a carbonyl group (C=O) bonded to two other carbon atom, i.e., R_3CCOCR_3, where R can be a variety of atoms and groups of atoms.

The carbonyl group is polar as a consequence of the fact that the electronegativity of the oxygen center is greater than that of carbonyl carbon. Thus, ketones are nucleophilic at oxygen and electrophilic at carbon.[1]

The carbonyl carbon is often described as "sp^2 hybridized" terminology, therefore, ketones are trigonal planar about the carbonyl carbon, with C-C-O and C-C-C bond angles of approximately 120°. Nucleophilic attack on the carbonyl carbon of ketones may occur from either face (Figure 4.1a). Ketone with α-hydrogen participates in a so-called keto-enol tautomerism (Figure 4.1b), which can be catalyzed by both acids and bases.[2] Table 4.1 shows the bond dissociation energies (BDE) of α-C-H and C(C=O)-C(α) bonds and the p*K*a values for some selected aromatic and aliphatic ketones.

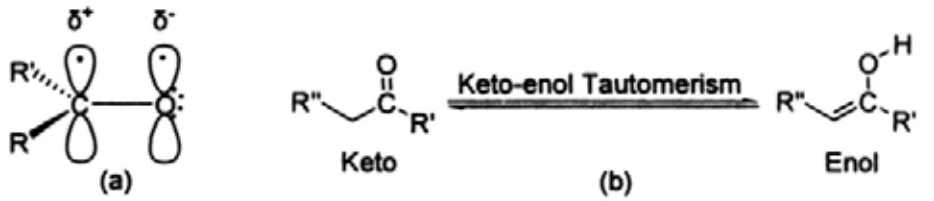

Figure 4.1 (a) Carbonyl compound (sp^2-hybridized); (b) Keto-enol tautomerism

Table 4.1 BDE of α-C-H and C(C=O)-C(α) Bonds and the p*K*a value for Selected Aromatic and Aliphatic Ketones

Ketone	BDE[3] / kcal mol^{-1}		p*K*a[4] (DMSO)
	α-C-H Bond	C(C=O)-C(α) Bond	
C_6H_5CO-**Me**	93	85.0	24.7
C_6H_5CO-**Et**	92.9	82.2	24.4
C_6H_5CO-**C_6H_5**	---	94.7	17.7
MeCO-**Me**	95.9	84.1	26.5
EtCO-**Et**	94.8	82.3	27.1
Et-CO-Me	93.8	83.0	---
Et-CO-**Me**	93.8	84.3	---
^{i}Pr-COMe	91.7	81.3	---
MeCO-C*H*$_2$COMe	---	80.8	*13.3*

4.1.2 Activation of C(C=O)-C(α) Bond of Ketones by Low-Valent Transition Metal Complexes

Activation of carbonyl carbon and α-carbon (C(C=O)-C(α)) bonds by transition metal complexes has been widely investigated not only due to its fundamental interests but also its potential utilities in organic synthesis.[5] Most examples for CCA reactions of carbonyl compounds involve strained systems by low-valent transition metal complexes.[5a-c] Among these, cyclobutanones or cyclobutenones are the most widely used substrates, and Table 4.2 lists some selected examples.[6-14]

Table 4.2 Application of C(C=O)-C(α) Bond Activation of Cyclobutanones and Cyclobutenones

Process	Example
Intermolecular alkyne insersion[6,7]	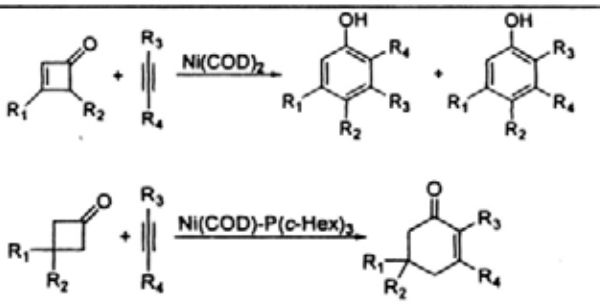
Lactone formation[8]	
Decarbonylation[9]	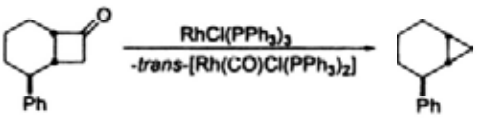
Double Cleavage[10]	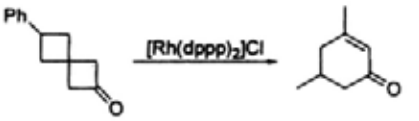
Arylation[11]	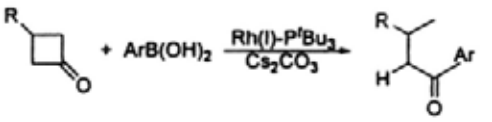
Intramolecular alkene insertion[12]	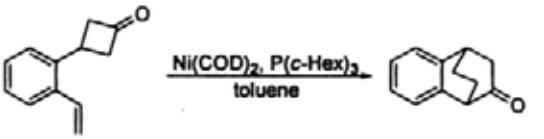
Intermolecular alkene insersion	
Phenol Formation[13]	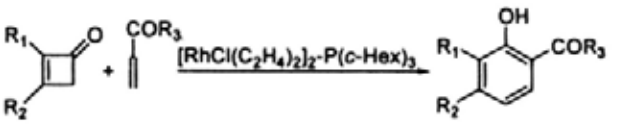
Decarbonylation[14]	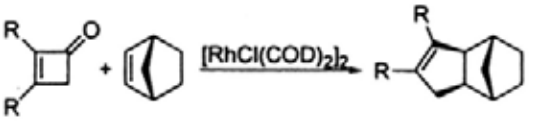

In addition, cyclobutenedions can also be used for the organic systhesis. Mitsudo *et al.* have reported an unusual coupling of cyclobutenedions with alkenes to synthesize cyclopentenones via C-C bond cleavage by ruthenium complexes (Scheme 4.1a).[15] Recently, Yamamoto and co-workers demonstrate a convergent synthesis of azabicycloalkenones involving the C-C bond cleavage of cyclobutenedions and intramolecular alkene insertion (Scheme 4.1b).[16]

Scheme 4.1 Activation of C(C=O)-C(α) Bond of Cyclobutenediones

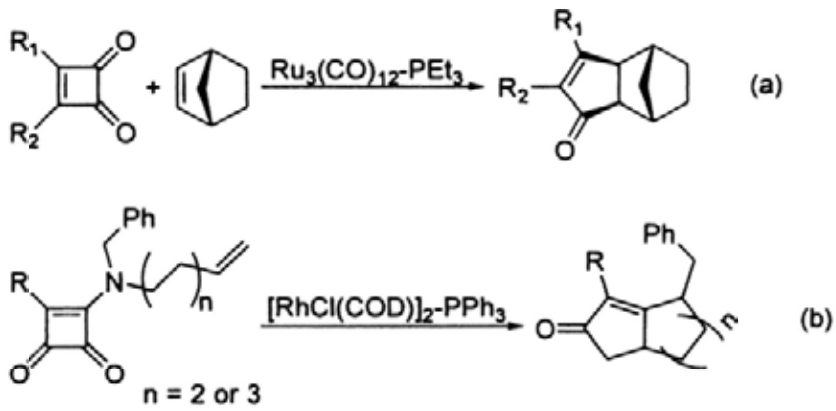

Besides the four-membered ring, three-membered ring of cyclopropenones was also reported to undergo C-C bond cleavage to give pyranopyrandiones in the presence of ruthenium catalyst via reconstructive carbonylation (Scheme 4.2a). In addition, this approach can also be used to synthesize the unsymmetrically substituted pyranopyrandiones via cross-carbonylation of cyclopropenones with internal alkynes (Scheme 4.2 b).[17]

Scheme 4.2 Activation of C(C=O)-C(α) Bond of Cyclopropenones

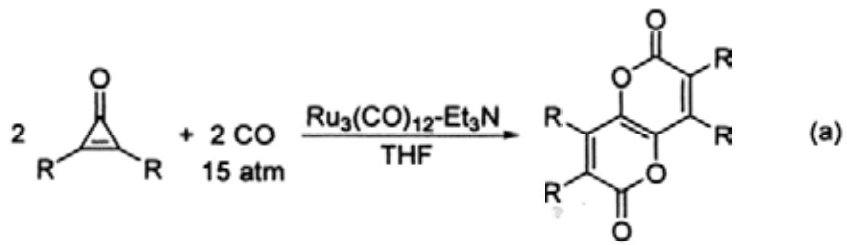

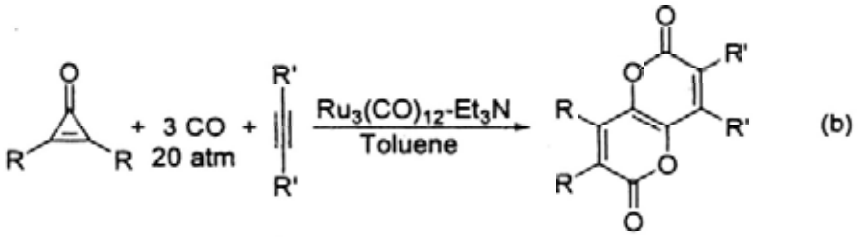

Another approach for the CCA reactions of carbonyl compounds is driven by chelation assistance of an adjacent coordinating atom.[5c-f] Scheme 4.3 shows an earlier example of activation of C(C=O)-C(α) bond by Rh(I) complex reported by Suggs and Jun.[18]

Scheme 4.3 Activation of C(C=O)-C(α) Bond Driven by Chelation Assistance

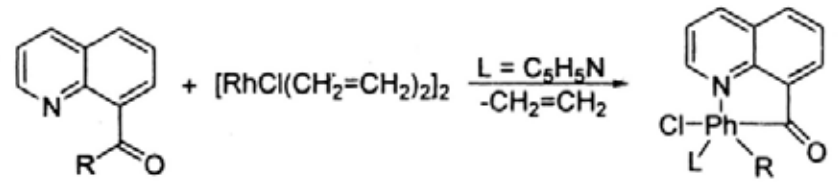

Recently, the catalytic approach for the synthesis of unsymmetrical ketones was achieved via the cleavage of C-C bond of unstrained ketones in chelation-assistant system. In 2006, Jun and co-workers reported a rhodium(I) catalyzed C-C bond activation of aliphatic ketones bearing with *β*-hydrogens with olefins using chelation-assistant system under microwave irradiation (Scheme 4.4).[19]

Scheme 4.4 Catalytic C(C=O)-C(α) Bond Activation of Unstrained Ketones

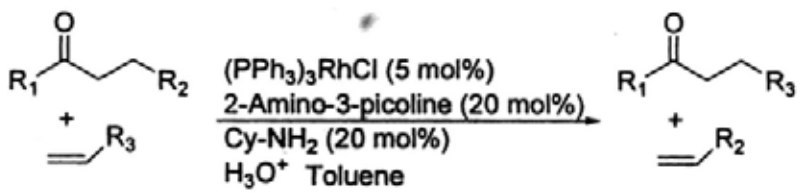

Douglas *et al.* reported an activation of an unstrained C-C bond and subsequent intermolecular carboacylation of olefin to form two new C-C bonds. In addition, this result provided a basis for the controlling C-C and C-H bond activation reaction pathways, and it can help in the development of further catalytic C-C bond activation

reactions (Scheme 4.5).[20] On the other hand, they also described an intramolecular carboacylation reaction with acylquinolines via the catalytic C-C bond activation by rhodium(I) complex (Scheme 4.6).[21]

Scheme 4.5 Selective C(C=O)-C(α) and C(α)-H Bond Activation

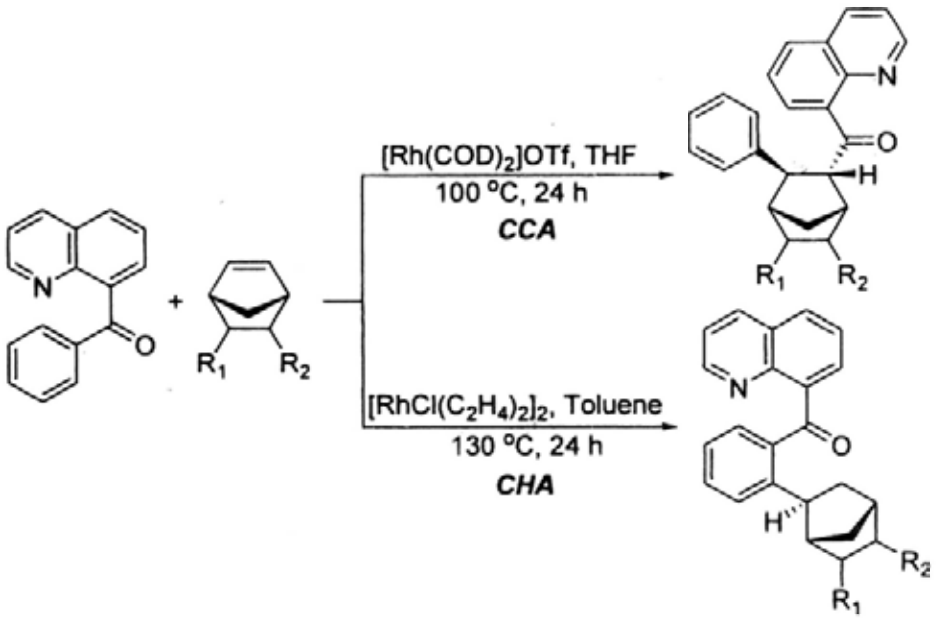

Scheme 4.6 Intramolecular Carboacylation via Catalytic C(C=O)-C(α) Bond Activation

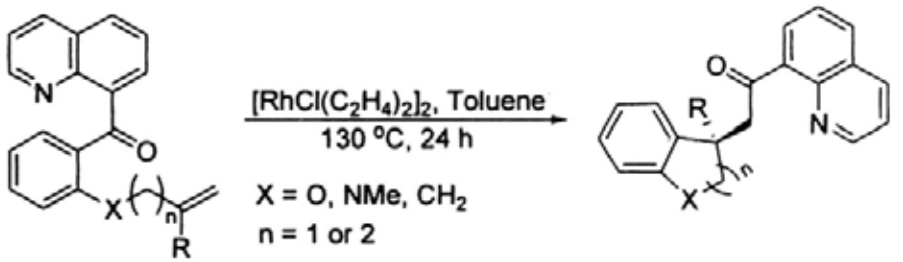

4.1.3 Activation of C-C Bond by High-Valent Transition Metal Complexes

High-valent transition metal complexes are much less known to cleave a C(C=O)-C(α) bond since oxidative addition of a C-C bond involves an uncommon high-valent transition metal complex intermediate. However, some important examples have been reported for other types of CCA reactions. A cationic silyl Rh(III) has been used to activate the aliphatic-nitrile bond.[22] A migratory aliphatic group of

nitrile to Rh via the η^2-iminoacyl intermediate constitutes the key CCA step without involving an oxidative addition (Scheme 4.7).

Scheme 4.7 CCA of Nitrile by Rh(III) via η^2-Iminoacyl Intermediate

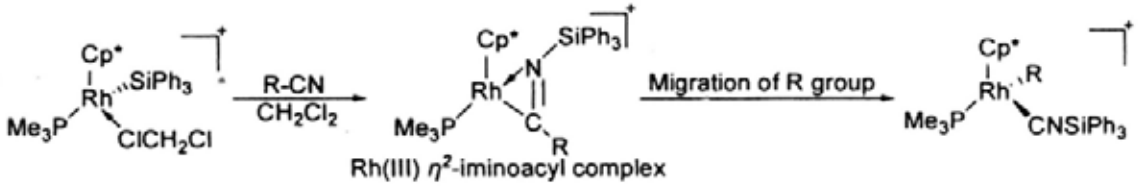

Rh(III) η^2-iminoacyl complex

A recent report by Bergman and coworkers has shown that $Cp^*(PMe_3)Ir(CH_3)OTf$ reacts with alkoxy and siloxysubstituted cyclopropanes to undergo CCA reaction and an Ir(V) alkyl intermediate was proposed (Scheme 4.8).[23]

Schem4.8 CCA of Cyclopropanes by Ir(III) via Oxidative Addition

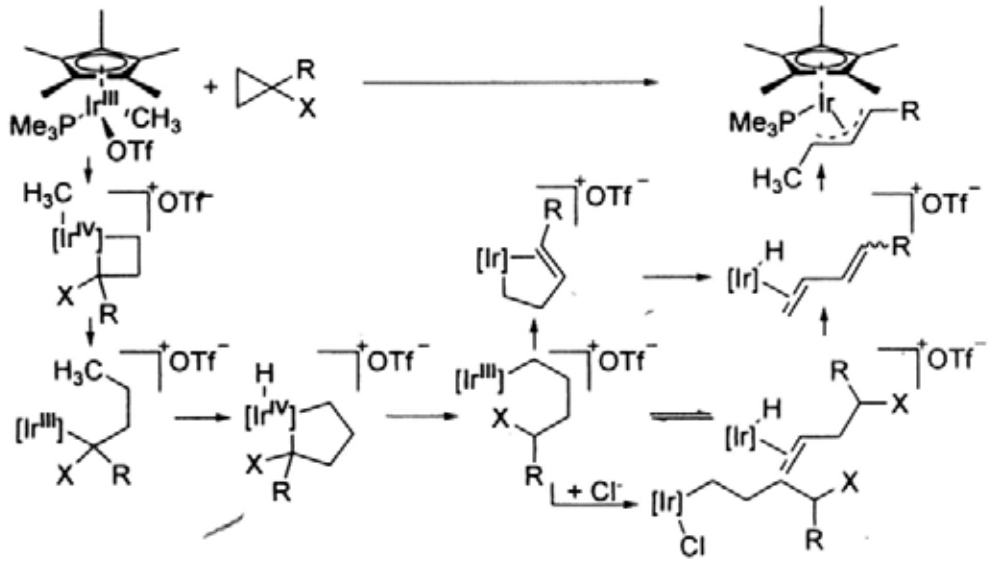

4.1.4 Possible Mechanisms on C(C=O)-C(α) Bond Activation by High-Valent Transition Metal Complexes

Even with limited examples of CCA of ketones, the C(C=O)-C(α) bond activation of ketones by high-valent transition metal complexes can be still divided into three mechanistic categories: (i) heterolysis; (ii) sigma-bond metathesis (SBM); (iii) oxidative addition, followed by reductive elimination (OA/RE) (Table 4.3). For high-valent transition metal complexes, difficulties exist for these three pathways.

Table 4.3 Possible Pathways for C(C=O)-C(α) Bond Activation by High-Valent Transition Metal Complexes

Process	Chemical Transformation
(i) Heterolysis	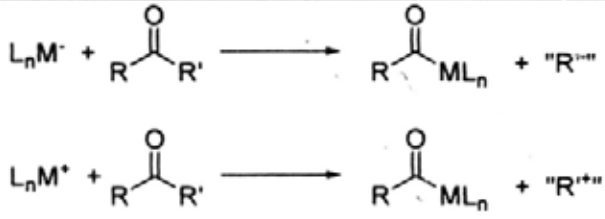
(ii) SBM	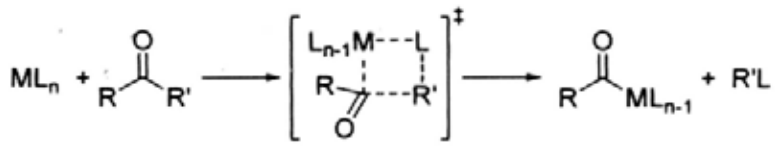
(iii) OA/RE	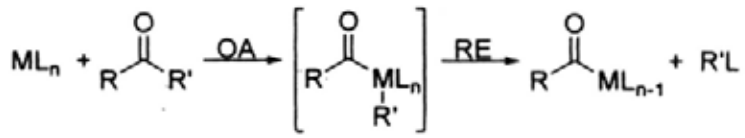

(i) Heterolysis: A C(C=O)-C(α) bond is surrounded by C-H bonds, especially the acidic enolizable C-H bonds. Therefore, the nucleophilic/electrophilic attack at an internal carbonyl carbon by a transition metal complex is kinetically unfavorable. The formation of a R^- or R^+ leaving group is energetically demanding.

(ii) SBM: Steric hindrance in the transition state is large. Up till now, no CCA via SBM reaction has been reported.[24]

(iii) OA/RE: Oxidative addition of C-C bond to a high-valent transition metal complex is rare. Furthermore, the formation of a sterically demanding intermediate is not favorable.

4.1.5 Discovery of C(C=O)-C(α) Bond Activation of Ketones by Iridium(III) Porphyrin Complexes

In Chan's group, the aldehydic carbon-hydrogen (C-H) bonds of aryl aldehydes

have been activated by high-valent metalloporphyrins of rhodium(III) and iridium(III) (eqs 4.1 and 4.2).[25]

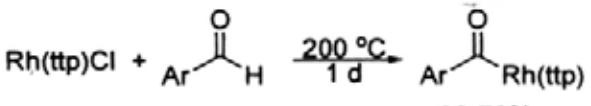

(4.1)

38-79%

Ar = C_6H_5, *p*-F-C_6H_4, *p*-Me-C_6H_4, *p*-^{t}Bu-C_6H_4, *p*-CF_3-C_6H_4, *p*-OMe-C_6H_4

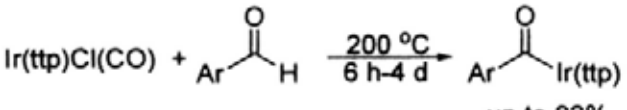

(4.2)

up to 92%

Ar = C_6H_5, *p*-F-C_6H_4, *p*-Me-C_6H_4, *p*-^{t}Bu-C_6H_4, *p*-CF_3-C_6H_4, *p*-OMe-C_6H_4

In addition, the C(C=O)-C(α) bond activation of acetophenones have been achieved by high-valent iridium(III) porphyrin complexes (eq 4.3), which was firstly discovered by Ms Song.[26] This type of reaction is mechanistically intriguing due to the difficulty of forming high-valent transition iridium(V) intermediates via OA, which are particularly sterically demanding with three substitutents locating in a *cis*-manner to the same face of a porphyrin plane. For a SBM process, attack at the internal carbonyl carbon by the Ir center via a four-centered transition state is also sterically hindered.

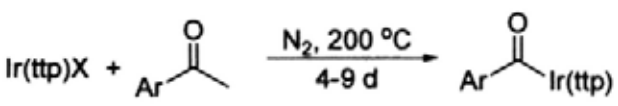

(4.3)

36-85%

X = Cl(CO), (BF_4)(CO), Me
Ar = C_6H_5, *p*-F-C_6H_4, *p*-Cl-C_6H_4, *p*-Me-C_6H_4, *p*-OMe-C_6H_4

4.1.6 Objectives of This Work

The objectives of this work are (1) to explore the scope of ketones in the C(C=O)-C(α) bond activation reaction with high-valent iridium(III) porphyrin complexes, and (2) to gain mechanistic understandings of the C(C=O)-C(α) bond activation of ketones.

4.2 C(C=O)-C(α) Bond Activation of Ketones by Iridium Porphyrin Complexes

4.2.1 C(C=O)-C(α) Bond Activation of Acetophenones by Electrophilic Iridium Porphyrin Complexes

Ir(ttp)Cl(CO) **1a** was found to undergo successful selective CCA reaction with a variety of *para*-substituted acetophenones in solvent-free conditions at the less steric hindered and weaker C(C=O)-C(methyl) bonds (85.0 kcal mol^{-1})[3] rather than the C(C=O)-C(aryl) bonds (94.7 kcal mol^{-1})[3] to yield Ir(ttp)COAr.[25b] Table 4.4 and eq 4.4 list the results of the optimized findings.

Table 4.4 CCA of Acetophenones by Ir(ttp)Cl(CO)

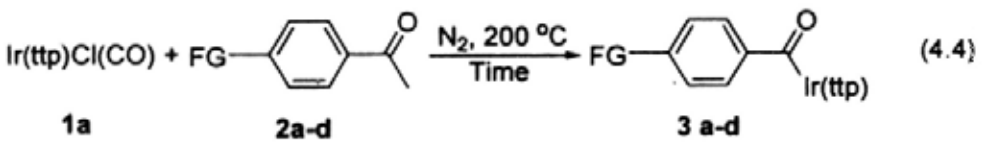

(4.4)

1a **2a-d** **3 a-d**

Entry	FG	Time / d	Product (Yield / %)
1	F **2a**	13	Ir(ttp)CO(4-F-C_6H_4) **3a** (74)
2	H **2b**	20	Ir(ttp)COC_6H_5 **3b** (71)[a]
3	Me **2c**	12	Ir(ttp)CO(4-Me-C_6H_4) **3c** (78)
4	OMe **2d**	15	Ir(ttp)CO(4-OMe-C_6H_4) **3d** (79)

[a] Aromatic CHA products of Ir(ttp)(*para*-COMe-C_6H_4) **4b** and Ir(ttp)(*meta*-COMe-C_6H_4) **4c** were also isolated in 4% and 8% yield, respectively.

For example, Ir(ttp)Cl(CO) **1a** reacted with the prototypical acetophenone **2b** in 200 °C for 20 days to give Ir(ttp)COC_6H_5 **3b** in 71% yield together with the aromatic CHA products Ir(ttp)(*para*-COMe-C_6H_4) **4b** in 4% yield and Ir(ttp)(*meta*-COMe-C_6H_4) **4c** in 8% yield, respectively (Table 4.4, entry 2). Both electron-rich and

electron-poor *para*-substituted acetophenones required shorter reaction time of 12 to 15 days to give **3a** and **3c-d** in similar CCA product yields (Table 4.4, entries 1, 3 and 4).

Table 4.5 CCA of Acetophenones by Ir(ttp)(BF_4)(CO)

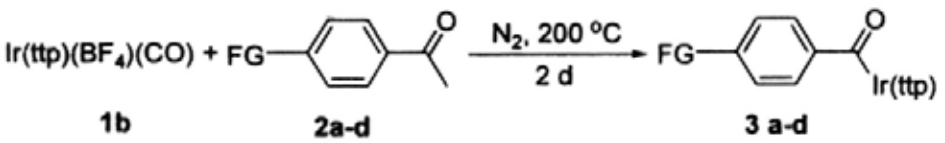

(4.5)

1b **2a-d** **3 a-d**

Entry	FG	Product (Yield / %)
1	F **2a**	Ir(ttp)CO(4-F-C_6H_4) **3a** (54)
2[a]	H **2b**	Ir(ttp)COC_6H_5 **3b** (58)
3	Me **2c**	Ir(ttp)CO(4-Me-C_6H_4) **3c** (75)
4	OMe **2d**	Ir(ttp)CO(4-OMe-C_6H_4) **3d** (80)

[a] Aromatic CHA products of **4b** and **4c** still remained in trace amount (<5%) according to TLC analysis, but was not isolated after chromatography due to the large amount impurities present.

The more electrophilic Ir(ttp)(BF_4)(CO) **1b** bearing the more labile BF_4 anion was found to be more reactive towards the silicon-hydrogen bond activation (SiHA) of silanes than Ir(ttp)Cl(CO) (Chapter 2), therefore, the reactivity of Ir(ttp)(BF_4)(CO) towards the C(C=O)-C(α) bond activation was examined (Table 4.5, eq 4.5). Indeed, Ir(ttp)(BF_4)(CO) **1b** reacted with acetophenones **2a-d** to give the corresponding CCA products **3a-d** faster than Ir(ttp)Cl(CO). However, the CCA product yields for **2a-b** were lower (Table 4.5, entries 1 and 2 vs Table 4.4, entries 1 and 2), while the CCA product yields for **2c-d** were similar (Table 4.5, entries 3 and 4 vs Table 4.4, entries 3 and 4). In addition, the aromatic CHA products **4b-c** still formed in trace amount

(<5%) in the reaction between Ir(ttp)(BF_4)(CO) **1b** and acetophenone according to TLC analysis.

4.2.2 C(C=O)-C(α) Bond Activation of Acetophenones by Electron-Rich Iridium Porphyrin Complexes

Besides the electrophilic iridium porphyrin complexes **1a-b**, electron-rich iridium porphyrin complexes, such as Ir(ttp)R (R = Me **1c**, C_6H_5 **1d** and $SiEt_3$ **1e**) can also cleave the C(C=O)-C(α) bonds of acetophenones at 200 °C.

Table 4.6 CCA of Acetophenones by Ir(ttp)Me

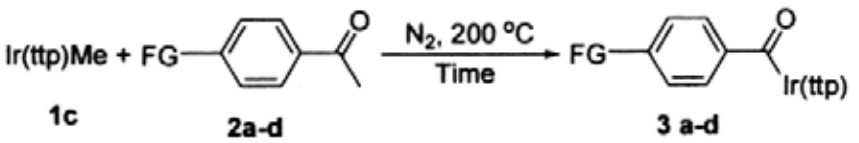

1c **2a-d** **3 a-d** (4.6)

Entry	FG	Time / d	Product (Yield / %)
1	F **2a**	6	Ir(ttp)CO(4-F-C_6H_4) **3a** (92)
2	H **2b**	26	Ir(ttp)COC_6H_5 **3b** (80)
3	Me **2c**	21	Ir(ttp)CO(4-Me-C_6H_4) **3c** (58)
4	OMe **2d**	24	Ir(ttp)CO(4-OMe-C_6H_4) **3d** (82)

Table 4.6 and eq 4.6 show the results of CCA of acetophenones by Ir(ttp)Me **1c**. Ir(ttp)Me reacted with acetophenone **2b** at 200 °C to cleave the C(C=O)-C(α) bond in slower rate than electrophilic iridium porphyrin complexes **1a-b** (Table 4.6, entry 2 vs Table 4.4, entry 2 and Table 4.5, entry 2). By TLC analysis of the reaction mixture, the α-CHA product **4a** was formed within 5 hours together with the aromatic CHA products **4b-c**, while the α-CHA product was converted to the aromatic CHA products after 1 day. After 2 days, the CCA product was observed, and Ir(ttp)Me still remained

but was completely consumed after 4 days. For electron-poor *para*-fluoro-acetophenone **2a**, the reaction rate and the product yield were much higher (Table 4.6, entry 1). However, for electron-rich *para*-substituent acetophenones **2c-d**, the reaction rate and the CCA product yields were similar (Table 4.6, entries 3 and 4).

In addition, Ir(ttp)C_6H_5 **1d** reacted poorly with acetophenone **2b**. Even after 26 days, only trace amount of the CCA product **3b** (<5%) formed and Ir(ttp)C_6H_5 was recovered in 88% yield (eq 4.7). The stronger Ir-C(sp^2) bond in Ir(ttp)C_6H_5 likely reduces the reactivity.[27]

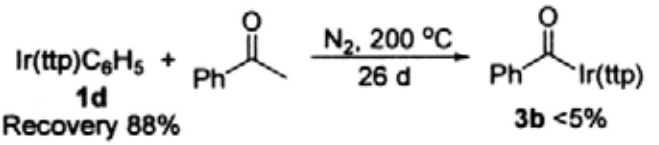

(4.7)

The more electron-rich Ir(ttp)$SiEt_3$ **1e** also reacted with acetophenone **2b** successfully after 1 day to give the α-CHA product **4a** in 58% yield as the sole product (eq 4.8). Upon prolong heating the reaction mixture for 8 days, the CCA product **3b** was isolated in 89% yield (eq 4.8). By TLC analysis of the reaction mixture, the α-CHA product **4a** was formed after 1 day and was converted to the aromatic CHA products **4b-c** and CCA product **3b** slowly.

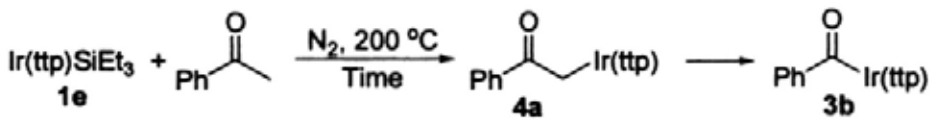

(4.8)

4.2.3 Steric Effect on the C(C=O)-C(α) Bond Activation of Aromatic Ketones

Unfortunately, the C(C=O)-C(α) bond activation of aromatic ketones was found to be limited to the steric unhindered enoliazble methyl ketones. Table 4.7 and eq 4.9 summarize the relative reactivity of iridium porphyrin complexes with propiophenone **2e**. For the more bulky propiophenone **2e**, the aromatic CHA products **4d-e** were isolated as the major products. The CCA product **3b** was only observed according to

TLC analysis and was isolated in less than 5% yield for all the iridium porphyrin complexes examined (Table 4.7, entries 1-4). The electrophilic Ir(ttp)Cl(CO) **1a** and Ir(ttp)(BF_4)(CO) **1b** and the more electron-rich Ir(ttp)$SiEt_3$ **1e** gave a high yield of the aromatic CHA products **4d-e** (Table 4.7, entries 1-2 and 4), while Ir(ttp)Me **1c** exhibited poor reactivity towards propiophenone, with the aromatic CHA products **4d-e** isolated in a low yield of 7% and 14%, respectively and Ir(ttp)Me recovered in 50% yield (Table 4.7, entry 3).

Table 4.7 Aromatic CHA of Propiophenone by Iridium Porphyrin Complexes[a]

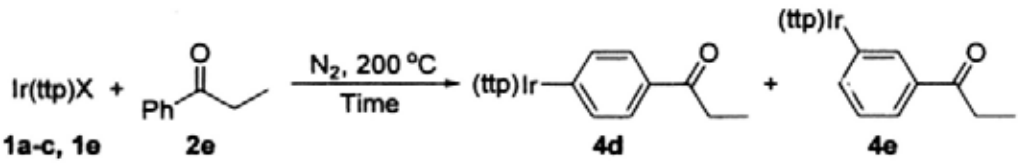

(4.9)

Entry	Ir(ttp)X	Time / d	Yield / % **4d**	Yield / % **4e**
1	Ir(ttp)Cl(CO) **1a**	12	23	46
2	Ir(ttp)(BF_4)(CO) **1b**	12	21	42
3[b]	Ir(ttp)Me **1c**	12	7	14
4	Ir(ttp)$SiEt_3$ **1e**	17	22	44

[a] **3b** was observed according to TLC analysis, and the yield was less than 5%. [b] Ir(ttp)Me was recovered in 50% yield.

4.2.4 C(C=O)-C(α) Bond Activation of Aliphatic Ketones

The C(C=O)-C(α) bond activation of aromatic ketones is therefore sensitive to the steric hindrance of the ketones. So the least hindered aliphatic ketone, acetone **2f**, was subject to reactions with various iridium porphyrin complexes. Table 4.8 and eq 4.10 summarize the results.

Ir(ttp)Cl(CO) **1a** reacted poorly with acetone **2f**, to give only trace amount C(C=O)-C(α) bond activation product of Ir(ttp)Me **1c** and Ir(ttp)COMe **3e** (Table 4.8, entry 1). Most of Ir(ttp)Cl(CO) remained unreacted according to TLC analysis, but

decomposed during column chromatography on alumina. Alumina chromatography was chosen since the products **1c** and **3e** can only be purified by alumina chromatography but Ir(ttp)Cl(CO) is only stable towards silica gel chromatography.

Fortunately, the more electrophilic Ir(ttp)(BF_4)(CO) **1b** was found to cleave the C(C=O)-C(α) bond of acetone **2f** in a faster rate than acetophenone to form Ir(ttp)Me **1c** and Ir(ttp)COMe **3e** in 74% and 11% yields, respectively (Table 4.8, entry 2).

Table 4.8 Reactivity of Iridium Porphyrin Complexes towards Acetone

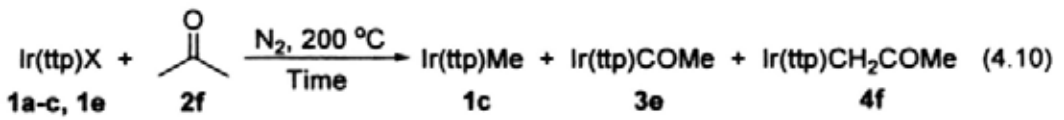

Entry	X	Time / d	Yield / %			
			1c	**3e**	**4f**	Total
1[a]	Cl(CO) **1a**	10	<5	<5	---	<5
2	(BF_4)(CO) **1b**	1	74	11	---	85
3[b]	(BF_4)(CO) **1b**	1	Ir(ttp-β-d_8)CD_3 **1c'**-β-d_8; Ir(ttp-β-d_8)$COCD_3$ **3e'**-β-d_8			ca 50
4[c]	Me **1c**	5	80	---	---	80
5	Ir(ttp)$SiEt_3$ **1e**	4	---	---	34	34

[a] Ir(ttp)Cl(CO) was still remained after 10 days according to TLC analysis, but decomposed upon column chromatography on alumina. [b] Acetone-d_6 **2g** used. [b] Ir(ttp)Me recovered.

In addition, when Ir(ttp)(BF_4)(CO) **1b** was heated in acetone-d_6 **2g**, a mixture of the C(C=O)-C(α) bond activation products containing Ir(ttp-β-d_8)CD_3 **1c'**-β-d_8 and Ir(ttp-β-d_8)$COCD_3$ **3e'**-β-d_8 with the protons of pyrrole exchanged to deuterium was isolated in ca 50% yield after 1 day (Table 4.8, entry 3).

There are two lines of evidence to support the formation of Ir(ttp-β-d_8)CD_3

1c'-β-d_8 and Ir(ttp-β-d_8)$COCD_3$ **3e'**-β-d_8. Firstly, the CCA of acetone **2f** has been achieved by Ir(ttp)(BF_4)(CO), and Ir(ttp)Me and Ir(ttp)COMe were isolated as a mixture (Table 4.8, entry 2). From the ^{1}H NMR spectrum shown in Figure 4.2a, the proton signals in the porphyrin ligands for Ir(ttp)Me and Ir(ttp)COMe completely overlap, except for pyrrole protons. They are identical isotopic mixture. Mass spectrometic results also revealed the presence of CCA products. The region of *m/z* = 883-888 was assignable to **1c'**-β-d_8, while *m/z* = 902-905 belonged to **3e'**-β-d_8 (Figure 4.3). Since this kind of H/D exchange reaction is not the focus in this work, the detailed mechanism was not examined. There are reports on the H/D exchange of octaalkylporphyrins at the *meso*-position.[28]

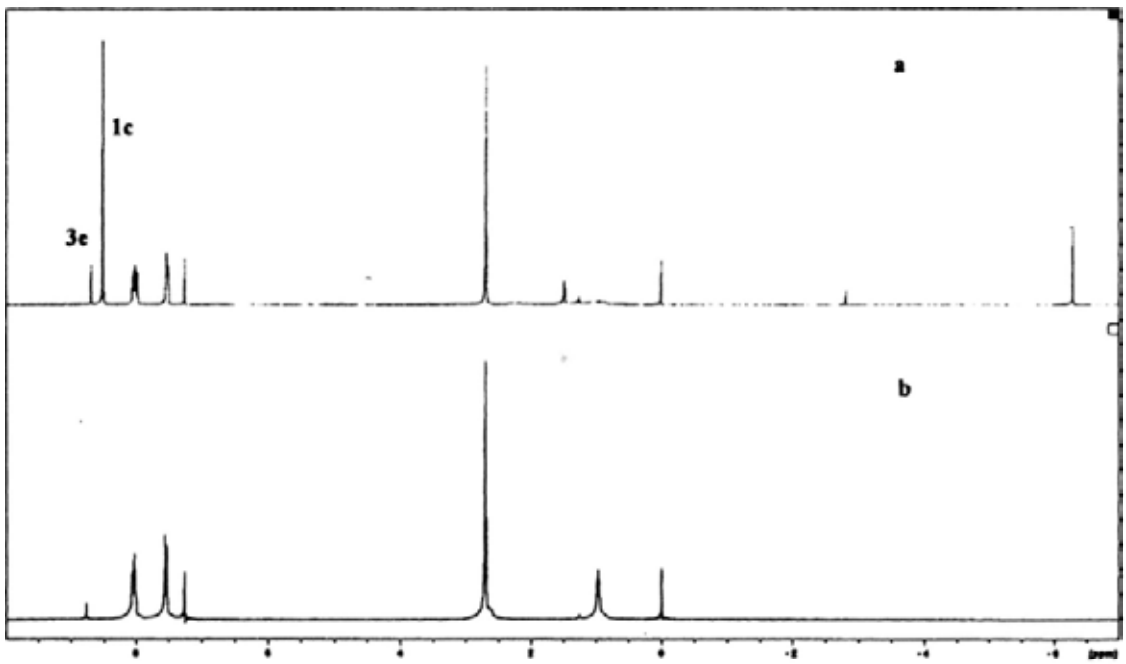

Figure 4.2 (a) ^{1}H NMR spectrum for the mixture of Ir(ttp)Me and Ir(ttp)COMe; (b)^{1}H NMR spectrum for the mixture of Ir(ttp-β-d_8)CD_3 and Ir(ttp-β-d_8)$COCD_3$

Ir(ttp)Me **1c** was found to be thermally stable in acetone at 200 °C in 5 days and was recovered in 80% yield (Table 4.8, entry 4). The thermal stability of Ir(ttp)Me **1c** in acetone-d_6 was ascertained as the reaction mixture in a sealed-NMR tube at 200 °C, after 34 days, gave no Ir(ttp)CD_3 **1c'**, but only Ir(ttp)Me **1c** in 72% yield. Finally,

Ir(ttp)$SiEt_3$ **1e** reacted with acetone in 4 days to give only the α-CHA product **4f** in 34% yield without any CCA product (Table 4.8, entry 5). The lower yield is likely due to the decomposition of the α-CHA product or the intermediates at high temperature of 200 °C.

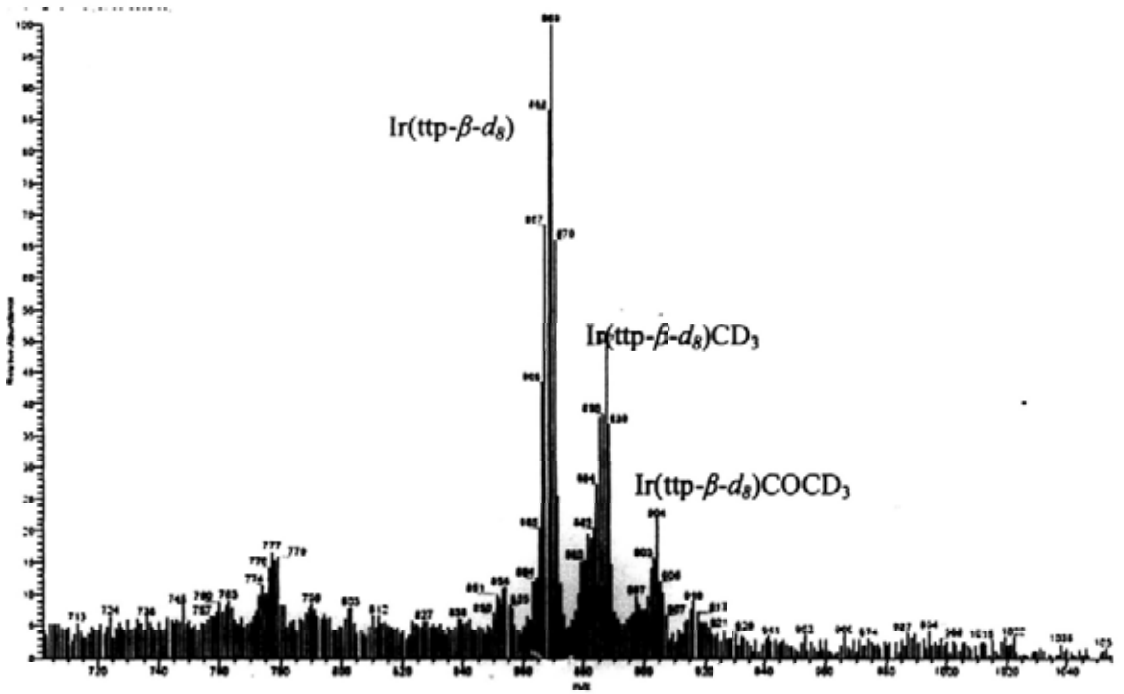

Figure 4.3 Mass Spectrum for the mixture of Ir(ttp-β-d_8)CD_3 and Ir(ttp-β-d_8)$COCD_3$

Therefore, only the most reactive Ir(ttp)(BF_4)(CO) **1b** was then used to react with various aliphatic ketones to examine the reactivity as well as the selectivity of the bond activation reaction (Table 4.9, eq 4.11).

Methyl ketones **2h-i** underwent C(C=O)-C(α) bond activation successfully to give **1c**, **3e** and **3f**, and the selectivity was found to be dependent on the sterics and the bond strengths of ketones (Table 4.1). Ir(ttp)(BF_4)(CO) **1b** reacted with 2-butanone **2h** at 200 °C after 4 days, and a mixture of Ir(ttp)Me **1c** (13%), Ir(ttp)COMe **3e** (24%) and Ir(ttp)Et **3f** (28%) was isolated (Table 4.9, entry 2). Most likely, the C(C=O)-C(ethyl) bond is more easily cleaved than the C(C=O)-C(methyl) bond. The same bond strength effect holds for acetylacetone **2i**, as the C(C=O)-C(CH_2) bond

cleavage product Ir(ttp)COMe **3e** was isolated in 50% yield, while the C(C=O)-C(methyl) bond activation product Ir(ttp)Me **1c** was isolated in a lower yield of 15%, when **1b** and **2i** were heated at 200 °C for 3 days (Table 4.9, entry 3). The more favored cleavage of a more bulky C(C=O)-C(α) bond is likely due to its lower bond dissociation energy than the C(C=O)-C(methyl) bond (83.0 kcal mol^{-1} for C(C=O)-C(ethyl) in **2h**, 80.8 kcal mol^{-1} for C(C=O)-C(CH_2) in **2i**, 84.1 kcal mol^{-1} for C(C=O)-C(methyl)).[3]

Table 4.9 CCA of Aliphatic Ketones by Ir(:tp)(BF_4)(CO)

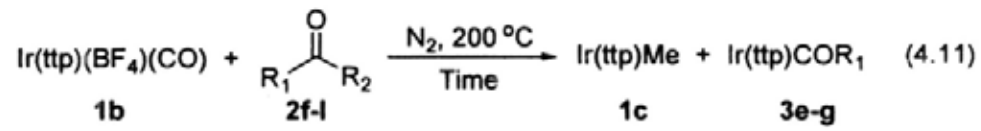

1b **2f-l** **1c** **3e-g**

Entry	R_1COR_2	Time / d	Product (Yield / %)
1	MeCOMe **2f**	1	Ir(ttp)Me **1c** (74); Ir(ttp)COMe **3e** (11)
2	MeCOEt **2h**	4	Ir(ttp)Me **1c** (13);Ir(ttp)COMe **3e** (24); Ir(ttp)Et **3f** (28)
3	$(MeCO)_2CH_2$ **2i**	3	Ir(ttp)Me **1c** (15); Ir(ttp)COMe **3e** (50)
4	$MeCO^iPr$ **2j**	4	Ir(ttp)Me **1c** (69)
5	EtCOEt **2k**	4	Ir(ttp)Me **1c** (<5); Ir(ttp)COMe **3e** (<5); Ir(ttp)Et **3f** (19); Ir(ttp)COEt **3g** (11)
6	$^iPrCO^iPr$ **2l**	4	A mixture of unknowns (ca 9)

In addition, for the more bulky 3-methyl-2-butanone **2j**, a selective C(C=O)-C(methyl) bond cleavage was achieved to give Ir(ttp)Me in 69% yield (Table 4.9, entry 4). Although the C(C=O)-C(isopropyl) bond (81.3 kcal mol^{-1})[3] is weaker than the C(C=O)-C(methyl) bond (ca 84.3 kcal mol^{-1})[3], the steric hindrance of isopropyl group inhibits the reaction.

However, for those non-methyl substituted ketones, such as **2k-l**, both the reaction rates and the CCA product yields were much lower. For the reaction between **1b** and 3-pentanone **2k**, besides the isolation of CCA products of Ir(ttp)Et **3f** and Ir(ttp)COEt **3g** in 19% and 11% yields, respectively, Ir(ttp)Me **1c** and Ir(ttp)COMe **3e** were also observed in trace amount after 4 days (Table 4.9, entry 5). We do not understand the origin of **1c** and **3e**. A possibility is that Ir(ttp)Me is generated from the reduction of CO by excess Ir(ttp)H,[29] while Ir(ttp)COMe is formed from the further reaction of Ir(ttp)Me via CO insertion.[30] For the more bulky 2,4-dimethyl-3-pentanone **2l**, no CCA product can be obtained due to the large steric hindrance of the isopropyl group (Table 4.9, entry 6).

4.2.5 Relative Reactivity for CHA and CCA of Ketones with Iridium Porphyrin Complexes

From the above results, the cleaveage rates of C(C=O)-C(α), C(α)-H and C(aryl)-H bonds of ketones are highly rate dependent on the properties of ketones and the iridium porphyrin complexes. Table 4.10 summarizes the relative reactivity. The more electrophilic Ir(ttp)(BF_4)(CO) is the most reactive iridium porphyrin complex for both aromatic and aliphatic ketones.

On the other hand, we also found that the CCA of *para*-substituted acetophenones exhibited a different reactivity towards the iridium porphyrin complexes (Table 4.11). Generally, *para*-fluorine substituted acetophenone reacted with iridium porphyrin complexes faster.

Table 4.10 Relative Reactivity Order of C(C=O)-C(α), C(α)-H and C(aryl)-H Bond Activation of Ketones by Iridium Porphyrin Complexes

Ketone	Process	Relative Rate for Iridium Porphyrin Complexes
C_6H_5COMe	CCA	$Ir(ttp)(BF_4)(CO) > Ir(ttp)SiEt_3 > Ir(ttp)Cl(CO) > Ir(ttp)Me > Ir(ttp)C_6H_5$
	α-CHA	$Ir(ttp)(BF_4)(CO) \sim Ir(ttp)SiEt_3 \sim Ir(ttp)Cl(CO) > Ir(ttp)Me >> Ir(ttp)C_6H_5$ (not observed)
	ArCHA	$Ir(ttp)(BF_4)(CO) > Ir(ttp)Cl(CO) > Ir(ttp)SiEt_3 \sim Ir(ttp)Me > Ir(ttp)C_6H_5$ (not observed)
MeCOMe	CCA	$Ir(ttp)(BF_4)(CO) >> Ir(ttp)Cl(CO)$
	CHA	$Ir(ttp)(BF_4)(CO) \sim Ir(ttp)SiEt_3$

Table 4.11 Relative Reactivity Order for CCA of *para*-Substituted Acetophenones by Ir(ttp)X (X = Cl(CO) or Me)

Ir(ttp)X	Relative Reactivity for Acetophenones
Ir(ttp)Cl(CO)	*p*-F ~ *p*-Me ~ *p*-OMe > H
Ir(ttp)Me	*p*-F > H ~ *p*-Me ~ *p*-OMe

In addition, when $Ir(ttp)(BF_4)(CO)$ reacted with various aromatic and aliphatic ketones, the relative reactivity was found to be dependent on the steric hindrance and the bond strengths[3] of the C(C=O)-C(α) bonds of ketones. The relative reactivity order for various ketones with $Ir(ttp)(BF_4)(CO)$ is also listed in Scheme 4.9. The less sterically hindered methyl, ethyl and methyl acyl groups are more easily cleaved, while the more bulky groups, such as phenyl and isopropyl, are stable toward cleavage.

Scheme 4.9 Relative Reactivity Order of the C(C=O)-C(α) Bond Activation of Various Ketones with Ir(ttp)(BF_4)(CO)

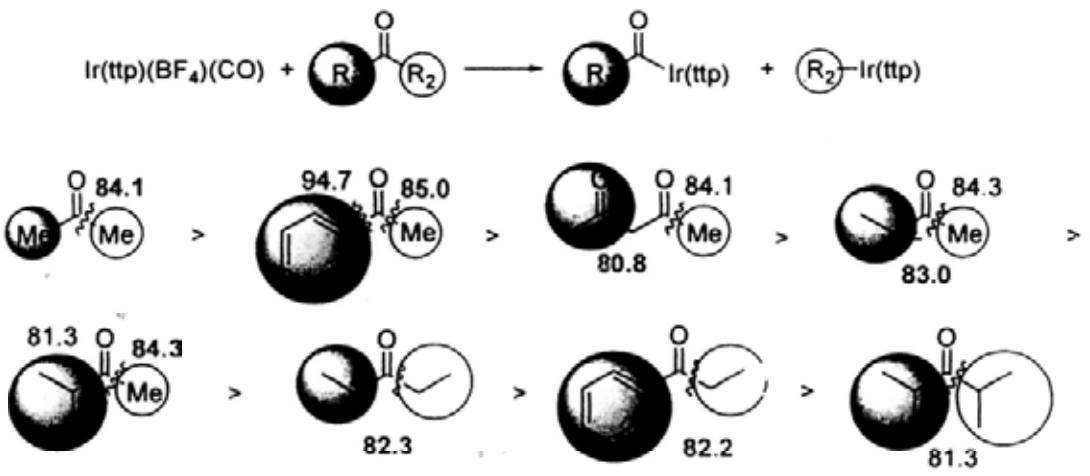

BDE[3]: kcal mol^{-1}

4.2.6 Mechanistic Studies on C(C=O)-C(α) Bond Activation of Ketones

4.2.6.1 C(C=O)-C(α) Bond Activation of Acetophenones by Electrophilic Iridium Porphyrin Complexes

In order to investigate the possible mechanism for the C(C=O)-C(α) bond activation of aromatic ketones, the reaction of **1a** and **2b** was studied in more details. TLC analysis of the reaction progress revealed the initial formation of the aromatic CHA products **4b-c** in 1 day and the CCA product **3b** was observed after 4 days. The aromatic CHA products **4b-c** were further converted to the CCA product slowly, but they were still present after 20 days (Table 4.4, entry 2). When the reaction was run in a shorter reaction time of 5 days at 200 °C, the aromatic CHA products **4b-c** were isolated in 10% and 20% yields, respectively, together with the CCA product **3b** formed in 16% yield (eq 4.12). Most likely, the aromatic CHA products **4b-c** are formed from a competitive parallel pathway and they are unlikely the active intermediates for the CCA reaction. In addition, the *para*- and *meta*- aromatic CHA products were isolated in about 1 to 2 ratio, according to the statistical aboundance of

para- and *meta*-protons. Therefore the reaction is unlikely via electrophilic aromatic substitution (S_EAr).[31]

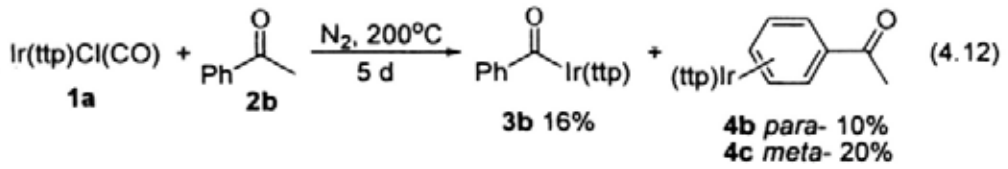

(4.12)

Furthermore, Ir(ttp)Cl(CO) reacted with acetophenone at a lower temperature of 120 °C, after 5 days the α-CHA product **4a** was isolated in 11% yield without any aromatic CHA and CCA products (eq 4.13). The α-CHA product **4a** is likely a kinetic product, preceeding the formation of aromatic CHA products.

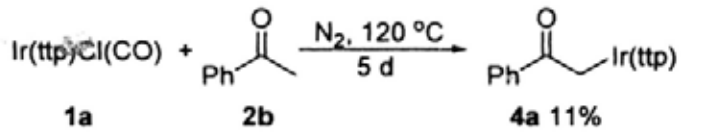

(4.13)

When the more reactive Ir(ttp)(BF_4)(CO) **1b** was reacted with acetophenone for 4 hours, the aromatic CHA products **4b** and **4c** were isolated in 8% and 16% yields, respectively, together with the α-CHA product **4a** in trace amount, and the CCA product **3b** in 15% yield (eq 4.14).

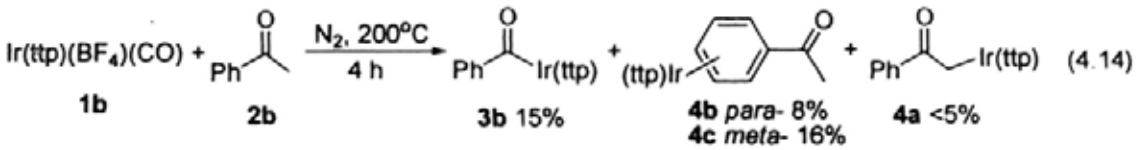

(4.14)

Most likely, the electrophilic iridium porphyrin complexes **1a-b** react with acetophenone **2b** to give the α-CHA product **4a** as the primary product, which can further convert to the aromatic CHA products **4b-c** as the secondary products at high temperature. Finally, the thermodynamic CCA product **3b** forms upon prolong heating.

During the reactions between iridium porphyrin complexes and acetophenones, immiscible liquid droplets, likely water, formed. The formation of water was reasoned to come from the iridium-catalyzed aldol condensation of acetophenones. Indeed, we

found that acetophenone independently did undergo a catalyzed aldol condensation reaction to give **5a** and **5b**[32] in the presence of 0.2 mol% of Ir(ttp)Cl(CO) **1a** even in a shorter reaction time of 1 day (eq 4.15).

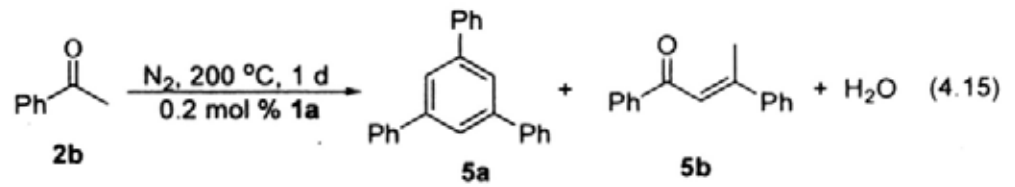

(4.15)

	5a	5b
Based on **2b**	0.5%	2%
Based on **1a**	250%	1000%

The α-CHA product **4a** has been found to be the kinetic product and the conversion to the CCA product was therefore examined by the reaction of **4a** with **2b** at 200 °C (eq 4.16). However, the reaction rate was slower than that of Ir(ttp)Cl(CO). The aromatic CHA products were also observed within 2 days before the formation of the CCA product after 4 days according to TLC analysis. After 15 days, the α-CHA product **4a** was consumed completely, and the aromatic CHA products **4b-c** were isolated in 21% and 42% yield, respectively, as well as the CCA product **3b** in 21% yield. At a longer reaction time of 26 days, the aromatic CHA products **4b-c** were converted to the CCA products slowly and **3b** was isolated in 75% yield.

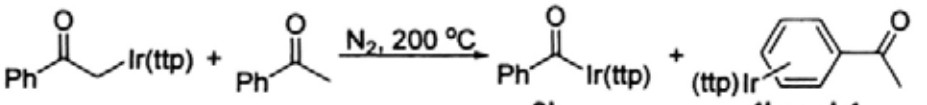

(4.16)

	3b	4b and 4c
t = 15 d	21%	21%, 42%
t = 26 d	75%	8%, 16%

Mechanistically, the direct SBM of M-C(sp^3) and C-C bonds is unlikely due to the steric hindrance. Furthermore, Ir(ttp)Me **1c** as an analogue of the α-CHA product **4a**, was found to be thermally stable in benzene, and no aromatic CHA product of Ir(ttp)C_6H_5 was observed at 200 °C after 10 days.[33] The sterically less demanding SBM of aromatic C-H bonds appears to be difficult. Therefore, the reaction of **4a** and

2b to give **4b-c** directly does not seem to be feasible. These results suggest that the α-CHA product **4a** is unlikely the direct active intermediate towards the CCA reaction, but a non-productive kinetic product.

In addition, Ir(ttp)C_6H_5 **1e**, an analogue of **4b-c**, reacted poorly with acetophenone at 200 °C (eq 4.7). Therefore, the aromatic CHA products are also not the intermediates involved in the CCA step, but another kind of non-productive kinetic products. Concerning the nature of the CCA step, the direct SBM of C-C bond and metal-C(sp^2) bond is difficult due to steric hindrance. D::rect SBM of C-C bond is unprecedented even it has been suggested but later corrected not to be the case.[24] Therefore, some other possible pathways were considered.

As water formed from the Ir(ttp)Cl(CO)-catalyzed aldol condensation of acetophenone (eq 4.15), and hydroxide anion (˙OH) has been found to undergo nucleophilic attack at the iridium center of iridium porphyrin aryls at 200 °C to give Ir(ttp)OH (Chapter 3, eqs 3.21 and 3.22, Figures 3.5 and 3.6), water especially at high temperature, can attack Ir(ttp)R, the kinetic CHA products **4a-c**, to give Ir(ttp)OH or Ir(ttp)H and co-products RH or ROH (Scheme 4.10).

Scheme 4.10 Possible Pathways for Hydrolyses of Ir(ttp)R with Water

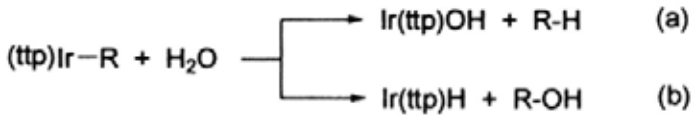

Indeed, Ir(ttp)H **1f** has been observed in 20% yield when the α-CHA product **4a** was heated at 200 °C in benzene-d_6 for 3 days in the presence of 100 equivalents of water (eq 4.17). Extensive decomposed iridium porphyrin species was observed. However, no 2-hydroxy-acetophenone ($C_6H_5COCH_2OH$), but only acetophenone **2b** was observed in 20% yield according to both ^{1}H NMR and GC-MS analyses. Therefore, water indeed hydrolyzes the Ir(ttp)R to give Ir(ttp)OH **1g** (as discussed in

details in Chapter 3).[34-35] Ir(ttp)OH has been proposed to convert to Ir(ttp)$^-$ in basic media (Chapter 3, Scheme 3.9), which further undergoes protonation in the presence of water (generated from the aldol condensation) to give Ir(ttp)H (p*K*a value of Ir(ttp)H is ca 15, Chapter 3).[36]

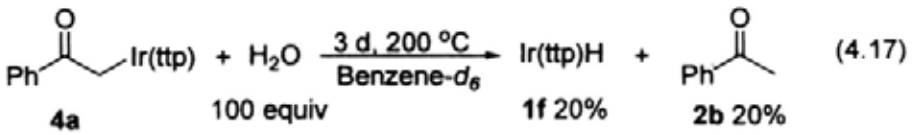

(4.17)

For the aromatic CHA products, the hydrolysis of Ir(ttp)C_6H_5 with water was much slower than that of the α-CHA product **4a**. Ir(ttp)C_6H_5 **1e** and acetophenone **2b** in the presence of water (100 equiv) at 200 °C after 28 days gave the CCA product **3b** only in 12% yield (eq 4.18). These results support that water can hydrolyze Ir(ttp)C_6H_5 to give Ir(ttp)OH via nucleophic substitution or SBM, and then gives Ir(ttp)H. Figure 4.4 illustrates the two possible transition states for the hydrolysis of Ir(ttp)C_6H_5 to Ir(ttp)OH.

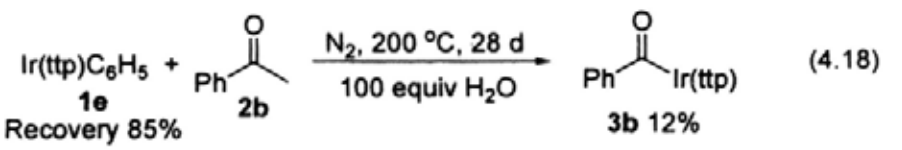

(4.18)

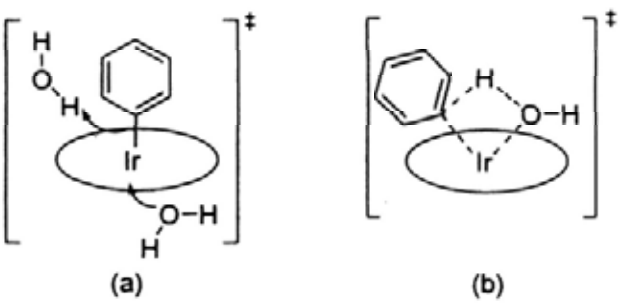

Figure 4.4 Possible pathways for the hydrolysis of Ir(ttp)C_6H_5 with water: (a) Nucleophilc substitution, (b) Sigma bond metathesis.

In addition, HCl is the co-product of the α-CHA reaction of ketones with Ir(ttp)Cl(CO). Therefore, 10 equivalents of HCl was added to the reaction mixture of Ir(ttp)C_6H_5 and acetophenone in order to promote the hydrolysis reaction. However,

$Ir(ttp)C_6H_5$ was completely decomposed after 15 hours at 200 °C. In order to find out the hydrolyzed organic co-product, Ir(ttp)(4-F-C_6H_4) **1e'** was heated in benzene-d_6 at 200 °C in the presence of 20 equivalents of HCl. After 13.5 hours, all the iridium porphyrin species was decomposed, and fluorobenzene was identified and quantified by GC-MS in 90% yield (eq 4.19). This result suggests that HCl indeed hydrolyzes Ir(ttp)Ar to give Ir(ttp)Cl. The failure to observe Ir(ttp)Cl is likely due to its instability towards possible demetallation by acid, especially in a large amount.[37]

$$\underset{\substack{\textbf{1e'}\\ \text{Decomposed}}}{Ir(ttp)(4\text{-}F\text{-}C_6H_4)} \xrightarrow[\substack{20\ \text{equiv HCl}\\ \text{Benzene-}d_6}]{200\ ^\circ\text{C, 13.5 h}} \text{"Ir(ttp)Cl"} + \underset{\substack{90\%\\ \text{(GC-MS)}}}{C_6H_5F} \qquad (4.19)$$

As Ir(ttp)H **1f** was observed to form in the reaction system, it is a possible active intermediate to cleave the C-C bond. However Ir(ttp)H **1f** reacted rapidly with acetophenone to give the α-CHA product of $Ir(ttp)CH_2COC_6H_5$ **4a** in 68% yield in just 1 day at 200 °C (Table 4.12, entry 1). Furthermore, the reaction mixture of **1f** and **2b** heated at 200 °C for 15 days gave both ArCHA products **4b-c** and CCA product **3b** in isolated yields of 8%, 16%, and 24%, respectively (Table 4.12, entry 2). Finally, **1f** reacted with **2b** at 200 °C for 26 days, and the CCA product **3b** was obtained as the major product in 72% yield (Table 4.12, entry 3). Therefore, the possible direct cleavage of C-C bond by Ir(ttp)H can not compete with the kinetic α- and aromatic C-H bond activation in the initial phase of the reaction. The hydrolysis pathway must be responsible for the re-conversion of α-CHA product **4a** back to Ir(ttp)OH and Ir(ttp)H.

Table 4.12 CCA of Acetophenone by Ir(ttp)H

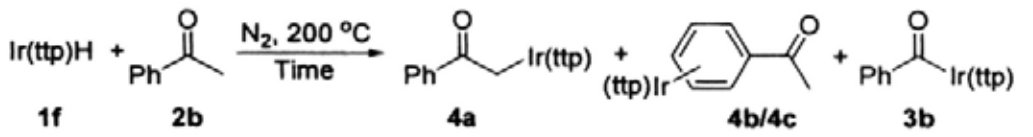

1f 2b 4a 4b/4c 3b (4.20)

Entry	Time / d	Yield / %				
		4a	**4b**	**4c**	**3b**	Total
1	1	68	---	---	---	68
2	15	42	8	16	24	90
3	26	9	5	10	72	87

4.2.6.2 Thermodynamic Estimation for the C(C=O)-C(α) Bond Activation of Acetophenone by Iridium Porphyrin Complexes

From above results, the CCA products were isolated as the thermodynamic product formed in the final step of the reaction. Since the C(C=O)-C(α) bond of acetophenone is surrounded by the kinetically accessible acidic C-H bonds, no CCA reaction was observed during the initial reaction. Therefore, the thermodynamics of the reaction step were estimated to gain some insight into the mechanism. Scheme 4.11 shows some possible intermediates for the CCA of acetophenone and the corresponding organic co-product together with the bond dissociation energies.[3,38-39] Among these, Ir(ttp)H and Ir(ttp)OH are considered to be the reasonable intermediates in the C(C=O)-C(α) bond activation. For Ir(ttp)H **1f**, the formation of Me-H (105.0 kcal mol^{-1})[3] (Scheme 4.11, pathway (v)) provides the driving force for the reaction, while for Ir(ttp)OH **1g**, the co-formation of MeOH also provides good driving force of the reaction (Scheme 4.11, pathway (vi)). Both these two species (Ir(ttp)H and Ir(ttp)OH) are more down hill than the rest. The intermediacy of **1e** is unlikely due to its demonstrated poor reactivity (eq 4.7).

Scheme 4.11 Possible Intermediates for the C(C=O)-C(α) Bond Activation of Acetophenone

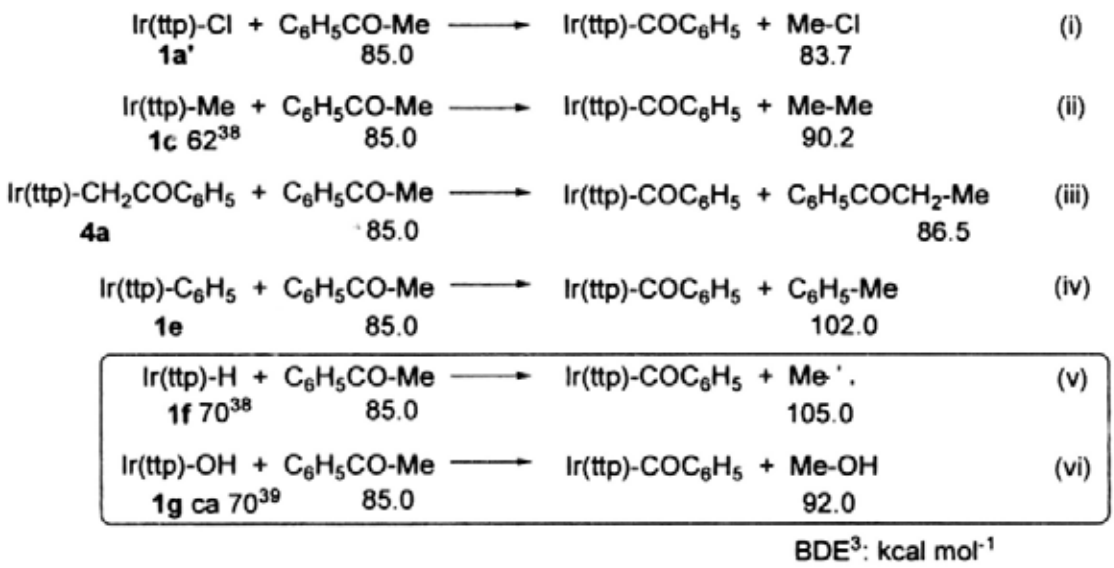

ΔH = BDE (Ir-X) + BDE (C_6H_5CO-Me) - BDE (Ir(ttp)-COC_6H_5) - BDE (X-Me)

$\Delta(\Delta H) = \Delta$ (BDE(Ir-X)) - Δ (BDE(X-Me))

4.6.2.3 Proposed Mechanism for the C(C=O)-C(α) Bond Activation of Acetophenones by Electrophilic Iridium Porphyrin Complexes

Based on the above findings, we propose a mechanism for the C(C=O)-C(α) bond activation of acetophenones by electrophilic iridium porphyrin complexes Ir(ttp)Cl(CO) **1a** and Ir(ttp)(BF_4)(CO) **1b** (Scheme 4.12). First, **1a-b** can react as a Lewis acid to catalyze the aldol condensation of acetophenone to give **5a-b** and water.[31] On the other hand, **1a-b** can also react with acetophenone **2b** to give the α-CHA product **4a** as a result of the nucleophilic attack of the enol form of **2b**.[31] **4a** undergoes interconversion with Ir(ttp)Cl **1a'** (Ir(ttp)(BF_4) **1b'**) or Ir(ttp)H **1f** via Ir(ttp)OH in acetophenone in the presence of HCl (HBF_4) (co-product of α-CHA) or H_2O (co-product from the aldol condensation). In addition, as discussed in chapter 3, Ir(ttp)OH, not Ir(ttp)H, was the intermediate to cleave the aromatic C-H bonds to give Ir(ttp)Ar. Therefore, Ir(ttp)OH is also the intermediate responsible for the aromatic

CHA of acetophenone, to give **4b-c**, which are more kinetically and thermodynamically stable than **4a**. On the other hand, **4b-c** can convert back to Ir(ttp)Cl (Ir(ttp)(BF_4)), or Ir(ttp)OH and Ir(ttp)H in the presence of HCl (HBF_4) or H_2O, respectively. Ir(ttp)H and/or Ir(ttp)OH then cleave(s) the C(C=O)-C(α) bond directly to give CCA product **3b** as the thermodynamic product. The cleavage of C(C=O)-C(α) bond is not kinetically favorable due to the steric hindrance than the more accessible C(α)-H bonds.

Scheme 4.12 Proposed Mechanism for C(C=O)-C(α) Bond Activation of Acetophenones by Electrophilic Iridium Porphyrin Complexes

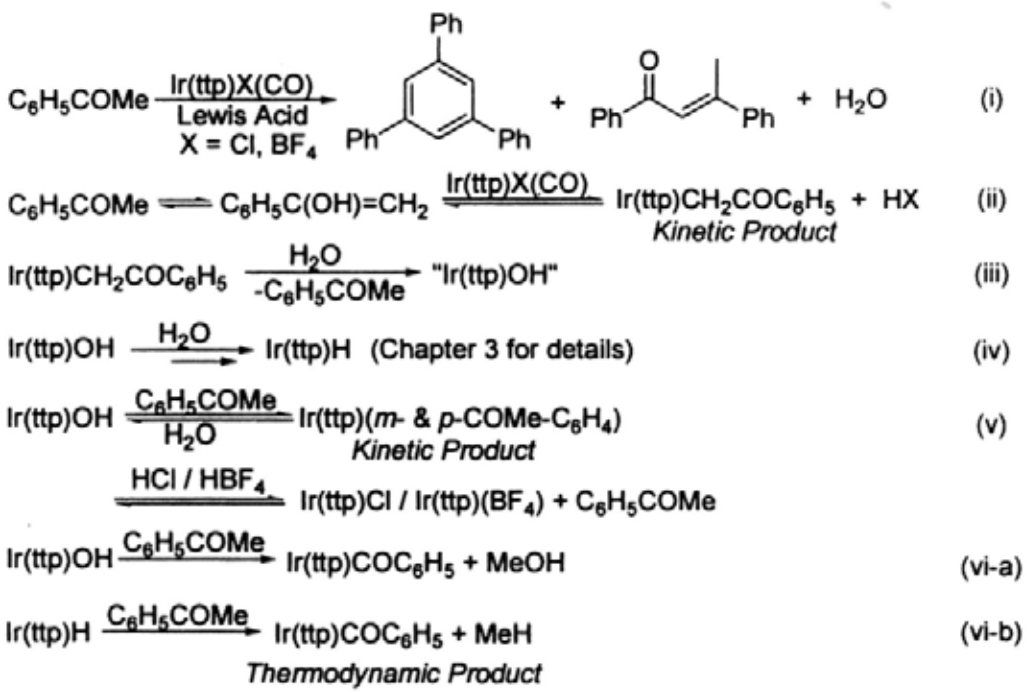

This proposed mechanism can also explain the higher yields obtained for *para*-substituted acetophenones (Tables 4.4 and 4.5) as the *para*-substituents hinder the formation of non-productive intermediates of aromatic CHA products.

In addition, the faster rate for the CCA reaction with Ir(ttp)(BF_4)(CO) (Table 4.5) is likely due to the more favored aldol condensation of acetophenone to form water. Besides iridium porphyrin complexes, the co-products of HBF_4 and HCl generated

from the α-CHA reaction can also catalyze the aldol condensation of acetophenones to form water.[2] The acidity of HBF_4 (p*K*a ca 0.1 in MeCN)[40] is stronger than that of HCl (p*K*a ca 8.6 in MeCN).[40] The boiling point of HBF_4 (130 °C (dec))[41] is also much higher than that of HCl (-85 °C).[42] Therefore, HBF_4 is a more efficient catalyst for the aldol condensation of acetophenone to give more water. For the more bulky propiophenone, the aldol condensation is unlikely due to the steric hindrance of ethyl group. Therefore, the re-conversion of the CHA products back to Ir(ttp)OH and Ir(ttp)H was inhibited. So the aromatic CHA reaction rate was slower, and the CCA product was difficult to form.

On the other hand, the p*K*a values decrease with more electron deficient acetophenones (Table 4.13).[43] Consequently, the more acidic acetophenones can undergo faster aldol condensation to give more water which enhances the hydrolysis of Ir(ttp)R and thus the CCA.

Table 4.13 p*K*a Value for Substituted Acetophenones[a]

Ketone	σ_p	p*K*a
C_6H_5COMe	0.00	18.38 ± 0.52
(*p*-F-C_6H_4)COMe	0.06	18.46 ± 0.51
(*p*-Me-C_6H_4)COMe	-0.17	---
(*p*-OMe-C_6H_4)COMe	-0.27	18.96 ± 0.51

[a] In water at 25 °C.

4.2.6.4 Kinetic and Thermodynamic Consideration of the CHA and CCA Products of Acetophenone

As the α-CHA product **4a** was formed in a lower reaction temperature of 120 °C (eq 4.13), and was converted to Ir(ttp)OH and then Ir(ttp)H with the addition of 100 equivalents of water (eq 4.17), it is the primary product.

The aromatic CHA products **4b-c** were formed after the α-CHA product, and were further converted to the CCA product at 200 °C (eq 4.16). Furthermore, Ir(ttp)C_6H_5 has been found to undergo hydrolysis with water very slowly, but promoted by HCl, so the aromatic CHA products **4b-c** are the secondary products.

Since the CCA products of iridium porphyrin acyl complexes were isolated as the final products in the reaction system, they are the thermodynamic ones. However, iridium porphyrin acyls were found to undergo acyl exchange with acetophenones (eq 4.21). Indeed, Ir(ttp)CO(4-Me-C_6H_4) was heated in acetophenone at 200 °C for 15 days, the acyl exchange product of Ir(ttp)COC_6H_5 via CCA reaction was isolatd in 80% yield, together with Ir(ttp)CO(4-Me-C_6H_4) was recovered in 17% yield. No α- and aromatic CHA products were observed by TLC analysis during the course of the reaction, which indicated that the CCA products are unlikely converted back to the CHA products, and they are indeed the thermodynamic products.

$$\underset{\substack{\textbf{3c}\\ \text{Recovery 17\%}}}{\text{Ir(ttp)CO(4-Me-C}_6\text{H}_4\text{)}} + \underset{\textbf{2b}}{\text{C}_6\text{H}_5\text{COMe}} \xrightarrow[15\ \text{d}]{\text{N}_2,\ 200\ ^\circ\text{C}} \underset{\textbf{3b 80\%}}{\text{Ir(ttp)COC}_6\text{H}_5} \qquad (4.21)$$

4.2.6.5 Proposed Mechanism for the C(C=O)-C(α) Bond Activation of Acetophenones by Electron-Rich Iridium Porphyrin Complexes

The electron-rich iridium porphyrin complexes, such as Ir(ttp)Me **1c** and Ir(ttp)$SiEt_3$ **1d**, can cleave the C(C=O)-C(α) bond of acetophenones to give the corresponding iridium porphyrin acyl complexes as the thermodynamic products, via the kinetic α-CHA and aromatic CHA products.

In addition, we have found that both α-CHA and aromatic CHA products underwent hydrolysis with water to give Ir(ttp)H, therefore, the reactivities of Ir(ttp)Me and Ir(ttp)$SiEt_3$ towards water were examined. When Ir(ttp)Me **1c** was heated in benzene-d_6 with the addition of 100 equivalents of water at 200 °C, after 6

days only trace amount of Ir(ttp)H was observed according to the ^{1}H NMR (Table 4.14, entry 1). Ir(ttp)Me was therefore stable towards hydrolysis by water in benzene. However, Ir(ttp)$SiEt_3$ dispalyed a faster hydrolysis rate with water, and 10% yield of Ir(ttp)H was obtained after 4 days at 200 °C, and Et_3SiOH[44] was also observed in 5% yield by ^{1}H NMR spectroscopy (Table 4.14, entry 3).

Table 4.14 Relative Reactivity for Hydrolysis of Ir(ttp)R

$$\underset{\textbf{1c, 4a, 1e}}{\text{Ir(ttp)R}} + \underset{100\text{ equiv}}{H_2O} \xrightarrow[\text{Benzene-}d_6]{200\ ^\circ\text{C, Time}} \underset{\textbf{1f}}{\text{Ir(ttp)H}} + \text{RH or ROH} \quad (4.22)$$

Entry	Ir(ttp)R	Time / d	Yield / %		
			Ir(ttp)R	Ir(ttp)H	RH or ROH
1	Ir(ttp)Me **1c**	6	>90%	<5	---
2	Ir(ttp)$CH_2COC_6H_5$ **4a**	3	---	20	C_6H_5COMe (20)
3	Ir(ttp)$SiEt_3$ **1e**	4	80	10	$HOSiEt_3$ (5)

Scheme 4.13 Proposed Mechanism for C(C=O)-C(α) Bond Activation of Acetophenones by Electron-Rich Iridium Porphyrin Complexes

$$C_6H_5COMe \xrightarrow[\text{Lewis Acid}\ (X = Me, SiEt_3)]{\text{Ir(ttp)R}} \underset{Ph}{\overset{Ph}{\overset{|}{\text{C}_6\text{H}_3}}}\underset{Ph}{} + \underset{Ph}{\overset{O}{\overset{\|}{\text{C}}}}\text{CH}=\text{C}(\text{Me})\text{Ph} + H_2O \quad \text{(i)}$$

$$C_6H_5COMe \rightleftharpoons C_6H_5C(OH)=CH_2 \xrightleftharpoons{\text{Ir(ttp)R}} \underset{\textit{Kinetic Product}}{\text{Ir(ttp)}CH_2COC_6H_5} + HR \quad \text{(ii)}$$

$$\text{Ir(ttp)}CH_2COC_6H_5 \xrightarrow[-C_6H_5COMe]{H_2O} \text{"Ir(ttp)OH"} \quad \text{(iii)}$$

$$\text{Ir(ttp)OH} \xrightarrow{H_2O} \text{Ir(ttp)H} \quad \text{(iv)}$$

$$\text{Ir(ttp)OH} \underset{H_2O}{\overset{C_6H_5COMe}{\rightleftharpoons}} \underset{\textit{Kinetic Product}}{\text{Ir(ttp)}(m\text{- \& }p\text{-COMe-}C_6H_4)} \quad \text{(v)}$$

$$\text{Ir(ttp)OH} \xrightarrow{C_6H_5COMe} \text{Ir(ttp)}COC_6H_5 + MeOH \quad \text{(vi-a)}$$

$$\text{Ir(ttp)H} \xrightarrow{C_6H_5COMe} \underset{\textit{Thermodynamic Product}}{\text{Ir(ttp)}COC_6H_5} + MeH \quad \text{(vi-b)}$$

From the above results, the rates of hydrolysis for both Ir(ttp)Me and Ir(ttp)$SiEt_3$ with water were much slower than that corresponding α-CHA reaction of acetophenone (4 days for **1c** and 1 day for **1e**), therefore, the α-CHA reaction most likely occurs directly between Ir(ttp)R (R = Me and $SiEt_3$) and acetophenone. Furthermore, water is essential to re-convert **4a** back to Ir(ttp)OH and Ir(ttp)H, therefore, the reacitivities of *para*-substituted acetophenones are highly related to the p*K*a values of ketones as disscused before. Scheme 4.13 shows the proposed mechanism for the C(C=O)-C(α) bond activation of acetophenones by electron-rich iridium porphyrin complexes, such as Ir(ttp)Me and Ir(ttp)$SiEt_3$.

4.2.6.6 Proposed Mechanism for the C(C=O)-C(α) Bond Activation of Aliphatic Ketones by Ir(ttp)(BF_4)(CO)

The more electrophilic Ir(ttp)(BF_4)(CO) exhibits the sole reactivity to cleave the C(C=O)-C(α) bond of aliphatic ketones, likely due to the stronger Lewis acidity and the co-formation of stronger acid of HBF_4 to promote the aldol condensation of less acidic aliphatic ketones (Table 4.1) and to form water. Scheme 4.14 shows the proposed mechanism for the C(C=O)-C(α) bond activation of aliphatic ketones by Ir(ttp)(BF_4)(CO) similar to Scheme 4.12.

Scheme 4.14 Proposed Mechanism for C(C=O)-C(α) Bond Activation of Acetophenones by Ir(ttp)(BF_4)(CO)

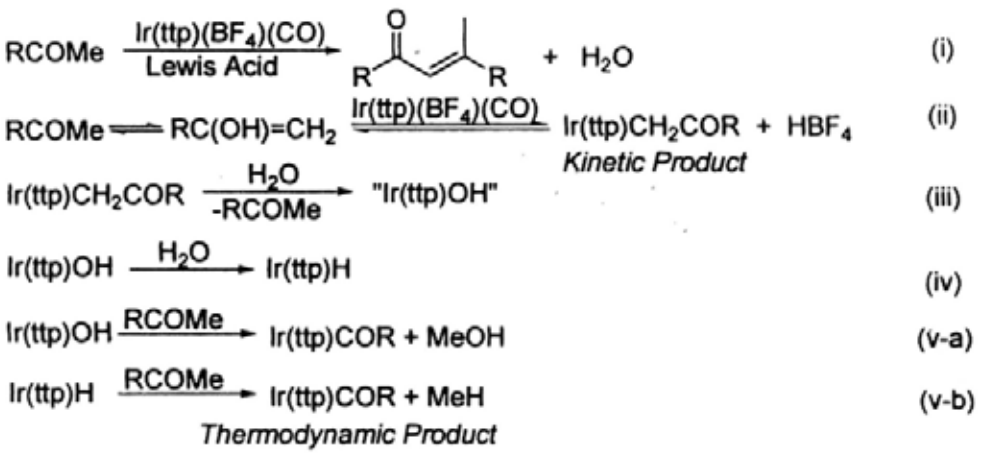

4.3 Conclusion

The C(C=O)-C(α) bond activation of enolizable ketones are successfully achieved by high-valent iridium(III) porphyrin complexes. Both α-CHA and aromatic CHA products were the kinetic products, while the CCA products were the thermodynamic ones. Ir(ttp)OH was the proposed intermediate for the aromatic CHA reaction of aromatic ketones, while both Ir(ttp)H and Ir(ttp)OH were the intermediates for the CCA reaction. Water, formed from the iridium-catalyzed aldol condensation of ketones, hydrolyzed the kinetic α-CHA and aromatic CHA products back to Ir(ttp)OH and Ir(ttp)H. Ir(ttp)(BF_4)(CO) exhibited a high reactivity towards aliphatic ketones, likely due to the stronger Lewis acidity in catalyzing the aldol condensation of aliphatic ketones to facilitate the formation of Ir(ttp)OH and Ir(ttp)H.

4.4 Experimental Section

Unless otherwise noted, all chemicals were obtained from commercial suppliers and used without further purification. Hexane for chromatography was distilled from anhydrous calcium chloride. Ketones were distilled from 4Å molecular sieve. Thin-layer chromatography was performed on precoated silica gel 60 F_{254} plates for thin-layer analyses for reaction mixture. All preparation reactions were carried out in a teflon screw-head stoppered tube in N_2. For purification of iridium porphyrin complexes, fresh column chromatography was used and carried out in air using aluminua (90 active neutral, 70-230 mesh). Samples for microanalyses were recrystallized from CH_2Cl_2/MeOH and were then dried at 40-60 °C in vacuum (0.005 mmHg) for 3 days.

^{1}H NMR spectra were recorded on a Bruker DPX-300 (300 MHz) or a Bruker 400. Chemical shifts were reported with reference to the residual solvent protons in $CDCl_3$ (δ 7.26 ppm) or C_6D_6 (δ 7.15 ppm) as the internal standard. Chemical shifts (δ)

were reported in parts per million (ppm) in δ scale downfield from TMS. Coupling constants (J) are reported in hertz (Hz). ^{13}C NMR spectra were recorded on a Bruker DPX 300 (75 MHz) or a Bruker 400 (100 MHz) spectrometer and referenced to $CDCl_3$ (δ 77.1 ppm) spectra. High-resolution mass spectra (HRMS) were performed on a Thermofinnign MAT 95 XL in FAB (using 3-nitrobenzyl alcohol (NBA) matrix and CH_2Cl_2 as the solvent) and ESI model (MeOH:CH_2Cl_2 = 1:1 as the solvent).

Reactions between Iridium Porphyrin Complexes and Ketones. General Procedure. The reaction of Ir(ttp)Cl(CO) **1a** with acetophenone (**2b**) is described as a typical example. Acetophenone (0.8 mL, 500 equiv) was added to Ir(ttp)Cl(CO) (12.4 mg, 0.013 mmol), and the mixture was degassed by the freeze-pump-thaw method (3 cycles). Then the mixture was heated at 200 °C for 20 days. The crude product was purified by column chromatography on alumina eluting with a mixture of hexane/CH_2Cl_2 (3:1). A purple solid of Ir(ttp)COC_6H_5[25b] **3b** (8.9 mg, 0.0092 mmol, 71%) was isolated. R_f = 0.28 (hexane/CH_2Cl_2 = 1:1). ^1H NMR (C_6D_6, 400 MHz): δ 2.42 (s, 12 H), 2.90 (d, 2 H, J = 7.2 Hz), 5.87 (t, 2 H, J = 7.6 Hz), 6.21 (t, 2 H, J = 7.2 Hz), 7.27 (d, 4 H, J = 7.6 Hz), 7.34 (d, 4 H, J = 7.2 Hz), 7.99 (d, 4 H, J = 7.6 Hz), 8.16 (d, 4 H, J = 7.6 Hz), 8.86 (s, 8 H). Then changed the solvent to hexane/CH_2Cl_2 (1:2), and a purple solid mixture of Ir(ttp)(*para*-COMe-C_6H_4)[26] **4b** (0.5 mg, 0.0005 mmol, 4%) and Ir(ttp)(*meta*-COMe-C_6H_4)[26] **4c** (1.0 mg, 0.0010 mmol, 8%) was isolated. Ir(ttp)(*para*-COMe-C_6H_4) **4b**: R_f = 0.14 (hexane/CH_2Cl_2 = 1:2). ^1H NMR (C_6D_6, 400 MHz): δ 0.95 (s, 3 H), 1.00 (d, 2 H, J = 8.8 Hz), 2.39 (s, 12 H), 5.24 (d, 2 H, J = 8.4 Hz), 7.20 (d, 4 H, J = 8.0 Hz), 7.34 (d, 4 H, J = 7.6 Hz), 7.93 (dd, 4 H, J = 1.6, 7.8 Hz), 8.12 (dd, 4 H, J = 1.2, 6.6 Hz), 8.82 (s, 8 H). Ir(ttp)(*meta*-COMe-C_6H_4) **4c**, R_f = 0.23 (hexane/CH_2Cl_2 = 1:2). ^1H NMR (C_6D_6, 400 MHz): δ 1.12 (s, 3 H), 1.19 (d, 1 H, J = 8.0 Hz), 1.69 (s, 1 H), 2.39 (s, 12 H), 4.73 (t, 1 H, J = 8.0 Hz), 5.53 (d, 1

H, J = 7.6 Hz), 7.23 (d, 4 H, J = 7.6 Hz), 7.34 (d, 4 H, J = 7.6 Hz), 8.09 (d, 4 H, J = 7.6 Hz), 8.14 (d, 4 H, J = 7.6 Hz), 8.82 (s, 8 H).

Reaction between Ir(ttp)Cl(CO) 1a and 4-Fluoroacetophenone (2a). 4-Fluoroacetophenone (0.8 mL, 500 equiv) and Ir(ttp)Cl(CO) (11.5 mg, 0.012 mmol) were heated at 200 °C for 13 days. A purple solid of Ir(ttp)CO(4-F-C_6H_4)[25b] **3a** (8.8 mg, 0.0089 mmol, 74%) was isolated after column chromatography. R_f = 0.28 (hexane/CH_2Cl_2 = 1:1). ^{1}H NMR (C_6D_6, 400 MHz): δ 2.41 (s, 12 H), 2.73 (dd, 2 H, $^4J_{H\text{-}F}$ = 5.4 Hz, J = 8.6 Hz), 5.50 (dd, 2 H, $^3J_{H\text{-}F}$ = 8.8 Hz, J = 8.8 Hz), 7.28 (d, 4 H, J = 8.0 Hz), 7.34 (d, 4 H, J = 7.6 Hz),7.98 (dd, 4 H, J = 1.6, 7.6 Hz), 8.14 (dd, 4 H, J = 1.6, 8.4 Hz), 8.85 (s, 8 H).

Reaction between Ir(ttp)Cl(CO) 1a and 4-Methylacetophenone (2c). 4-Methylacetophenone (0.8 mL, 500 equiv) and Ir(ttp)Cl(CO) (10.8 mg, 0.012 mmol) were heated at 200 °C for 12 days. A purple solid of Ir(ttp)CO(4-Me-C_6H_4)[25b] **3c** (9.2 mg, 0.0094 mmol, 78%) was isolated after column chromatography. R_f = 0.28 (hexane/CH_2Cl_2 = 1:1). ^{1}H NMR (C_6D_6, 400 MHz): δ 1.65 (s, 3 H), 2.42 (s, 12 H), 2.83 (d, 2 H, J = 8.0 Hz), 5.67 (d, 2 H, J = 8.0 Hz), 7.28 (d, 4 H, J = 7.6 Hz), 7.35 (d, 4 H, J = 7.6 Hz), 7.96 (dd, 4 H, J = 1.6, 7.6 Hz), 8.17 (dd, 4 H, J = 1.6, 7.6 Hz), 8.86 (s, 8 H).

Reaction between Ir(ttp)Cl(CO) 1a and 4-Methoxylacetophenone (2d). 4-Methoxylacetophenone (0.9 mL, 500 equiv) and Ir(ttp)Cl(CO) (12.8 mg, 0.014 mmol) were heated at 200 °C for 15 days. A purple solid of Ir(ttp)CO(4-MeO-C_6H_4)[25b] **3d** (11.1 mg, 0.0111 mmol, 79%) was isolated after column chromatography. R_f = 0.11 (hexane/CH_2Cl_2 = 1:1). ^{1}H NMR (C_6D_6, 400 MHz): δ 2.42 (s, 12 H), 2.90 (d, 2 H, J = 6.8 Hz), 2.92 (s, 3H), 5.45 (d, 2H, J = 8.8 Hz), 7.27 (d, 4 H, J = 8.1 Hz), 7.35 (d, 4 H, J = 7.6 Hz), 8.01 (d, 4 H, J = 7.6 Hz), 8.17 (d, 4 H, J = 7.6 Hz), 8.87 (s, 8 H).

Reaction between Ir(ttp)(BF_4)(CO) 1b and Acetophenone (2b). Acetophenone (0.8 mL, 500 equiv) and Ir(ttp)(BF_4)(CO) (12.5 mg, 0.013 mmol) were heated at 200 °C for 2 days. A purple solid of Ir(ttp)COC_6H_5[25b] **3b** (7.3 mg, 0.0075 mmol, 58%) was isolated after column chromatography. The aromatic CHA products of Ir(ttp)(*para*-COMe-C_6H_4)[26] **4b** and Ir(ttp)(*meta*-COMe-C_6H_4)[26] **4c** were still remained in trace amount (<5%).

Reaction between Ir(ttp)(BF_4)(CO) 1b and 4-Fluoroacetophenone (2a). 4-Fluoroacetophenone (0.8 mL, 500 equiv) and Ir(ttp)(BF_4)(CO) (12.6 mg, 0.013 mmol) were heated at 200 °C for 2 days. A purple solid of Ir(ttp)CO(4-F-C_6H_4)[25b] **3a** (6.9 mg, 0.0070 mmol, 54%) was isolated after column chromatography.

Reaction between Ir(ttp)(BF_4)(CO) 1b and 4-Methylacetophenone (2c). 4-Methylacetophenone (0.8 mL, 500 equiv) and Ir(ttp)(BF_4)(CO) (12.5 mg, 0.013 mmol) were heated at 200 °C for 2 days. A purple solid of Ir(ttp)CO(4-Me-C_6H_4)[25b] **3c** (9.6 mg, 0.0098 mmol, 75%) was isolated after column chromatography.

Reaction between Ir(ttp)(BF_4)(CO) 1b and 4-Methoxylacetophenone (2d). 4-Methoxylacetophenone (0.8 mL, 500 equiv) and Ir(ttp)(BF_4)(CO) (12.4 mg, 0.013 mmol) were heated at 200 °C for 2 days. A purple solid of Ir(ttp)CO(4-MeO-C_6H_4)[25b] **3d** (10.4 mg, 0.0104 mmol, 80%) was isolated after column chromatography.

Reaction between Ir(ttp) Me 1c and Acetophenone (2b). Acetophenone (0.8 mL, 500 equiv) and Ir(ttp)Me (12.7 mg, 0.014 mmol) were heated at 200 °C for 26 days. A purple solid of Ir(ttp)COC_6H_5[25b] **3b** (10.8 mg, 0.0112 mmol, 80%) was isolated after column chromatography.

Reaction between Ir(ttp)Me 1c and 4-Fluoroacetophenone (2a). 4-Fluoroacetophenone (0.9 mL, 500 equiv) and Ir(ttp)Me (13.1 mg, 0.015 mmol)

were heated at 200 °C for 6 days. A purple solid of Ir(ttp)CO(4-F-C_6H_4)[25b] **3a** (13.6 mg, 0.0138 mmol, 92%) was isolated after column chromatography.

Reaction between Ir(ttp)Me 1c and 4-Methylacetophenone (2c). 4-Methylacetophenone (0.9 mL, 500 equiv) and Ir(ttp)Me (11.5 mg, 0.013 mmol) were heated at 200 °C for 21 days. A purple solid of Ir(ttp)CO(4-Me-C_6H_4)[25b] **3c** (7.4 mg, 0.0075 mmol, 58%) was isolated after column chromatography.

Reaction between Ir(ttp)Me 1c and 4-Methoxylacetophenone (2d). 4-Methylacetophenone (0.9 mL, 500 equiv) and Ir(ttp)Me (12.5 mg, 0.014 mmol) were heated at 200 °C for 24 days. A purple solid of Ir(ttp)CO(4-MeO-C_6H_4)[25b] **3d** (11.4 mg, 0.0114 mmol, 82%) was isolated after column chromatography.

Reaction between Ir(ttp)$SiEt_3$ 1d and Acetophenone (2b) for One Day. Acetophenone (0.7 mL, 500 equiv) and Ir(ttp)$SiEt_3$ (12.0 mg, 0.012 mmol) were heated at 200 °C for 1 day. A purple solid of Ir(ttp)$CH_2COC_6H_5$ **4a** (6.8 mg, 0.0069 mmol, 58%) was isolated after column chromatography eluting with a mixture of hexane/CH_2Cl_2 (1:2). R_f = 0.18 (hexane/CH_2Cl_2 = 1:2). ^{1}H NMR (C_6D_6, 400 MHz): δ -3.53 (s, 2 H), 2.42 (s, 12 H), 5.13 (d, 2 H, J = 7.6 Hz), 6.48 (t, 2 H, J = 7.8 Hz), 6.81 (t, 1 H, J = 7.2 Hz), 7.30 (dd, 8 H, J = 8.0, 8.0 Hz), 8.04 (d, 4 H, J = 7.6 Hz), 8.14 (d, 4 H, J = 7.6 Hz), 8.75 (s, 8 H). ^{13}C NMR ($CDCl_3$, 100 MHz): δ -19.7, 21.7, 123.8, 124.4, 125.4, 126.8, 127.5, 127.6, 130.6, 131.5, 133.6, 134.2, 137.3, 138.8, 143.0, 198.3. HRMS (FAB): calcd for $(C_{56}H_{43}N_4O_1Ir_1)^+$ *m/z* 980.3061; found *m/z* 980.3064.

Reaction between Ir(ttp)$SiEt_3$ 1d and Acetophenone (2b) for Eight Days Acetophenone (0.8 mL, 500 equiv) and Ir(ttp)$SiEt_3$ (14.0 mg, 0.014 mmol) were heated at 200 °C for 8 days. A purple solid of Ir(ttp)COC_6H_5[25b] **3b** (12.0 mg, 0.0124 mmol, 89%) was isolated after column chromatography.

Reaction of Ir(ttp)C_6H_5 1e with Acetophenone (2b). Acetophenone (0.9 mL, 500 equiv) and Ir(ttp)C_6H_5 (15.5 mg, 0.016 mmol) were heated at 200 °C for 26 days. A purple solid of Ir(ttp)C_6H_5 **1b** (13.2 mg, 0.0141 mmol, 88%) was recovered. Then a purple solid of Ir(ttp)COC_6H_5[25b] **3b** (<5%) was isolated as the second fraction.

Reaction between Ir(ttp)Cl(CO) 1a and Propiophenone (2e). Propiophenone (0.9 mL, 500 equiv) and Ir(ttp)Cl(CO) (12.6 mg, 0.014 mmol) were heated at 200 °C for 12 days. A purple solid mixture of Ir(ttp)(*para*-COEt-C_6H_4) **4d** (3.2 mg, 0.0032 mmol, 23%) and Ir(ttp)(*meta*-COEt-C_6H_4) **4e** (6.4 mg, 0.0064 mmol, 46%; was isolated after column chromatography eluting with a mixture of hexane/CH_2Cl_2 (1:2). Ir(ttp)(*para*-COEt-C_6H_4) **4d**: R_f = 0.14 (hexane/CH_2Cl_2 = 1:2). ^{1}H NMR (C_6D_6, 400 MHz): δ 0.40 (t, 3 H, J = 7.6 Hz), 1.04 (d, 2 H, J = 8.8 Hz), 1.37 (q, 2 H, J = 7.2 Hz), 2.39 (s, 12 H), 5.43 (d, 2 H, J = 8.8 Hz), 7.20 (d, 4 H, J = 8.4 Hz), 7.34 (d, 4 H, J = 7.2 Hz), 7.93 (dd, 4 H, J = 2.0, 7.4 Hz), 8.15 (d, 4 H, J = 7.6 Hz), 8.83 (s, 8 H). Ir(ttp)(*meta*-COEt-C_6H_4) **4e**, R_f = 0.23 (hexane/CH_2Cl_2 = 1:2). ^{1}H NMR (C_6D_6, 400 MHz): δ 0.49 (t, 3 H, J = 7.2 Hz), 1.18 (d, 1 H, J = 8.0 Hz), 1.43 (q, 2 H, J = 7.2 Hz), 1.70 (t, 1 H, J = 1.6 Hz), 2.39 (s, 12 H), 4.76 (t, 1 H, J = 7.6 Hz), 5.66 (d, 1 H, J = 7.6 Hz), 7.22 (d, 4 H, J = 8.8 Hz), 7.34 (d, 4 H, J = 7.2 Hz), 8.08 (dd, 4 H, J = 1.6, 7.8 Hz), 8.15 (d, 4 H, J = 7.6 Hz), 8.83 (s, 8 H). HRMS (ESI): calcd for $(C_{57}H_{45}IrN_4O)^+$ *m/z* 994.3217; found *m/z* 994.321042.

Reaction between Ir(ttp)(BF_4)(CO) 1b and Propiophenone (2e). Propiophenone (0.9 mL, 500 equiv) and Ir(ttp)(BF_4)(CO) (12.9 mg, 0.013 mmol) were heated at 200 °C for 12 days. A purple solid mixture of Ir(ttp)(*para*-COEt-C_6H_4) **4d** (2.7 mg, 0.0027 mmol, 21%) and Ir(ttp)(*meta*-COEt-C_6H_4) **4e** (5.4 mg, 0.0054 mmol, 42%) was isolated after column chromatography.

Reaction between Ir(ttp)Me 1c and Propiophenone (2e). Propiophenone (1.0 mL, 500 equiv) and Ir(ttp)Me (13.5 mg, 0.015 mmol) were heated at 200 °C for 12 days. A purple solid of Ir(ttp)Me **1c** (6.6 mg, 0.0075 mmol, 50%) was recovered after column chromatography eluting with a mixture of hexane/CH_2Cl_2 (2:1). Then changed the solvent to hexane/CH_2Cl_2 (1:2), and a purple solid mixture of Ir(ttp)(*para*-COEt-C_6H_4) **4d** (1.0 mg, 0.0010 mmol, 7%) and Ir(ttp)(*meta*-COEt-C_6H_4) **4e** (2.0 mg, 0.0020 mmol, 14%) was isolated after column chromatography.

Reaction between Ir(ttp)$SiEt_3$ 1d and Propiophenone (2e). Propiophenone (1.0 mL, 500 equiv) and Ir(ttp)$SiEt_3$ (14.6 mg, 0.015 mmol) were heated at 200 °C for 17 days. A purple solid mixture of Ir(ttp)(*para*-COEt-C_6H_4) **4d** (3.3 mg, 0.0033 mmol, 22%) and Ir(ttp)(*meta*-COEt-C_6H_4) **4e** (6.6 mg, 0.0066 mmol, 44%) was isolated after column chromatography.

Reaction between Ir(ttp)Cl(CO) 1a and Acetone (2f). Acetone (0.5 mL, 500 equiv) and Ir(ttp)Cl(CO) (12.2 mg, 0.013 mmol) were heated at 200 °C for 10 days. A purple solid mixture of Ir(ttp)Me **1c** and Ir(ttp)COMe[26] **3e** was isolated in trace amount (<5%). Most Ir(ttp)Cl(CO) was still remained unreacted, while it was decomposed after column chromatography, and could not be recovered.

Reaction between Ir(ttp)(BF_4)(CO) 1b and Acetone (2f). Acetone (0.6 mL, 500 equiv) and Ir(ttp)(BF_4)(CO) (14.9 mg, 0.015 mmol) were heated at 200 °C for 1 day. A purple solid mixture of Ir(ttp)Me **1c** (9.7 mg, 0.0111 mmol, 74%) and Ir(ttp)COMe[26] **3e** (1.5 mg, 0.0016 mmol, 11%) was isolated after column chromatography eluting with a mixture of hexane/CH_2Cl_2 (2:1). Ir(ttp)COMe **3e**, R_f = 0.35 (hexane/CH_2Cl_2 = 1:2). ^1H NMR ($CDCl_3$, 300 MHz): δ -2.82 (s, 3 H), 2.69 (s, 12 H), 7.53 (d, 8 H, J = 6.0 Hz), 8.03 (d, 8 H, J = 6.0 Hz), 8.68 (s, 8 H).

Reaction between Ir(ttp)Me 1c and Acetone (2f). Acetone (0.5 mL, 500 equiv) and Ir(ttp)Me (12.8 mg, 0.015 mmol) were heated at 200 °C for 5 days. A purple solid of Ir(ttp)Me **1c** (10.5 mg, 0.0120 mmol, 80%) was recovered after column chromatography.

Reaction between Ir(ttp)$SiEt_3$ 1d and Acetone (2f). Acetone (0.5 mL, 500 equiv) and Ir(ttp)$SiEt_3$ (12.2 mg, 0.012 mmol) were heated at 200 °C for 4 days. A purple solid of Ir(ttp)CH_2COMe **4f** (3.8 mg, 0.0041 mmol, 34%) was isolated after column chromatography eluting with a mixture of hexane/CH_2Cl_2 (1:2). Ir(ttp)CH_2COMe **4f**, R_f = 0.23 (hexane/CH_2Cl_2 = 1:2). ^1H NMR ($CDCl_3$, 300 MHz): δ -4.32 (s, 2 H), -1.69 (s, 3 H), 2.69 (s, 12 H), 7.51 ~ 7.54 (m, 8 H), 8.00 ~ 8.05 (m, 8 H), 8.57 (s, 8 H). ^{13}C NMR ($CDCl_3$, 400 MHz): δ -12.8, 21.7, 29.9, 123.9, 127.5, 127.7, 131.7, 133.3, 134.2, 137.4, 138.7, 143.2, 208.0. HRMS (FAB): calcd for $(C_{51}H_{41}N_4O_1Ir_1)^+$ *m/z* 918.2904; found *m/z* 918.289941.

Reaction between Ir(ttp)(BF_4)(CO) 1b and Acetone-d_6 (2f'). Acetone-d_6 (0.5 mL, 500 equiv) and Ir(ttp)(BF_4)(CO) (12.4 mg, 0.013 mmol) were heated at 200 °C for 1 day. A purple solid mixture of Ir(ttp-β-d_8)CD_3 **1c'**-β-d_8 and Ir(ttp-β-d_8)$COCD_3$ **3e'**-β-d_8 (6.4 mg, ca 50%) was obtained after column chromatography.

Reaction between Ir(ttp)(BF_4)(CO) 1b and 2-Butanone (2h). 2-Butanone (0.6 mL, 500 equiv) and Ir(ttp)(BF_4)(CO) (14.0 mg, 0.014 mmol) were heated at 200 °C for 4 days. A purple solid mixture of Ir(ttp)Me **1c** (1.6 mg, 0.0018 mmol, 13%), Ir(ttp)COMe[26] **3e** (3.0 mg, 0.0033 mmol, 24%) and Ir(ttp)Et[45] **3f** (3.5 mg, 0.0039 mmol, 28%) was isolated after column chromatography. Ir(ttp)Et **3f**, R_f = 0.25 (hexane/CH_2Cl_2 = 2:1). ^1H NMR (C_6D_6, 400 MHz): δ -5.20 (q, 2 H, J = 7.2 Hz), -4.27 (t, 3 H, J = 7.2 Hz), 2.41 (s, 12 H), 7.22 (d, 4 H, J = 7.6 Hz), 7.35 (d, 4 H, J = 7.6 Hz), 7.99 (dd, 4 H, J = 2.0, 7.6 Hz), 8.19 (dd, 4 H, J = 1.6, 7.8 Hz), 8.76 (s, 8 H).

Reaction between Ir(ttp)(BF_4)(CO) 1b and 3-Methyl-2-butanone (2i). 3-Methyl-2-butanone (0.7 mL, 500 equiv) and Ir(ttp)(BF_4)(CO) (12.0 mg, 0.012 mmol) were heated at 200 °C for 4 days. A purple solid of Ir(ttp)Me **1c** (7.3 mg, 0.0083 mmol, 69%) was isolated after column chromatography.

Reaction between Ir(ttp)(BF_4)(CO) 1b and Acetylacetone (2j). Aectylacetone (0.6 mL, 500 equiv) and Ir(ttp)(BF_4)(CO) (11.8 mg, 0.012 mmol) were heated at 200 °C for 3 days. A purple solid mixture of Ir(ttp)Me **1c** (1.6 mg, 0.0018 mmol, 15%) and Ir(ttp)COMe[26] **3e** (5.4 mg, 0.0060 mmol, 50%) was isolated after column chromatography.

Reaction between Ir(ttp)(BF_4)(CO) 1b and 3-Pentanone (2k). 3-Pentanone (0.7 mL, 500 equiv) and Ir(ttp)(BF_4)(CO) (13.0 mg, 0.013 mmol) were heated at 200 °C for 4 days. A purple solid mixture of Ir(ttp)Et[45] **3f** (2.2 mg, 0.0024 mmol, 19%), Ir(ttp)COEt[25b] **3g** (1.3 mg, 0.0014 mmol, 11%) and Ir(ttp)Me **1c** (<5%), Ir(ttp)COMe[26] **3e** (<5%) was isolated after column chromatography. Ir(ttp)COEt **3g**, R_f = 0.66 (hexane/CH_2Cl_2 = 1:2). ^{1}H NMR ($CDCl_3$, 300 MHz): δ -3.20 (q, 2 H, J = 7.2 Hz), -1.71 (t, 3 H, J = 7.2 Hz), 2.69 (s, 12 H), 7.52 (d, 8 H, J = 8.1 Hz), 8.02 (d, 8 H, J = 7.8 Hz), 8.67 (s, 8 H).

Reaction between Ir(ttp)(BF_4)(CO) 1b and 2,4-Dimethyl-3-pentanone (2l). 2,4-Dimethyl-3-pentanone (0.9 mL, 500 equiv) and Ir(ttp)(BF_4)(CO) (12.3 mg, 0.013 mmol) were heated at 200 °C for 4 days. A purple solid mixture of unknowns (1.1 mg, ca 9%) was isolated after column chromatography. No CCA products were observed.

Reaction between Ir(ttp)Cl(CO) 1a and Acetophenone (2b) at a 200 °C for Five Days. Acetophenone (0.8 mL, 500 equiv) and Ir(ttp)Cl(CO) (13.2 mg, 0.014 mmol) were heated at 200 °C for 5 days. A purple solid of Ir(ttp)COC_6H_5[25b] **3b** (2.2 mg, 0.0023 mmol, 16%) was isolated after column chromatography eluting with a mixture

of hexane/CH_2Cl_2 (3:1). Then changed the solvent to hexane/CH_2Cl_2 (1:2), and a purple solid mixture of Ir(ttp)(*para*-COMe-C_6H_4)[26] **4b** (1.4 mg, 0.0014 mmol, 10%) and Ir(ttp)(*meta*-COMe-C_6H_4)[26] **4c** (2.8 mg, 0.0028 mmol, 20%) was isolated. According to TLC analysis, Ir(ttp)Cl(CO) **1a** was still remained unreacted, while it was decomposed in column chromatography and could not be recovered.

Reaction between Ir(ttp)(BF_4)(CO) 1b and Acetophenone (2b) at a 200 °C for Four Hours. Acetophenone (0.8 mL, 500 equiv) and Ir(ttp)(BF_4)(CO) (12.6 mg, 0.013 mmol) were heated at 200 °C for 4 hours. A purple solid of Ir(ttp)COC_6H_5[25b] **3b** (1.9 mg, 0.0019 mmol, 15%) was isolated after column chromatography eluting with a mixture of hexane/CH_2Cl_2 (3 : 1). Then changed the solvent to hexane/CH_2Cl_2 (1:2), and a purple solid mixture of Ir(ttp)(*para*-COMe-C_6H_4)[26] **4b** (1.0 mg, 0.0010 mmol, 8%), Ir(ttp)(*meta*-COMe-C_6H_4)[26] **4c** (2.0 mg, 0.0020 mmol, 16%) and Ir(ttp)CH_2CO C_6H_5 **4a** (<5%) was isolated.

Reaction between Ir(ttp)Cl(CO) 1a and Acetophenone (2b) at a 120 °C. Acetophenone (0.8 mL, 500 equiv) and Ir(ttp)Cl(CO) (12.9 mg, 0.014 mmol) were heated at 120 °C for 5 days. A purple solid Ir(ttp)$CH_2COC_6H_4$ **4a** (1.5 mg, 0.0015 mmol, 11%) was isolated after column chromatography. Most of Ir(ttp)Cl(CO) **1a** still remained unreacted, while it was decomposed in column chromatography and could not be recovered.

Reaction between Ir(ttp)$CH_2COC_6H_5$ 4a and Acetophenone (2b) for Fifteen Days. Acetophenone (0.8 mL, 500 equiv) and Ir(ttp)$CH_2COC_6H_5$ (12.4 mg, 0.013 mmol) were heated at 200 °C for 15 days. The crude product was purified by column chromatography eluting with a mixture of hexane/CH_2Cl_2 (3:1), and a purple solid of Ir(ttp)COC_6H_5[25b] **3b** (2.7 mg, 0.0028 mmol, 21%) was isolated. Then changed the solvent to hexane/CH_2Cl_2 (1:2), and a purple solid mixture of Ir(ttp)(*para*-COMe-

C_6H_4)[26] **4b** (2.7 mg, 0.0028 mmol, 21%) and Ir(ttp)(*meta*-COMe-C_6H_4)[26] **4c** (5.4 mg, 0.0055 mmol, 42%) was isolated.

Reaction between Ir(ttp)$CH_2COC_6H_5$ 4a and Acetophenone (2b) for Twenty Six Days. Acetophenone (0.9 mL, 500 equiv) and Ir(ttp)$CH_2COC_6H_5$ (14.7 mg, 0.015 mmol) were heated at 200 °C for 26 days. The crude product was purified by column chromatography eluting with a mixture of hexane/CH_2Cl_2 (3:1), and a purple solid of Ir(ttp)COC_6H_5[25b] **3b** (10.8 mg, 0.0112 mmol, 75%) was isolated. Then changed the solvent to hexane/CH_2Cl_2 (1:2), and a purple solid mixture of Ir(t:p)(*para*-COMe-C_6H_4)[26] **4b** (1.2 mg, 0.0012 mmol, 8%) and Ir(ttp)(*meta*-COMe-C_6H_4)[26] **4c** (2.4 mg, 0.0024 mmol, 16%) was isolated.

Reaction between Ir(ttp)H 1c and Acetophenone (2b) for One Day. Acetophenone (0.9 mL, 500 equiv) and Ir(ttp)H (12.7 mg, 0.015 mmol) were heated at 200 °C for 1 day. The crude product was purified by column chromatography eluting with a mixture of hexane/CH_2Cl_2 (1:2), and a purple solid of Ir(ttp)$CH_2COC_6H_5$ **4a** (10.0 mg, 0.0102 mmol, 68%) was isolated.

Reaction between Ir(ttp)H 1c and Acetophenone (2b) for Fifteen Days. Acetophenone (1.0 mL, 500 equiv) and Ir(ttp)H (15.3 mg, 0.018 mmol) were heated at 200 °C for 15 days. The crude product was purified by column chromatography eluting with a mixture of hexane/CH_2Cl_2 (3:1), and a purple solid of Ir(ttp)COC_6H_5[25b] **3b** (4.2 mg, 0.0043 mmol, 24%) was isolated. Then changed the solvent to hexane/CH_2Cl_2 (1:2), and a purple solid mixture of Ir(ttp)$CH_2COC_6H_5$ **4a** (7.4 mg, 0.0075 mmol, 42%), Ir(ttp)(*para*-COMe-C_6H_4)[26] **4b** (1.4 mg, 0.0014 mmol, 8%) and Ir(ttp)(*meta*-COMe- C_6H_4)[26] **4c** (2.8 mg, 0.0029 mmol, 16%) was isolated.

Reaction between Ir(ttp)H 1c and Acetophenone (2b) for Twenty Six Days. Acetophenone (1.0 mL, 500 equiv) and Ir(ttp)H (15.2 mg, 0.018 mmol) were heated

at 200 °C for 26 days. The crude product was purified by column chromatography eluting with a mixture of hexane/CH_2Cl_2 (3:1), and a purple solid of Ir(ttp)COC_6H_5[25b] **3b** (12.6 mg, 0.0130 mmol, 72%) was isolated. Then changed the solvent to hexane/CH_2Cl_2 (1:2), and a purple solid mixture of Ir(ttp)$CH_2COC_6H_5$ **4a** (1.6 mg, 0.0016 mmol, 9%), Ir(ttp)(*para*-COMe-C_6H_4)[26] **4b** (0.9 mg, 0.0009 mmol, 5%) and Ir(ttp)(*meta*-COMe- C_6H_4)[26] **4c** (1.8 mg, 0.0018 mmol, 10%) was isolated.

Aldol Condensation of Acetophenone (2b) Catalyzed by Ir(ttp)Cl(CO) 1a. Acetophenone (0.8 mL) was added to Ir(ttp)Cl(CO) (13.5 mg, 0.0015 mmol), and the mixture was degassed by the freeze-pump-thaw method (3 cycles). Then the mixture was heated at 200 °C for 1 day. The aldol condensation products **5a-b**[32] were observed in 0.5% and 2% based on **2b**, while 250% and 1000% based on **1a**, respectively, according ^{1}H NMR of crude reaction mixture by using $Si(SiMe_3)_4$ as internal standard. In addition, Ir(ttp)$CH_2COC_6H_5$ **4a**, Ir(ttp)(*para*-COMe-C_6H_4)[26] **4b** and Ir(ttp)(*meta*-COMe-C_6H_4)[26] **4c** were observed according to ^{1}H NMR of the crude reaction mixture, and most of Ir(ttp)Cl(CO) **1a** was still remained unreacted.

Reaction between Ir(ttp)C_6H_5 1e and Acetophenone (2b) with the Addition of Water. Acetophenone (0.9 mL, 500 equiv) and H_2O (29 μL, 1.60 mmol, 100 equiv) were added to Ir(ttp)C_6H_5 (15.1 mg, 0.016 mmol), and the mixture was degassed by the freeze-pump-thaw method (3 cycles). Then the mixture was heated at 200 °C for 28 days. The crude product was purified by column chromatography on alumina eluting with a mixture of hexane/CH_2Cl_2 (3:1), and purple solid of Ir(ttp)C_6H_5 **1b** (12.8 mg, 0.0136 mmol, 85%) was recovered. Then another purple solid of Ir(ttp)COC_6H_5[25b] **3b** (1.8 mg, 0.0019 mmol, 12%) was isolated as the second fraction.

Reaction between Ir(ttp)C_6H_5 1e and Acetophenone (2b) with the Addition of HCl. Acetophenone (1.0 mL, 500 equiv) and HCl (15 μL, 37%, 10 equiv) were added

to Ir(ttp)C_6H_5 (16.4 mg, 0.017 mmol), and the mixture was degassed by the freeze-pump-thaw method (3 cycles). Then the mixture was heated at 200 °C for 15 hours. The reaction mixture was changed to green in color and the Ir(ttp)(C_6H_5) **1e** was decomposed.

Reaction between Ir(ttp)CO(4-Me-C_6H_4) 3c and Acetophenone (2b). Acetophenone (1.0 mL, 500 equiv) was added to Ir(ttp)CO(4-Me-C_6H_4) (16.2 mg, 0.016 mmol), and the mixture was degassed by the freeze-pump-thaw method (3 cycles). Then the mixture was heated at 200 °C for 15 days. The crude product was purified by column chromatography on alumina eluting with a mixture of hexane/CH_2Cl_2 (3:1), and a purple solid mixture of Ir(ttp)COC_6H_5 **3b** (12.4 mg, 0.0128 mmol, 80%) and Ir(ttp)CO(4-Me-C_6H_4) **3c** (2.7 mg, 0.0027 mmol, 17%) was isolated.

Reaction between Ir(ttp)Me 1c and Acetone-d_6 (2f') in a Sealed-NMR Tube. Acetone-d_6 (0.4 mL, 1000 equiv) was added to Ir(ttp)Me (4.7 mg, 0.0054 mmol) in a NMR tube with a rotaflo stopper, and the mixture was degassed by the freeze-pump-thaw method (3 cycles), then the NMR-tube was flamed-sealed under vacuum. The mixture was heated at 200 °C and was monitored with ^{1}H NMR spectroscopy. No Ir(ttp)CD_3 **1c'** was observed after 34 days and a purple solid of Ir(ttp)Me **3d** (3.4 mg, 0.0039 mmol, 72%) was recovered after column chromatography.

Reaction of Ir(ttp)$CH_2COC_6H_5$ 4a in Benzene-d_6 with the Addition of water in a Sealed-NMR Tube. Benzene-d_6 (0.5 mL) and H_2O (8 μL, 0.44 mmol, 100 equiv) were added to Ir(ttp)$CH_2COC_6H_5$ (4.3 mg, 0.0044 mmol) in a NMR tube with a rotaflo stopper, and the mixture was degassed by the freeze-pump-thaw method (3 cycles), then the NMR tube was flame-sealed under vacuum. The mixture was heated

at 200 °C and was monitored with ^{1}H NMR spectroscopy with the NMR yields measured using the residual benzene signal as the internal standard. Ir(ttp)$CH_2COC_6H_5$ **4a** consumed completely after 3 days, and Ir(ttp)H **1f** was formed as the major product (20%), as well as the decomposition products (ca 80%). According to the integration of ^{1}H NMR and GC-MS with naphthalene as the internal standard, the yield of acetophenone was 20%.

Reaction of Ir(ttp)(4-F-C_6H_4) 1e' in Benzene-d_6 with the Addition of HCl in a Sealed-NMR Tube Benzene-d_6 (0.5 mL) and HCl (7 μL, 37%, 20 equiv) were added to Ir(ttp)(4-F-C_6H_4) (4.1 mg, 0.0043 mmol) in a NMR tube with a rotaflo stopper, and the mixture was degassed by the freeze-pump-thaw method (3 cycles), then the NMR tube was flame-sealed under vacuum. The mixture was heated at 200 °C and was monitored with ^{1}H NMR spectroscopy. Iridium species were decomposed after 13.5 hours and fluorobenzene was observed in 90% yield according to GC-MS analysis by using naphthalene as the internal standard.

Reaction of Ir(ttp)Me 1c in Benzene-d_6 with the Addition of water in a Sealed-NMR Tube. Benzene-d_6 (0.5 mL) and H_2O (11 μL, 0.63 mmol, 100 equiv) were added to Ir(ttp)Me (5.5 mg, 0.0063 mmol) in a NMR tube with a rotaflo stopper, and the mixture was degassed by the freeze-pump-thaw method (3 cycles), then the NMR tube was flame-sealed under vacuum. The mixture was heated at 200 °C and was monitored with ^{1}H NMR spectroscopy with the NMR measured using the residual benzene signal as the internal standard. Ir(ttp)H was formed in trace amount (< 5%) after 6 days, and Ir(ttp)Me (> 90%) was still remained unreacted.

Reaction of Ir(ttp)$SiEt_3$ 1d in Benzene-d_6 with the Addition of water in a Sealed-NMR Tube. Benzene-d_6 (0.5 mL) and H_2O (13 μL, 0.70 mmol, 100 equiv) were added to Ir(ttp)$SiEt_3$ (6.8 mg, 0.0070 mmol) in a NMR tube with a rotaflo

stopper, and the mixture was degassed by the freeze-pump-thaw method (3 cycles), then the NMR tube was flame-sealed under vacuum. The mixture was heated at 200 °C and was monitored with ^{1}H NMR spectroscopy with the NMR measured using the residual benzene signal as the internal standard. Ir(ttp)H was formed (10%) after 4 days with the co-formation of $OHSiEt_3$ (5%), and $Ir(ttp)SiEt_3$ (80%) was still remained unreacted.

References

(1) Anslyn, E. V.; Dougherty, D. A. *Modern Physical Organic Chemistry*; Sausalito, California, University Science Book, 2006.

(2) Smith, M. B.; March, J. *March's Advanced Organic Chemistry; Reactions, Mechanisms, Structure*, 5th Ed.; Wiley-Interscience: New York, 2001.

(3) Luo, Y.-R. *Handbook of Bond Dissociation Energies in Organic Compounds*; CRC Press: Boca Raton, FL, 2003.

(4) *http://evans.harvard.edu/pdf/evans_pKa_table.pdf.* Accessed on 27 November 2009.

(5) (a) Jun, C.-H. *Chem. Soc. Rev.* **2004**, *33*, 610-618. (b) Winter, C.; Krause, N. *Angew. Chem., Int. Ed.* **2009**, *48*, 2460-2462. (c) Nečas, D.; Kotora, M. *Curr. Org. Chem.* **2007**, *11*, 1566-1591. (d) Rybtchinski, B.; Milstein, D. *Angew. Chem., Int. Ed.* **1999**, *38*, 870-883. (e) Park, Y. J.; Park, J.-W.; Jun, C.-H. *Acc. Chem. Res.* **2008**, *41*, 222-234. (f) Jun, C.-H.; Moon, C. W.; Lee, D.-Y. *Chem. Eur. J.* **2002**, *8*, 2422-2428.

(6) (a) Huffman, M. A.; Liebeskind, L. S. *J. Am. Chem. Soc.* **1991**, *113*, 2771-2772. (b) Murakami, M.; Ashida, S.; Matsuda, T. *J. Am. Chem. Soc.* **2005**, *127*, 6932-6933.

(7) Murakami, M.; Ashida, S.; Matsuda, T. *Tetrahedron* **2006**, *62*, 7540-7546.

(8) Murakami, M.; Tsuruta, T.; Ito, Y. *Angew. Chem., Int. Ed.* **2000**, *39*, 2484-2486.

(9) (a) Murakami, M.; Amii, H.; Shigeto, K.; Ito, Y. *J. Am. Chem. Soc.* **1996**, *118*, 8285-8290. (b) Çelenligil-Çetin, R.; Watson, L. A.; Guo, C.; Foxman, B. M.; Ozerov, O. V. *Organometallics* **2005**, *24*, 186-189.

(10) Murakami, M.; Takahashi, K.; Amii, H.; Ito, Y. *J. Am. Chem. Soc.* **1997**, *119*, 9307-9308.

(11) (a) Matsuda, T.; Makino, M.; Murakami, M. *Org. Lett.* **2004**, *6*, 1257-1259. (b) Matsuda, T.; Makino, M.; Murakami, M. *Bull. Chem. Soc. Jpn.* **2005**, *78*, 1528-1533.

(12) Murakami, M.; Ashida, S. *Chem. Commun.* **2006**, 4599-4601.

(13) Kondo, T.; Niimi, M.; Nomura, M.; Wada, K.; Mitsudo, T. *Tetrahedron Lett.* **2007**, *48*, 2837-2839.

(14) Kondo, T.; Taguchi, Y.; Kaneko, Y.; Niimi, M.; Mitsudo, T. *Angew. Chem., Int. Ed.* **2004**, *43*, 5369-5372.

(15) Kondo, T.; Nakamura, A.; Okada, T.; Suzuki, N.; Wada, K.; Mitsudo, T. *J. Am. Chem. Soc.* **2000**, *122*, 6319-6320.

(16) Yamamoto, Y.; Kuwabara, S.; Hayashi, H.; Nishiyama, H. *Adv. Synth. Catal.* **2006**, *348*, 2493-2500.

(17) Kondo, T.; Kaneko, Y.; Taguchi, Y.; Nakamura, A.; Okada, T.; Shiotsuki, M.; Ura, Y.; Wada, K.; Mitsudo, T. *J. Am. Chem. Soc.* **2002**, *124*, 6824-6825.

(18) (a) Suggs, J. W.; Jun, C.-H. *J. Am. Chem. Soc.* **1984**, *106*, 3054-3056. (b) Suggs, J. W.; Jun, C.-H. *J. Am. Chem. Soc.* **1986**, *108*, 4679-4681.

(19) Ahn, J.-A.; Chang, D.-H.; Park, Y. J.; Yon, Y. R.; Loupy, A.; Jun, C.-H. *Adv. Synth. Catal.* **2006**, *348*, 55-58.

(20) Wentzel, M. T.; Reddy, V. J.; Hyster, T. K.; Douglas, C. J. *Angew. Chem., Int. Ed.*

2009, *48*, 6121-6123.

(21) Dreis, A. M.; Douglas, C. J. *J. Am. Chem. Soc.* **2009**, *131*, 412-413.

(22) Taw, F. L.; Mueller, A. H.; Bergman, R. G.; Brookhart, M. *J. Am. Chem. Soc.* **2003**, *125*, 9808-9813.

(23) Anstey, M. R.; Yung, C. M.; Du, J.; Bergman, R. G. *J. Am. Chem. Soc.* **2007**, *129*, 776-777.

(24) Direct σ-bond metathesis is unprecedented, see: Soulivong, D.; Copéret, C.; Thivolle-Cazat, J.; Basset, J.-M.; Maunders, B. M.; Pardy, R. B. A.; Sunley, G. J. *Angew. Chem., Int. Ed.* **2004**, *43*, 5366-5369.

(25) (a) Chan, K. S.; Lau, C. M. *Organometallics* **2006**, *25*, 260-265. (b) Song, X.; Chan, K. S. *Organometallics* **2007**, *26*, 965-970.

(26) Song, X. *M. Phil. Thesis,* The Chinese University of Hong Kong, 2007.

(27) (a) Jones, W. D.; Feher, F. J. *J. Am. Chem. Soc.* **1982**, *104*, 4240-4242. (b) Clot, E.; Mégret, C.; Eisenstein, O.; Perutz, R. N. *J. Am. Chem. Soc.* **2006**, *128*, 8350-8357.

(28) (a) Stolzenberg, A. M.; Laliberte, M. A. *J. Org. Chem.* **1987**, *52*, 1022-1027. (b) Hickman, D. L.; Goff, H. M. *J. Am. Chem. Soc.* **1984**, *106*, 5013-5014. (c) Godziela, G. M.; Kramer, S. K.; Goff, H. M. *Inorg. Chem.* **1986**, *25*, 4286-4288.

(29) Cheung, C. W.; Chan, K. S. *Organometallics* **2008**, *27*, 3043-3055.

(30) Wayland, B. B.; Van Voorhees, S. L.; Wilker, C. *Inorg. Chem.* **1986**, *25*, 4039-4042.

(31) Pankratov, A. N. *J. Mol. Struct. Theochem.* **2000**, *507*, 239-244.

(32) For the Lewis acid catalyzed aldol condensation of acetophenone via the $Rh(oep)CH_2COR$ intermediate from a more reactive $Rh(oep)ClO_4$: (a) Aoyama,

Y.; Yoshida, T.; Ogoshi, H. *Tetrahedron Lett.* **1985**, *26*, 6107-6108. (b) Aoyama, Y.; Tanaka, Y.; Yoshida, T.; Toi, H.; Ogoshi, H. *J. Organomet. Chem.* **1987**, *329*, 251-266.

(33) Cheung, C. W. Unpublished Results, **2009**.

(34) For Rh(oep)OH, see: (a) Del Rossi, K. J.; Wayland, B. B. *J. Am. Chem. Soc.* **1985**, *107*, 7941-7944. For Rh(tspp)OH, see: (b) Fu, X.; Wayland, B. B. *J. Am. Chem. Soc.* **2004**, *126*, 2623-2631. (c) Fu, X.; Li, S.; Wayland, B. B. *J. Am. Chem. Soc.* **2006**, *128*, 8947-8954. For $Ir(acac)_2OH$, see: (d) Te::n, W. J., III; Young, K. J. H.; Oxgaard, J.; Nielsen, R. J.; Goddard, W. A., III; Periana, R. A. *Organometallics* **2006**, *25*, 5173-5175.

(35) Analogous disproportionation reaction of Rh^{II}, see: (a) In excess MeOH, see: Li, S.; Cui, W.; Wayland, B. B. *Chem. Commun.* **2007**, 4024-4025. (b) By strong ligand, see: Wayland, B. B.; Balkus, K. J., Jr.; Farnos, M. D. *Organometallics* **1989**, *8*, 950-955. (c) Wayland, B. B.; Sherry, A. E.; Bunn, A. G. *J. Am. Chem. Soc.* **1993**, *115*, 7675-7684.

(36) (a) Nelson, A. P.; DiMagno, S. G. *J. Am. Chem. Soc.* **2000**, *122*, 8569-8570. (b) Sanford, M. S.; Groves, J. T. *Angew. Chem., Int. Ed.* **2004**, *43*, 588-590. (c) Ogoshi, H.; Setsune, J.-I.; Yoshida, Z.-I. *J. Organomet. Chem.* **1978**, *159*, 317-328.

(37) Smith, K. M. *Porphyrins and Metalloporphyrins*, Ed.; Elservier Scientific Pub. Co.: New York, 1975.

(38) Wayland, B. B. Temple University, Philadelphia, PA. Personal communication, 2007.

(39) From the literature report by Wayland *et al.*, the bond strength of Rh(TMPS)OD is slighter weaker than Rh(TMPS)D by 1.8 kcal mol^{-1}, therefore, we assumed

that the BDE of Ir(ttp)OH was similar to Ir(ttp)H. See: Fu, X.; Li, S.; Wayland, B. B. *Inorg. Chem.* **2006**, *45*, 9884-9889.

(40) (a) Hu, X.; Cossairt, B. M.; Brunschwig, B. S.; Lewis, N. S.; Peters, J. C. *Chem. Commun.* **2005**, 4723-4725. (b) Kosuke, I. *Acid–Base Dissociation Constants in Dipolar Aprotic Solvents*, Blackwell Scientific Publications, Oxford, 1990.

(41) *http://www.nanotech.wisc.edu/CNT_LABS/MSDS/Acids/MSDS%20Fluoroboric%20Acid.htm.* Accessed on 26 November 27, 2009.

(42) Lide, D. R., Ed. *CRC Handbook of Chemistry and Physics*, 84th ed., CRC Press: Boca Raton, FL, 2003.

(43) Guthrie, J. P.; Cossar, J.; Klym, A. *Can. J. Chem.* **1987**, *65*, 2154-2159.

(44) Lee, Y.; Seomoon, D.; Kim, S.; Han, H.; Chang, S.; Lee, P. H. *J. Org. Chem.* **2004**, *69*, 1741-1743.

(45) Yeung, S. K. *Ph.D. Thesis*, The Chinese University of Hong Kong, 2005.

Appendix

Appendix I (Chapter 2)

I.I Crystal Data for Iridium Porphyrin Silyls 3a-c and 3g

Table 1 Details of Data Collection and Processing Parameters for Ir(ttp)$SiEt_3$, Ir(ttp)$Si(OEt)_3$, Ir(ttp)$SiBnMe_2$ and Ir(ttp)$SiPh_2Me$

	Ir(ttp)$SiEt_3$ **3a**	Ir(ttp)$Si(OEt)_3$ **3b**	Ir(ttp)$SiBnMe_2$ **3c**	Ir(ttp)$SiPh_2Me$ **3g**
empirical formula	$C_{54}H_{51}IrN_4Si$	$C_{54}H_{51}IrN_4O_3Si$	$C_{57}H_{49}IrN_4Si \cdot 1/4CH_2Cl_2$	$C_{61}H_{49}IrN_4Si$
cryst syst	Monoclinic	Triclinic	Monoclinic	Orthorhombic
space group	$P2_1/c$	$P\bar{1}$	$P2_1/c$	Pnma
Fw	976.28	1024.28	1031.52	1058.33
a (Å)	14.3493 (5)	11.743 (6)	13.780 (2)	16.2845 (5)
b (Å)	23.2821 (7)	12.886 (6)	51.702 (9)	14.3385 (4)
c (Å)	15.6998 (4)	16.755 (8)	15.311 (3)	22.3058 (7)
α (deg)	90	83.320 (10)	90	90

	Ir(ttp)$SiEt_3$ **3a**	Ir(ttp)$Si(OEt)_3$ **3b**	Ir(ttp)$SiBnMe_2$ **3c**	Ir(ttp)$SiPh_2Me$ **3g**
β (deg)	94.6240 (10)	84.748 (9)	97.874 (4)	90
γ (deg)	90	85.872 (10)	90	90
Z	4	2	8	4
D_{calc} (mg/m^3)	1.240	1.359	1.268	1.350
absorp coeff (mm^{-1})	2.612	2.736	2.555	2.628
V (Å^3)	5227.9 (3)	2503 (2)	10806 (3)	5208.3(3)
F (000)	1876	1036	4164	2136
cryst size (mm)	0.50 x 0.40 x 0.30	0.50 x 0.40 x 0.30	0.50 x 0.40 x 0.30	0.50 x 0.40 x 0.30
reflcns collcd	54561	13356	57969	46320
absorp corr	Multiscan	SADABS	SADABS	Multiscan
max. and min. transmn	0.7456 and 0.5073	1.0000 and 0.480014	1.0000 and 0.500568	1.0000 and 0.498708
no. of data / restraints / params	9211 / 9 / 541	8740 / 16 / 577	19016 / 156 / 1216	6452 / 310 / 574
goodness-of-fit on F^2	1.087	1.072	1.138	1.073
refinement method	Full-matrix least-squares on F^2			

	Ir(ttp)SiEt$_3$ **3a**	Ir(ttp)Si(OEt)$_3$ **3b**	Ir(ttp)SiBnMe$_2$ **3c**	Ir(ttp)SiPh$_2$Me **3g**
final R_1 [a] / wR_2 [b] [I>2σ(I)]	0.0338 / 0.899	0.0545 / 0.1436	0.0986 / 0.2632	0.0770 / 0.2474
final R_1 [a] / wR_2 [b] (all data)	0.0477 / 0.0957	0.0677 / 0.1555	0.1371 / 0.2851	0.1002 / 0.2586
w_1/w_2 [c]	0.059800 / 0.018300	0.1018 / 0.8042	0.1040 / 232.8366	0.1290 / 65.9459

[a] $R_1 = \sum(\| F_0 \| - \| F_c \|) / \sum \| F_0 \|$. [b] $wR_2 = \{\sum[w(F_0^2 - F_c^2)^2] / \sum[w(F_0^2)^2]\}^{1/2}$.

[c] Weighting scheme $w^{-1} = \sigma^2(F_0^2) + (w_1 P)^2 + w_2 P$, where $P = (F_0^2 + 2F_c^2)/3$.

I.II ^{1}H and ^{13}C NMR Spectra of $Ir(ttp)SiR_3$ (3a-g)

Table 2 List of ^{1}H and ^{13}C NMR Spectra of $Ir(ttp)SiR_3$ (3a-g)

^{1}H NMR of Ir(ttp)SiEt$_3$ **3a**

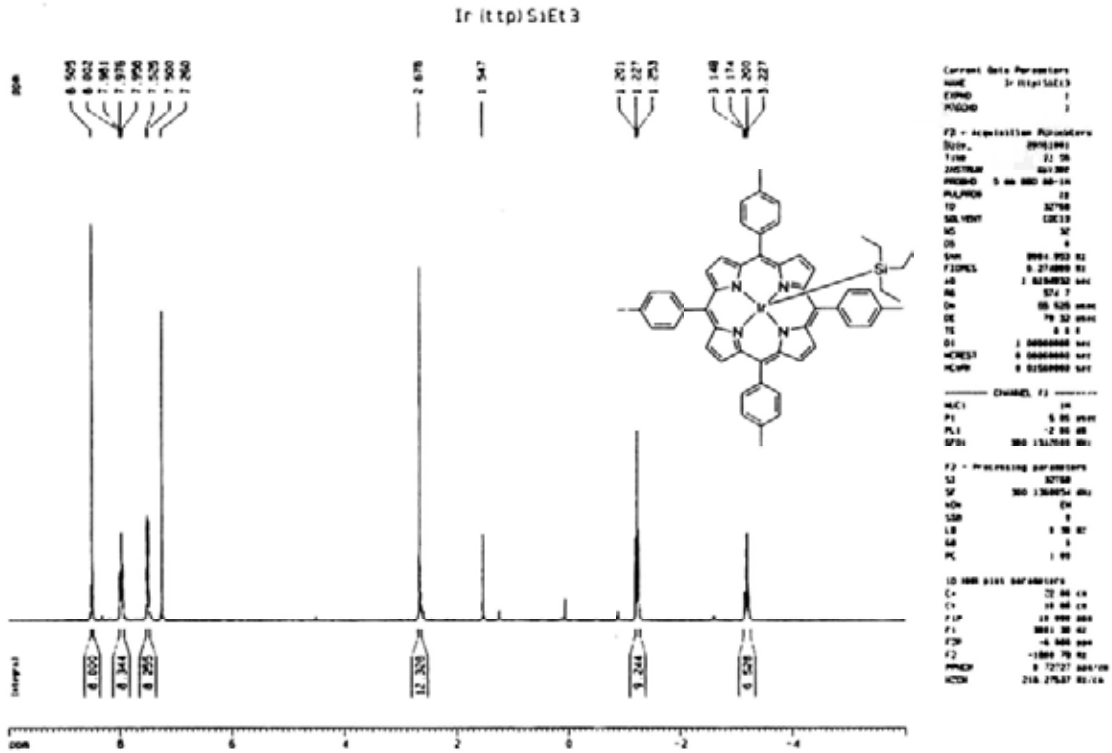

^{13}C NMR of Ir(ttp)SiEt$_3$ **3a**

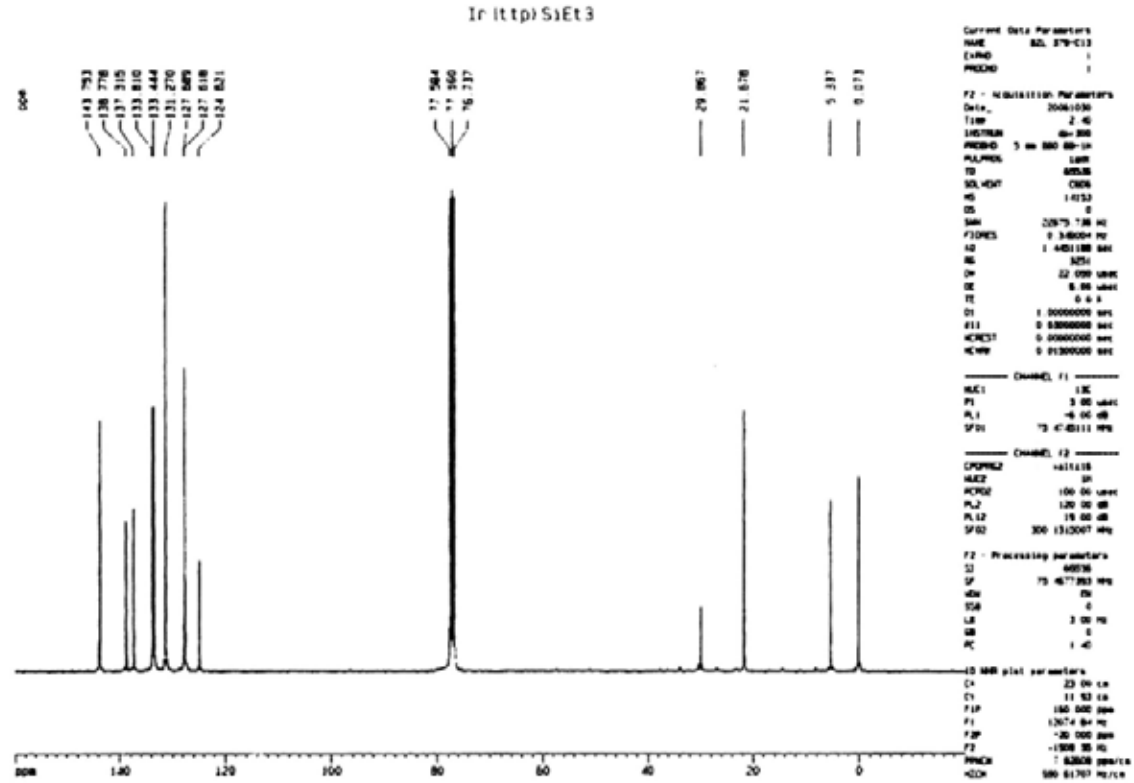

^{1}H NMR of Ir(ttp)Si(OEt)$_3$ **3b**

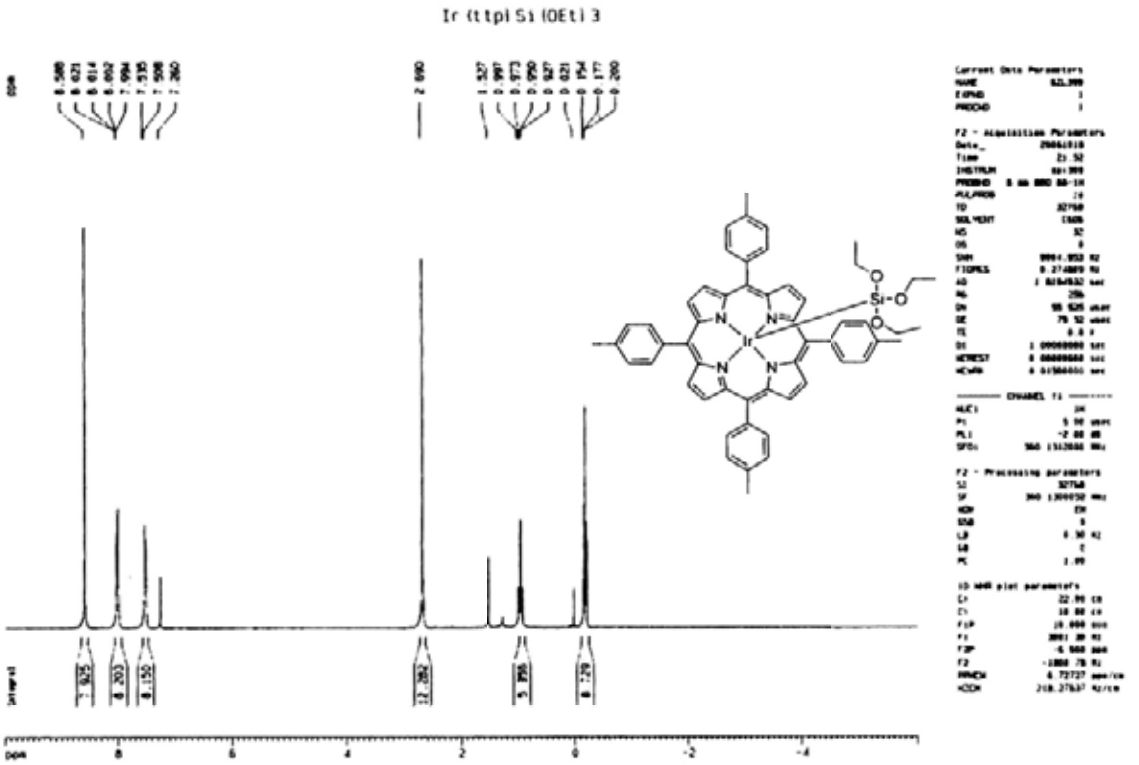

^{13}C NMR of Ir(ttp)Si(OEt)$_3$ **3b**

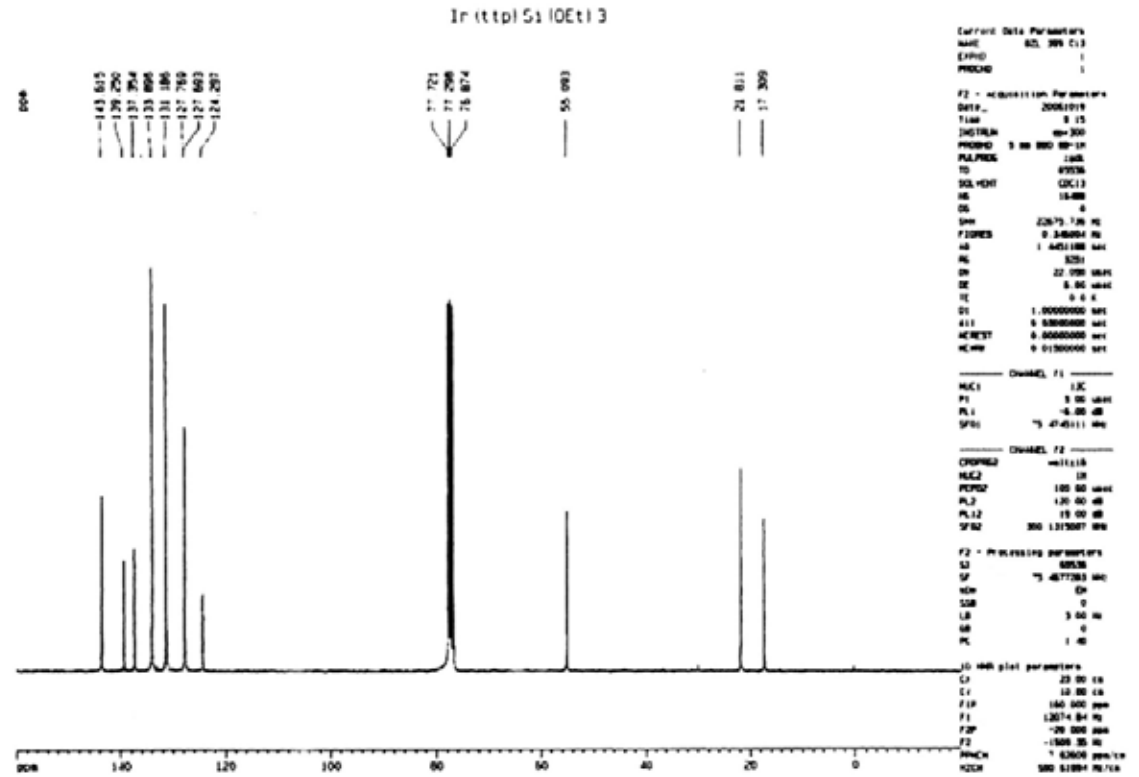

^{1}H NMR of Ir(ttp)SiBnMe$_2$ **3c**

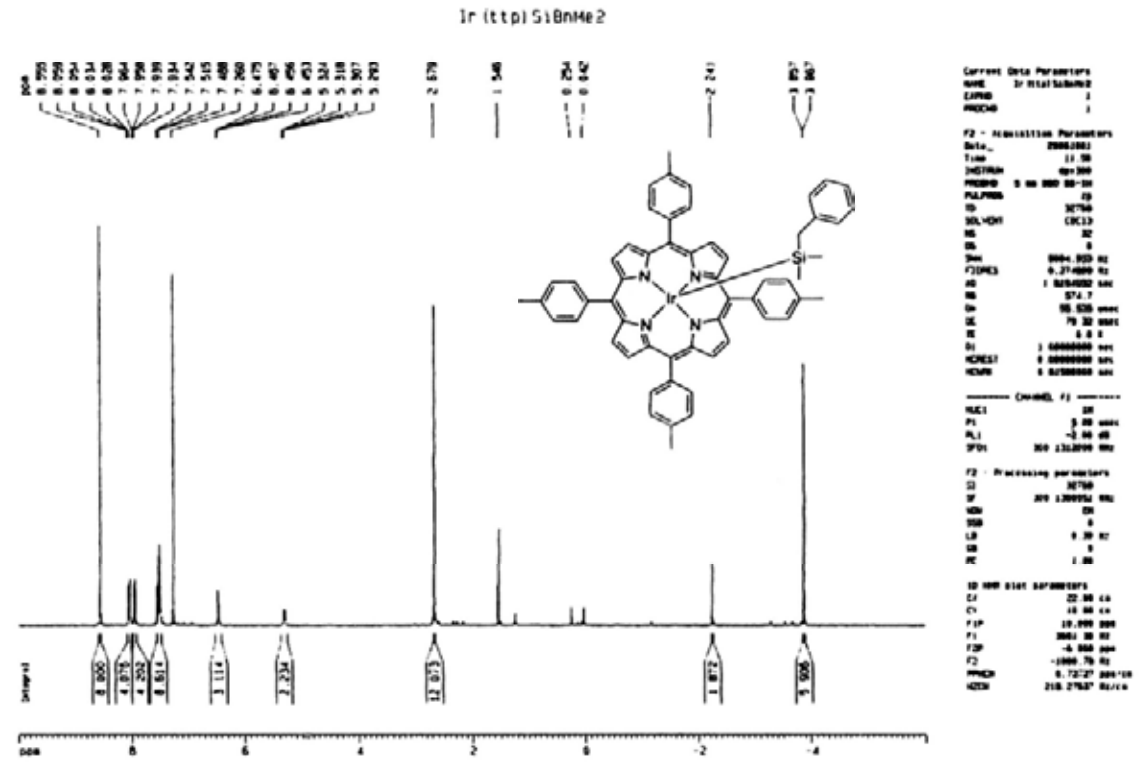

^{13}C NMR of Ir(ttp)SiBnMe$_2$ **3c**

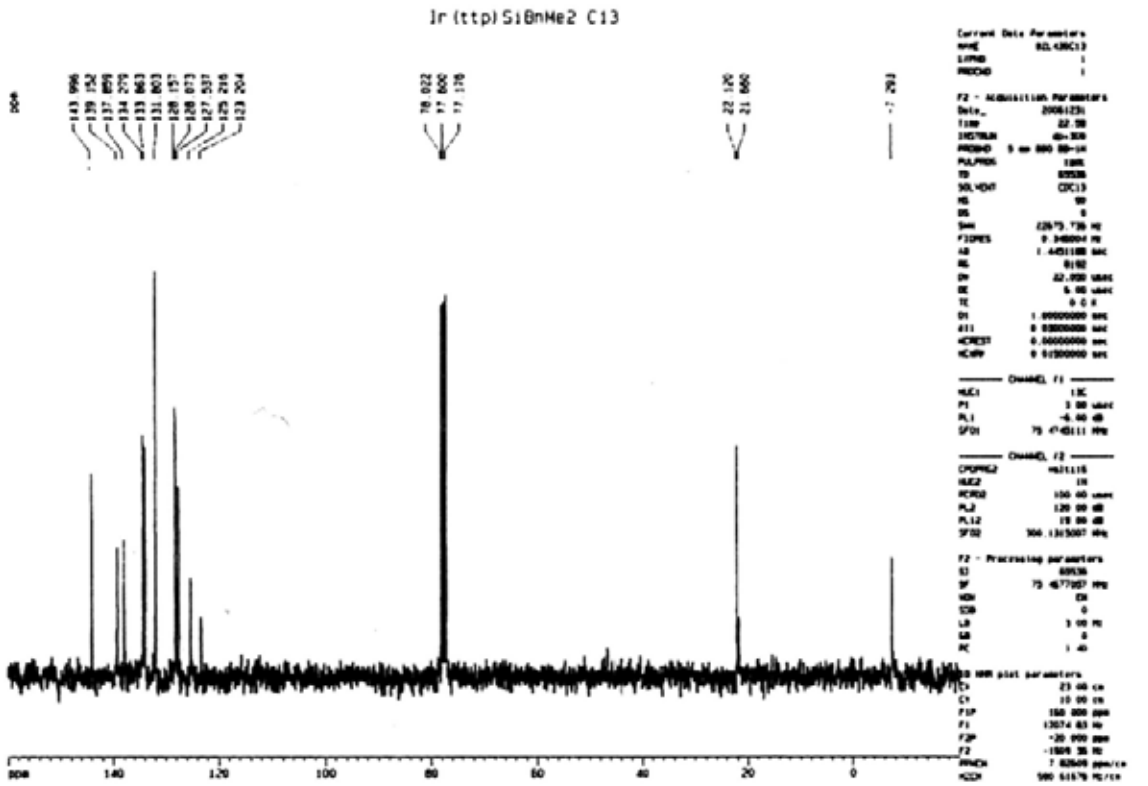

^{1}H NMR of Ir(ttp)SiPhH$_2$ **3d**

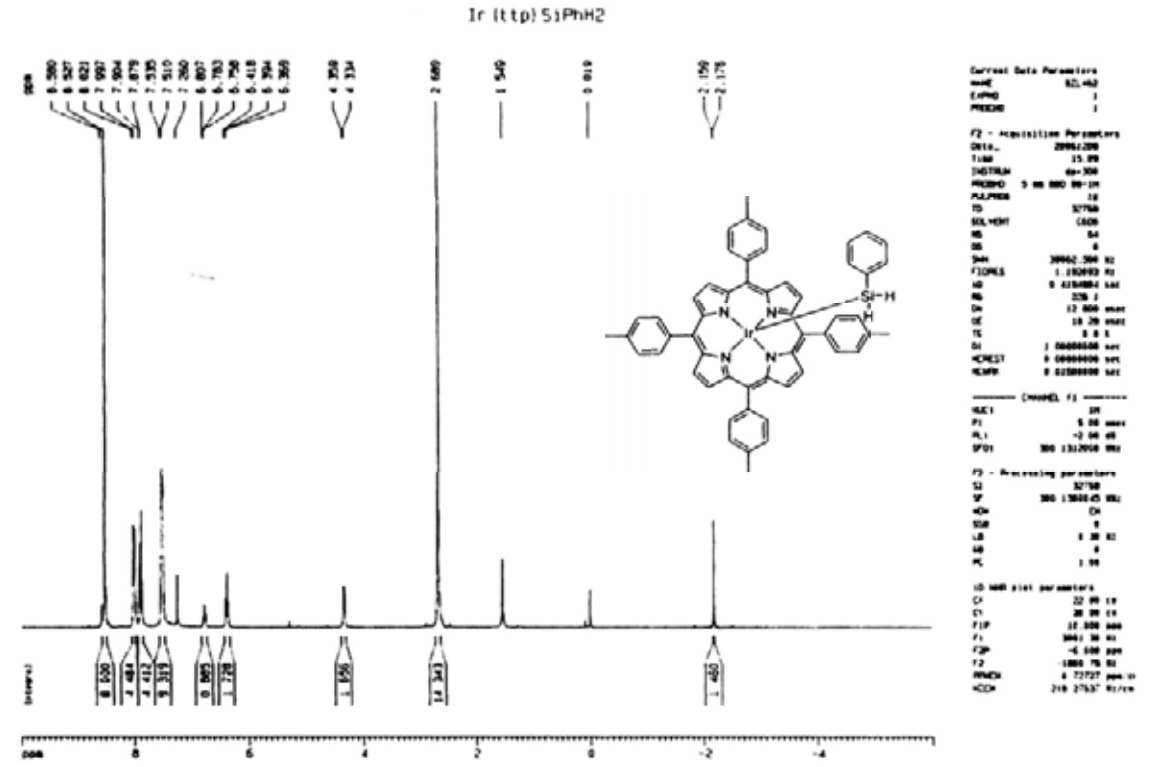

^{13}C NMR of Ir(ttp)SiPhH$_2$ **3d**

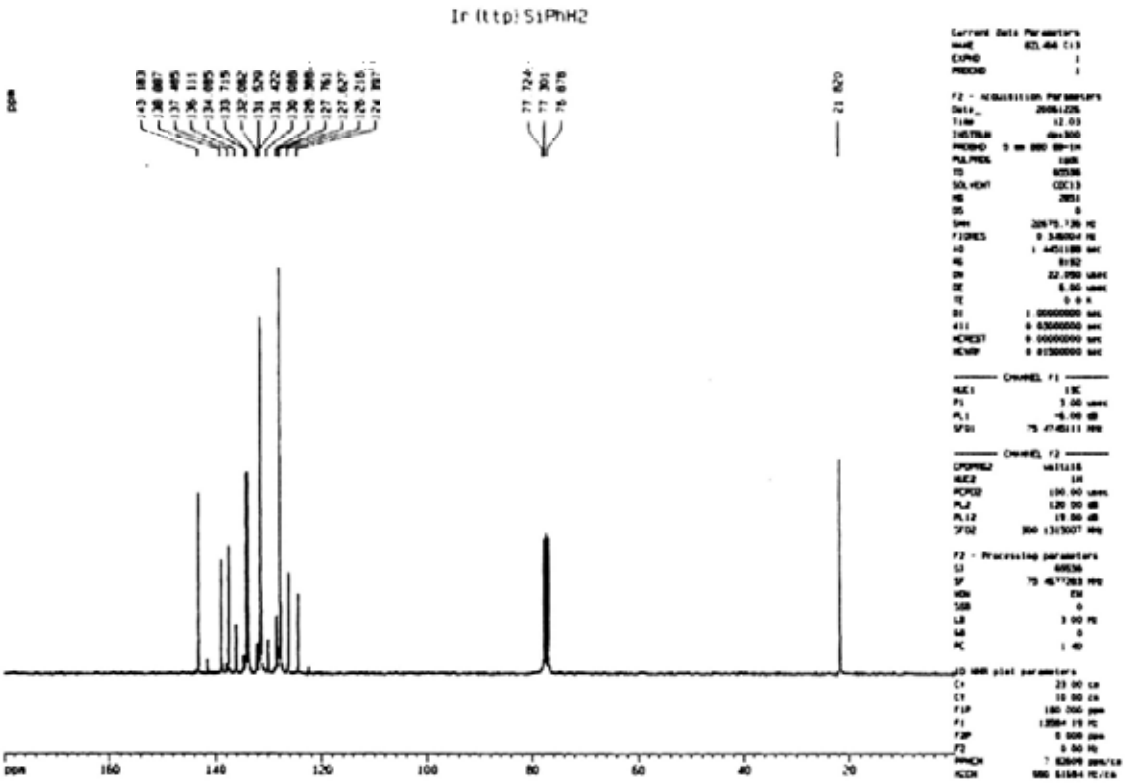

^{1}H NMR of Ir(ttp)SiPhMeH **3e**

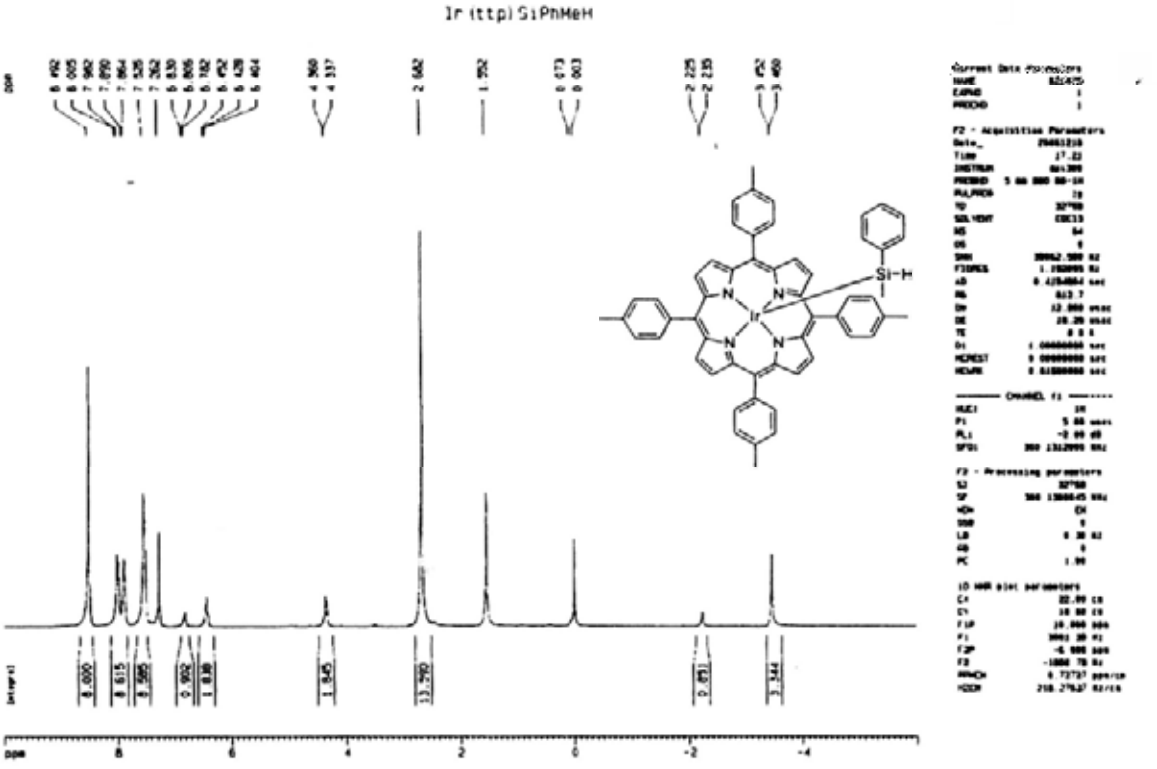

^{13}C NMR of Ir(ttp)SiPhMeH **3e**

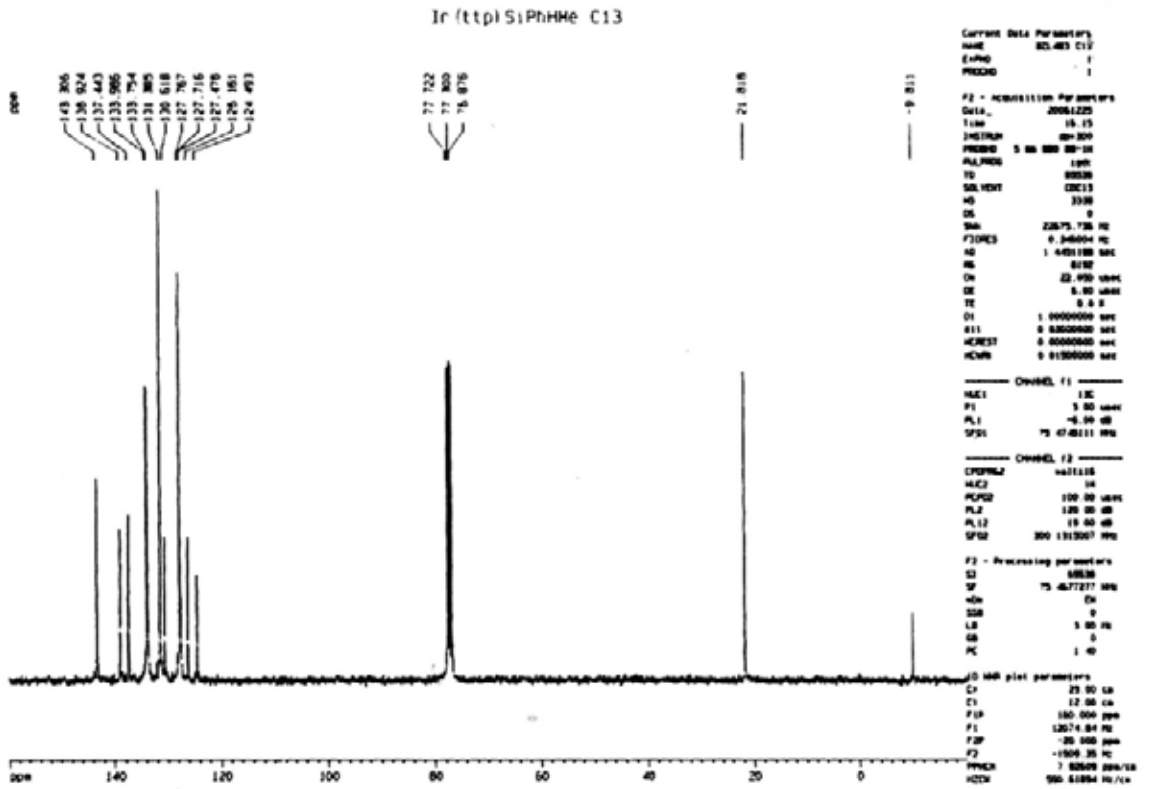

^{1}H NMR of Ir(ttp)SiPh$_2$H **3f**

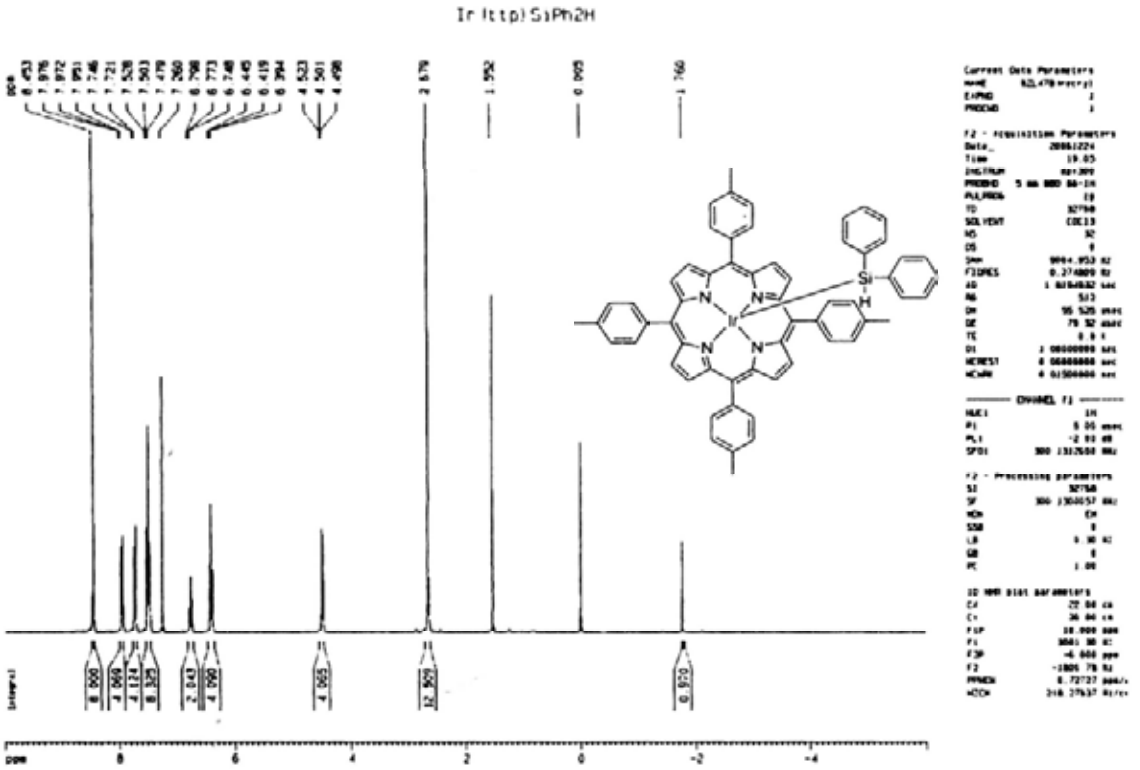

^{13}C NMR of Ir(ttp)SiPh$_2$H **3f**

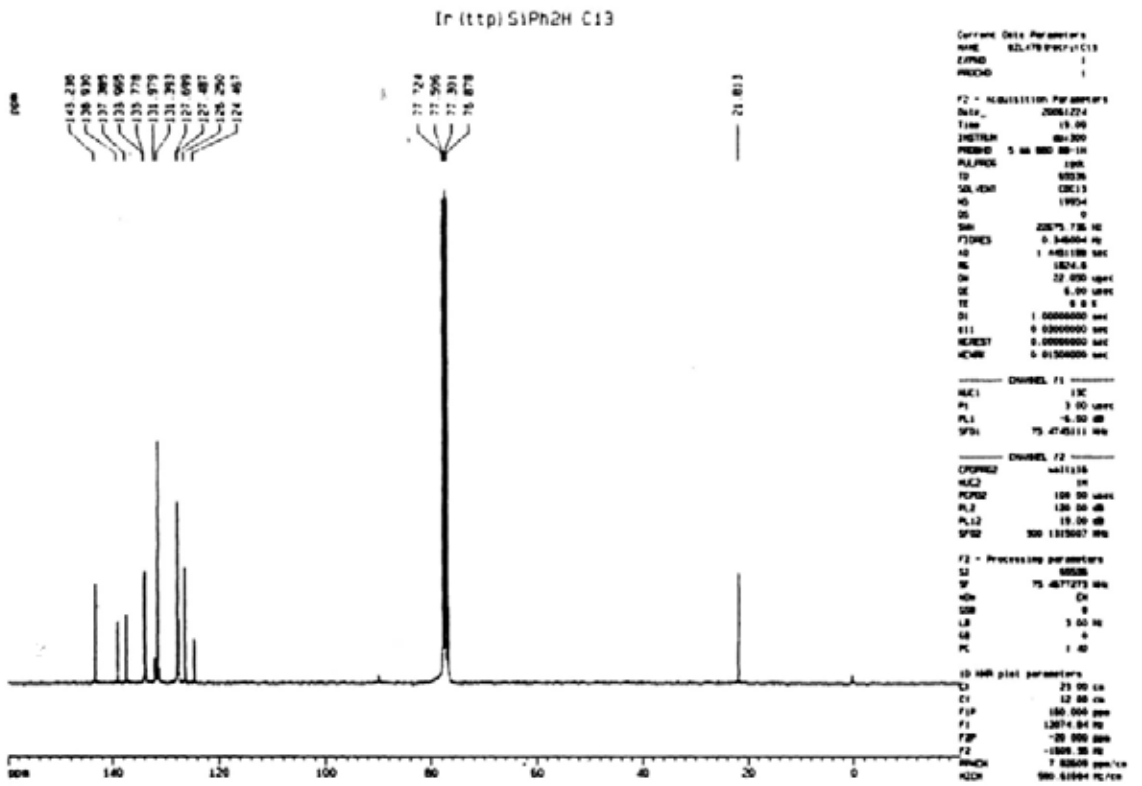

^{1}H NMR of Ir(ttp)SiPh$_2$Me **3g**

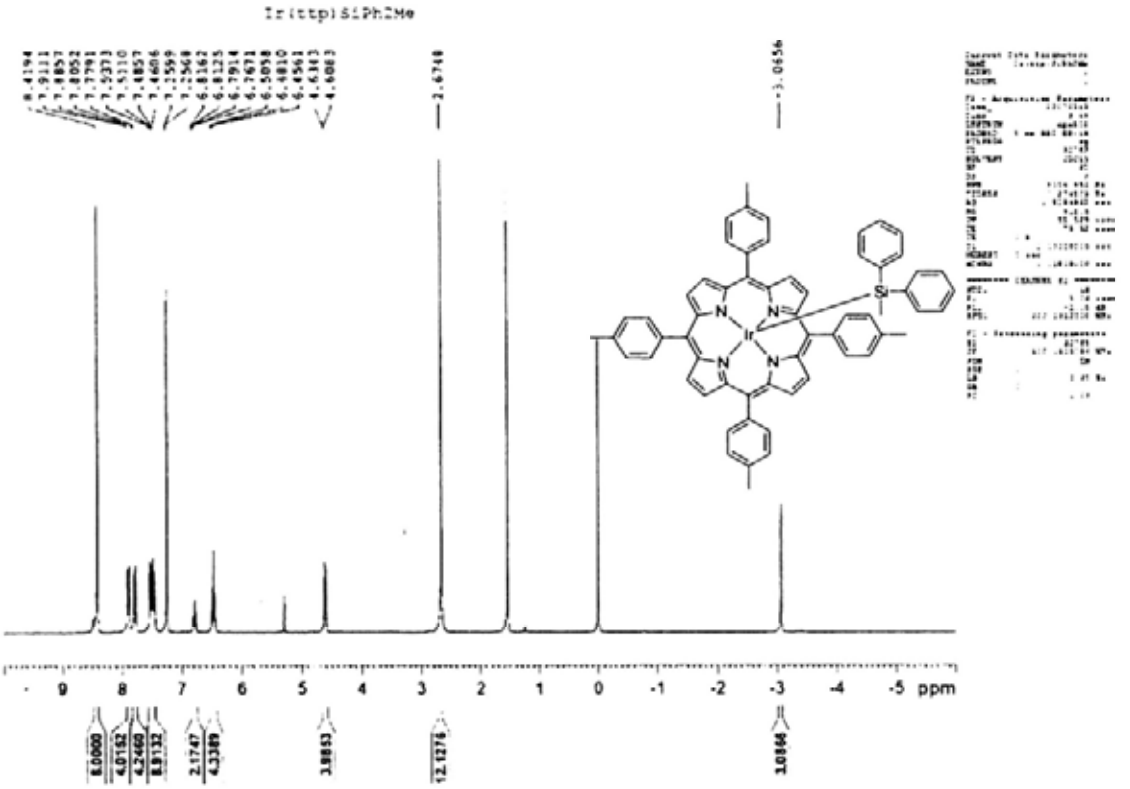

^{13}C NMR of Ir(ttp)SiPh$_2$Me **3g**

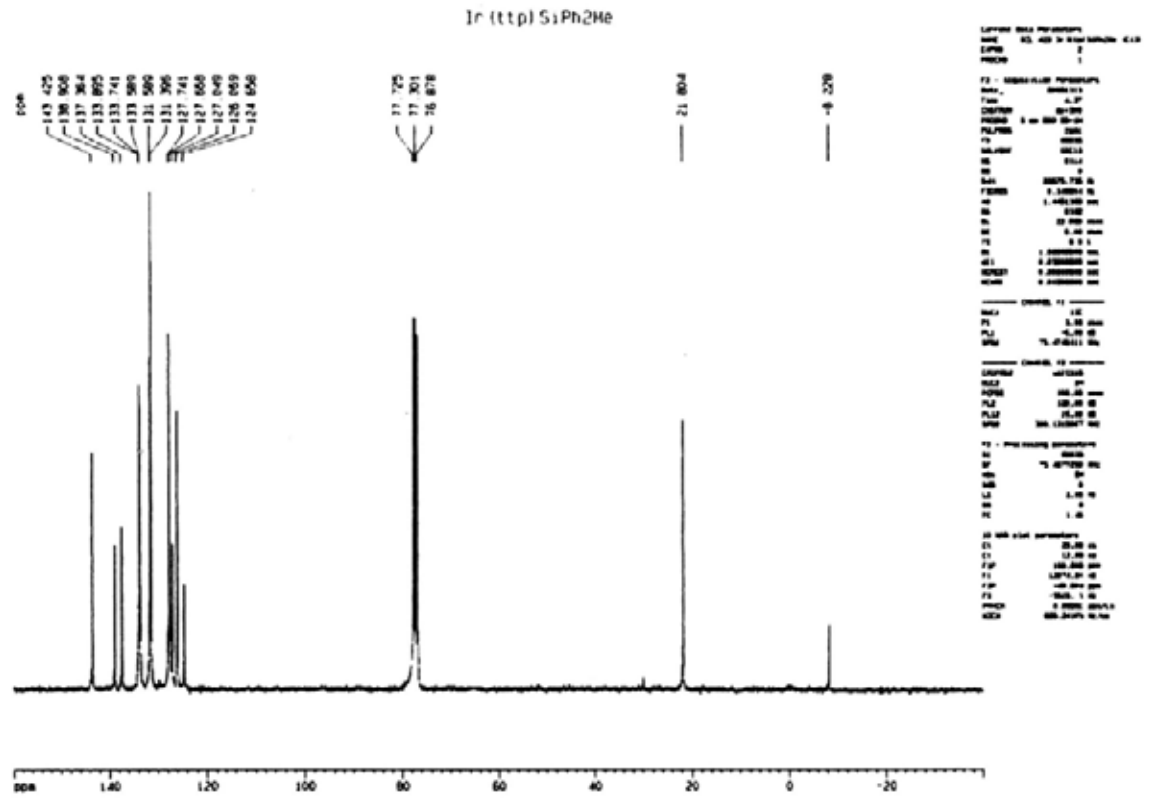

Appendix II (Chapter 3)

II.I Data for the Reaction of Ir(ttp)$SiEt_3$ in the Presence of KOH in Benzene-d_6

Table 3 Data for the Reaction of Ir(ttp)$SiEt_3$ in the Presence of KOH in Benzene-d_6

Time / d	Yield / %					
	Ir(ttp)$SiEt_3$	Ir(ttp)$^{\cdot}$	Unknown	Ir(ttp)H	$(Et_3Si)_2O$	$KOSiEt_3$
0	100	0	0	0	0	0
1	87	0	0	0	0	0
2	26	5	0	0	0	9
3	16	11	0	0	0	15
4	25	28	0	0	0	46
5	11	11	0	0	3	20
6	7	14	0	0	3	29
7	6	10	0	0	5	27
8	3	6	4	0	4	19
9	7	13	10	0	4	64
10	2	6	0	0	2	15
11	4	19	0	0	2	48
12	3	15	0	0	2	35
13	8	32	0	0	2	65
14	6	26	0	0	2	66
15	6	22	0	0	7	46
16	6	20	0	0	10	30
17	7	20	0	0	14	24
18	7	17	0	0	16	10
19	7	12	0	0	15	4
20	7	11	0	0	17	4
23	7	11	0	7	21	0
24	8	13	0	5	21	0
27	6	14	0	2	17	0

II.II Thermodynamic Estimation of Free Energy, Enthalpy and Entropy of Water and KF in Different Temperature

Table 4 Data and Equations for Calculation

	H_2O (G)	H_2O (L)	KF (Cr)
C_{pm} @ 298 K / J mol^{-1} K^{-1}	36.5[a]	75.55[a]	49.114[a]
C_{vm} @ 298 K / J mol^{-1} K^{-1}	27.5[b]	75.55[b]	49.114[a]
S_f @ 298 K / J mol^{-1} K^{-1}	-44.27[a]	-163.3[c]	-99.47[d]
S @ 298 K / J mol^{-1} K^{-1}	188.80[a]	69.99[a]	64.670[a]
H_f @ 298 K / KJ mol^{-1}	-24.80[a]	-286.03[a]	-568.606[a]
G_f @ 298 K / KJ mol^{-1}	-228.60[a]	-237.35[a]	-538.934[a]
Equations for Calculation:			
Low Temperature (≤298 K)	$\Delta S(T_2, L) = \Delta S(298K, L) + C_{pm} * \ln(T_2/298)$		
H_2O (L)	$\Delta H_f(T_2, L) = \Delta H_f(298K, L) + C_{pm} * (T_2 - 298)$		
	$\Delta G_f(T_2, L) = \Delta H_f(T_2, L) - T * \Delta S_f(T_2, L)$		
High Temperature (≥298 K)	$\Delta S(T_2, G) = \Delta S(298K, G) + C_{vm} * \ln(T_2/298)$		
H_2O (G)	$\Delta H_f(T_2, G) = \Delta H_f(298K, G) + C_{pm} * (T_2 - 298)$		
	$\Delta G_f(T_2, G) = \Delta H_f(T_2, G) - T * \Delta S_f(T_2, G)$		
KF (S)	$\Delta S(T_2, S) = \Delta S(298K, S) + C_{pm} * \ln(T_2/298)$		
	$\Delta H_f(T_2, S) = \Delta H_f(298K, S) + C_{pm} * (T_2 - 298)$		
	$\Delta G_f(T_2, S) = \Delta H_f(T_2, S) - T * \Delta S_f(T_2, S)$		

[a] Ref (1). [b] Ref (2). [c] Calculated according to $\Delta S_f(H_2O, L) = \Delta S(H_2O, L) - \Delta S(H_2, G) - 0.5\,\Delta S(O_2, G)$. [d] Calculated according to $\Delta S_f(KF, S) = \Delta S(KF, S) - \Delta S(K, S) - 0.5\,\Delta S(F_2, G)$.

Table 5 Gibbs Free Energy (ΔG_f / KJ mol^{-1}), Enthalpy (ΔH_f / KJ mol^{-1}) and Entropy (ΔS_f / J mol^{-1} K^{-1}) of H_2O and KF in Different Temperature

Temp / K	ΔS_f / J mol^{-1} K^{-1}		ΔH_f / KJ mol^{-1}		ΔG_f / KJ mol^{-1}	
	H_2O	HF	H_2O	HF	H_2O	HF
298	-163.30 (l)	-99.47 (s)	-286.03 (l)	-568.61 (s)	-237.37 (l)	-538.96 (s)
353	-150.50 (l)	-91.15 (s)	-281.87 (l)	-565.90 (s)	-228.75 (l)	-533.73 (s)
373	-146.34 (l)	-88.44 (s)	-280.36 (l)	-564.92 (s)	-225.78 (l)	-531.93 (s)
	-38.10 (g)		-239.74 (g)		-225.53 (g)	
393	-36.66 (g)	-85.88 (s)	-239.19 (g)	-563.94 (s)	-224.78 (g)	-530.19 (s)
423	-34.64 (g)	-82.27 (s)	-238.36 (g)	-562.47 (s)	-223.71 (g)	-527.67 (s)
473	-31.56 (g)	-76.78 (s)	-228.58 (g)	-560.01 (s)	-213.65 (g)	-523.69 (s)
523	-28.80 (g)	-71.84 (s)	-235.61 (g)	-557.56 (s)	-220.55 (g)	-519.98 (s)

References:

(1) *http://en.wikipedia.org/wiki/Water_(data_page)*. Accessed on 05 December 5, 2009.

(2) Yaws, C. L. *Chemical Properties Handbook: Physical, Thermodynamic, Environmental, Transport, Safety, and Health Related Properties for Organic and Inorganic Chemicals*; McGraw-Hill: New York, 1999.

(3) Kuburović, M.; Đurić, S.; Jovović, A.; Karan, M. *Thermal. Science* **2002**, *6*, 71-79.

II.III Crystal Data for Ir(ttp)Ar 3b-e, 3g and 3i

Table 6a Details of Data Collection and Processing Parameters for 3b and 3b'

	Ir(ttp)(2-F-C_6H_4) **3b**	Ir(ttp)(2-F-C_6H_4)(PPh_3) **3b'**
empirical formula	$C_{54}H_{40}FIrN_4$	$C_{73}H_{57}Cl_2FIrN_4P$
cryst syst	Triclinic	Triclinic
space group	$P\bar{1}$	$P\bar{1}$
Fw	956.10	1303.30
a (Å)	11.5587(3)	11.677(4)
b (Å)	11.7996(4)	13.392(4)
c (Å)	19.3485(6)	19.058(6)
α (deg)	92.2800(10)	91.994(6)
β (deg)	105.4820(10)	93.622(7)
γ (deg)	108.9740(10)	95.864(6)
Z	2	2
D_{calc} (mg/m^3)	1.333	1.464
absorp coeff (mm^{-1})	2.845	2.427
V (Å^3)	2381.66(13)	2956.0(16)
F (000)	956	1316
cryst size (mm)	0.50 x 0.30 x 0.20	0.40 x 0.30 x 0.20
reflcns collcd	3379 / 8622	32812 / 10663
absorp corr	Multi-scan	Multi-scan
max. and min. transmn	0.7456 and 0.6105	0.7456 and 0.4898
refinement method	Full-matrix least-squares on F^2	
no. of data / restraints / params	8622 / 189 / 1010	10663 / 28 / 739
goodness-of-fit on F^2	1.178	1.087
final R_1 [a] / wR_2 [b] [I>2σ(I)]	0.0978 / 0.3168	0.0368 / 0.0980
final R_1 [a] / wR_2 [b] (all data)	0.1034 / 0.3210	0.0428 / 0.103
w_1/w_2 [c]	0.098600 / 99.287903	0.053000 / 6.070400

[a] $R_1 = \Sigma(\| F_0 \| - \| F_c \|) / \Sigma \| F_0 \|$. [b] $wR_2 = \{\Sigma[w(F_0^2 - F_c^2)^2] / \Sigma[w(F_0^2)^2]\}^{1/2}$.

[c] Weighting scheme $w^{-1} = \sigma^2(F_0^2) + (w_1 P)^2 + w_2 P$, where $P = (F_0^2 + 2F_c^2)/3$.

Table 6b Details of Data Collection and Processing Parameters for 3c and 3c'

	Ir(ttp)(2,3-F-C_6H_4)(MeOH) **3c**	Ir(ttp)(2,3-F-C_6H_4)(PPh_3) **3c'**
empirical formula	$C_{58}H_{49}F_2IrN_4O_2$	$C_{72.50}H_{55}ClF_2IrN_4P$
cryst syst	Monoclinic	Triclinic
space group	P2(1)/c	$P\bar{1}$
Fw	1064.21	1278.82
a (Å)	10.7728(9)	11.6958(10)
b (Å)	19.5092(16)	13.4667(12)
c (Å)	24.1139(19)	19.1165(17)
α (deg)	90	92.258(2)
β (deg)	94.213(2)	93.569(2)
γ (deg)	90	96.187(2)
Z	4	2
D_{calc} (mg/m^3)	1.399	1.423
absorp coeff (mm^{-1})	2.694	2.361
V (Å^3)	5054.3(7)	2984.4(5)
F (000)	2144	1290
cryst size (mm)	0.40 x 0.30 x 0.20	0.50 x 0.40 x 0.30
reflcns collcd	76406 / 9024	27081 / 10670
absorp corr	Multi-scan	Multi-scan
max. and min. transmn	0.7456 and 0.5552	0.7456 and 0.4690
refinement method	Full-matrix least-squares on F^2	
no. of data / restraints / params	9024 / 0 / 604	10670 / 8 / 748
goodness-of-fit on F^2	1.099	1.074
final R_1 [a] / wR_2 [b] [I>2σ(I)]	0.0546 / 0.1676	0.0446 / 0.1278
final R_1 [a] / wR_2 [b] (all data)	0.0733 / 0.1817	0.0505 / 0.1321
w_1/w_2 [c]	0.125100	0.082200 / 6.717200

[a] $R_1 = \Sigma(\| F_0 \| - \| F_c \|) / \Sigma \| F_0 \|$. [b] $wR_2 = \{\Sigma[w(F_0^2 - F_c^2)^2] / \Sigma[w(F_0^2)^2]\}^{1/2}$.

[c] Weighting scheme $w^{-1} = \sigma^2(F_0^2) + (w_1 P)^2 + w_2 P$, where $P = (F_0^2 + 2F_c^2)/3$.

Table 6c Details of Data Collection and Processing Parameters for 3g and 3g'

	Ir(ttp)(3,5-F-C_6H_4)(MeOH) **3g**	Ir(ttp)(3,5-F-C_6H_4)(PPh_3) **3g'**
empirical formula	$C_{54}H_{39}F_2IrN_4$	$C_{73}H_{56}Cl_2F_2IrN_4P$
cryst syst	Triclinic	Triclinic
space group	$P\bar{1}$	$P\bar{1}$
Fw	974.09	1321.29
a (Å)	11.1507(19)	11.7246(4)
b (Å)	12.266(2)	13.4858(4)
c (Å)	18.754(4)	19.0437(6)
α (deg)	75.317(4)	92.8660(10)
β (deg)	72.776(3)	93.5180(10)
γ (deg)	72.964(3)	96.6670(10)
Z	2	2
D_{calc} (mg/m^3)	1.405	1.472
absorp coeff (mm^{-1})	2.946	2.411
V (Å^3)	2303.2(7)	2980.15(16)
F (000)	972	1332
cryst size (mm)	0.50 x 0.30 x 0.20	0.40 x 0.30 x 0.20
reflcns collcd	25635 / 7818	42958 / 10652
absorp corr	Multi-scan	Multi-scan
max. and min. transmn	0.7456 and 0.4576	0.7456 and 0.5184
refinement method	Full-matrix least-squares on F^2	
no. of data / restraints / params	7818 / 42 / 625	10652 / 0 / 748
goodness-of-fit on F^2	1.163	1.046
final R_1 [a] / wR_2 [b] [I>2σ(I)]	0.0765 / 0.1884	0.0235 / 0.0610
final R_1 [a] / wR_2 [b] (all data)	0.1088 / 0.2027	0.0284 / 0.0667
w_1/w_2 [c]	0.069800 / 17.314798	0.037000 / 1.784400

[a] $R_1 = \Sigma(\| F_0 \| - \| F_c \|) / \Sigma \| F_0 \|$. [b] $wR_2 = \{\Sigma[w(F_0^2 - F_c^2)^2] / \Sigma[w(F_0^2)^2]\}^{1/2}$.

[c] Weighting scheme $w^{-1} = \sigma^2(F_0^2) + (w_1 P)^2 + w_2 P$, where $P = (F_0^2 + 2F_c^2)/3$.

Table 6d Details of Data Collection and Processing Parameters for 3i and 3i'

	Ir(ttp)(C_6F_5)(MeOH) **3i**	Ir(ttp)(C_6F_5)(PPh_3) **3i'**
empirical formula	$C_{55}H_{40}F_5IrN_4O$	$C_{73}H_{53}Cl_2F_5IrN_4P$
cryst syst	Triclinic	Triclinic
space group	$P\bar{1}$	$P\bar{1}$
Fw	1060.11	1375.26
a (Å)	13.3088(15)	11.7524(4)
b (Å)	13.3281(15)	13.4812(4)
c (Å)	15.3974(18)	19.1743(6)
α (deg)	86.718(3)	91.8440(10)
β (deg)	65.479(2)	94.2440(10)
γ (deg)	76.756(2)	96.9460(10)
Z	2	2
D_{calc} (mg/m^3)	1.457	1.520
absorp coeff (mm^{-1})	2.824	2.401
V (Å^3)	2416.6(5)	3004.75(17)
F (000)	1056	1380
cryst size (mm)	0.40 x 0.30 x 0.20	0.40 x 0.30 x 0.20
reflcns collcd	27538 / 8393	33642 / 10755
absorp corr	Multi-scan	Multi-scan
max. and min. transmn	0.7456 and 0.5465	0.7456 and 0.5175
refinement method	Full-matrix least-squares on F^2	
no. of data / restraints / params	8393 / 0 / 595	10755 / 0 / 775
goodness-of-fit on F^2	1.011	1.029
final R_1 [a] / wR_2 [b] [I>2σ(I)]	0.0398 / 0.0969	0.0236 / 0.0613
final R_1 [a] / wR_2 [b] (all data)	0.0509 / 0.1014	0.0279 / 0.0677
w_1/w_2 [c]	0.066000	0.036300 / 2.614300

[a] $R_1 = \Sigma(\| F_0 \| - \| F_c \|) / \Sigma \| F_0 \|$. [b] $wR_2 = \{\Sigma[w(F_0^2 - F_c^2)^2] / \Sigma[w(F_0^2)^2]\}^{1/2}$.

[c] Weighting scheme $w^{-1} = \sigma^2(F_0^2) + (w_1 P)^2 + w_2 P$, where $P = (F_0^2 + 2F_c^2)/3$.

Table 6e Details of Data Collection and Processing Parameters for 3d and 3d'

	Ir(ttp)(3-F-C_6H_4) **3d** (100(2) K)	Ir(ttp)(3-F-C_6H_4)(PPh_3) **3d'**
empirical formula	$C_{54}H_{40}FIrN_4$	$C_{73}H_{57}Cl_2FIrN_4P$
cryst syst	Triclinic	Triclinic
space group	$P\bar{1}$	$P\bar{1}$
Fw	956.10	1303.30
a (Å)	11.3610(10)	11.7587(4)
b (Å)	11.3686(10)	13.4435(4)
c (Å)	19.4448(16)	19.1110(6)
α (deg)	91.965(2)	92.3110(10)
β (deg)	104.496(2)	93.6820(10)
γ (deg)	107.177(2)	96.3990(10)
Z	2	2
D_{calc} (mg/m^3)	1.376	1.446
absorp coeff (mm^{-1})	2.937	2.397
V (Å^3)	2307.1(3)	2992.58(16)
F (000)	956	1316
cryst size (mm)	0.40 x 0.30 x 0.20	0.40 x 0.30 x 0.20
reflcns collcd	26351 / 7855	29457 / 10750
absorp corr	Multi-scan	Multi-scan
max. and min. transmn	0.7456 and 0.4704	0.7456 and 0.5612
refinement method	Full-matrix least-squares on F^2	
no. of data / restraints / params	7855 / 175 / 1072	10750 / 2 / 739
goodness-of-fit on F^2	1.357	1.020
final R_1 [a] / wR_2 [b] [I>2σ(I)]	0.0941 / 0.2744	0.0358 / 0.0911
final R_1 [a] / wR_2 [b] (all data)	0.0967 / 0.2757	0.0466 / 0.0975
w_1/w_2 [c]	0.000100 / 129.480301	0.053800 / 3.451600

[a] $R_1 = \Sigma(\| F_0 \| - \| F_c \|) / \Sigma \| F_0 \|$. [b] $wR_2 = \{\Sigma[w(F_0^2 - F_c^2)^2] / \Sigma[w(F_0^2)^2]\}^{1/2}$.

[c] Weighting scheme $w^{-1} = \sigma^2(F_0^2) + (w_1 P)^2 + w_2 P$, where $P = (F_0^2 + 2F_c^2)/3$.

Table 6f Details of Data Collection and Processing Parameters for 3e and 3f

	Ir(ttp)(4-F-C_6H_4) **3e**	Ir(ttp)(2,5-F_2-C_6H_3)(DMSO) **3f**
empirical formula	$C_{54}H_{40}FIrN_4$	$C_{56}H_{45}F_2IrN_4OS$
cryst syst	Monoclinic	Triclinic
space group	P2(1)/n	$P\bar{1}$
Fw	956.10	1052.22
a (Å)	15.642(2)	11.5968(6)
b (Å)	18.657(3)	12.2172(7)
c (Å)	15.828(2)	28.8734(16)
α (deg)	90	80.6860(10)
β (deg)	107.604(3)	86.0440(10)
γ (deg)	90	69.4080
Z	4	3
D_{calc} (mg/m^3)	1.442	1.387
absorp coeff (mm^{-1})	3.078	2.741
V (Å^3)	4403.0(12)	3778.6(4)
F (000)	1912	1584
cryst size (mm)	0.40 x 0.30 x 0.20	0.50 x 0.40 x 0.30
reflcns collcd	49129 / 7976	58069 / 13623
absorp corr	Multi-scan	Multi-scan
max. and min. transmn	0.7456 and 0.5104	0.7456 and 0.5526
refinement method	Full-matrix least-squares on F^2	
no. of data / restraints / params	7976 / 0 / 541	13623 / 24 / 925
goodness-of-fit on F^2	1.052	1.171
final R_1 [a] / wR_2 [b] [I>2σ(I)]	0.0214 / 0.0488	0.0728 / 0.1505
final R_1 [a] / wR_2 [b] (all data)	0.0283 / 0.0509	0.0942 / 0.1571
w_1/w_2 [c]	0.024200 / 1.841100	0.031100 / 32.321499

[a] $R_1 = \Sigma(\| F_0 \| - \| F_c \|) / \Sigma \| F_0 \|$. [b] $wR_2 = \{\Sigma[w(F_0^2 - F_c^2)^2] / \Sigma[w(F_0^2)^2]\}^{1/2}$.

[c] Weighting scheme $w^{-1} = \sigma^2(F_0^2) + (w_1 P)^2 + w_2 P$, where $P = (F_0^2 + 2F_c^2)/3$.

II.IV X-Ray Structures for 3b-g, 3i and 3b'-d', 3g', 3i'

Table 7 X-Ray Structures of Ir(ttp)Ar 3b-g and 3i

Compound Name	X-Ray Structures
Ir(ttp)(2-F-C_6H_4) **3b**	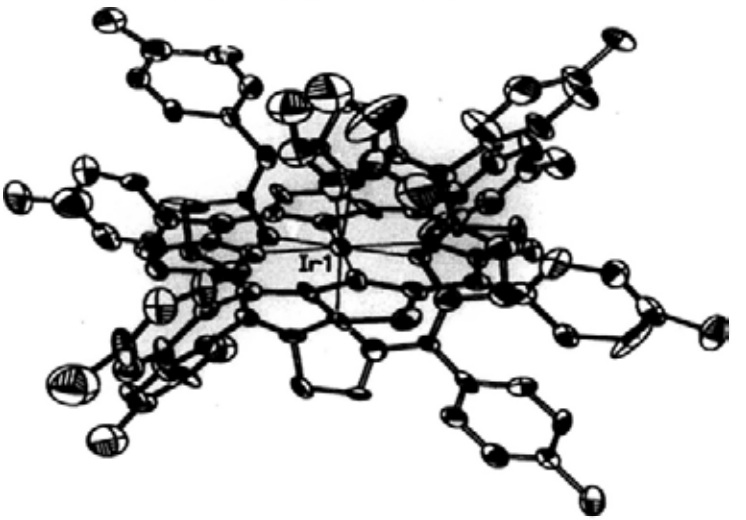
Ir(ttp)(2,3-F_2-C_6H_3)(MeOH) **3c**	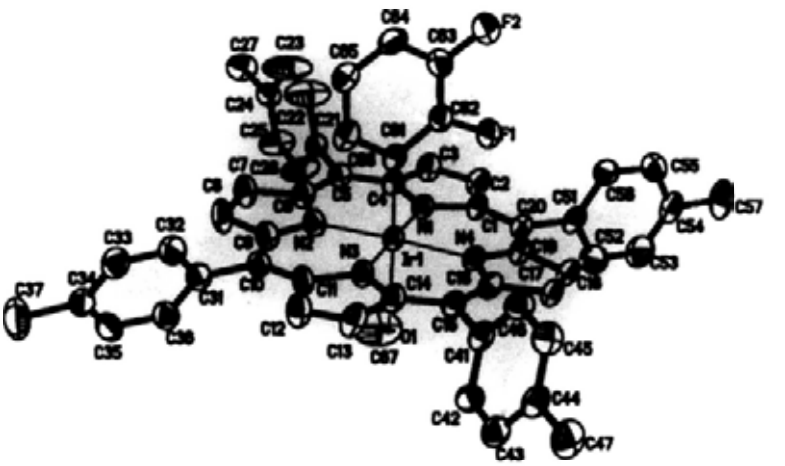
Ir(ttp)(3-F-C_6H_4) **3d**	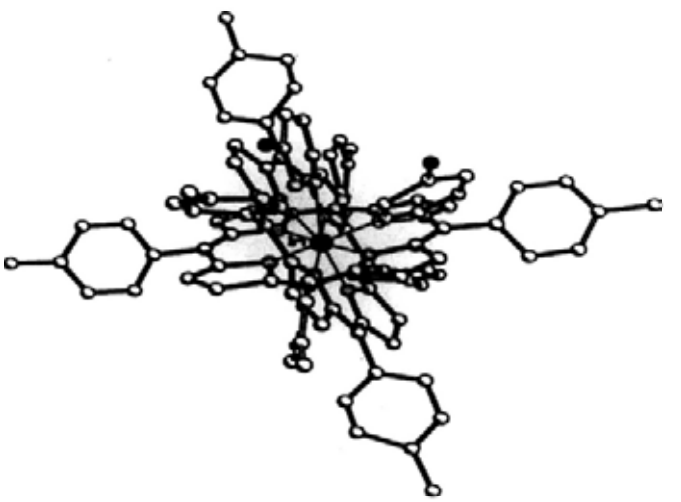

Compound Name	X-Ray Structures
Ir(ttp)(4-F-C_6H_4) **3e**	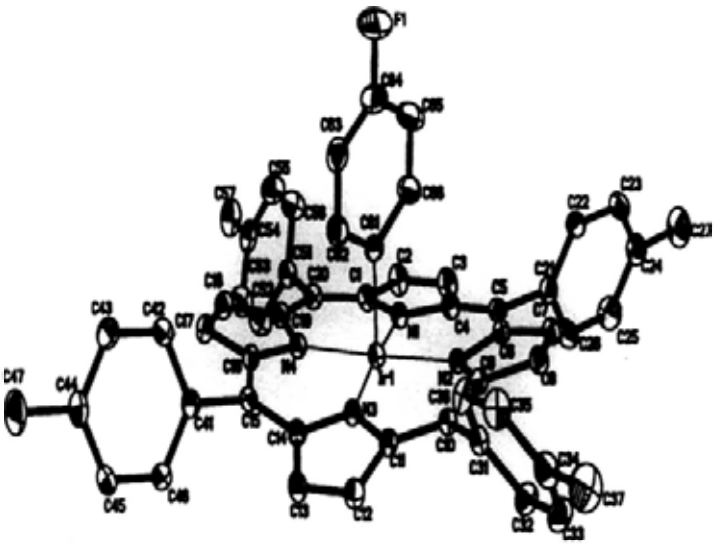
Ir(ttp)(2,5-F_2-C_6H_3)(DMSO) **3f**	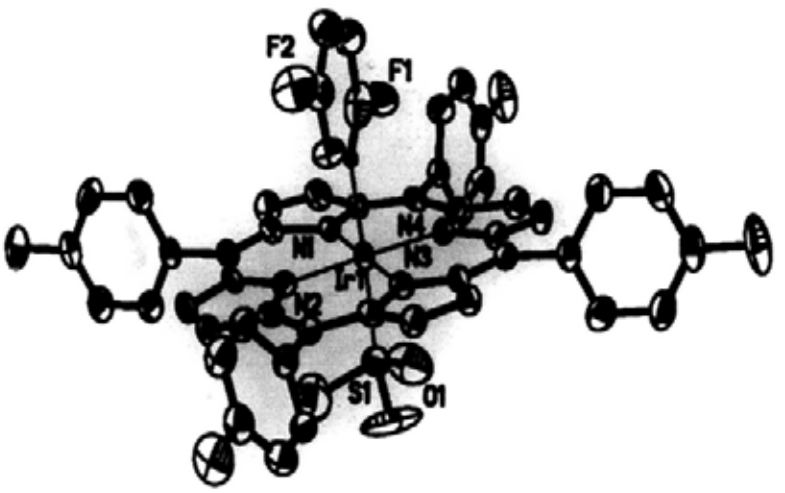
Ir(ttp)(3,5-F_2-C_6H_3) **3g**	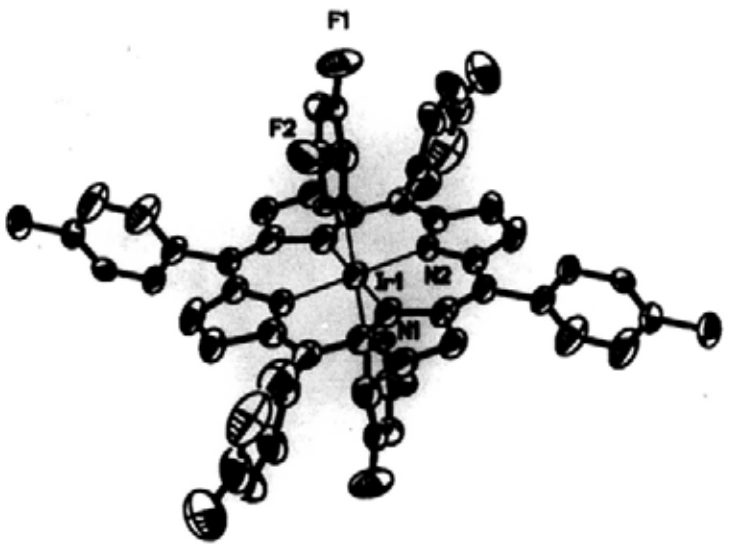

Compound Name	X-Ray Structures
Ir(ttp)(C_6F_5)(MeOH) **3i**	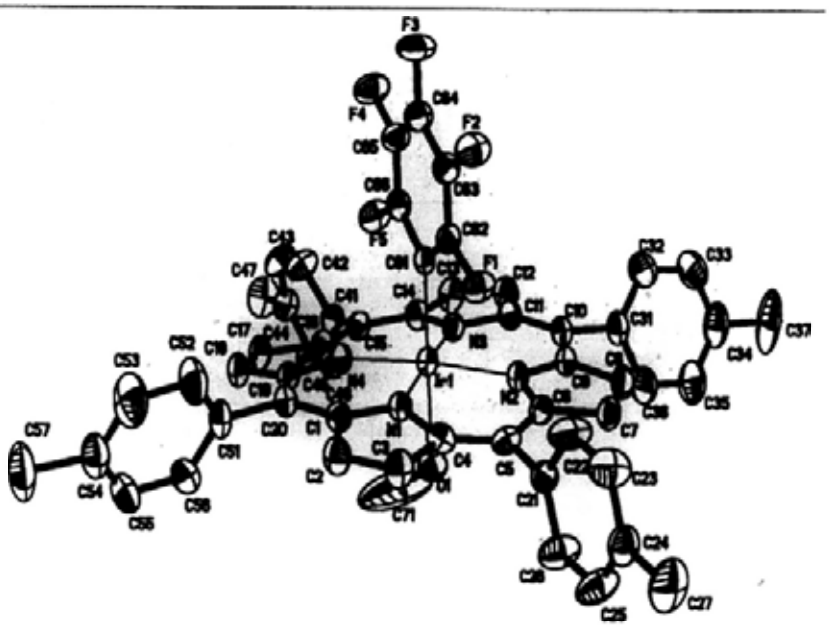

Table 8 X-Ray Structures of Ir(ttp)Ar 3b-g and 3i

Compound Name	X-Ray Structures
Ir(ttp)(2-F-C_6H_4)(PPh_3) **3b'**	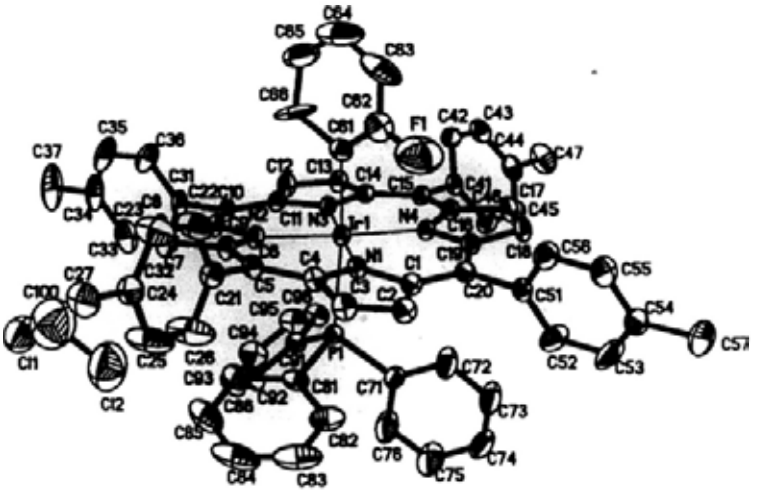
Ir(ttp)(2,3-F_2-C_6H_3)(PPh_3) **3c'**	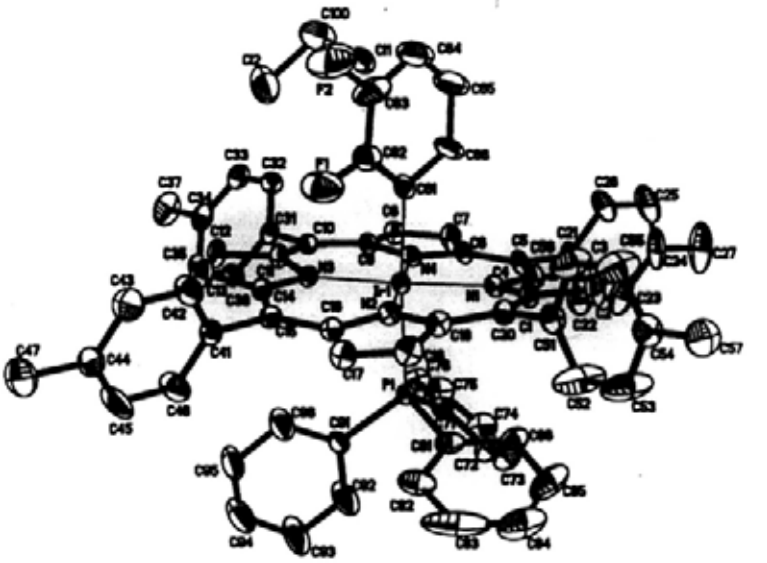
Ir(ttp)(3-F-C_6H_4)(PPh_3) **3d'**	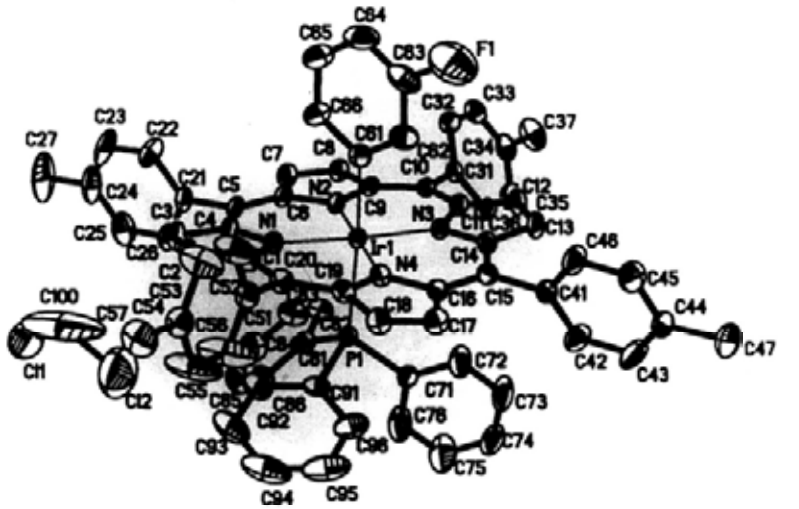

Compound Name	X-Ray Structures
Ir(ttp)(3,5-F_2-C_6H_3)(PPh_3) **3g'**	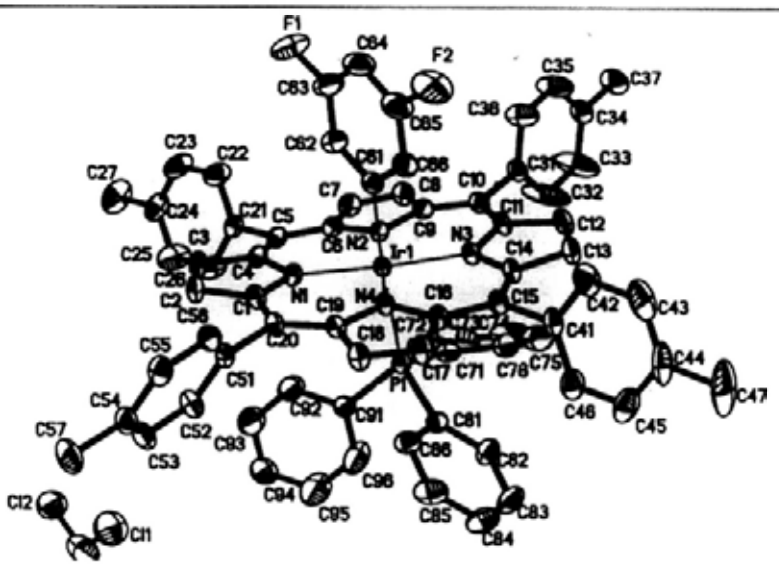
Ir(ttp)(C_6F_5)(PPh_3) **3i'**	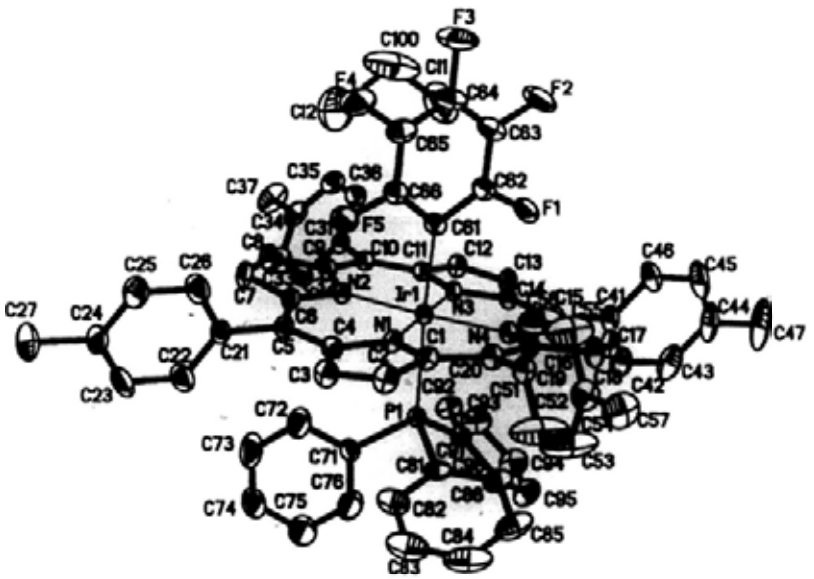

II.V ^{1}H , ^{13}C and ^{19}F NMR Spectra of Ir(ttp)Ar 3a-i

Table 9 List of ^{1}H and ^{13}C NMR Spectra of Ir(ttp)Ar 3a-i

^{1}H NMR of Ir(ttp)C_6H_5 **3a**

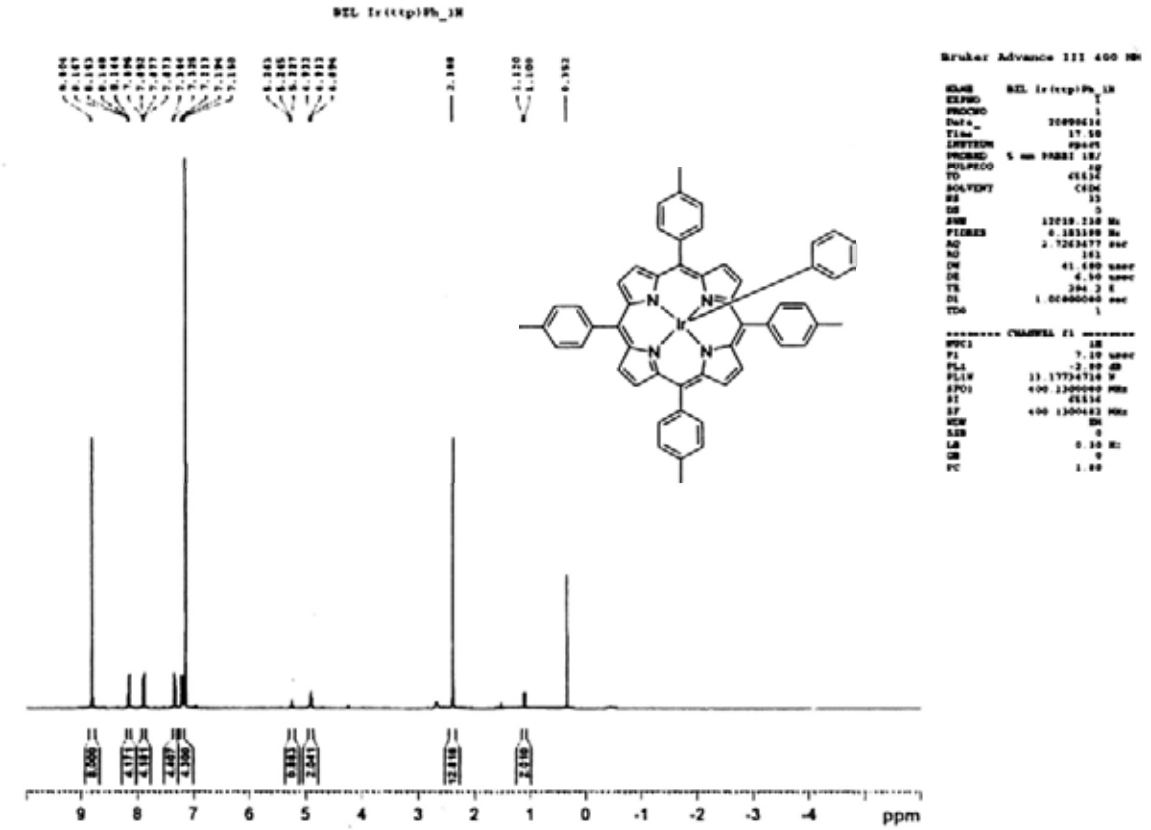

^{13}C NMR of Ir(ttp)C_6H_5 **3a**

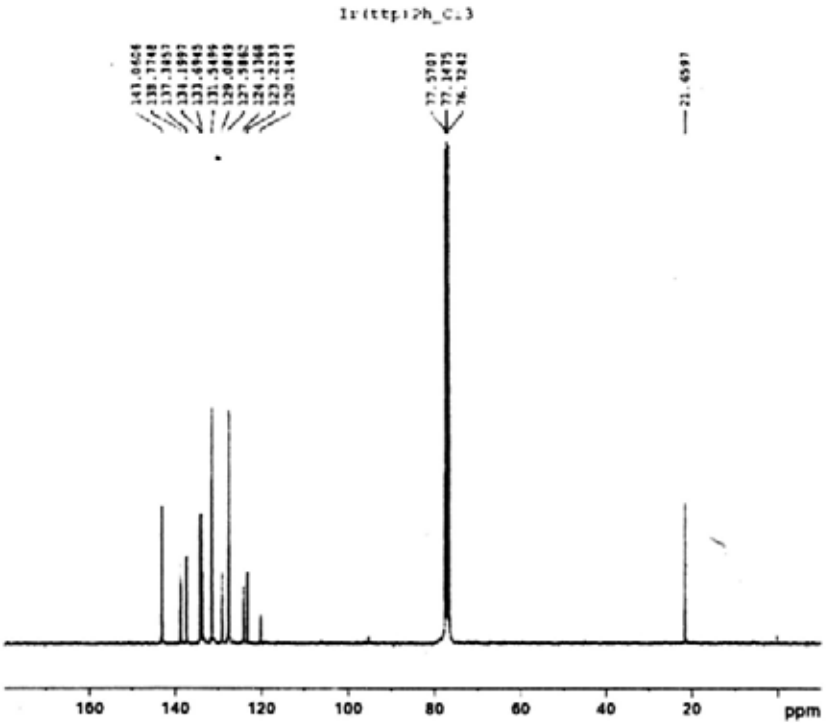

^{13}C NMR of Ir(ttp)(2-F-C_6H_4) **3b**

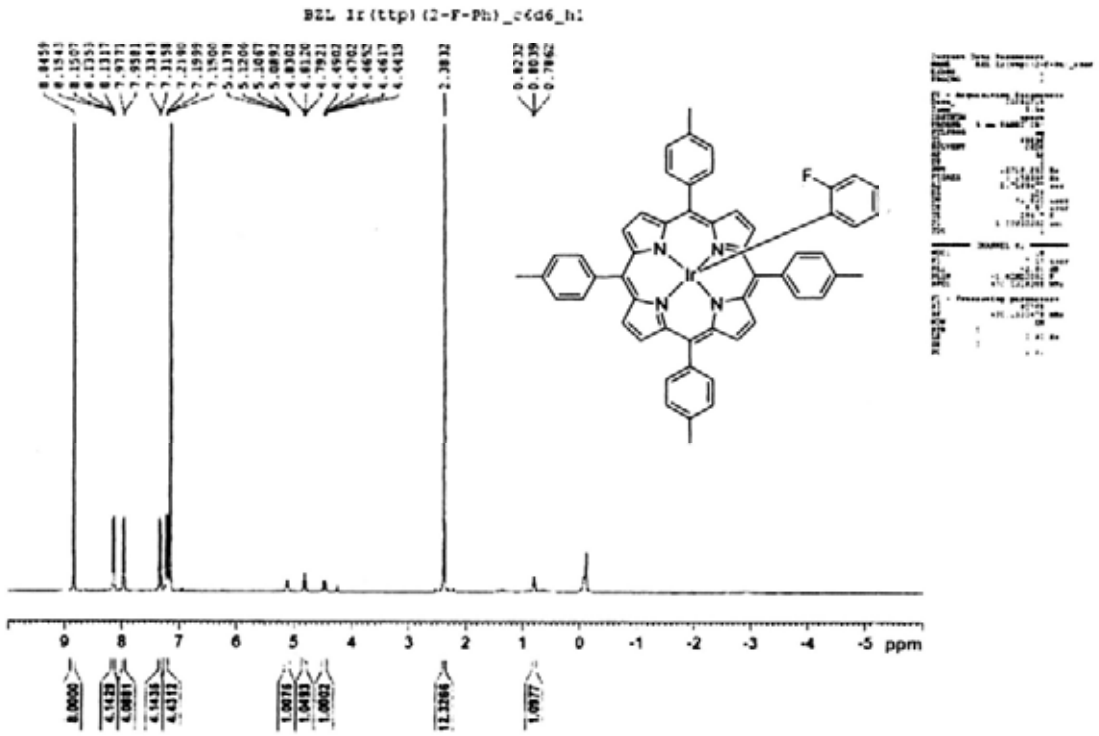

^{13}C NMR of Ir(ttp)(2-F-C_6H_4) **3b**

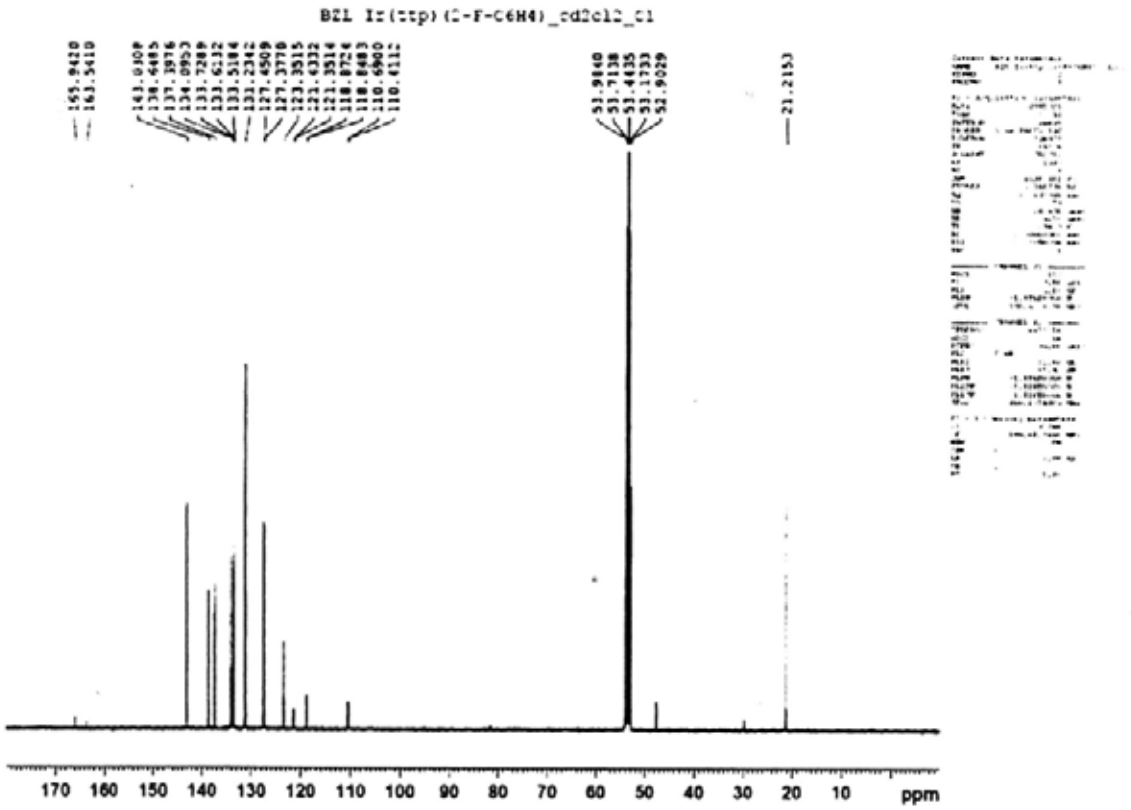

^{1}H NMR of Ir(ttp)(2,3-F_2-C_6H_3) **3c**

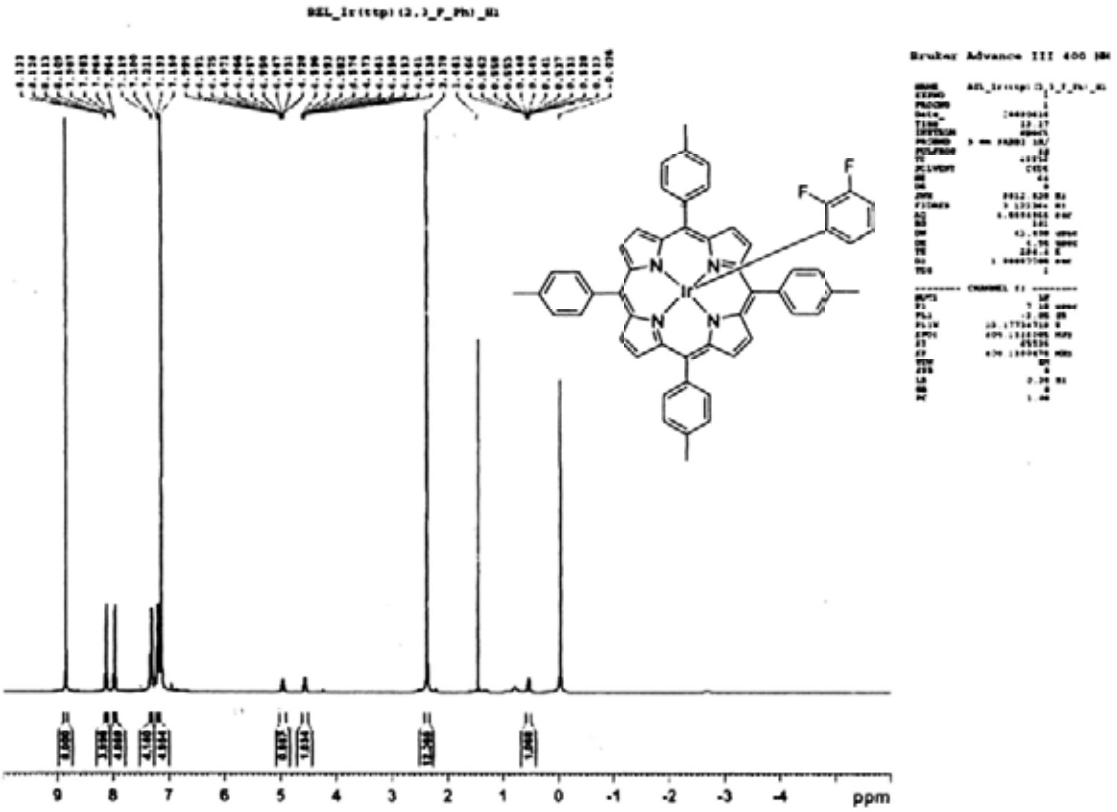

^{13}C NMR of Ir(ttp)(2,3-F_2-C_6H_3) **3c**

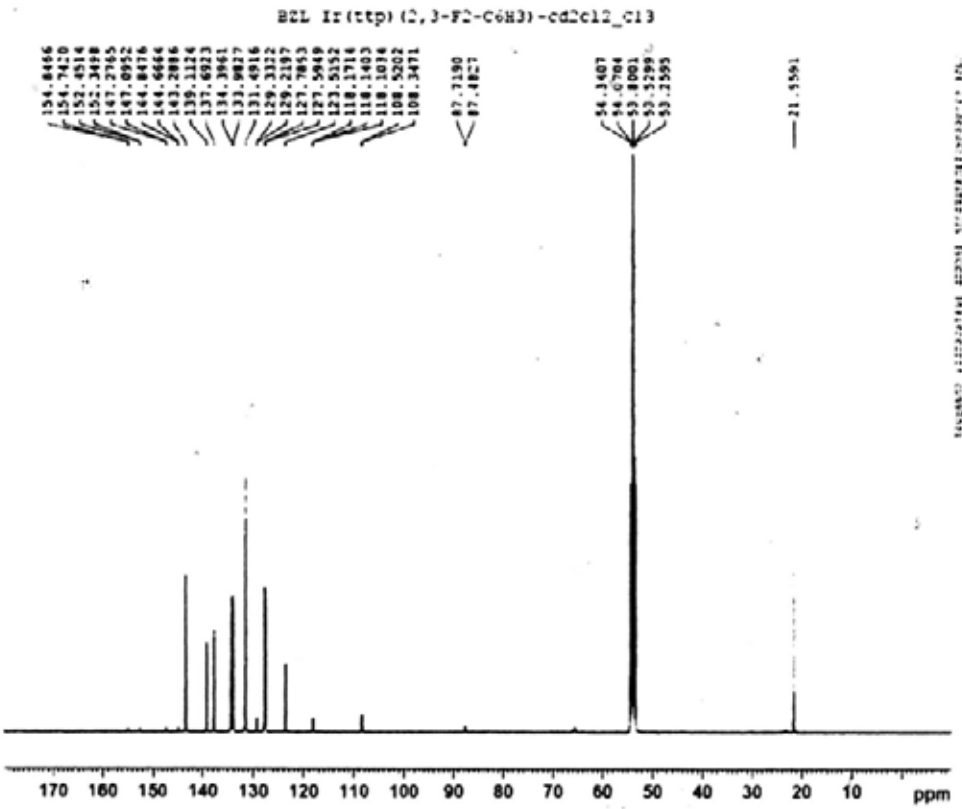

^{1}H NMR of Ir(ttp)(3-F-C_6H_4) **3d**

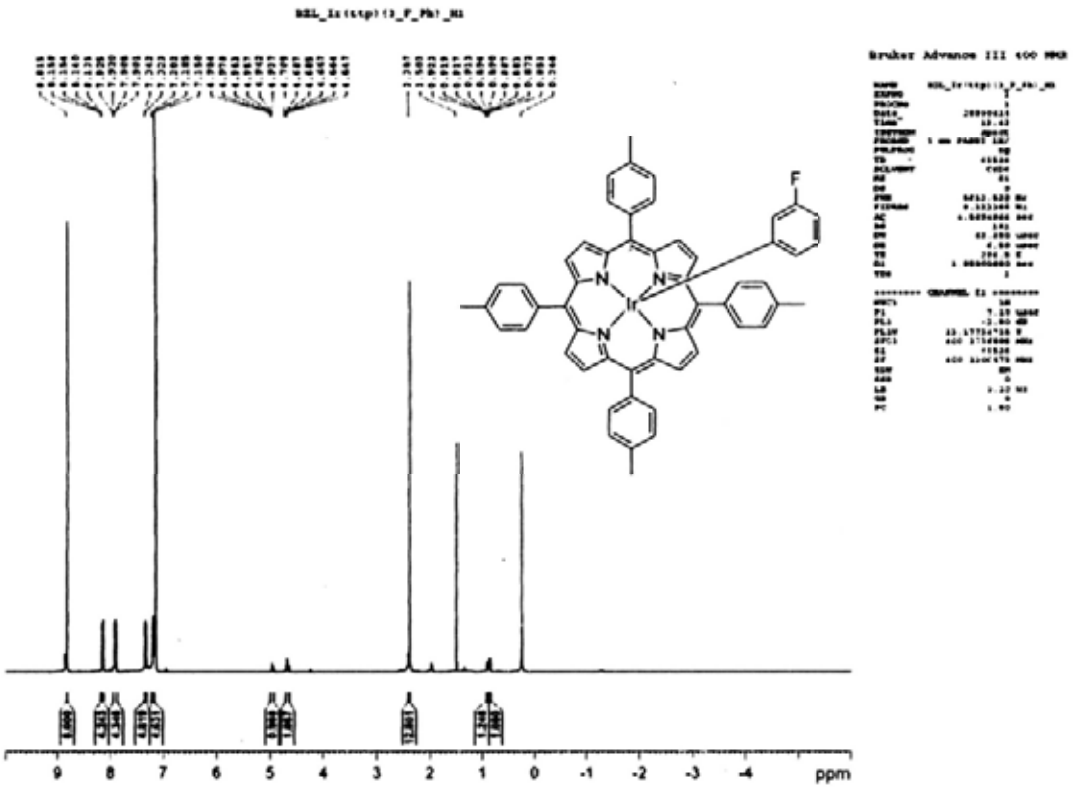

^{13}C NMR of Ir(ttp)(3-F-C_6H_4) **3d**

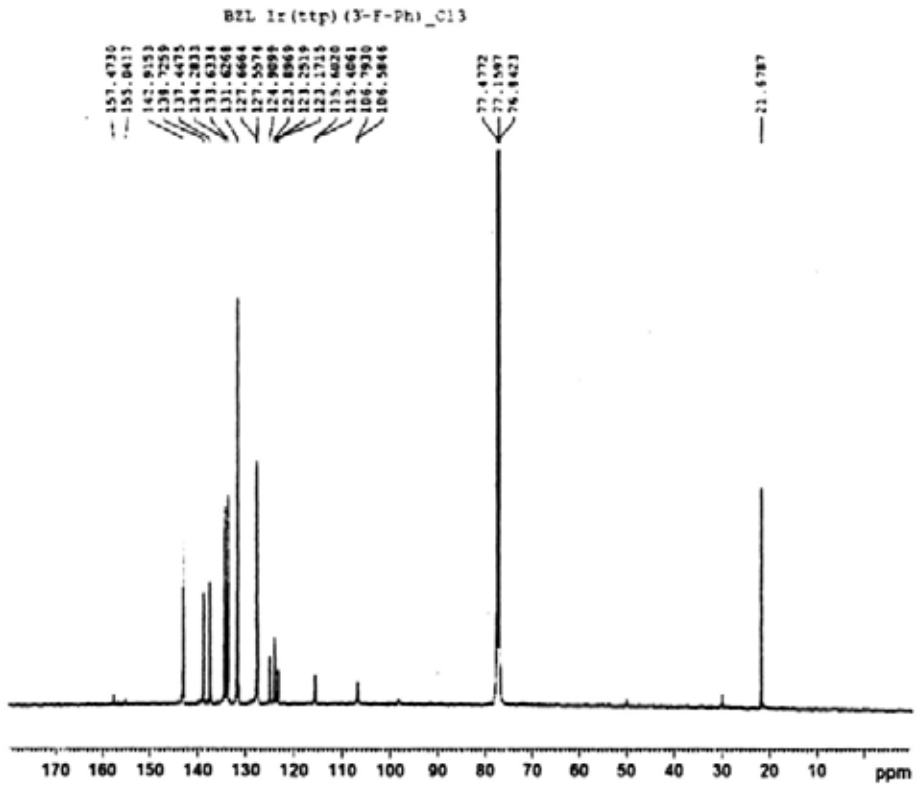

^{1}H NMR of Ir(ttp)(4-F-C_6H_4) **3e**

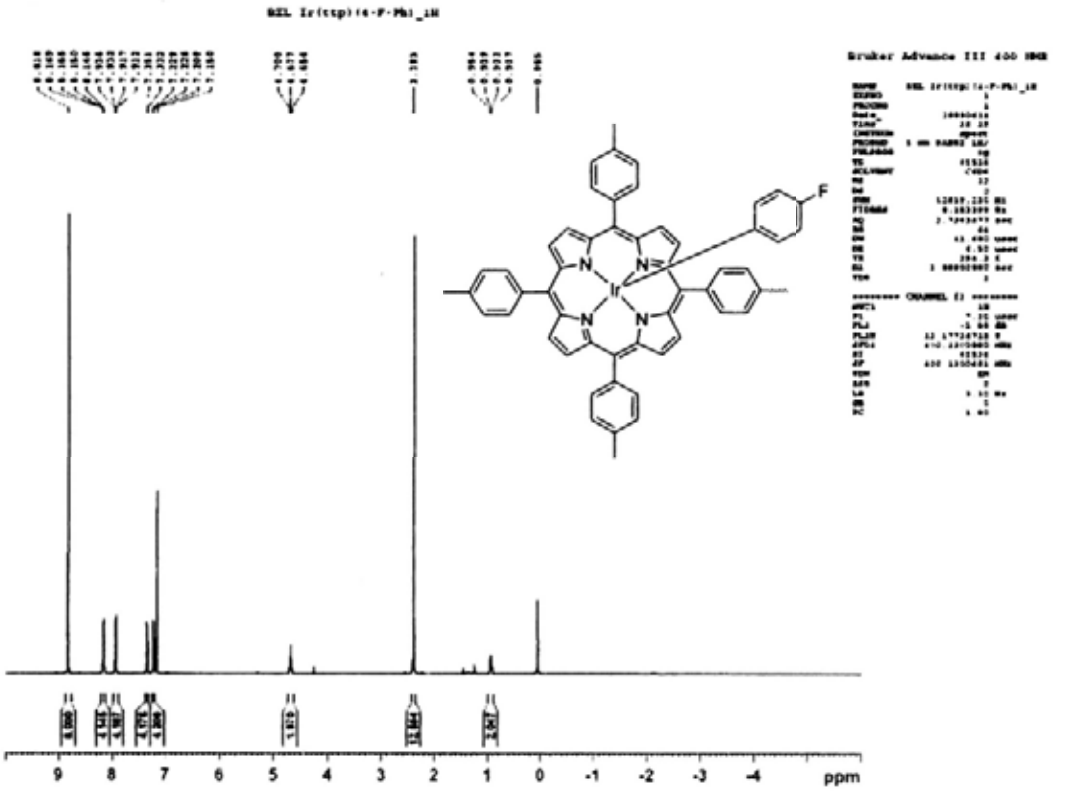

^{13}C NMR of Ir(ttp)(4-F-C_6H_4) **3e**

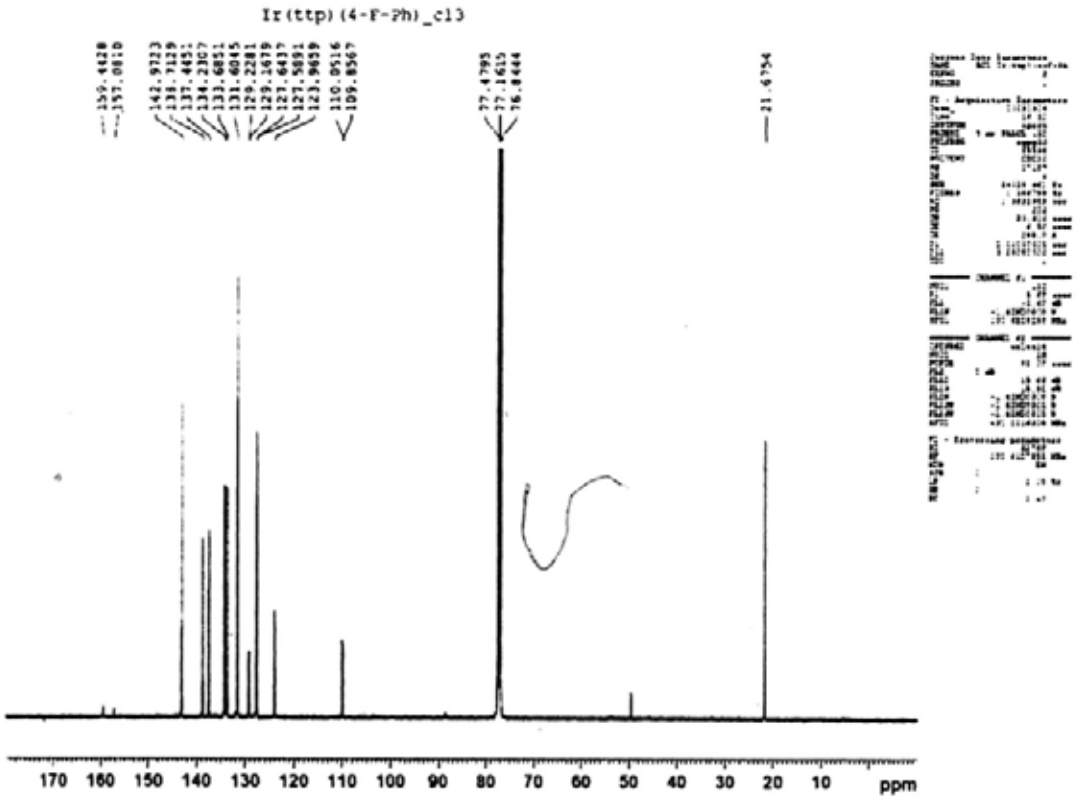

^{1}H NMR of Ir(ttp)(2,5-F_2-C_6H_3) **3f**

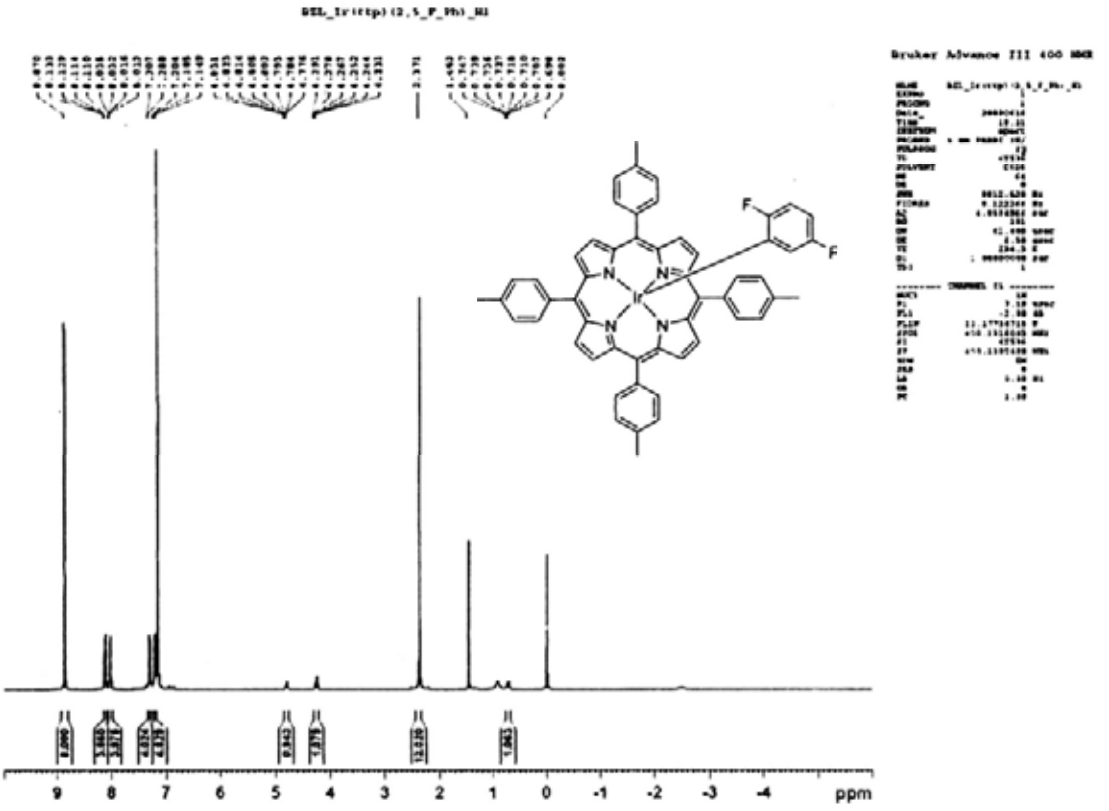

^{13}C NMR of Ir(ttp)(2,5-F_2-C_6H_3) **3f**

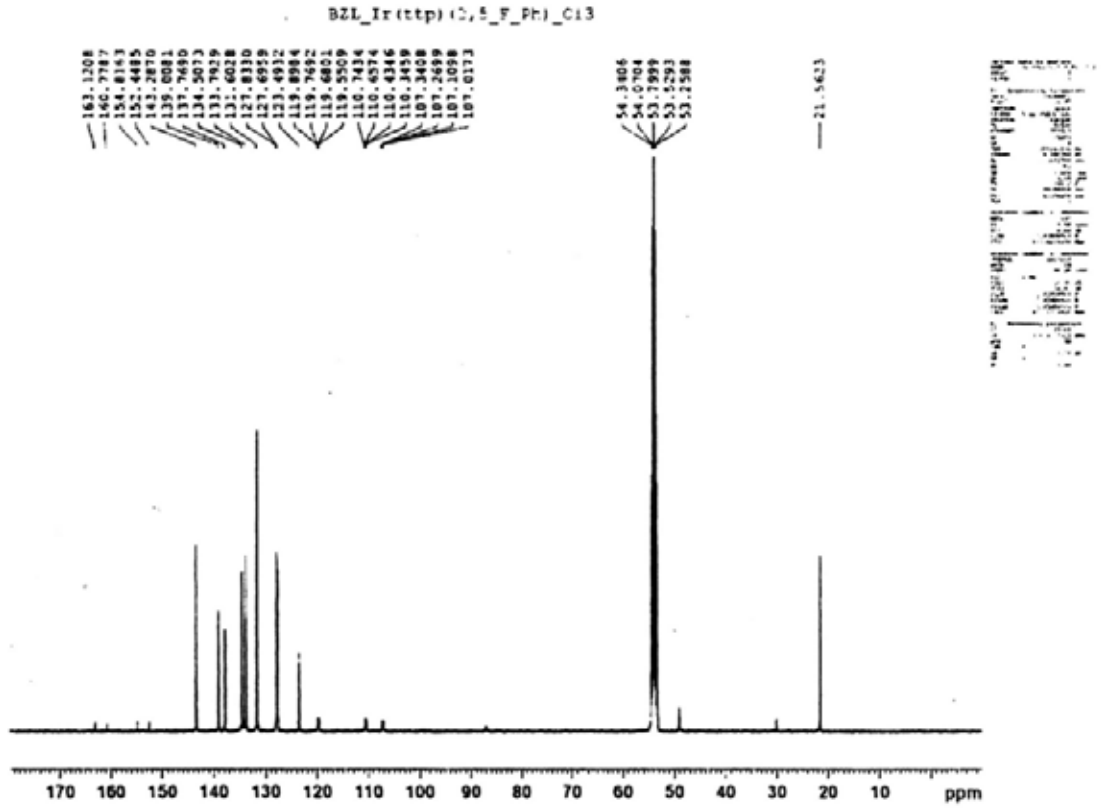

^{1}H NMR of Ir(ttp)(3,5-F_2-C_6H_3) **3g**

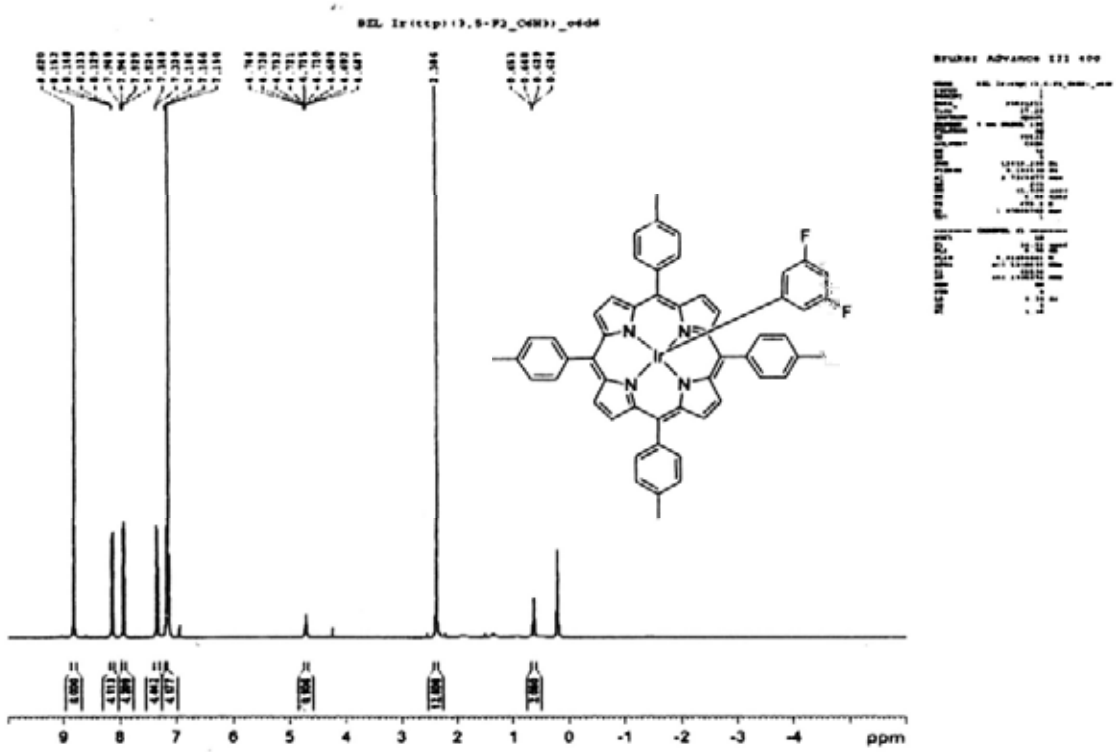

^{1}H NMR of Ir(ttp)(2,3,4,6-F_4-C_6H) **3h** .

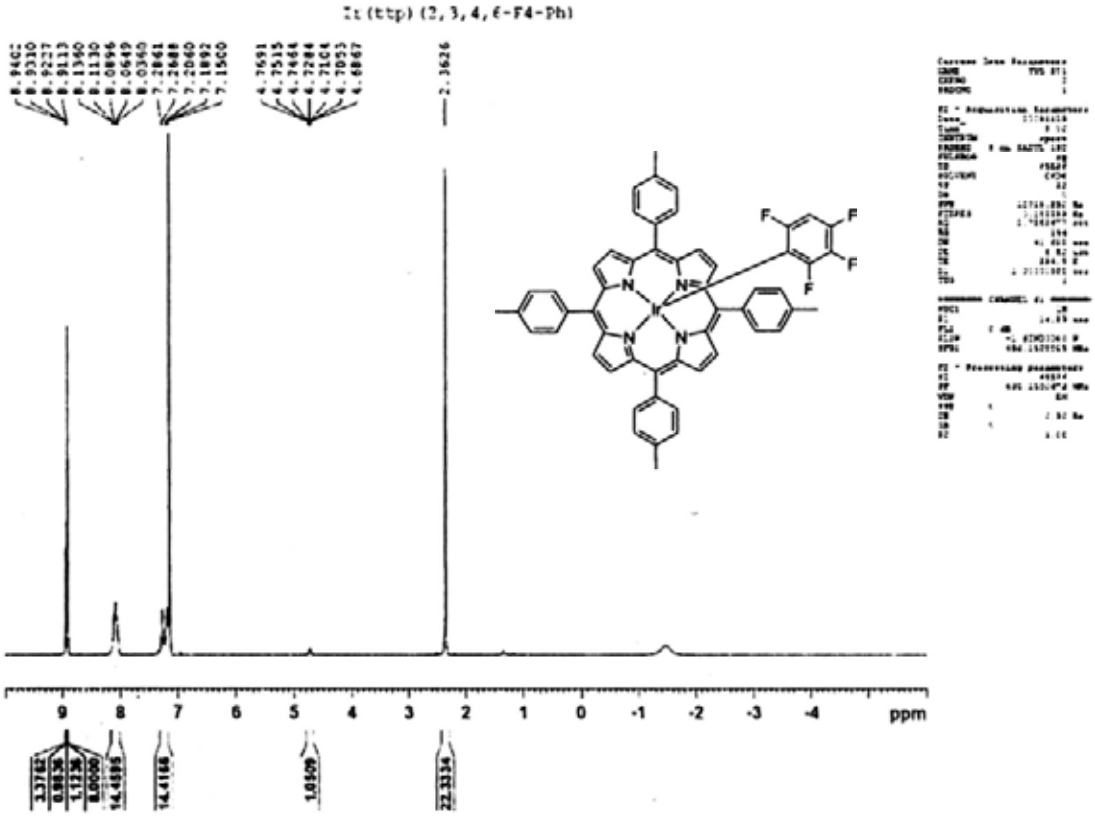

^{1}H NMR of Ir(ttp)C_6F_5 3i

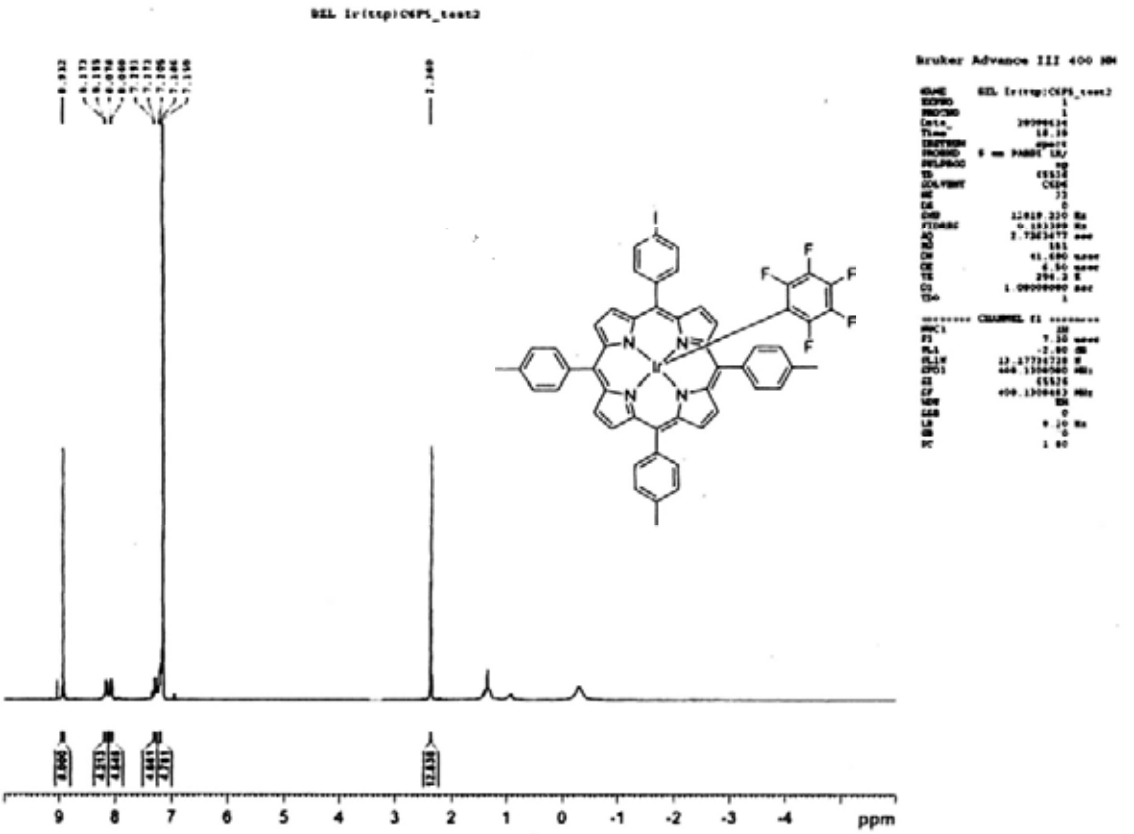

^{13}C NMR of Ir(ttp)C_6F_5 3i

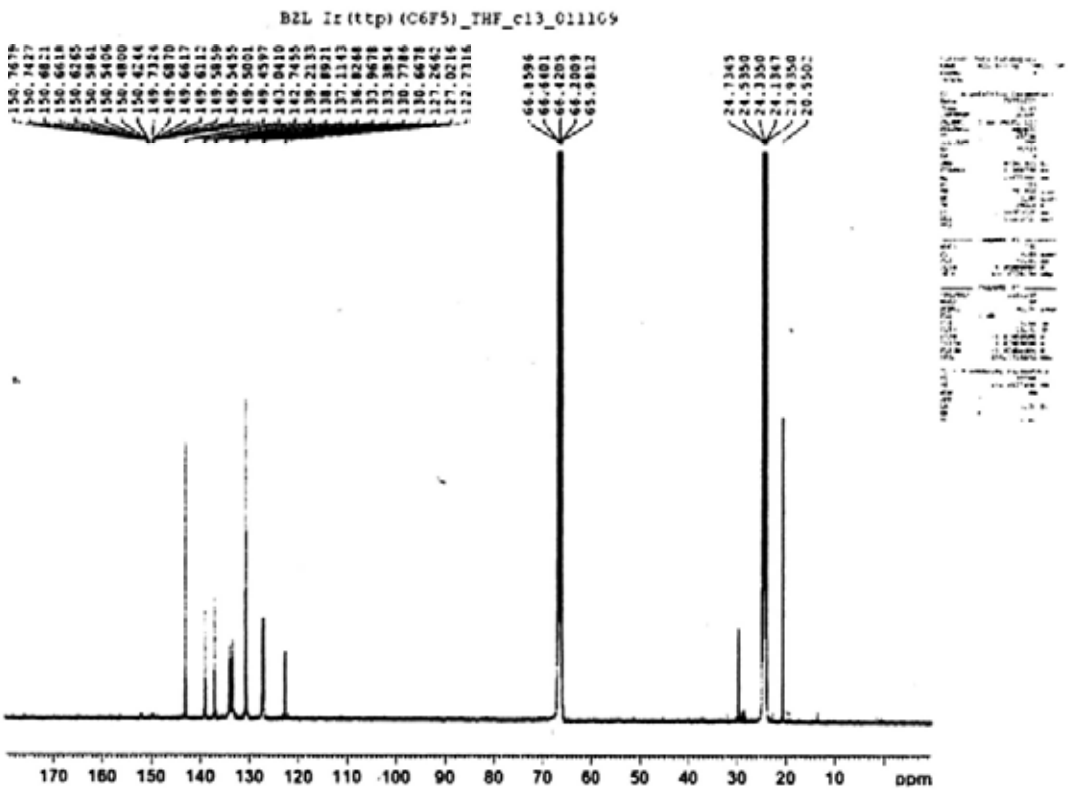

Table 10 List of ^{19}F NMR Spectra of Ir(ttp)Ar 3b-f, 3h-i

^{19}F NMR of Ir(ttp)(2-F-C_6H_4) **3b**

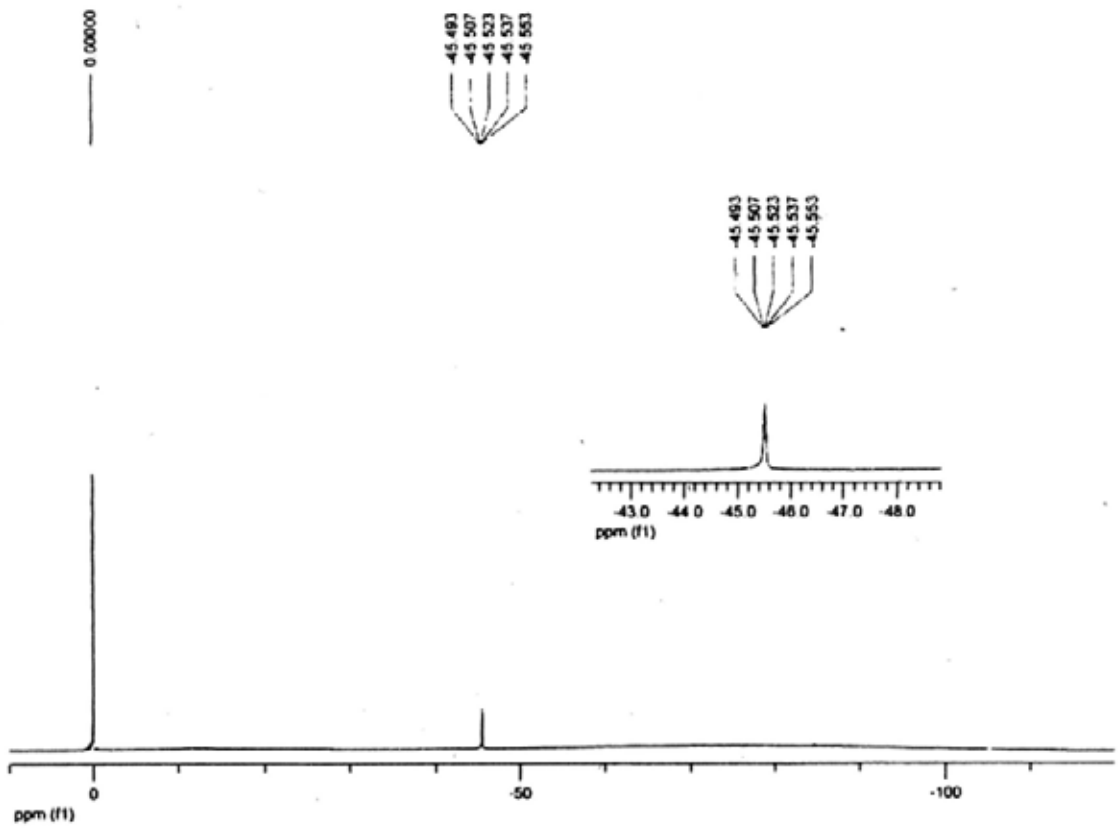

^{19}F NMR of Ir(ttp)(2,3-F_2-C_6H_3) **3c**

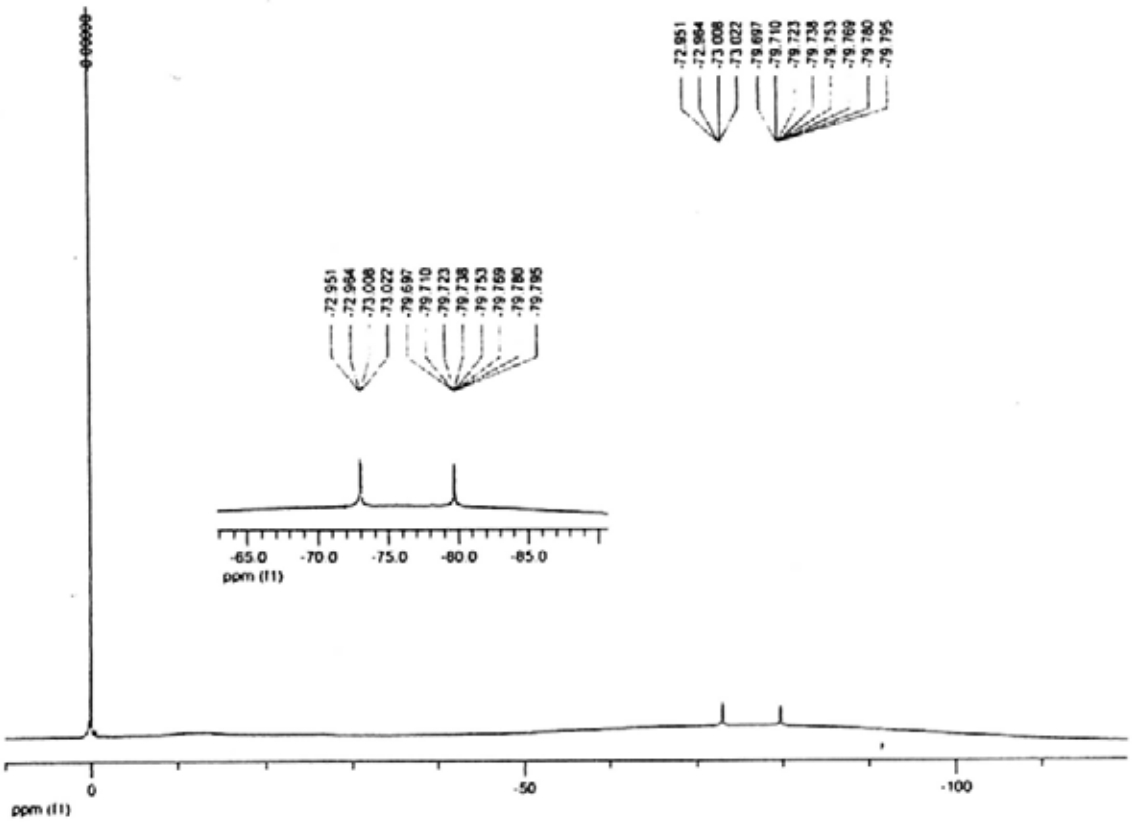

^{19}F NMR of Ir(ttp)(3-F-C_6H_4) **3d**

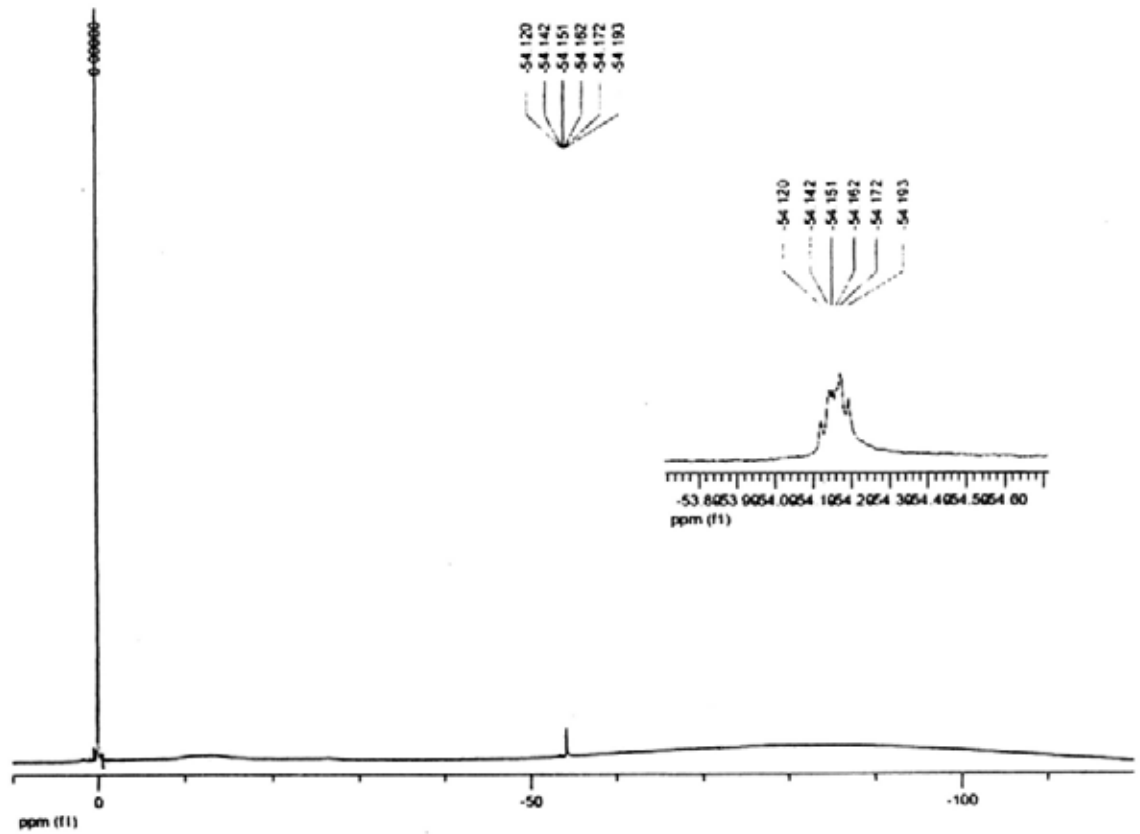

^{19}F NMR of Ir(ttp)(4-F-C_6H_4) **3e**

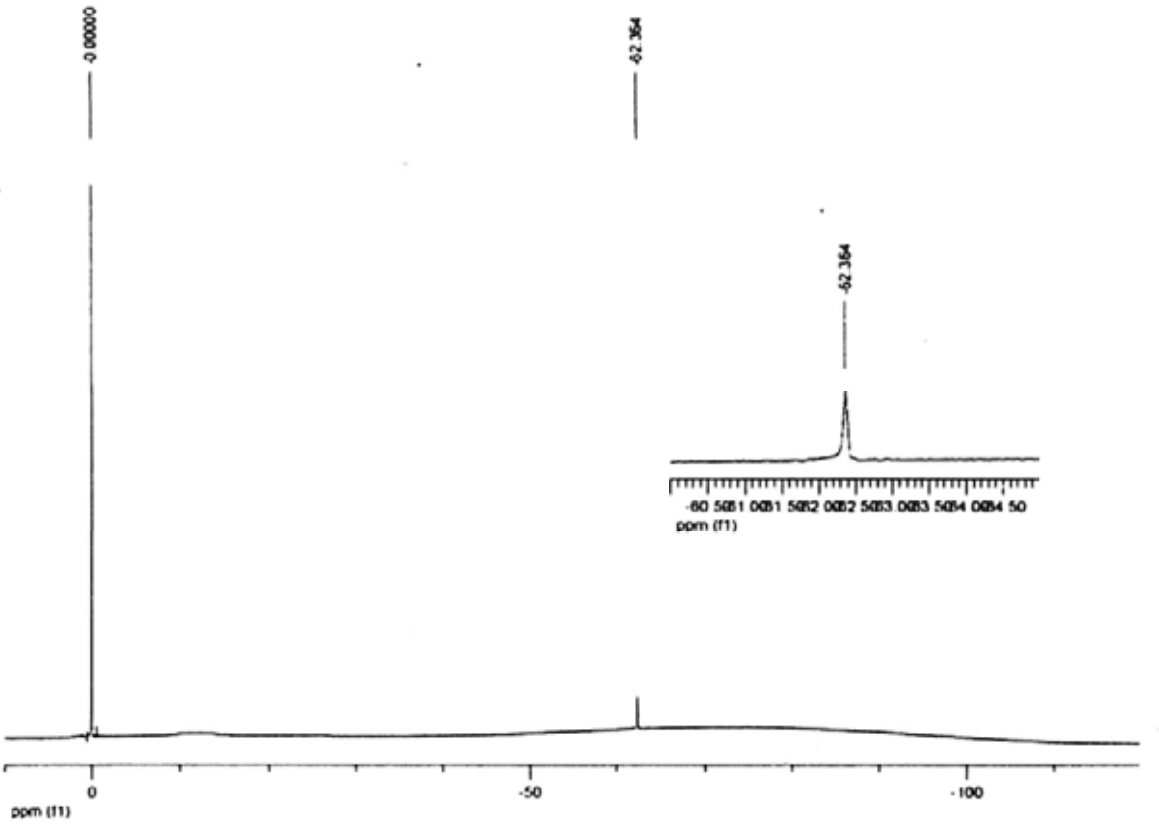

^{19}F NMR of Ir(ttp)(2,5-F_2-C_6H_3) **3f**

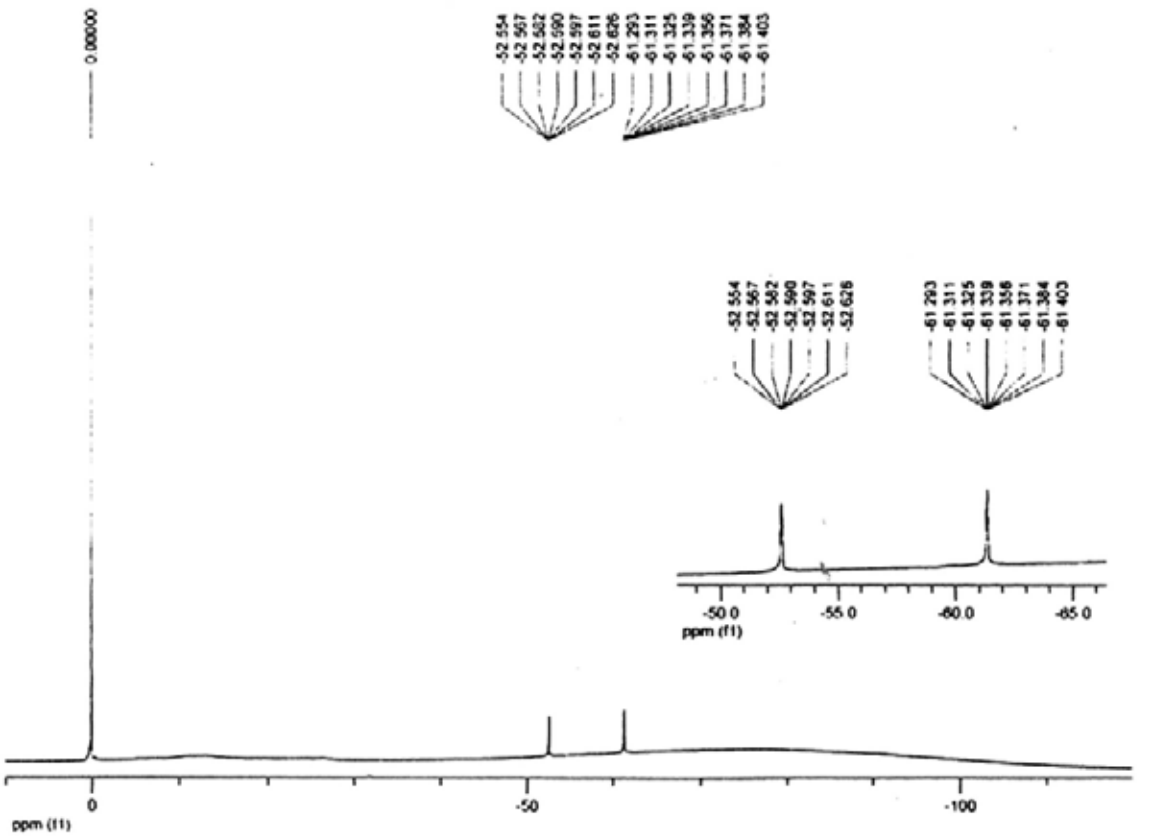

^{19}F NMR of Ir(ttp)(2,3,4,6-F_4-C_6H) **3h**

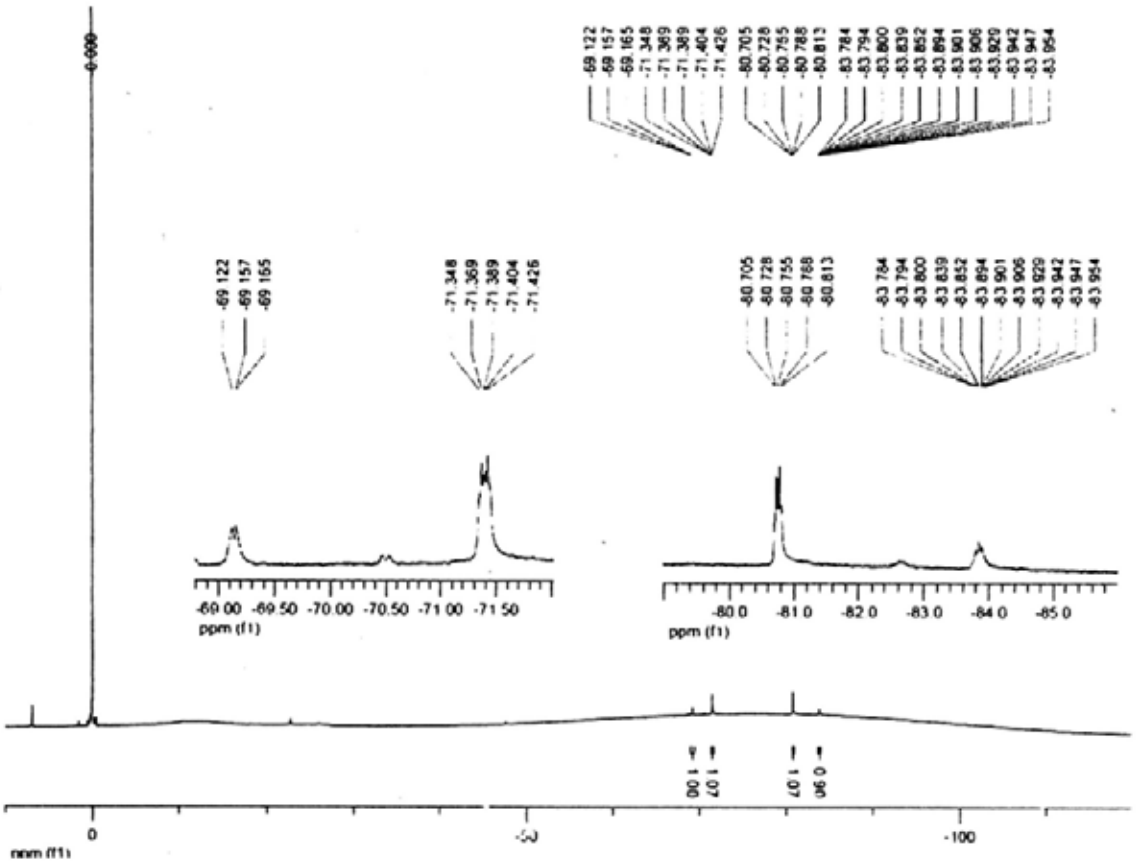

^{19}F NMR of Ir(ttp)C_6F_5 **3i**

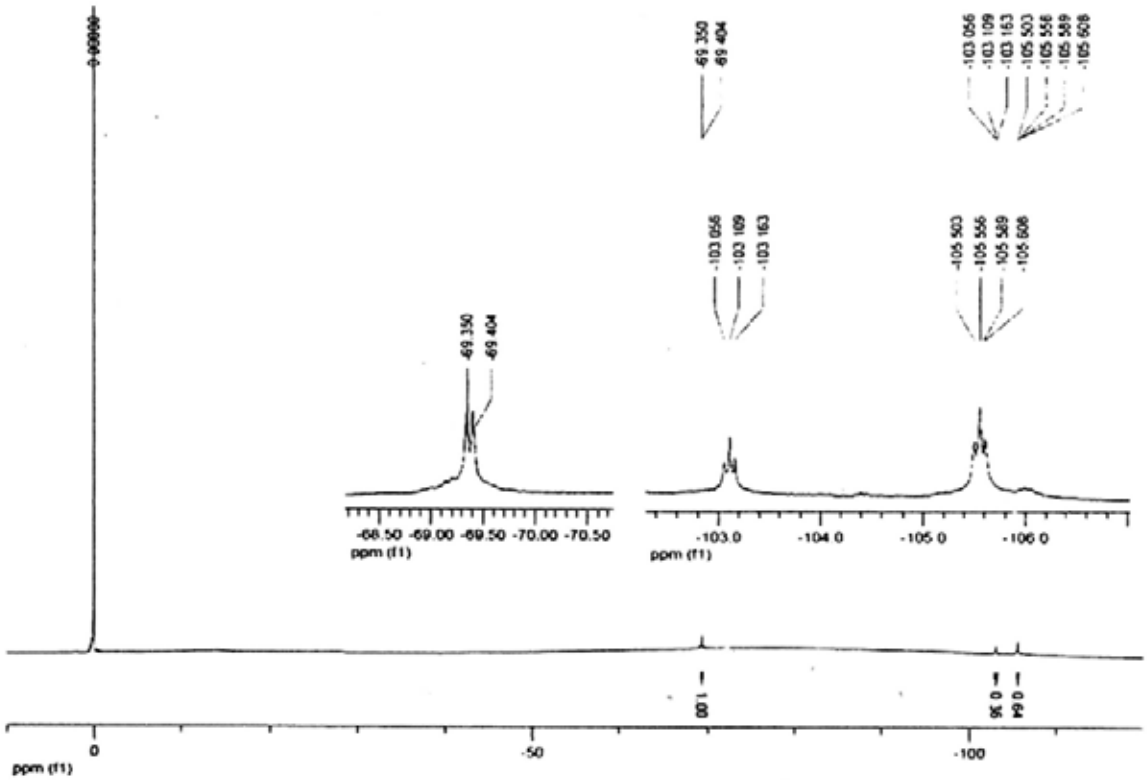

Table 11 List of ^{1}H NMR Spectra of Ir(ttp)Ar(PPh_3) 3a'-g' and 3i'

^{1}H NMR of Ir(ttp)(C_6H_5)(PPh_3) **3a'**

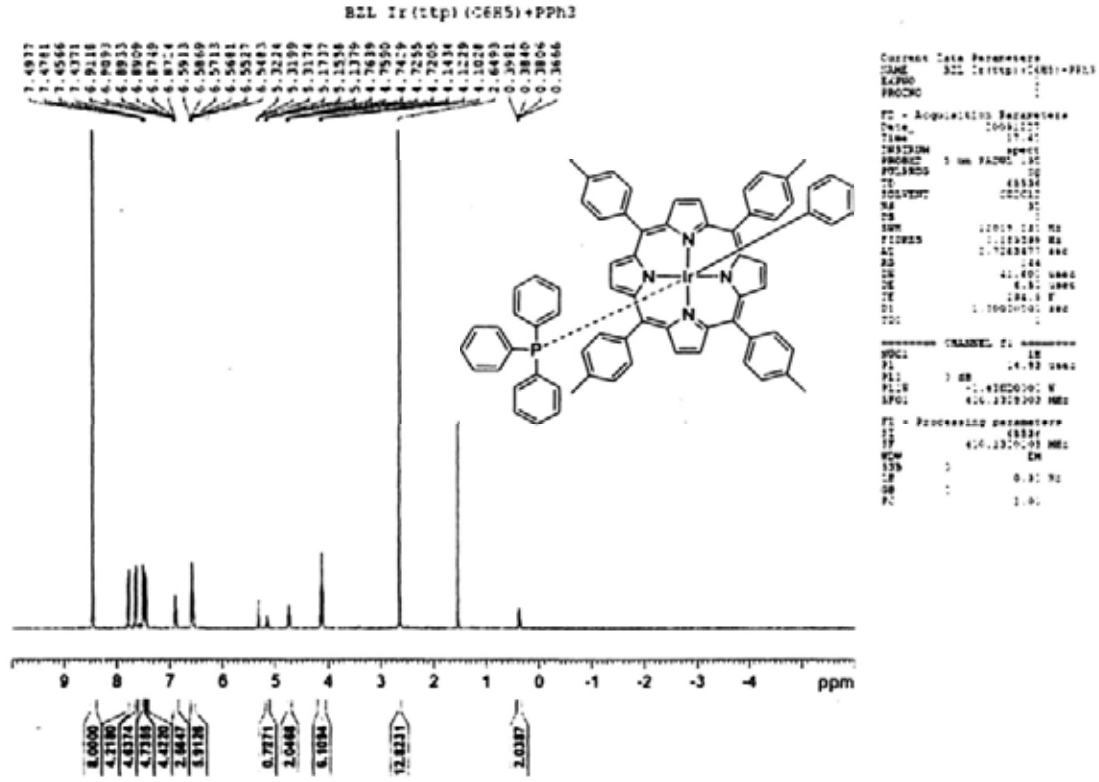

^{1}H NMR of Ir(ttp)(2-F-C_6H_4)(PPh_3) **3b'**

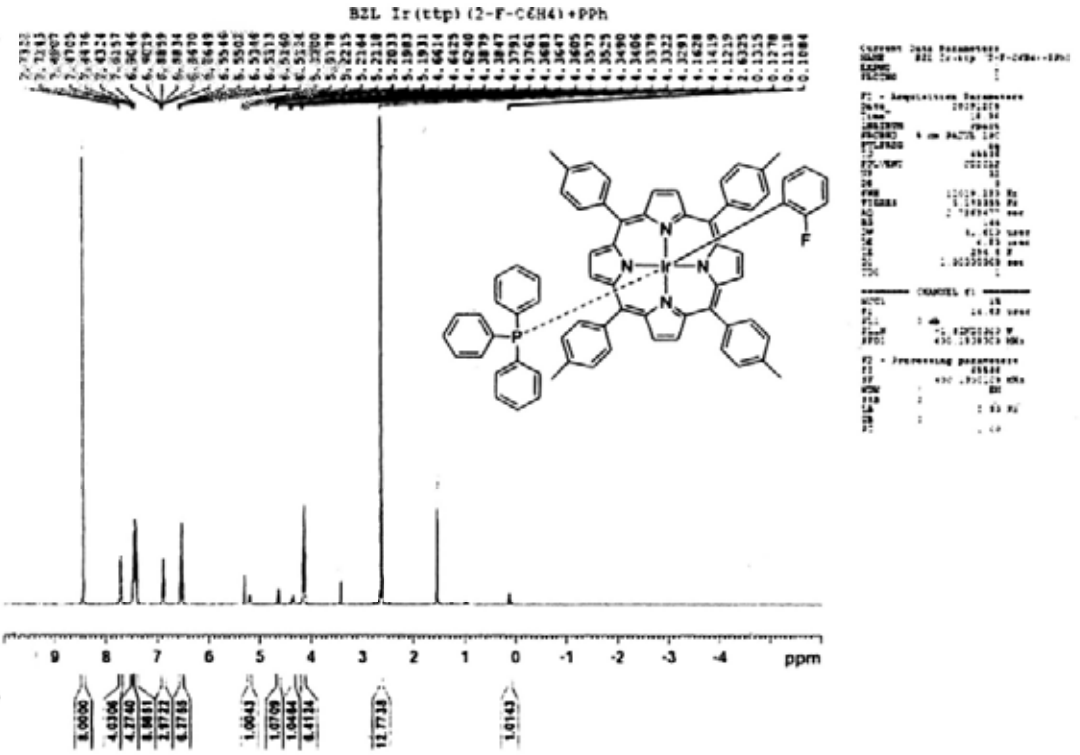

^{1}H NMR of Ir(ttp)(2,3-F_2-C_6H_3)(PPh_3) **3c'**

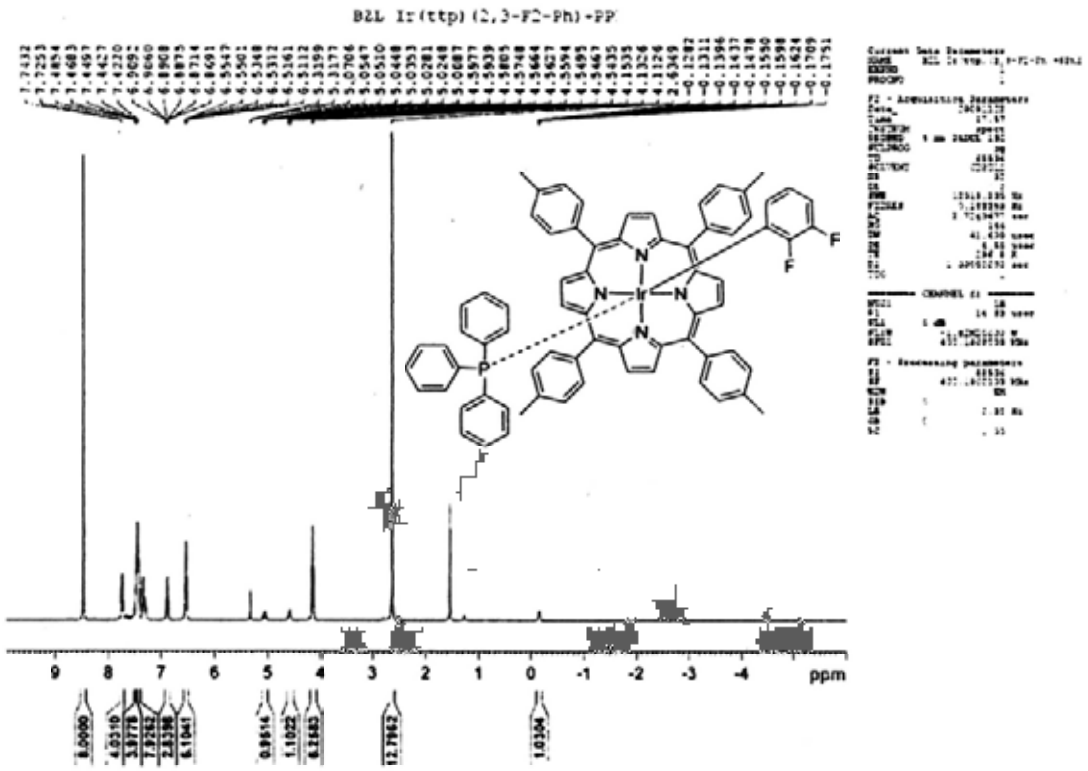

^{1}H NMR of Ir(ttp)(3-F-C_6H_4)(PPh_3) **3d'**

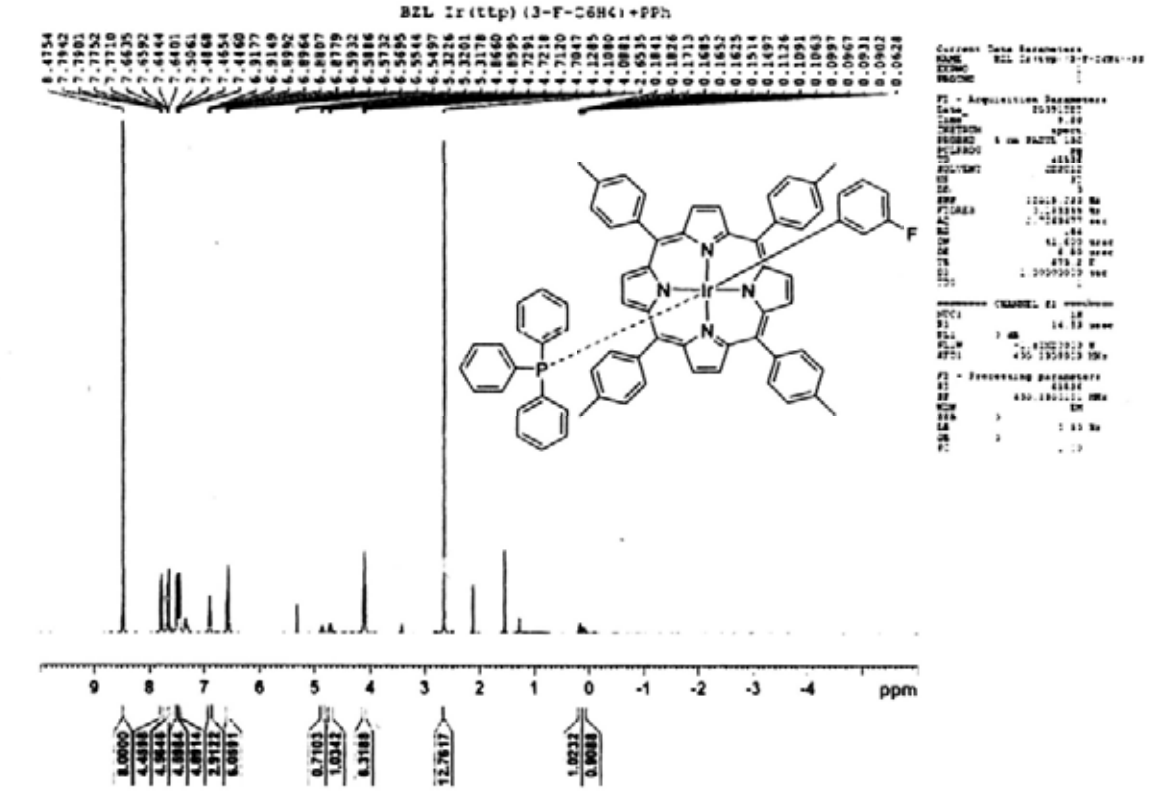

^{1}H NMR of Ir(ttp)(4-F-C_6H_4)(PPh_3) **3e'**

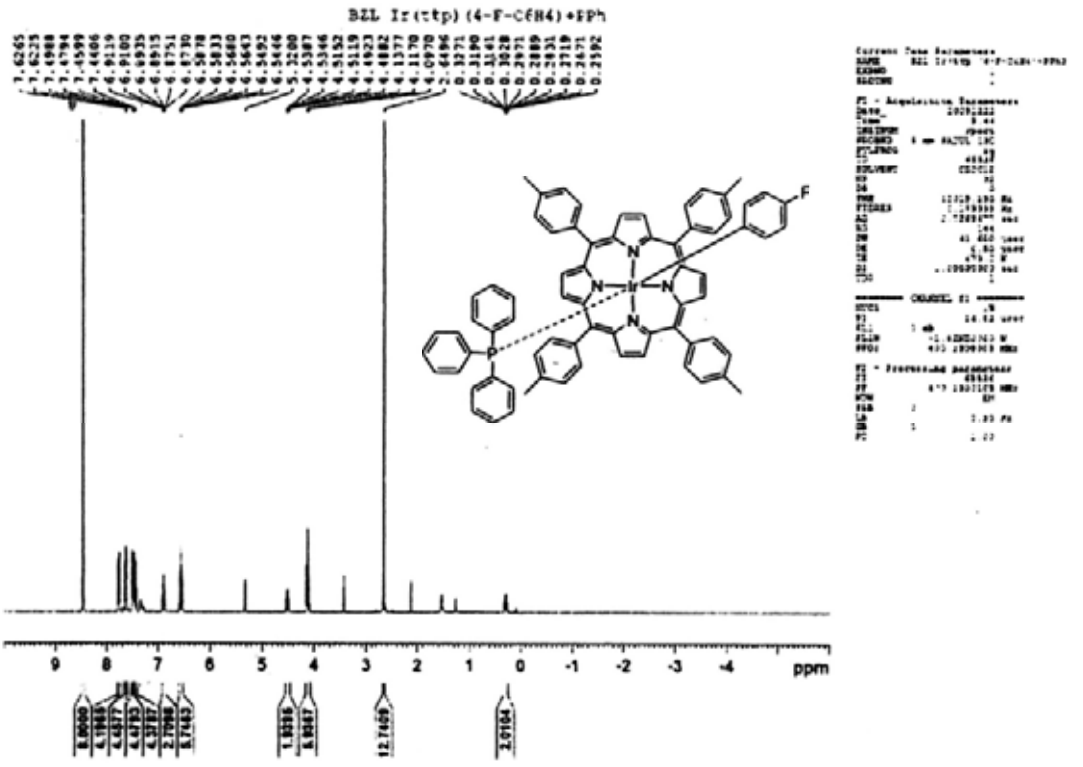

^{1}H NMR of Ir(ttp)(2,5-F_2-C_6H_3)(PPh_3) **3f'**

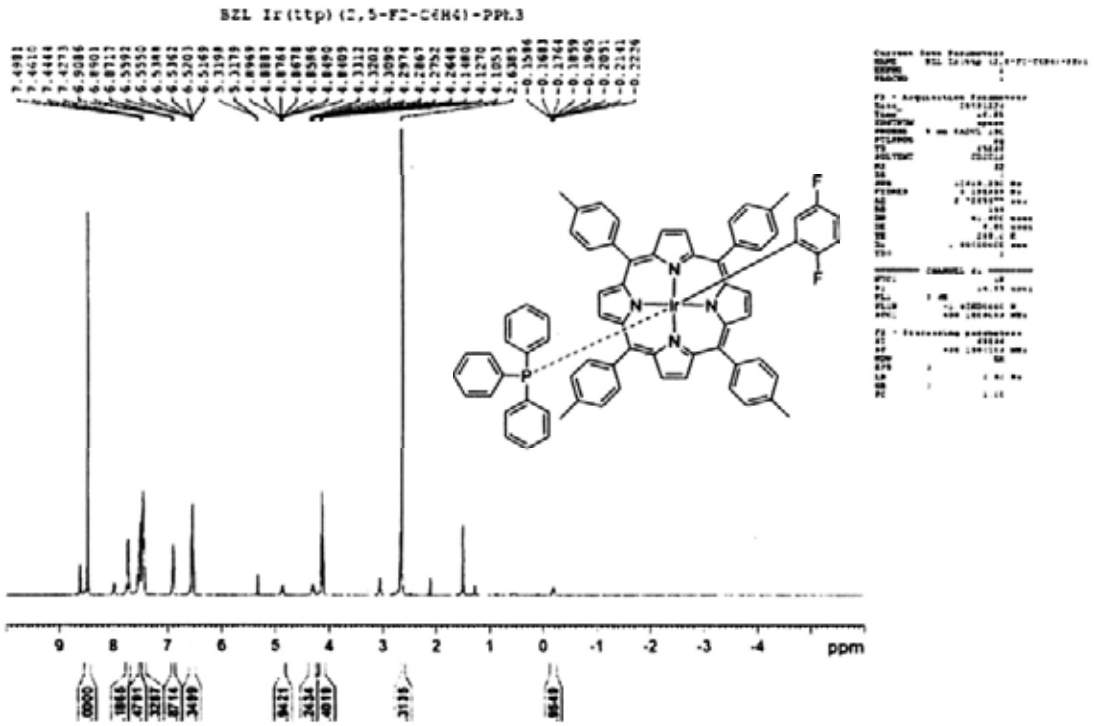

^{1}H NMR of Ir(ttp)(3,5-F_2-C_6H_3)(PPh_3) **3g**

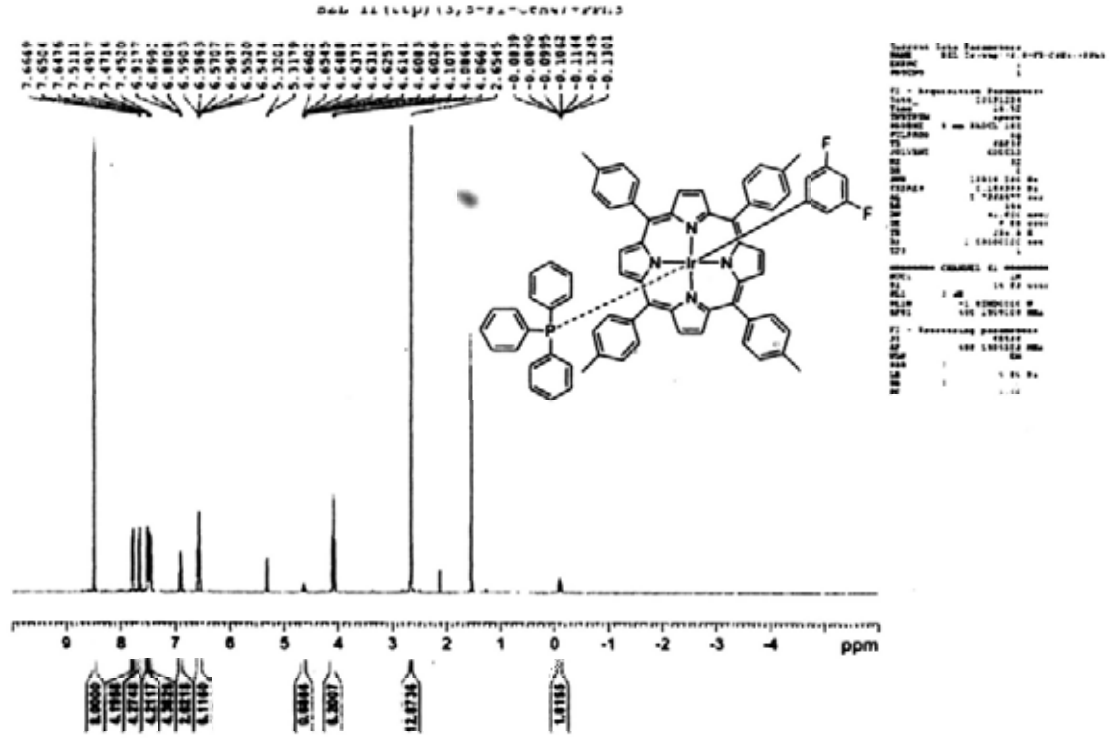

^{1}H NMR of Ir(ttp)(C_6F_5)(PPh_3) **3i'**

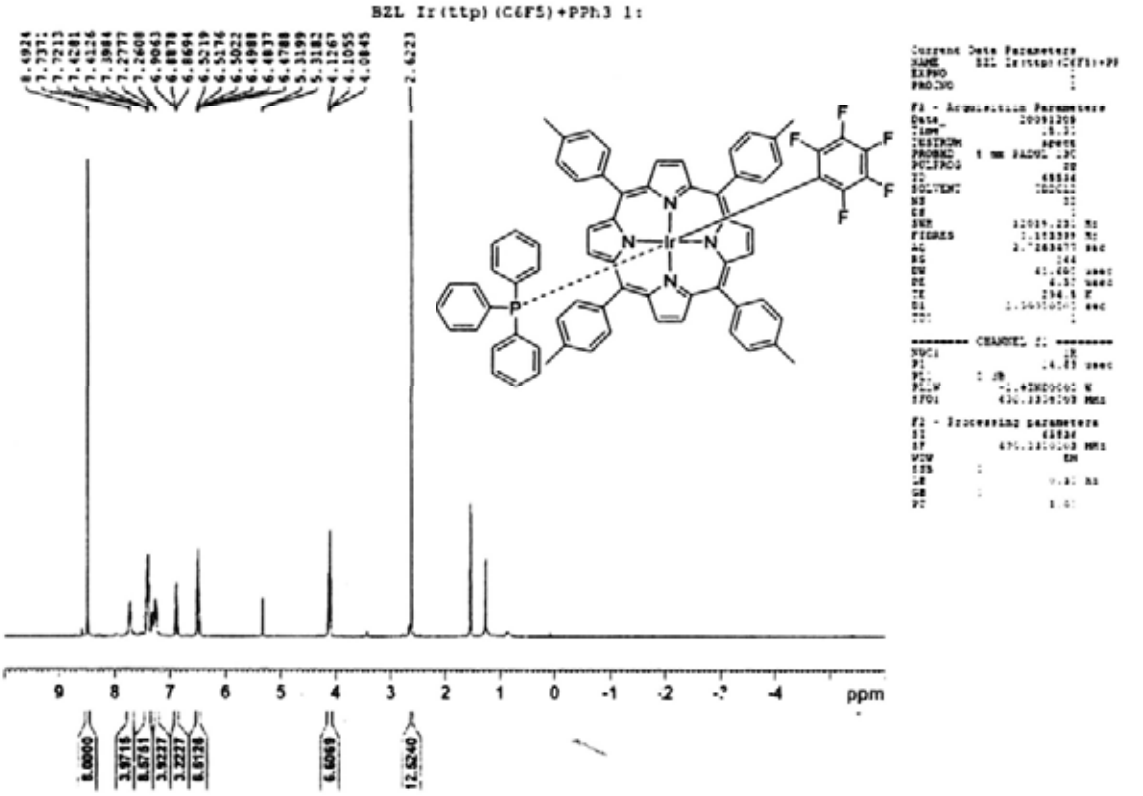

II.VI Chemical Shift for [ArIr(ttp)OH]⁻ 4a-d in Benzene-d_6

Table 12 ^{1}H NMR Spectra for 4a-d

Entry	Compound Name	Chemical Shift
1	$[C_6H_5Ir(ttp)OH]^-$ **4c** 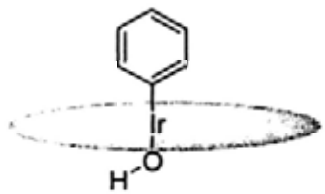	-10.95 (s, 1 H), 1.49 (d, 2 H, J = 7.8 Hz), 2.38 (s, 12 H), 4.91 (t, 2 H, J = 7.3 Hz), 5.21 (tt, 1 H, J = 1.1, 6.5 Hz), 7.07 (dd, 4 H, J = 1.2, 7.2 Hz), 7.24 (ddd, 8 H, J = 1.3, 7.2, 16.2[a] Hz), 7.76 (dd, 4 H, J = 1.2, 7.8 Hz), 8.16 (s, 8 H)
2	$[(4\text{-}F\text{-}C_6H_4)Ir(ttp)OH]^-$ **4a** 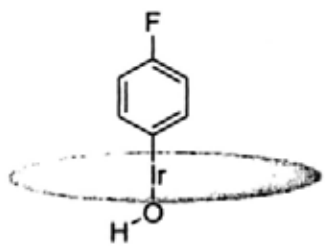	-10.94 (s, 1 H), 1.37 (d, 2 H, J = 4.8 Hz), 2.36 (s, 12 H), 4.73 (dd, 2 H, $^3J_{H\text{-}F}$ = 8.8 Hz, J = 8.8 Hz), 7.06 (d, 4 H, J = 7.6 Hz), 7.27 (s, 8 H), 7.59 (d, 4 H, J = 6.8 Hz), 8.16 (s, 8 H)
3	$[(2,5\text{-}F_2\text{-}C_6H_3)Ir(ttp)OH]^-$ **4b** 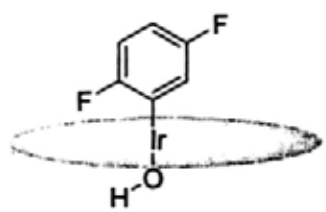	-11.14 (s, 1 H), 0.91[b] (m, 1 H), 2.34 (s, 12 H), 4.31 (m, 1 H), 4.57 (m, 1 H), 7.06 (s, 4 H), 7.25 (s, 8 H), 7.67 (s, 4 H), 8.23 (s, 8 H)
4	$[C_6F_5Ir(ttp)OH]^-$ **4d** 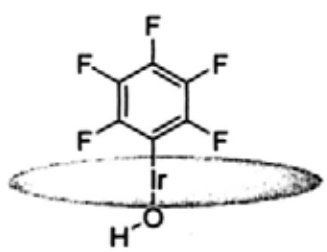	-6.80[c] (s, 1H), 2.37 (s, 12 H), 7.08 (s, 4 H), 7.33 (s, 8 H), 7.81 (s, 4 H), 8.41 (s, 8 H)

[a] The protons may be affected by fluorine in added 1,4-difluorobenzene. [b] Most likely, the proton was overlapped with the impurities. [c] No peak was observed at around -10 ~ -12 ppm, most likely, -6.80 ppm was possible peak for hydroxyl group.

^{1}H NMR Spectrum of $[C_6H_5Ir(ttp)OH]^-$ **4c**

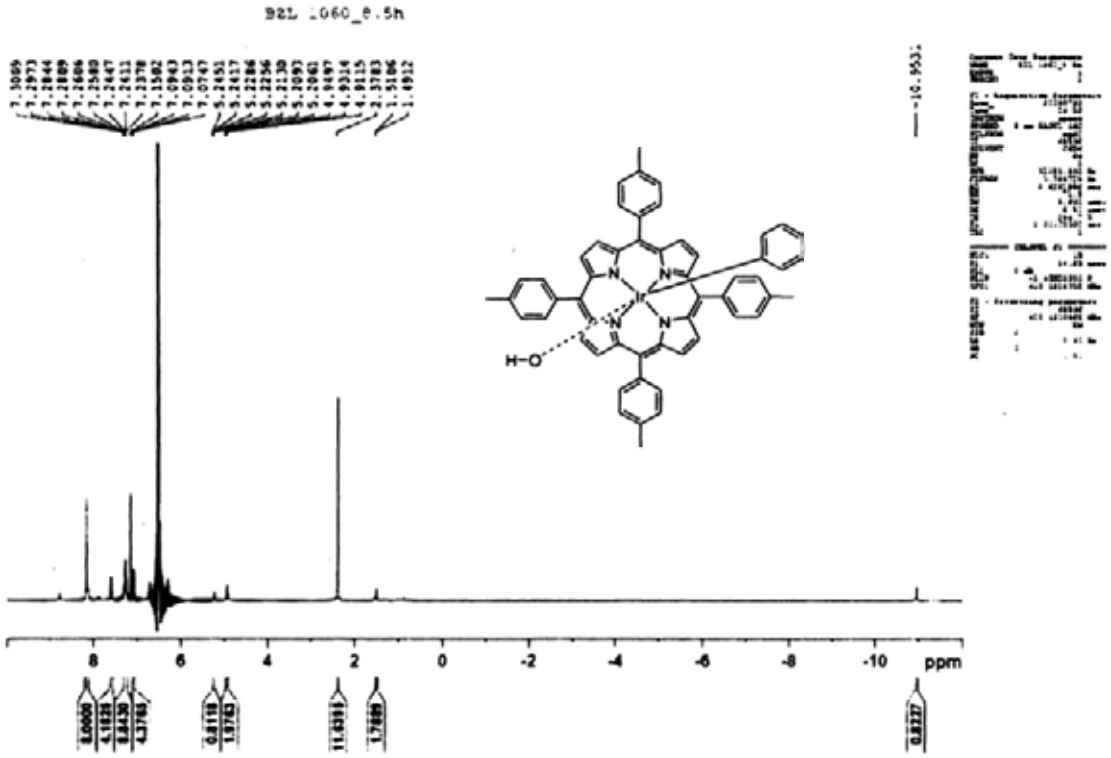

^{1}H NMR Spectrum of $[(4\text{-}F\text{-}C_6H_4)Ir(ttp)OH]^-$ **4a**

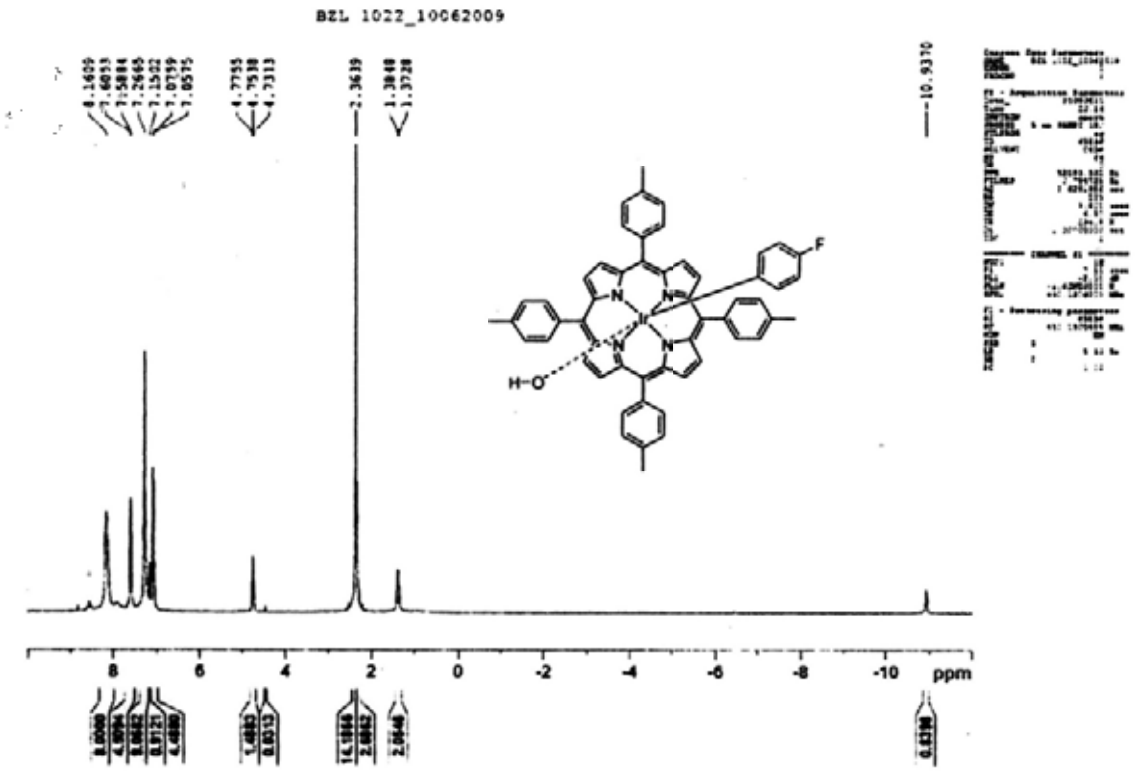

^{1}H NMR Spectrum of [(2,5-F_2-C_6H_3)Ir(ttp)OH]$^-$ **4b**

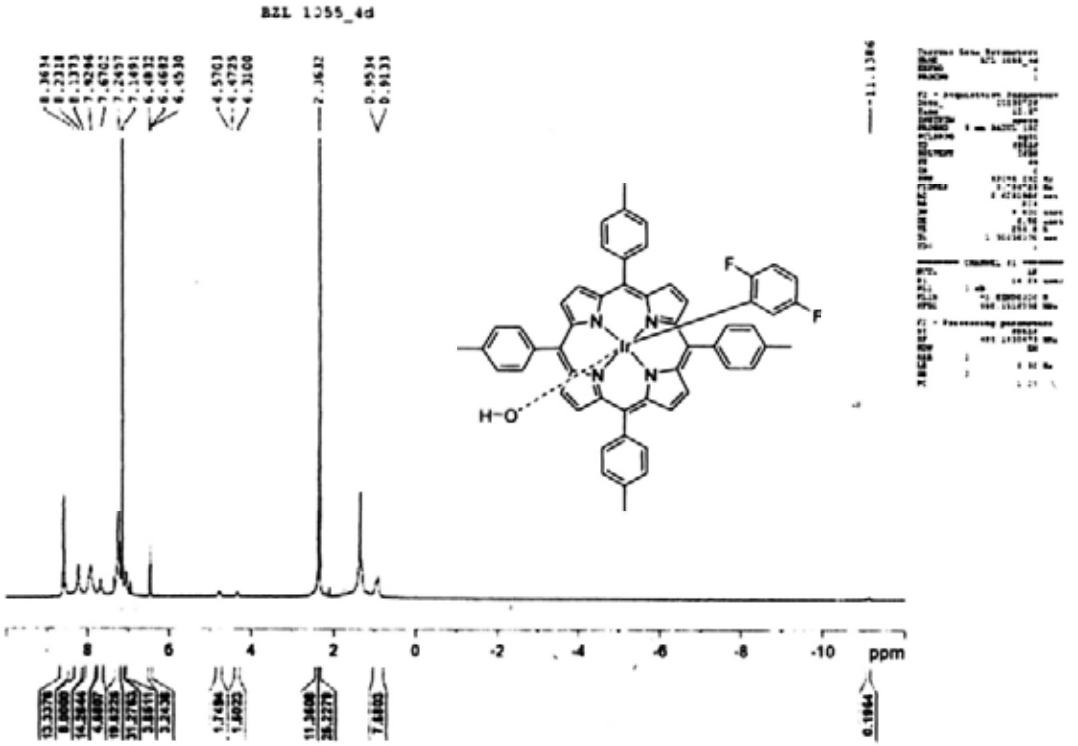

^{1}H NMR Spectrum of [C_6F_5Ir(ttp)OH]$^-$ **4d**

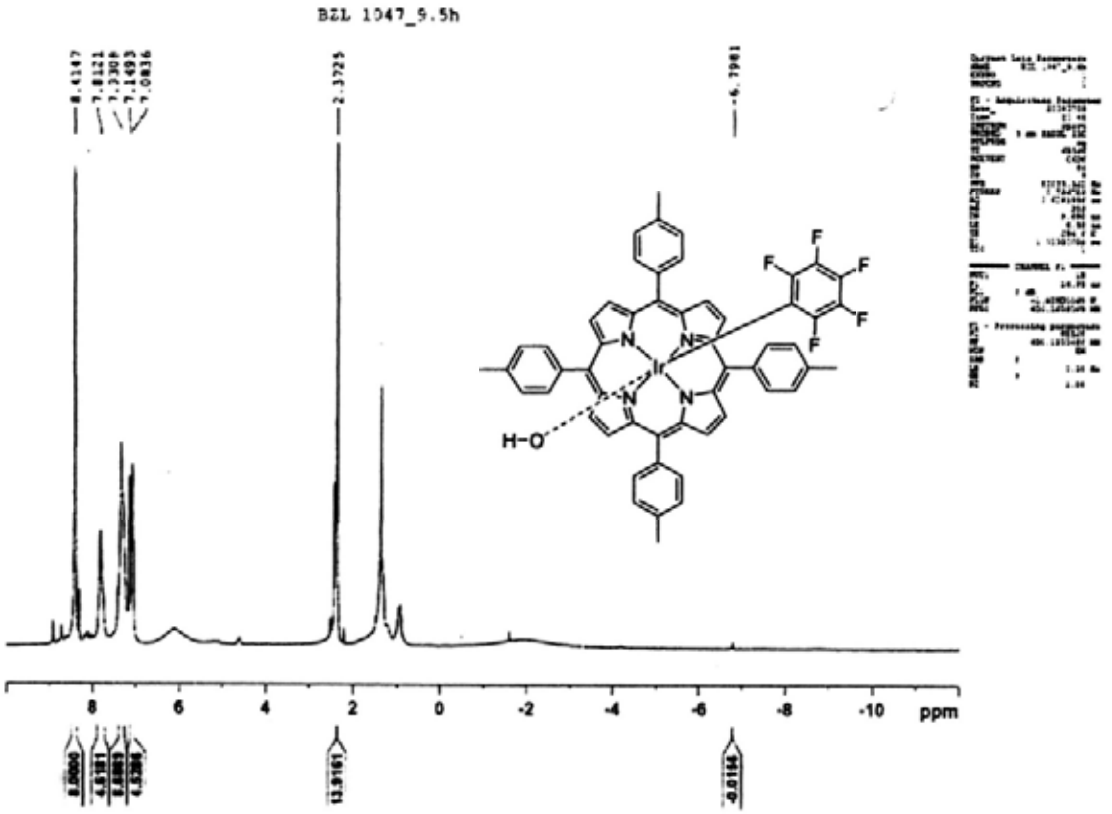

Appendix III (Chapter 4)

III.I ^{1}H and ^{13}C NMR Spectra of Ir(ttp)R 4a-f and 3a-d, 3f

Table 13 List of ^{1}H and ^{13}C NMR Spectra of Ir(ttp)R 4a-f and 3a-d, 3f,

^{1}H NMR of Ir(ttp)CO(4-F-C_6H_4) **3a**

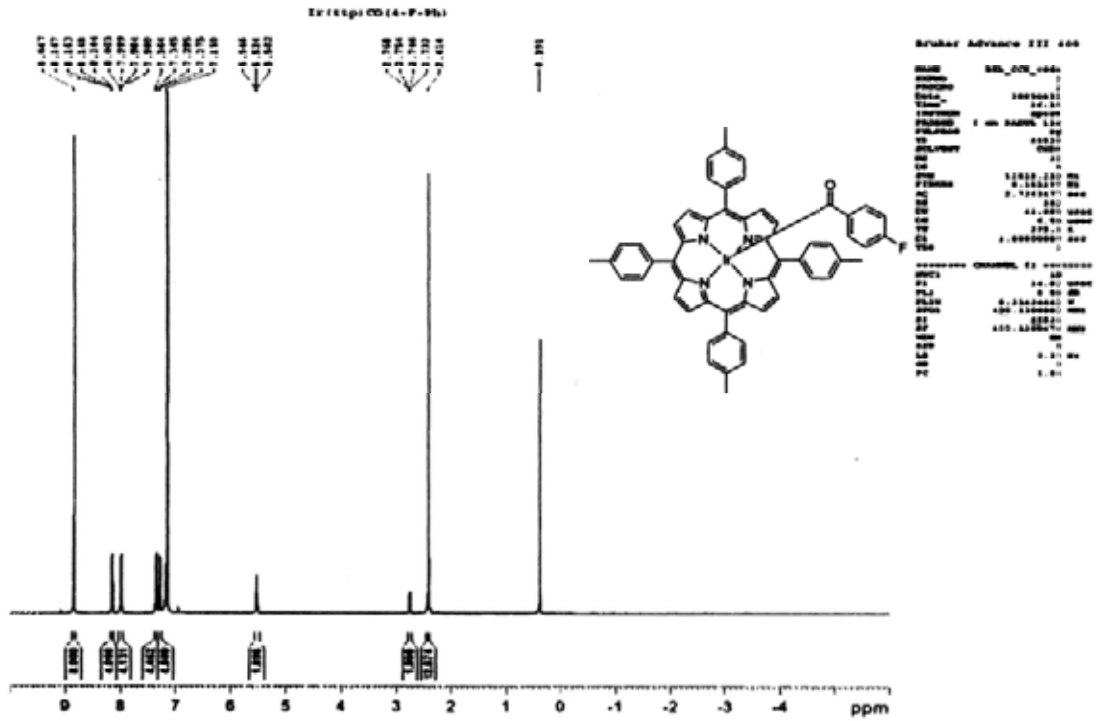

^{1}H NMR of Ir(ttp)COC_6H_5 **3b**

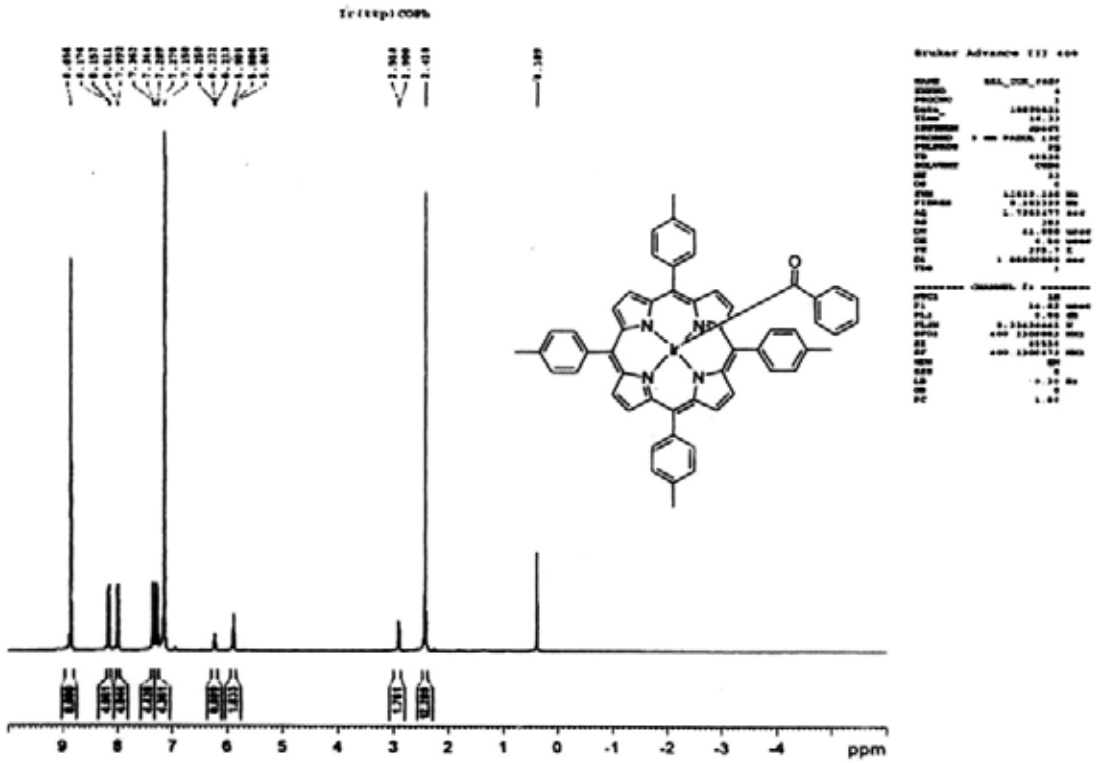

^{1}H NMR of Ir(ttp)CO(4-Me-C_6H_4) **3c**

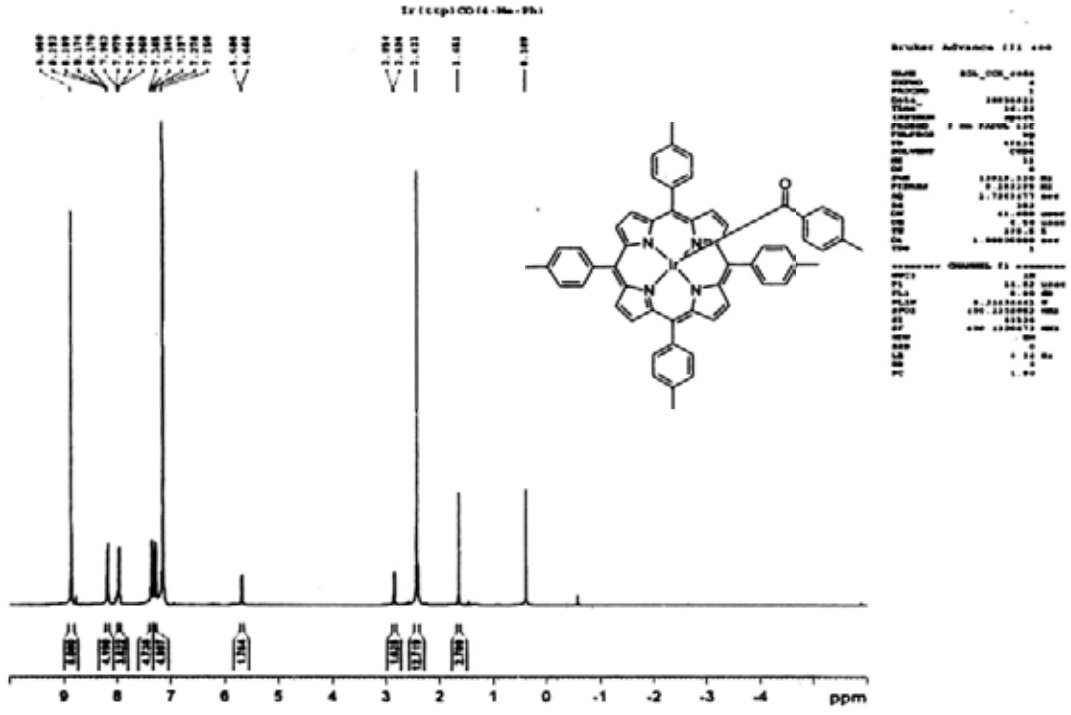

^{1}H NMR of Ir(ttp)CO(4-OMe-C_6H_4) **3d**

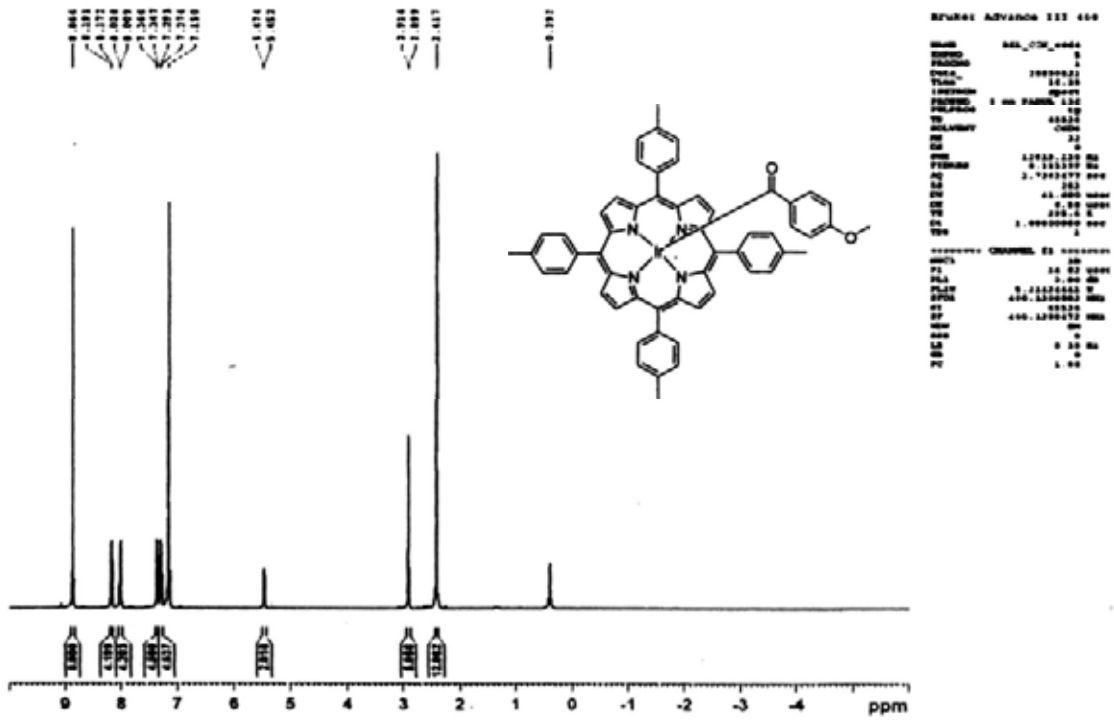

^{1}H NMR of Ir(ttp)$CH_2COC_6H_5$ **4a**

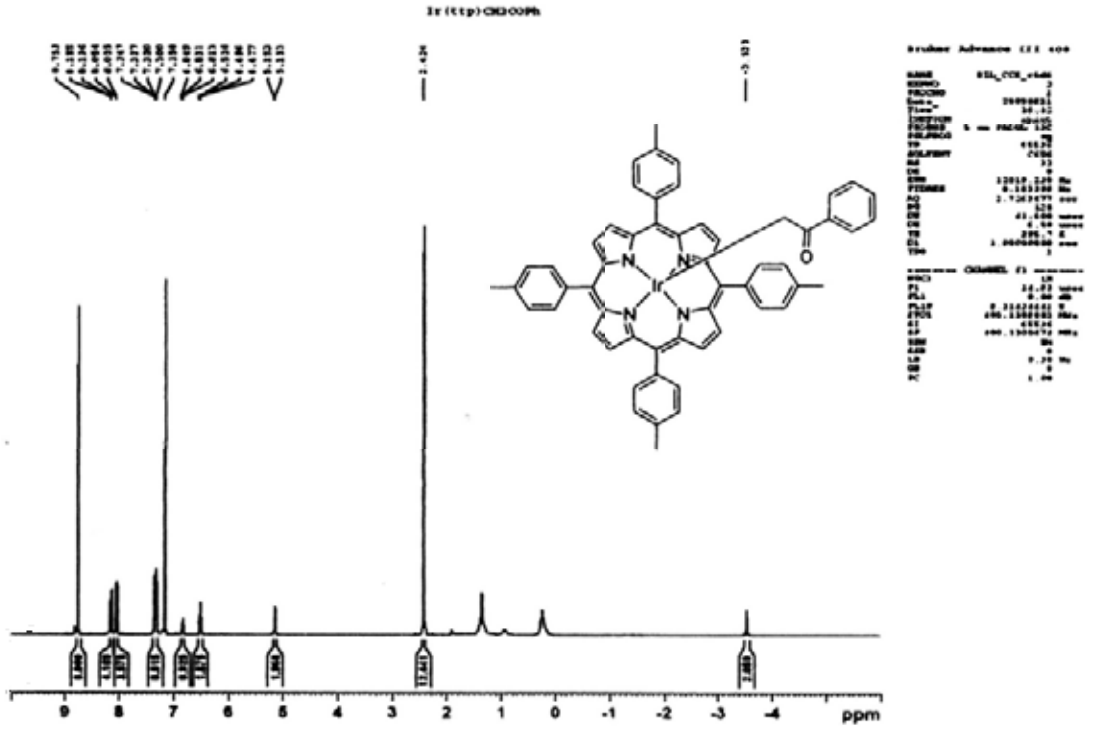

^{13}C NMR of Ir(ttp)$CH_2COC_6H_5$ **4a**

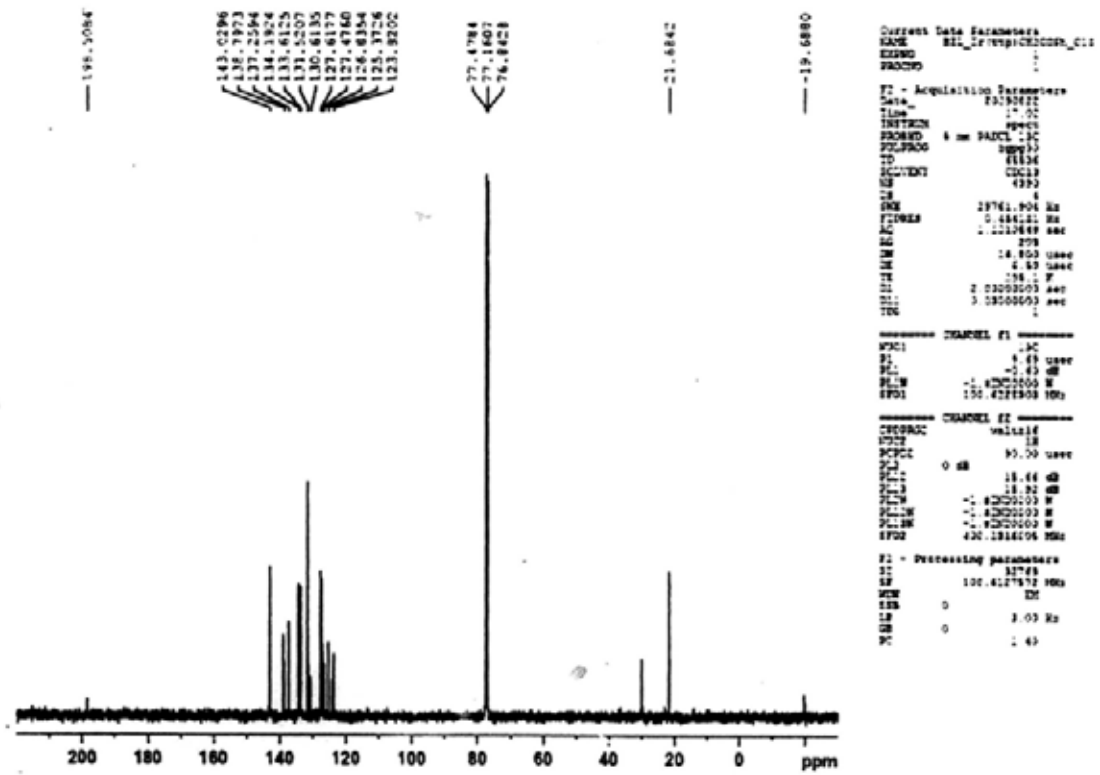

^{1}H NMR of Ir(ttp)(*meta*-&*para*-COMe-C_6H_4) **4b-c**

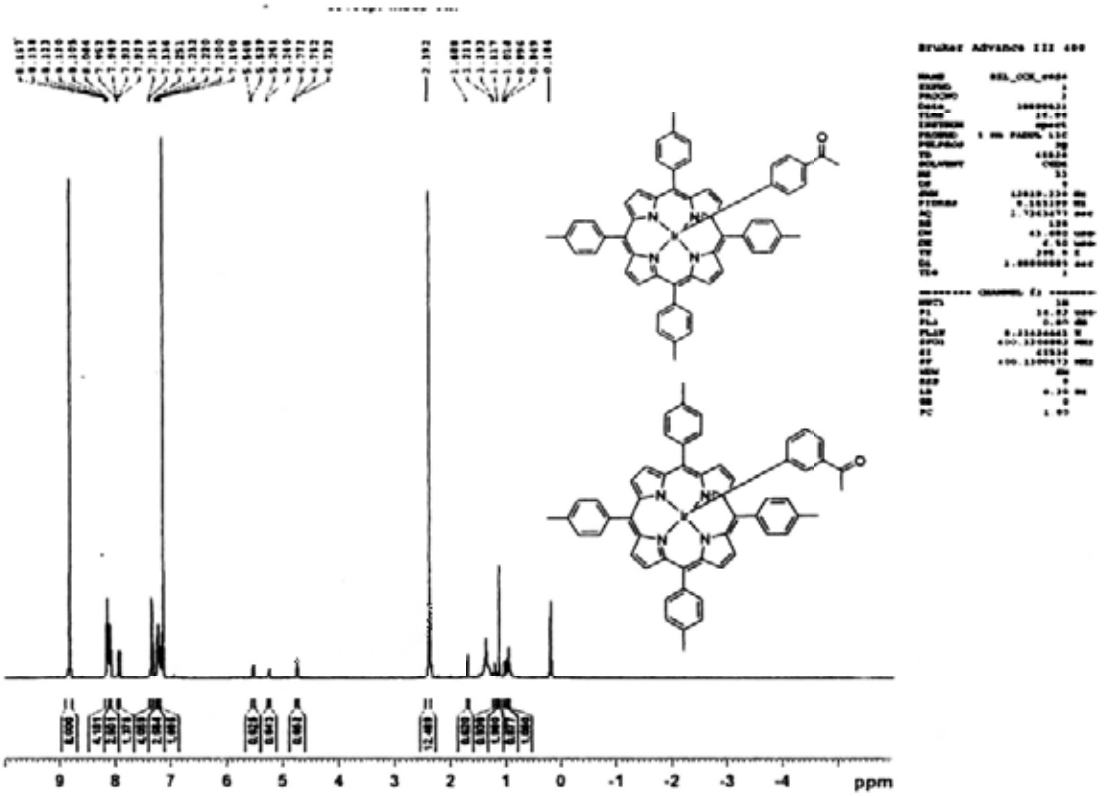

^{1}H NMR of Ir(ttp)CH_2COMe **4f**

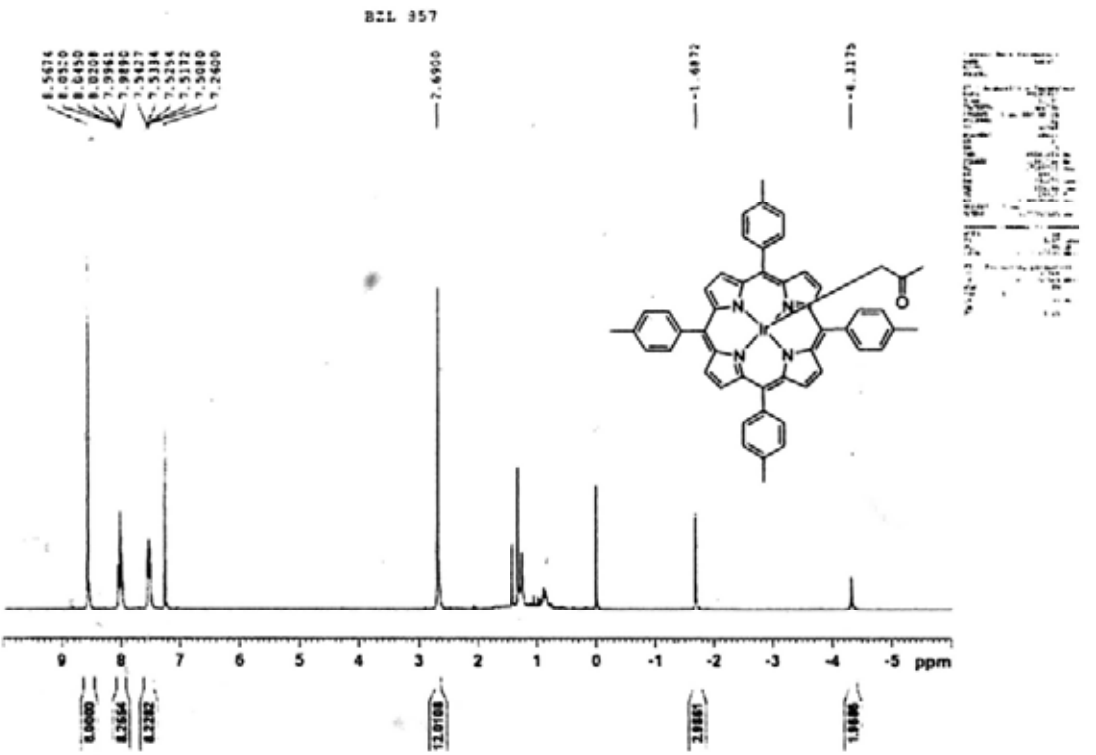

^{13}C NMR of Ir(ttp)CH_2COMe **4f**

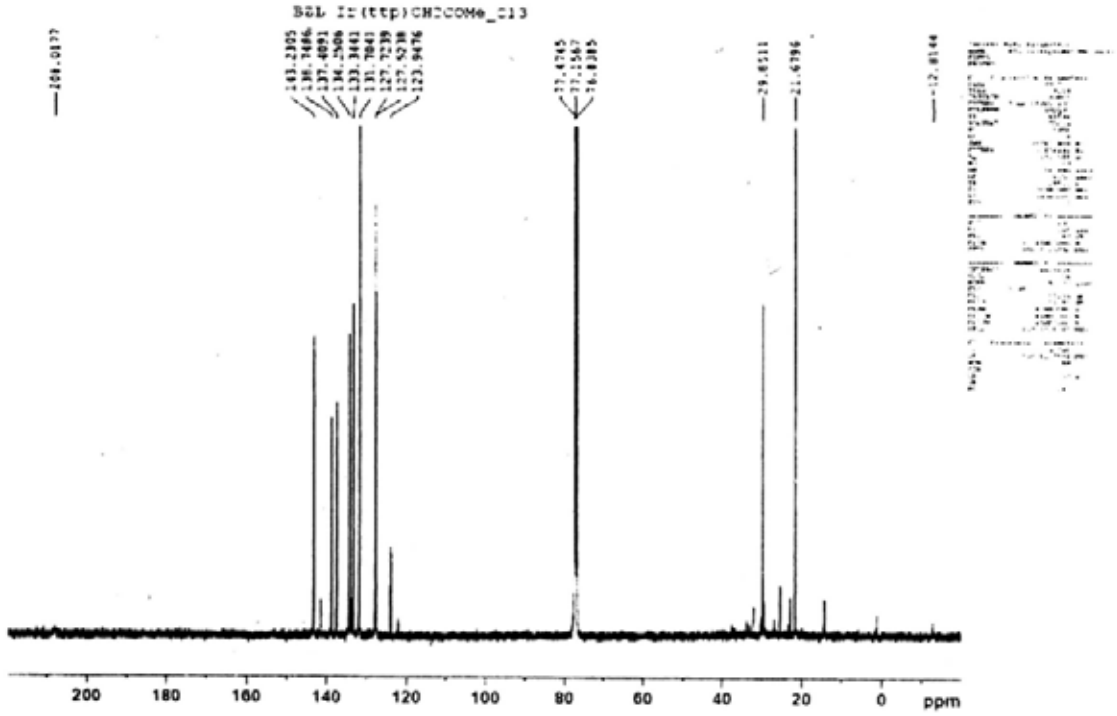

^{1}H NMR of Ir(ttp)Et **3f**

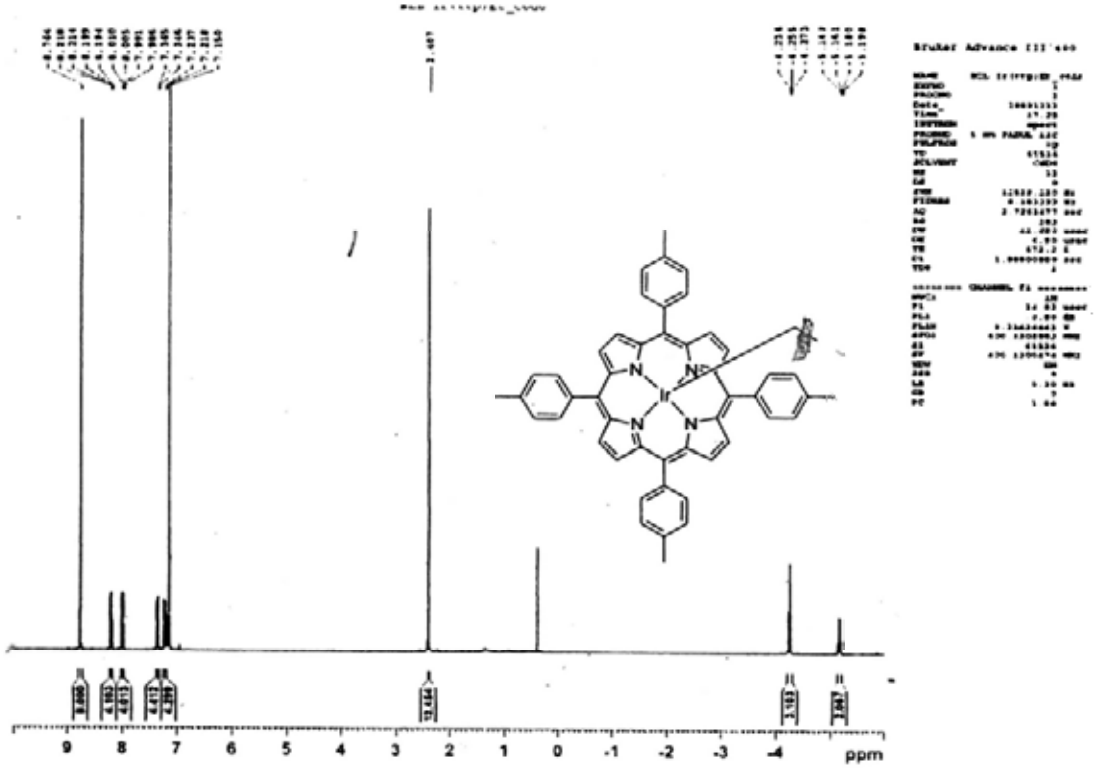

^{1}H NMR of Ir(ttp)(*meta*-&*para*-COEt-C_6H_4) **4d-e**

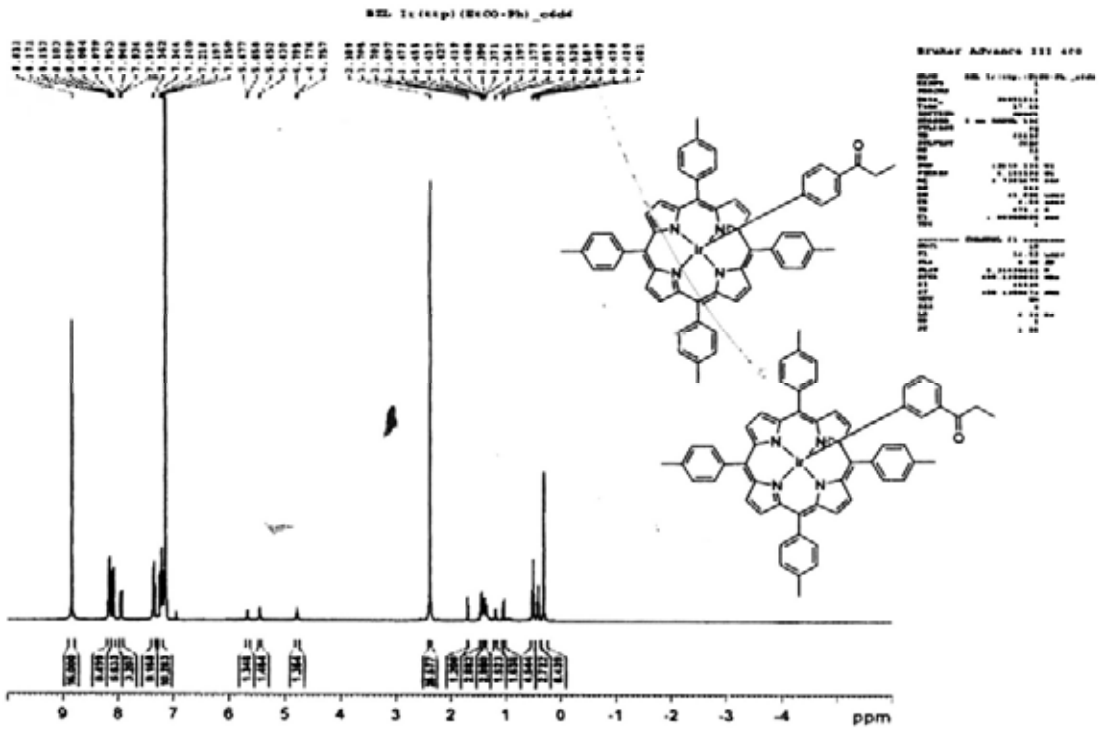

^{1}H NMR of the formation of 5a-b catalyzed by 1a

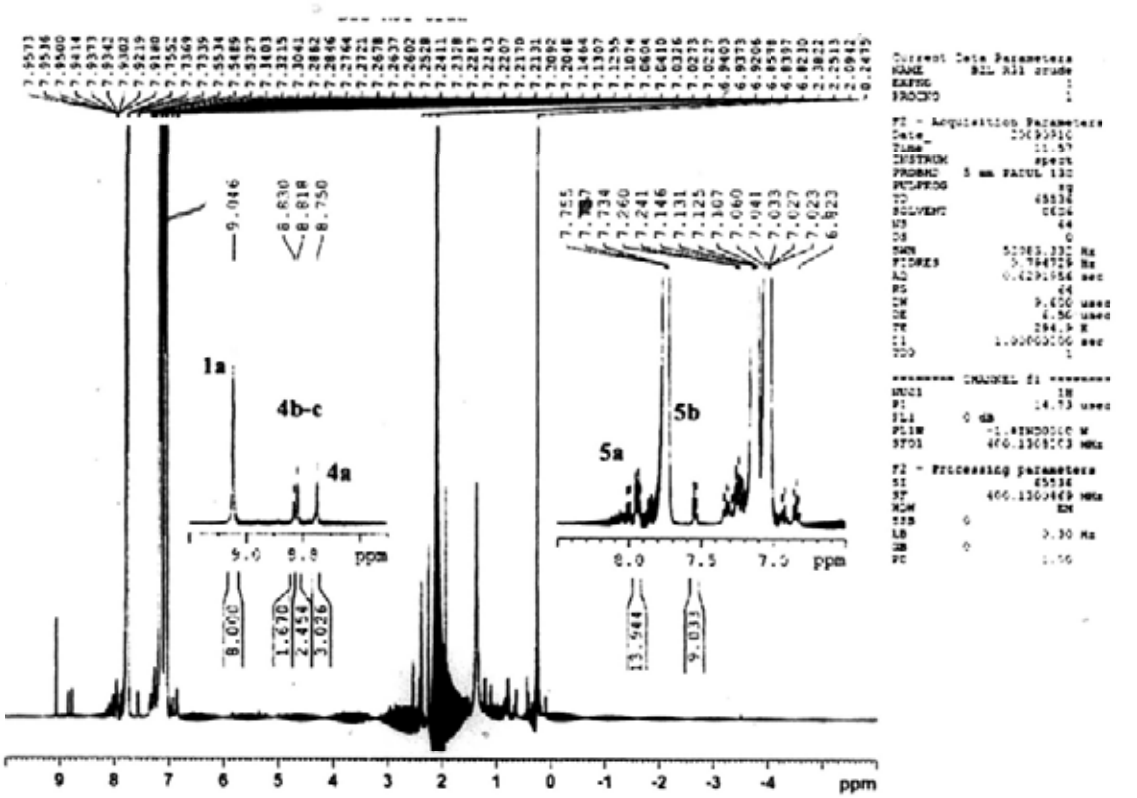

^{1}H NMR of the reaction between 4a in benzene-d_6 with H_2O

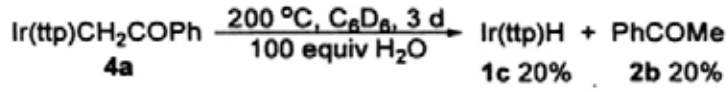

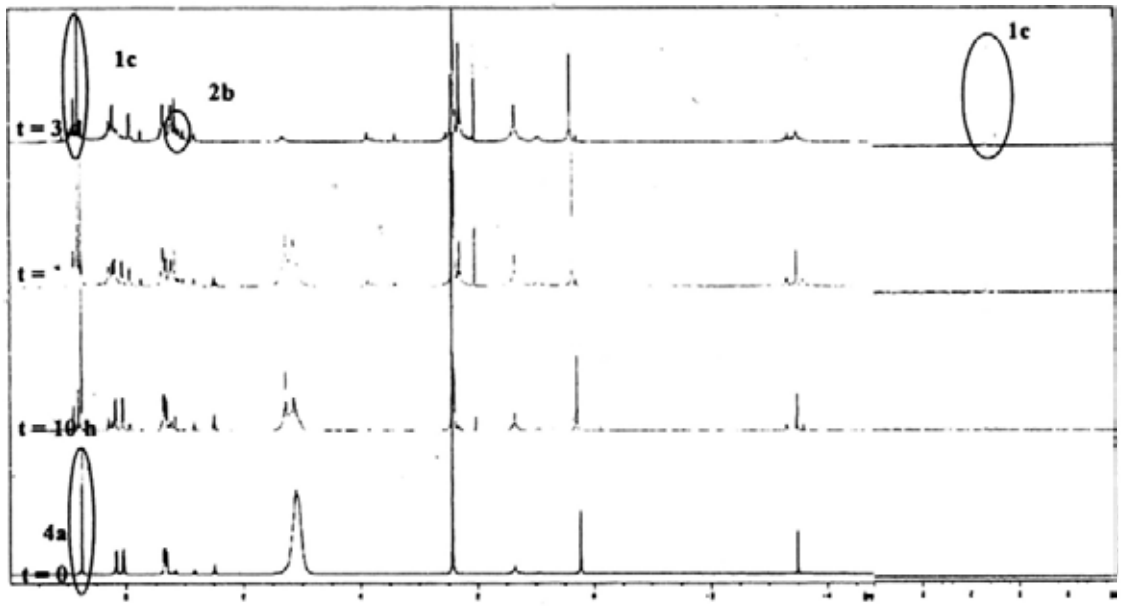

III.II GC-MS Spectra for Formation of Acetophenone and Fluorobenzene

Table 14 List of GC-MS Spectra for Formation of Acetophenone and Fluorobenzene with Naphthalene as Internal Standard

GC-MS Spectrum for Acetophenone with Naphthalene

Sample Information

Analyzed by	Admin
Analyzed	10/2/2009 4:25:11 PM
Sample Type	Unknown
Level #	1
Sample Name	BZL_R32_org
Sample ID	
IS Amount	[1]=1
Sample Amount	1
Dilution Factor	1
Vial #	5
Injection Volume	1
Data File	C:\GCMSsolution\Data\Project1\BZL_R32_org.qgd
Org Data File	C:\GCMSsolution\Data\Project1\BZL_R32_org.qgd
Method File	C:\GCMSsolution\Data\SANG\General.qgm
Org Method File	C:\GCMSsolution\Data\SANG\General.qgm
Report File	
Tuning File	C:\GCMSsolution\System\Tune1\02092009.qg
Modified by	Admin
Modified	10/2/2009 5:26:34 PM

Chromatogram BZL_R32_org C:\GCMSsolution\Data\Project1\BZL_R32_org.qgd

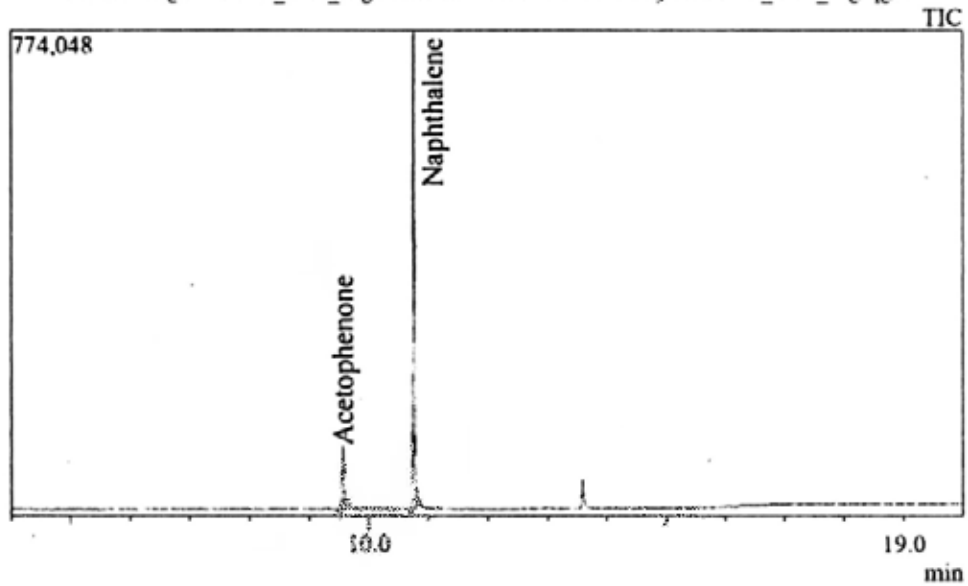

Quantitative Result Table

Name	ID#	R.Time	m/z	Area	Height	Conc.
Acetophenone	1	9.561	105.00	77154	34844	0.000
Naphthalene	2	10.755	128.00	681884	379490	0.000

GC-MS Spectrum for Fluorobenzene with Naphthalene

Sample Information

Analyzed by	: Admin
Analyzed	: 10/13/2009 5:21:29 PM
Sample Type	: Unknown
Level #	: 1
Sample Name	: BZL_R39_org
Sample ID	:
IS Amount	: [1]=1
Sample Amount	: 1
Dilution Factor	: 1
Vial #	: 4
Injection Volume	: 1
Data File	: C:\GCMSsolution\Data\Project1\BZL_R39_org2.qgd
Org Data File	: C:\GCMSsolution\Data\Project1\BZL_R39_org2.qgd
Method File	: C:\GCMSsolution\Data\Project1\Shing_1c(PhH&PhF)4.qgm
Org Method File	: C:\GCMSsolution\Data\Project1\Shing_1c(PhH&PhF)4.qgm
Report File	:
Tuning File	: C:\GCMSsolution\System\Tune1\07102009.qgt
Modified by	: Admin
Modified	: 10/13/2009 5:50:07 PM

Chromatogram BZL_R39_org C:\GCMSsolution\Data\Project1\BZL_R39_org2.qgd

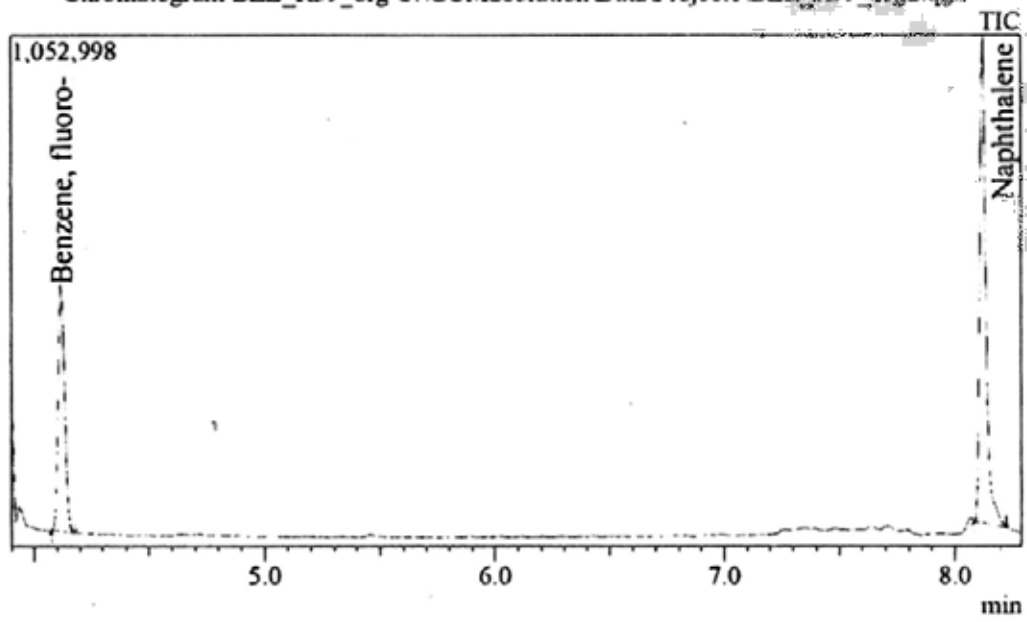

Quantitative Result Table

Name	ID#	R.Time	m/z	Area	Height	Conc.
Benzene, flu	1	4.120	96.00	525635	256895	0.000
Naphthalene	2	8.122	128.00	903961	486763	0.000